COMMUNICATIONS QUARTERLY

THE JOURNAL OF COMMUNICATIONS TECHNOLOGY

Winter 1993

$9.95

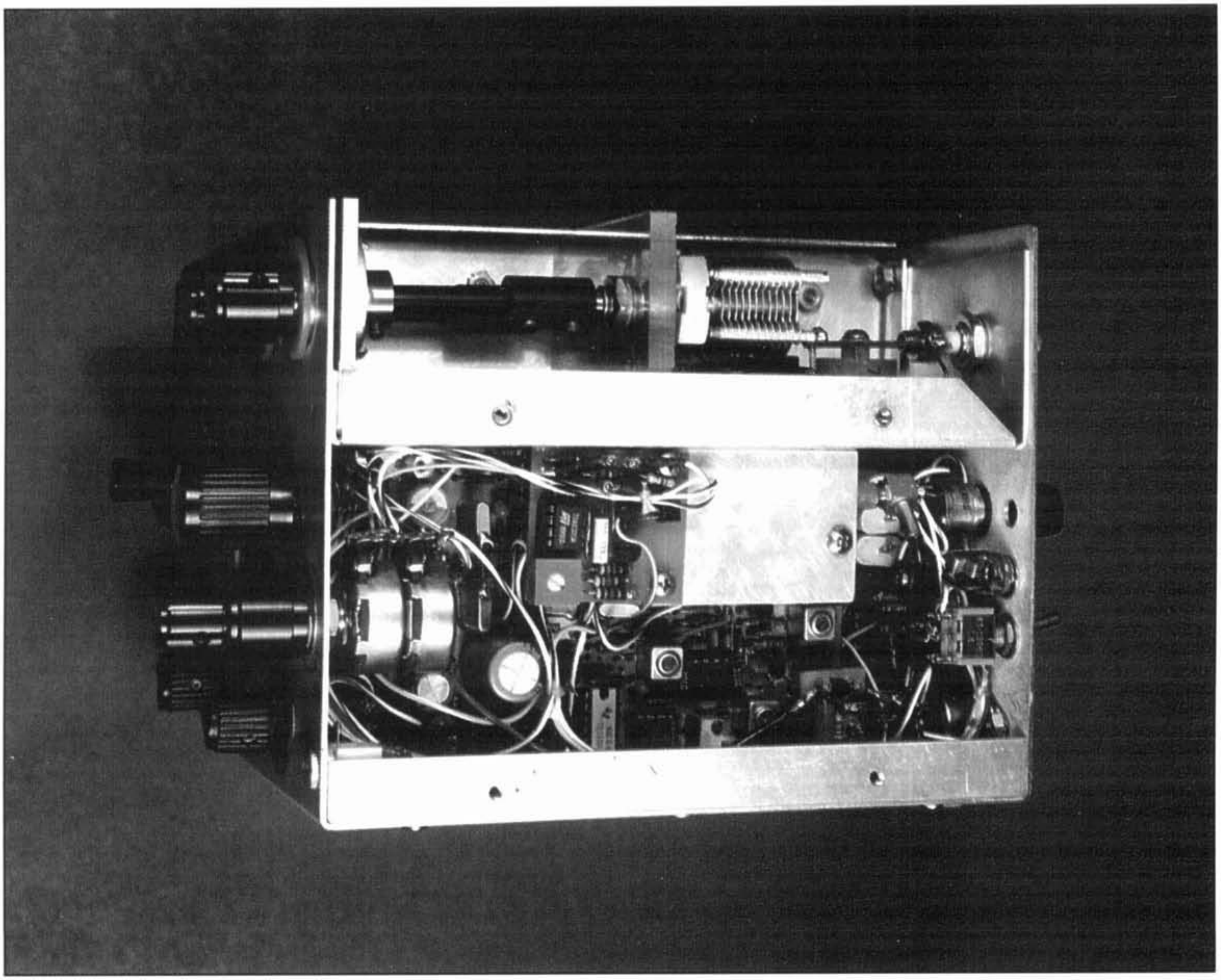

ISSN 1053-9433

REMOTE CONTROL JUST GOT EASIER

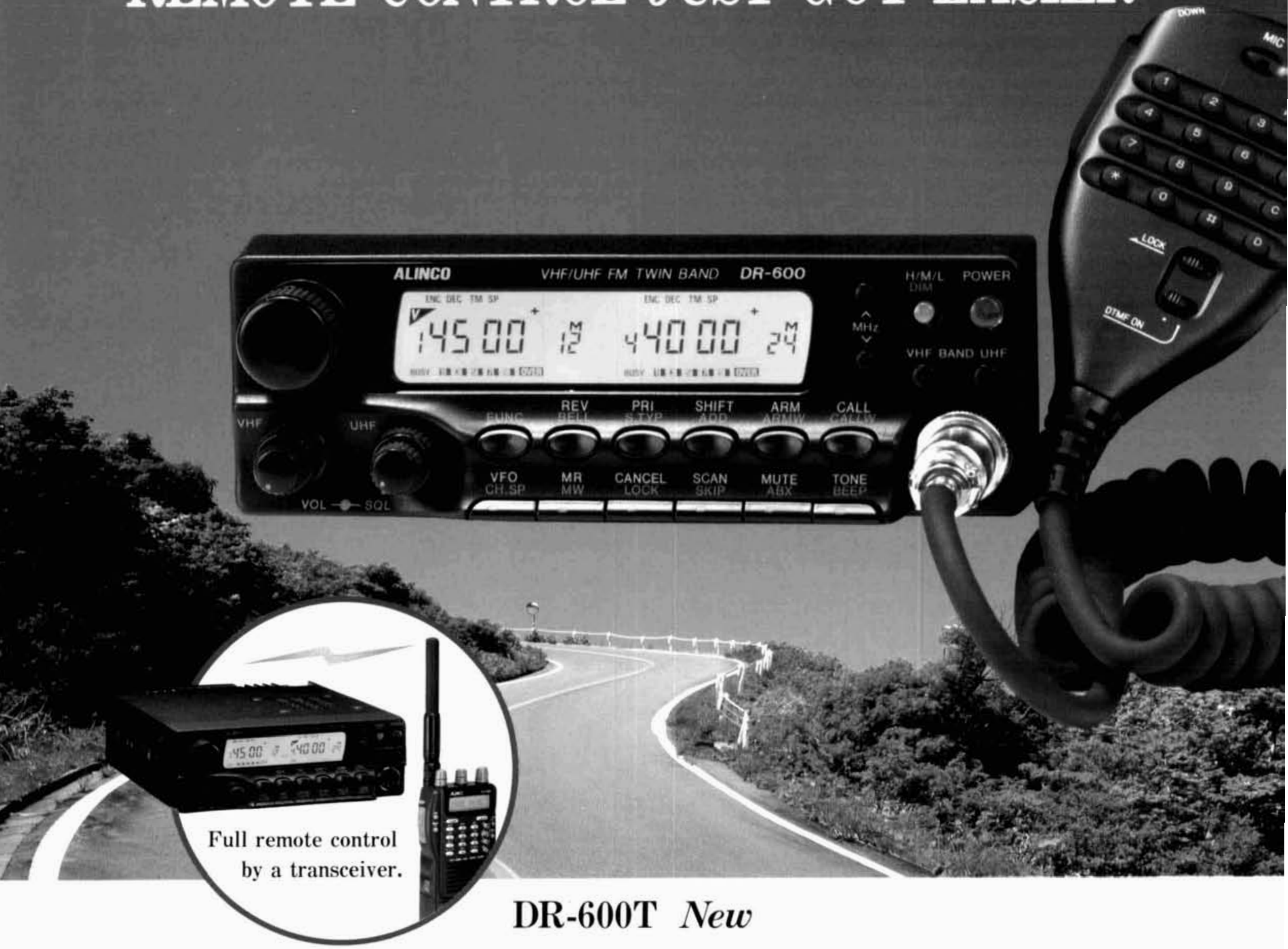

DR-600T *New*

We invented the remote control transceiver in 1990, and we are redefining it today. Hams have been asking for a high-power remote-control rig that is more flexible, more powerful, and less complicated: This is it.

Standard features include FULL remote control with or without a security code. The user can exercise control over both bands from one control channel. This means that a single band HT is all that is required to take full advantage of this feature. The DTMF decoder board that makes all this possible is now factory installed as standard equipment. Also included is DSQ for private paging, autodialer channels, direct frequency input from microphone, CTCSS encode, and odd splits on every memory channel.

This rig features state of the art sensitivity and selectivity, including Airband reception capability with a simple modification. For security and convenience, the head can be mounted separately from the main unit with the optional separation kit.

Check out the affordable technology of the 90's.
Check out ALINCO.

Alinco New Warranty program
One Full Year, Parts and Labor Factory Warranty from Alinco Electronics.
Extended Coverage Plan (ECP) available.
See your Authorized Alinco Dealer for details.

ALINCO
ELECTRONICS INC.

ALINCO ELECTRONICS INC.
438 Amapola Avenue, Unit 130, Torrance, CA 90501
Tel.(310)618-8616 Fax(310)618-8758

Specifications and features are subject to change without notice or obligation.

CIRCLE 15 ON READER SERVICE CARD

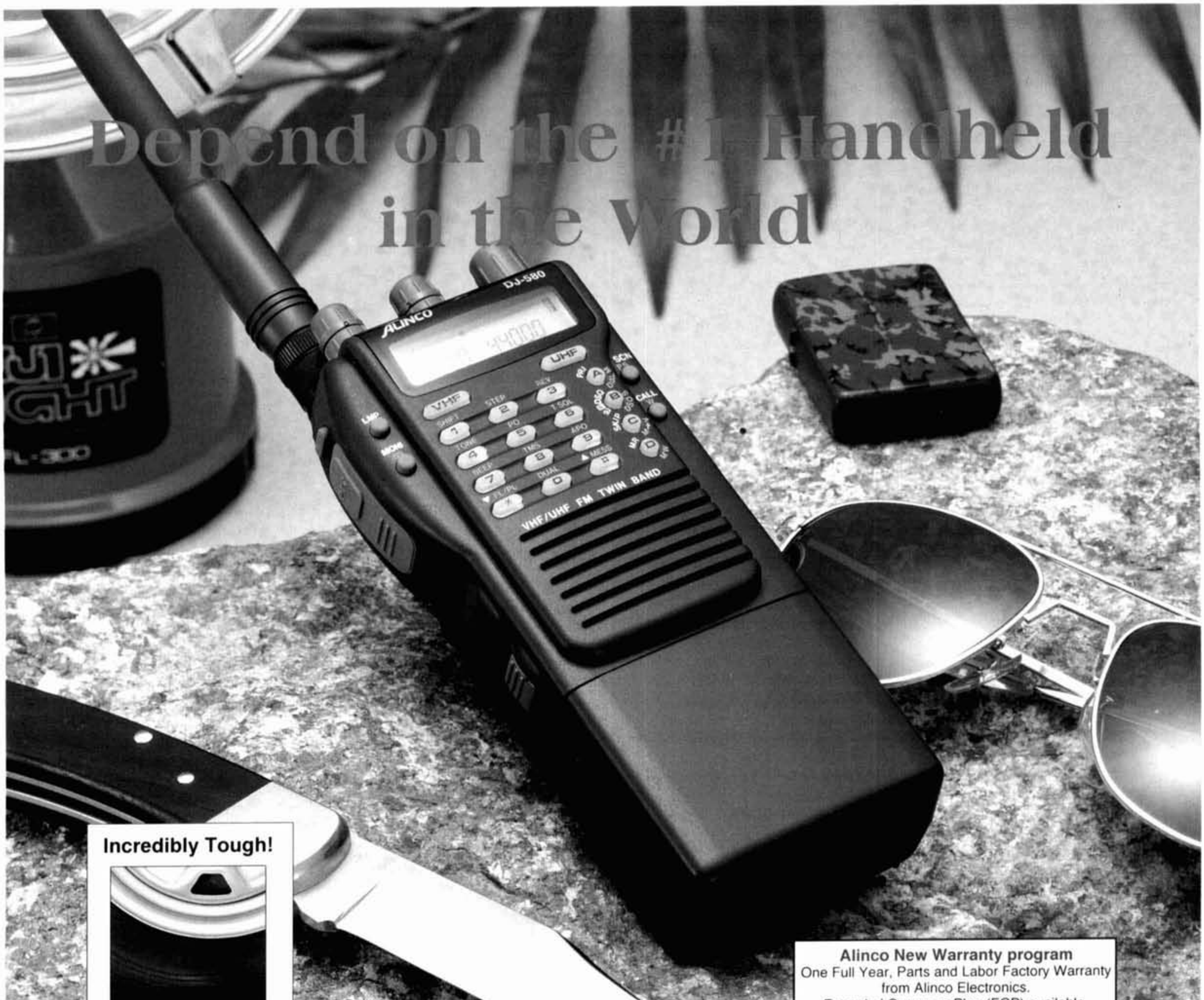

Alinco New Warranty program
One Full Year, Parts and Labor Factory Warranty from Alinco Electronics.
Extended Coverage Plan (ECP) available.
See your Authorized Alinco Dealer for details.

Incredibly Tough!

DJ-580T Dual Bander
Photo for Demonstration only-Abuse to the transceiver will void the warranty.

Model DJ-580TA

The new DJ-580TA takes the lead in super-compact, handheld technology. Generously loaded with all the best features, this is the smallest twin - band HT you will find with so much power going for it.

Great sound, excellent sensitivity, and a comfortable, ergonomic design make this mini very hard to beat.

Alinco's DJ-580TA has Full-Duplex Cross Band Operation and Cross Band Repeater Functions with real world power and excellent sensitivity. Airband receive with simple modification.

This unit has built in DSQ for paging, CTCSS encode and decode standard, various scanning functions, 3 power level selections for each band, bell function, and an illuminated keypad.

New MCF function allows you to set the 40 memory channels regardless of which channels you want for VHF or UHF. Any combination is possible.

If the battery is depleted to less than 5 volts, Alinco's Patented Super Low Battery Consumption Function is automatically activated. You can continue to operate the radio all the way down to 3.5 volts. This feature is effective with dry cell batteries only.

Check out the affordable technology of the 90's.
Check out ALINCO.

ALINCO
ELECTRONICS INC.

ALINCO ELECTRONICS INC.
438 Amapola Avenue, Unit 130, Torrance, CA 90501
TeL:(310) 618-8616 Fax:(310) 618-8758

Kenwood's new TM-742A (144MHz/440MHz) and TM-942A (144MHz/440MHz/1200MHz) FM multibanders offer prime performance plus unparalleled freedom of choice for installation (optional kit).

- **High power**
  Maximum RF output is 50 watts (144MHz), 35 watts (440MHz), and 10 watts (1200MHz).
- **Wideband receiver coverage**
  The TM-742A receives from 118 to 174MHz and 410 to 470MHz; transmit ranges are 144–148MHz and 438–450MHz. The TM-942A adds the 1240–1300MHz range.
- **New & improved detachable front panel**
  The display and control sections can be separated for 3-way convenience. (with DFK-3,4,7)
- **100 memory channels**
  The 100 multi-function memory channels (all available for split operation) can be grouped into 5 banks for added convenience.
- **Multiple scan modes**
  Choose from 8 scan modes per band, plus CO (carrier-operated) and TO (time-operated) scan stops.
- **Tri-band receive/display**
  The TM-942A can receive/display all three bands (144MHz/440MHz/1200MHz) simultaneously. For the TM-742A there are four optional band units: 28MHz (50 watts), 50MHz (50 watts), 220MHz (25 watts), and 1200MHz (10 watts).
- **Cross-band repeater, dual-in repeater, fixed-band repeater**
- **Single-bander simplicity**
  Independent SQL and VOL controls for each band enable rapid response.
- **S meter squelch and auto squelch**
  Weak signals can be shut out. Noise squelch is also available.
- **Supplied multi-function microphone**
  Enables direct frequency entry.
- **Clock and timer**
  Includes stopwatch, alarm and on/off timer functions.
- **Wireless remote control function**
  A DTMF transceiver can be used to control various settings on the TM-742A/942A.
- **Built-in DTSS and pager function**
  The TM-742A/942A offers DTSS (Dual-Tone Squelch System) for selective calling and paging using standard DTMF tones. Elapsed time is shown by the tone alert system.
- **Supplied accessories**
  Mounting bracket, DC cable, fuses, mic, mic hook.
- **Choice of accessories**
  A full line of mics, speakers, and other accessories is available. See your authorized Kenwood Amateur Radio dealer for details!

Specifications guaranteed for Amateur band use only.

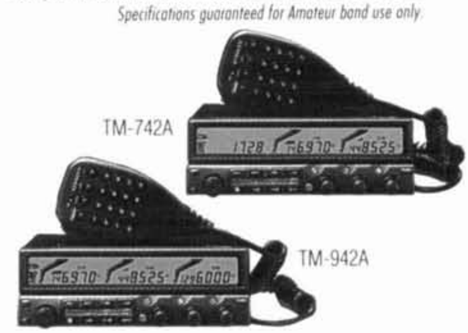

TM-742A/942A

Mobile Transceivers

KENWOOD U.S.A. CORPORATION
COMMUNICATIONS & TEST EQUIPMENT GROUP
P.O. BOX 22745, 2201 E. Dominguez Street,
Long Beach, CA 90801-5745

KENWOOD ELECTRONICS CANADA INC.
6070 Kestrel Road, Mississauga,
Ontario, Canada L5T 1S8

COMMUNICATIONS QUARTERLY
THE JOURNAL OF COMMUNICATIONS TECHNOLOGY

CONTENTS

Volume 3, Number 1 — Winter 1993

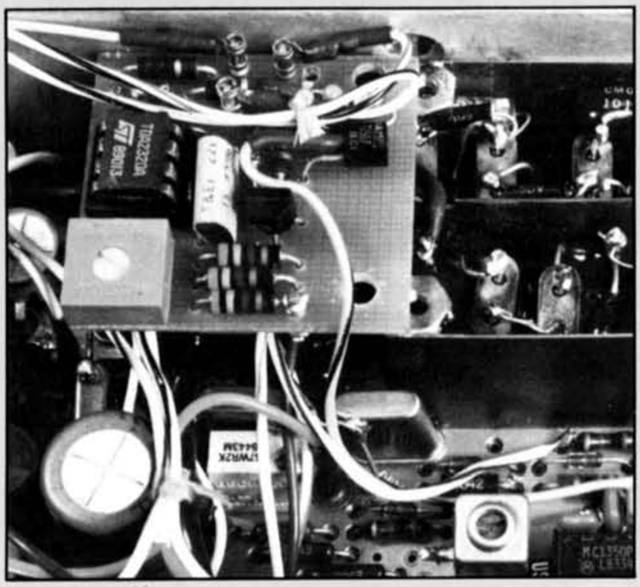
Carver, page 11

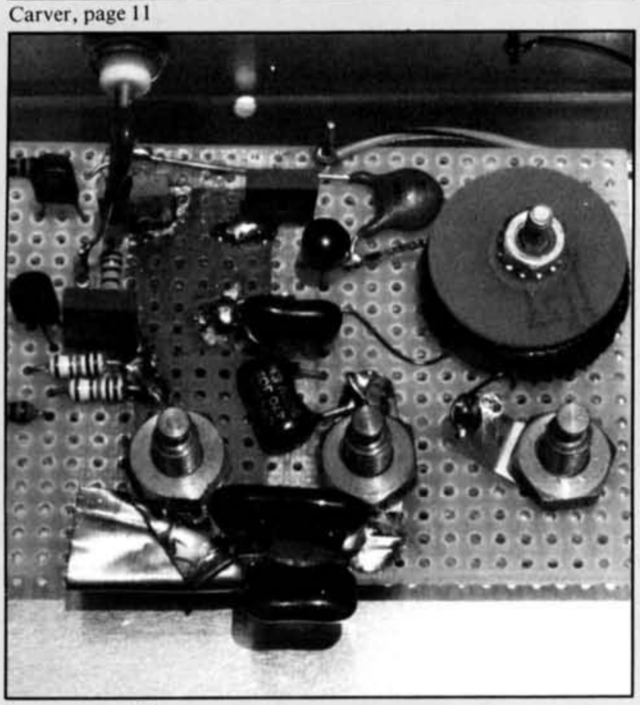
Carver, page 19

Cover photo: High-performance crystal filter designed by K6OLG for use in his homebrew 40-meter mobile radio (see story beginning page 11). Photo by Mike Berman.

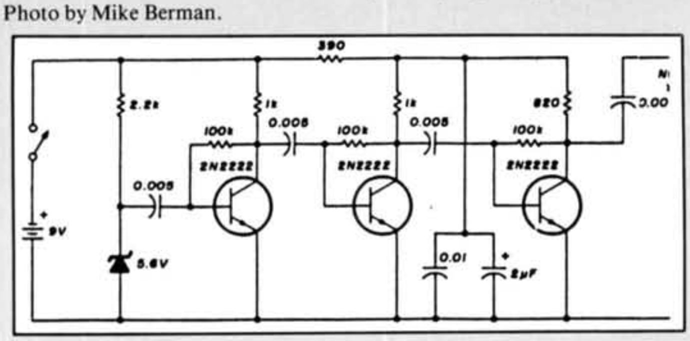

Shapiro, page 83

EDITORIAL

The Lost Art of Homebrewing

With all the good commercial amateur radio gear on the market, why would anyone want to build anything from scratch anymore? Parts are harder to obtain these days, and the more exotic components are expensive in small lots—if you can find someone willing to sell them to you. Besides, you need to be an RF engineer to design anything with the bells and whistles you'll find in a manufactured rig. Don't you?

While today's projects may be more complicated than the super-regens and 2-tube Cw rigs you used to build, there are now many more tools available to help you create and implement the more complex designs rattling around in your brain. Commercial manufacturers offer inexpensive integrated circuits that reduce the need for more intricate and involved circuitry. There are computer programs for designing pc boards, filters, and generic circuits. Board designs can now be copied directly onto acetate using a computer printer. With photosensitive GC material, these designs can be transferred to a pc board with a minimum of effort.

I know you're busy these days, and it's easier to buy than build. But didn't it feel great to create something of your own . . . you know, smell that solder? If you don't want to deal with messy and time-consuming board preparations using chemical etchants and baths, use protoboards to develop designs. If you've always hated soldering, wire wrap. If the complete scratch-built route isn't to your liking, build one of the many kits available. A friend of mine, upon receiving her ham ticket, decided she wanted to know more about the technical side of the hobby and built her own radio from just such a kit. My 11-year old son built a working 2-meter receiver in a couple of days last winter. Don't let these novice technical people put you to shame! After all, isn't the challenge of homebrewing what drew you to amateur radio in the first place?

If you aren't interested in building for yourself, how about helping to nurture one of the engineers of the future? Homebrewing provides a research and development playground for budding technical minds. No number of classroom lectures or computer simulations can provide the knowledge garnered from hands-on design work. By building their own test equipment, receivers, transceivers, and antennas, novice technicians can learn a lot about the inner workings of electronics. And once they've learned how things work, they'll be more intelligent consumers of commercial gear. They'll even be able to modify their commercial toys to include additional features. With all the technical knowledge you've accumulated from your own homebrew efforts, you can help those coming up through the ranks.

If you once did lots of homebrewing, let the bug bite you again. Imagine the excitement you'll feel when you talk to Tasmania with that little transceiver you built on a six by six piece of board using generic components, and he gives you an S9+ signal report! You can casually mention that your rig is homebrew and wait for the response. And there's always someone on the air who's willing to work with you in on-the-air tests. Sharing your efforts via the airwaves can generate a creative vitality for both you, the builder, and those you contact, as you work together to refine a radio design.

Let's remember that amateur radio priviledges were granted by the FCC not only to provide public assistance during times of disaster, but to encourage technological experimentation and advancement in the field of communications. Perhaps you're one of many hams who began his ham career at an early age, who built his own equipment because he couldn't afford to buy manufactured items, who parlayed the knowledge he accrued into a career as an RF design engineer or technician. Or maybe your experience led you to work in radio communications for the military or a commercial company. Some of us have even been lucky enough to become "professional" hams—designing amateur radio gear that we package and sell ourselves, or working as a design engineer for a company that produces ham gear. Some write for or edit amateur radio publications or design ham related software.

If homebrewing no longer appeals to you, fine. Amateur radio offers options for everyone. But if you've never fulfilled your Walter Mitty dream of building the perfect transceiver or antenna, roll up your sleeves and get back to work! There's never been a greater diversity of parts to build with or a better array of tools to help you reach your goal. Remember, some day you could hear those sweet words, "Your signal is S9+," coming back to your from some faraway country. And while you're at it, write about what you've built. Don't let homebrewing become a lost art; rediscover the fun, and pass it along!

Terry Littlefield, KA1STC
Editor

A publication of
CQ Communications, Inc.
76 North Broadway
Hicksville, NY 11801-USA

Editorial Offices: P.O. Box 465, Barrington, NH 03825. Telephone/Fax: 603-664-2515.

Business Offices: 76 North Broadway, Hicksville, NY 11801. Telephone: (516) 681-2922. FAX: (516) 681-2926.

Communications Quarterly is published four times a year (quarterly) by *CQ Communications, Inc.* Subscription prices: Domestic—one year $29.95, two years $56.95. Foreign—one year $39.95, two years $76.95. Foreign Air Mail—one year $60.95, two years $118.95.

Allow six weeks for change of address.

Second-class postage paid at Hicksville, NY and additional mailing offices.

Postmaster: Please send change of address to Communications Quarterly, CQ Communications, Inc., 76 North Broadway, Hicksville, NY 11801. ISSN 1053-9344

LETTERS

A bit of SSB history

In *Communications Quarterly*, Summer '92, Jon dyer G40BU/VE1JAD in "HF Receiver Design" gave a rather interesting history of SSB radio. AT&T started using HF SSB radio circuits in 1927 and they were in use until satellites took over. As for amateurs, there was an article on an SSB transmitter in magazine *Radio/R9* in the middle-late '30s. In that period according to an interview Bill Orr had with Jim Lamb and published in *Ham Radio* several years ago he designed an SSB transceiver but the idea was (misguidedly) turned down by the *QST* editors as too complexed and costly for hams in the depression years!

A pioneer that really got amateur SSB going was Don Norgaard, W2KUJ, in his series of articles in 1948 *QST* on the phasing method for generating SSB. In the early '50s Central Electronics brought out its popular 10A kit for a phasing method SSB transmitter. I got one while I was YN1WC and took off on SSB with a hundred or so others around the world at the time.

The filter type method of SSB generation has been used since day one for commercial communication equipment. I never saw, heard of or had any stability problem all of the years before frequency synthesis was developed.

Wayne Cooper, AG4R
Miami Shores, Florida

Some comments coherer operation

In rereading the article "Radio Receivers of the Past" in the Spring 1992 issue of your magazine, I find the description of the operation of a coherer on page 94 is in error.

The device does not provide a "non-linear impedance" as we think of that term today. The coherer is a latching device. It has a high resistance (around 50k ohms) when "reset" and a low resistance (around 100 ohms) when triggered by the signal. The resistance stays low until the coherer is tapped or reset. The telegraph relay in the system or the sounder has the tapper or reset device attached to it so when the signal pulse sets the resistance low and the relay pulls up, the tapper resets the coherer dropping the current to the relay because of the high resistance causing the relay to drop out.

For a spark signal the coherer-relay-sounder-tapper sequence is repeated at the spark rate and the sounder provides a tone at the spark rate.

The breakdown voltage of the oxide film on the metal filings in the coherer is about 16 volts and, according to a book I found at Illinois Tech in Chicago entitled *Radio Up to 1912* (author unknown), the filings are welded (very lightly) by the signal, not activated magnetically as stated in the article.

A coherer is easy to build. I have built a number to satisfy my curiosity about how they operate.

I even built a radio control system using a spark transmitter and a coherer receiver that worked at about a 50 foot range (just like the RC boats in the 1890s).

If a how-to-build article on a coherer sounds like something you might be able to use, I will be glad to send you the information because I don't have a word processor to put it in the right format for publishing.

The Germans used coherers in WWII in local air raid warning systems after the central warning systems were bombed out. The coherers were set to trigger on the allied bomber's radars. The locals systems gave people a few minutes warning in which to head for shelter.

Len Petraitts, W0NU
Pittsboro, North Carolina

Some super sleuthing

Thank you very much for sending me a copy of the article, "The Triangle Antenna," and the spring 1992 issue of *Communications Quarterly*.

Today I ordered all the back issues except the spring 1992. I hope this will bring me up-to-date on all the "Good Stuff" that I have been missing.

While reviewing the contents of the "spring 1992" issue, I became aware of a couple of items. First, I noticed that your call has been issued to Terry Northup who is listed as the Editor of Communications Quarterly. Second, there is an article in the spring issue by a Rick Littlefield, K1BQT. Third, seems like you were Northup and got together with Littlefield and changed your name to Littlefield. Congratulations to you and Rick. Must be a lot of QRM around the Shack now, Hi.

I have enclosed some stamps to reimburse the "Petty Cash" fund for the mailing costs you used in sending me the material. Thanks again for your cooperation in this matter.

Ted Simmington, W1JOT
Needham, MA

Good detective work Ted! K1BQT and I "merged our shacks" in May of this year. Ed.

(Continued on page 106)

ASTRON CORPORATION
9 Autry
Irvine, CA 92718
(714) 458-7277 • FAX (714) 458-0826

ASTRON POWER SUPPLIES

• HEAVY DUTY • HIGH QUALITY • RUGGED • RELIABLE •

MODEL VS-50M

SPECIAL FEATURES

- *SOLID STATE ELECTRONICALLY REGULATED*
- FOLD-BACK CURRENT LIMITING Protects Power Supply from excessive current & continuous shorted output
- CROWBAR OVER VOLTAGE PROTECTION on all Models except RS-3A, RS-4A, RS-5A, RS-4L, RS-5L
- MAINTAIN REGULATION & LOW RIPPLE at low line input Voltage
- HEAVY DUTY HEAT SINK • CHASSIS MOUNT FUSE
- THREE CONDUCTOR POWER CORD except for RS-3A
- ONE YEAR WARRANTY • MADE IN U.S.A.

PERFORMANCE SPECIFICATIONS

- INPUT VOLTAGE: 105-125 VAC
- OUTPUT VOLTAGE: 13.8 VDC ± 0.05 volts (Internally Adjustable: 11-15 VDC)
- RIPPLE Less than 5mv peak to peak (full load & *low line*)
- All units available in 220 VAC input voltage (except for SL-11A)

SL SERIES

• LOW PROFILE POWER SUPPLY

MODEL	Colors Gray	Colors Black	Continuous Duty (Amps)	ICS* (Amps)	Size (IN) H × W × D	Shipping Wt. (lbs.)
SL-11A	•	•	7	11	2⅝ × 7⅝ × 9¾	12
SL-11R	•	•	7	11	2⅝ × 7 × 9¾	12
SL-11S	•	•	7	11	2⅝ × 7⅝ × 9¾	12
SL-11R-RA		•	7	11	4¾ × 7 × 9¾	13

RS-L SERIES

• POWER SUPPLIES WITH BUILT IN CIGARETTE LIGHTER RECEPTACLE

MODEL	Continuous Duty (Amps)	ICS* (Amps)	Size (IN) H × W × D	Shipping Wt. (lbs.)
RS-4L	3	4	3½ × 6⅛ × 7¼	6
RS-5L	4	5	3½ × 6⅛ × 7¼	7

RM SERIES

MODEL RM-35M

• 19" RACK MOUNT POWER SUPPLIES

MODEL	Continuous Duty (Amps)	ICS* (Amps)	Size (IN) H × W × D	Shipping Wt. (lbs.)
RM-12A	9	12	5¼ × 19 × 8¼	16
RM-35A	25	35	5¼ × 19 × 12½	38
RM-50A	37	50	5¼ × 19 × 12½	50
RM-60A	50	55	7 × 19 × 12½	60
• Separate Volt and Amp Meters				
RM-12M	9	12	5¼ × 19 × 8¼	16
RM-35M	25	35	5¼ × 19 × 12½	38
RM-50M	37	50	5¼ × 19 × 12½	50
RM-60M	50	55	7 × 19 × 12½	60

RS-A SERIES

MODEL RS-7A

MODEL	Colors Gray	Colors Black	Continuous Duty (Amps)	ICS* (Amps)	Size (IN) H × W × D	Shipping Wt. (lbs.)
RS-3A		•	2.5	3	3 × 4¾ × 5¾	4
RS-4A	•	•	3	4	3¾ × 6½ × 9	5
RS-5A		•	4	5	3½ × 6⅛ × 7¼	7
RS-7A	•	•	5	7	3¾ × 6½ × 9	9
RS-7B	•	•	5	7	4 × 7½ × 10¾	10
RS-10A	•	•	7.5	10	4 × 7½ × 10¾	11
RS-12A	•	•	9	12	4½ × 8 × 9	13
RS-12B		•	9	12	4 × 7½ × 10¾	13
RS-20A	•	•	16	20	5 × 9 × 10½	18
RS-35A	•	•	25	35	5 × 11 × 11	27
RS-50A	•		37	50	6 × 13¾ × 11	46

RS-M SERIES

MODEL RS-35M

MODEL	Continuous Duty (Amps)	ICS* (Amps)	Size (IN) H × W × D	Shipping Wt. (lbs.)
• Switchable volt and Amp meter				
RS-12M	9	12	4½ × 8 × 9	13
• Separate volt and Amp meters				
RS-20M	16	20	5 × 9 × 10½	18
RS-35M	25	35	5 × 11 × 11	27
RS-50M	37	50	6 × 13¾ × 11	46

VS-M AND VRM-M SERIES

MODEL VS-35M

• Separate Volt and Amp Meters • Output Voltage adjustable from 2-15 volts • Current limit adjustable from 1.5 amps to Full Load

MODEL	Continuous Duty (Amps) @13.8VDC	@10VDC	@5VDC	ICS* (Amps) @13.8V	Size (IN) H × W × D	Shipping Wt. (lbs.)
VS-12M	9	5	2	12	4½ × 8 × 9	13
VS-20M	16	9	4	20	5 × 9 × 10½	20
VS-35M	25	15	7	35	5 × 11 × 11	29
VS-50M	37	22	10	50	6 × 13¾ × 11	46
• Variable rack mount power supplies						
VRM-35M	25	15	7	35	5¼ × 19 × 12½	38
VRM-50M	37	22	10	50	5¼ × 19 × 12½	50

RS-S SERIES

MODEL RS-12S

• Built in speaker

MODEL	Colors Gray	Colors Black	Continuous Duty (Amps)	ICS* Amps	Size (IN) H × W × D	Shipping Wt. (lbs.)
RS-7S	•	•	5	7	4 × 7½ × 10¾	10
RS-10S	•	•	7.5	10	4 × 7½ × 10¾	12
RS-12S	•	•	9	12	4½ × 8 × 9	13
RS-20S	•	•	16	20	5 × 9 × 10½	18
SL-11S	•	•	7	11	2¾ x 7⅝ x 9¾	12

*ICS—Intermittent Communication Service (50% Duty Cycle 5min. on 5 min. off)

NEW!

HAL Announces the PCI-4000 PC-CLOVER System

For Fast, Bandwidth-Efficient HF Data

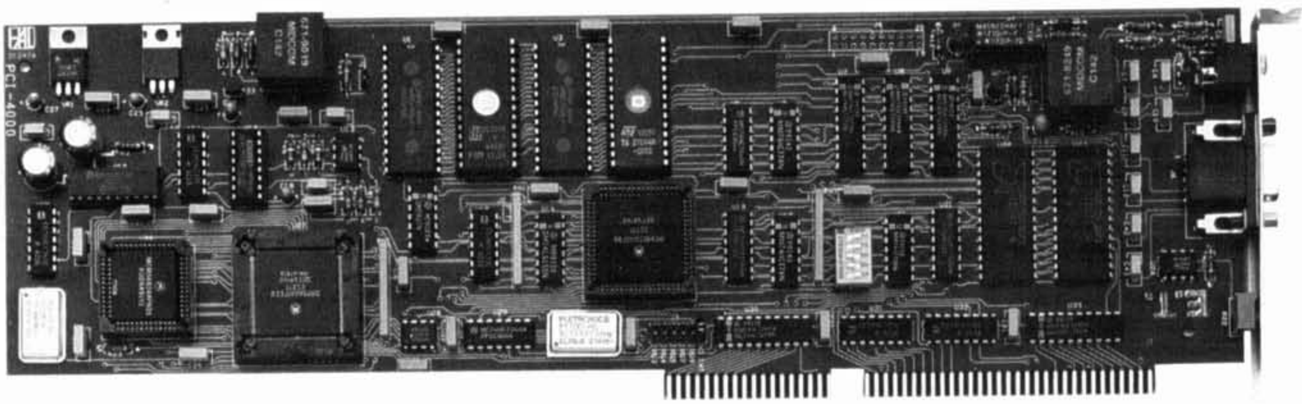

The PCI-4000 uses the latest development in HF data transfer methods–CLOVER-II. CLOVER-II is designed to maximize the amount of data which can be transferred in a narrow bandwidth over HF radio frequencies. It uses a combination of four tone frequencies with phase and amplitude modulation to achieve data transfer rates as high as 60 characters per second–about ten times faster than AMTOR. The PC-CLOVER system incorporates Reed-Solomon error correction, not simply a retransmission scheme. The PCI-4000 is a full-sized PC card which operates in a 80286-based PC or higher.

The PCI-4000 PC CLOVER system features:

- Higher throughput than RTTY, AMTOR, Packet, or PACTOR on similar HF channel
- Simple pull-down menu operation
- Signal bandwidth of 500 Hz (@50 dB down)
- Plugs into your PC (286, 386SX, 386, or 486 machines)
- Easy interface to your transceiver
- Automatically adapts to HF band conditions
- Error correcting using Reed-Solomon error correction

You've read about it in the articles. Now you can operate CLOVER!
Order your PC-CLOVER system today from HAL Communications Corp.

PCI-4000 PC-CLOVER System Only $995.00

HAL

HAL Communications Corp.
P.O. Box 365
Urbana, IL 61801
Phone (217) 367-7373
FAX (217) 367-1701

MasterCard

VISA

Bill Carver, *K6OLG*
1952 Royal Oak Road
Tustin, California 92680

HIGH-PERFORMANCE CRYSTAL FILTER DESIGN

Produce precisely shaped, very narrow CW filters that don't ring and SSB filters with incredible selectivity, without black magic

Wes Hayward's ladder filter articles [1,2] described the design and construction of inexpensive crystal filters having good performance. In the years since these articles were published, ham literature has been full of homebrew rigs with ladder filters. Cohn filters, using identical crystal frequencies and capacitors throughout, are particularly attractive for simple cut-and-try filters.

But you don't need to stop at cut-and-try filters. With the same number of parts, just different component values, you can produce precisely shaped and very narrow CW filters that don't ring, and SSB filters with incredible selectivity. Making them requires neither luck nor black magic; this article explains the process, shares some practical ideas, and shows a few actual filter examples.

The schematic of, say, an 8-pole filter is always the same. The only difference between Chebychev, Butterworth, Gaussian, (or any response shape) lies in the component values. With perfect lossless coils, capacitors, and crystals, for a given impedance there is a set of component values that will produce a Butterworth frequency response. Another set of component values will make a 0.1-dB Chebychev frequency response, and so on.

Parts cost for filters is minimal. Once you're comfortable with the process, you can produce quite exotic filters inexpensively, essentially substituting time for money—a time-honored homebrew tradition.

Equipment requirements

- **Counter.** A frequency counter with 1-Hz resolution.
- **Crystal tester.** Several adequate dedicated testers have already been described.[1,3] Some interesting variations are available from the author for an SASE.
- **Test oscillator.** The test oscillator needs to be more stable than a general-purpose signal generator. I threw together a VXO using a crystal from the batch being tested and tuned it with an ARC-5 tuning capacitor to get plenty of bandspread. In the tester, the

selectivity of the crystal being tested will filter out oscillator harmonics, but the substitution pot won't. This will cause an error in the crystal Q measurement. Use a simple five-pole low-pass filter to remove harmonics from the test oscillator signal.

- **Ohmmeter.** A bridge or DMM that's accurate to within 1 ohm is required and 0.1-ohm resolution is even better.
- **Computer and software.** This article assumes you'll use Wes Hayward's LADPAC software,* which runs on an IBM PC or clone. The software contains a group of interconnected general-purpose ladder network programs for designing of ordinary impedance-matching networks, and one program, **X**, used specifically for designing crystal filters.

LADPAC lets you see what selectivity you can obtain from 6 crystals, 8 crystals, or 15 crystals; you decide how much selectivity is "enough." You can change terminations, find out what the insertion loss will be, make matching networks to other impedances, and see how badly the filter shape will change if the capacitors are in error by 5 percent. I find the actual filters closely match the computer prediction.

Throughout the text, I list the actual keystrokes to run the program at certain points. Obviously, this will be meaningless without the program, so I apologize to the casual reader. However, for those who take the plunge and buy the program, this detail is useful to quickly see how the process is done.

The design process

The steps of the design process are:

- Measure the parameters of your crystals. Crystal matching isn't too important, because crystals can be *tuned* during filter construction.**
- Choose a filter and bandwidth that you'll be able to make with the crystals you have.
- Perform the theoretical design using the LADPAC design program. It will estimate the performance you can obtain. Repeat steps 2 and 3 as many times as necessary to get the desired filter.
- Select the coupling capacitors specified by LADPAC.
- Match the series-resonant frequencies of your set of crystals to one *loop frequency*. If you can't obtain this with your crystals, *tune* a crystal with a series capacitor.
- Solder the parts together and make sure the design works as predicted.

Measuring crystal parameters

To calculate a filter, you'll need to know crystal series-resonant frequency, series resistance, Q, and the parallel "holder" capacitance. Be as careful as possible because doing an accurate design hinges on knowing these parameters. I offer the following hints in addition to those mentioned in previous articles.

- The crystal case must be grounded in the finished filter and it's prudent to carefully solder the grounding wire to the case *before* you start testing. Use minimum heat; the heat of soldering might alter a crystal parameter.
- While crystals are stable, you'll be measuring in *cycles*. After inserting some crystals into the tester, I noticed that 20 to 30 seconds were required for the series-resonant frequency to stabilize fully. I finally traced this phenomenon to the warmth generated by my hands and eliminated the problem by handling the crystals with a sock during testing!

A crystal tester has resistors on each side of the crystal. With the tester off, measure the sum of those resistances by connecting the ohmmeter to the crystal leads. Call this resistance r_t.

Power up the tester, find the series-resonant frequency of a crystal, and record the relative amplitude. Tuning is relatively broad at the peak. Tune higher and lower and record the -3 dB frequencies, f_H, and f_L. Now substitute a pot for the crystal, and adjust it for the same maximum reading as the crystal. Measure and record the resistance of the pot, calling it R_p. You can now calculate the crystal parameters as follows:

series-resonant frequency	f_o	$= (f_H + f_L)/2$
3-dB width	df	$= f_H - f_L$
crystal Q	Q	$= (f_o/df)(r_t + r_p/r_p)$
crystal equivalent inductance	L	$= (r_t + r_p)/(2\pi df)$

For example, if f_H = 4,434,320 and f_L = 4,434,120, then f_o = 4,434,220 and df = 200. If the tester resistance, r_t, is 100 ohms and the substitution pot measured 20 ohms, then:

$$Q = (f_o/df)(r_t + r_p/r_p) = 133{,}026.6$$

$$L = 120/400\pi = 0.3/\pi = .0955 \text{ Hy}$$

*Unfortunately, as we went to press, we found out that LADPAC has been discontinued. However, an improved filter design program has evolved from LADPAC and is available at a *reduced price*. For more information contact Hayward Electronic Systems, Inc., 7700 S.W. Danielle Street, Beaverton, Oregon 97005. Ed.

**This will provoke the same philosophical argument as using the phrase "antenna tuner." Of course you aren't really tuning the crystal, you are adjusting the circuit to accept the crystal you have. From the circuit's standpoint, however, the crystal plus C_t looks like a different crystal having the desired series-resonant frequency.

Crystal capacitors

A crystal is usually modeled as a series-tuned circuit in parallel with a holder capacitance, C_p. A more complete model has three capacitors: the capacitance between the two crystal leads, C_L, and two capacitances, C_C, from each lead to the case (see **Figure 1**). I measured capacitance between the case and the two crystal leads *tied together*. I assigned half to each lead-case capacitance, C_C. Next, I measured and reduced the lead-lead capacitance by $C_C/2$. I measured the average capacitance of a wide variety of crystals. You can use the results shown in **Table 1**.

Wide filters operate at higher impedances and have smaller coupling capacitors. C_C is in parallel with, and adds to the coupling capacitors, so you must subtract it from the physical capacitor you're soldering in. For example, if a theoretical filter design shows an 18-pF coupling capacitor between two HC-18 crystals, it should be reduced by 0.6 pF for each crystal (or 1.2 pF), to 16.8 pF. When only one crystal is connected to a capacitor (at the end of the filter) the calculated value should be reduced by only 0.6 pF. This correction isn't particularly important for narrow filters where coupling capacitors are hundreds of picofarads.

In most cases, the value used for C_L isn't terribly critical. If you don't measure these capacitances for your actual crystals, you may use the LADPAC defaults and subtract the capacitance shown in **Table 1** from the coupling capacitor values, as I just described.

Calculation of the average crystal

After you've tested all the crystals, look for groups of high Q crystals with similar values of inductance. Try to find a few more than you think you'll need. Once you get the hang of it, it's easy to add a few more poles to get better selectivity! After choosing your set, calculate the average Q and average inductance for LADPAC use.

Filters that don't ring: Gaussian and linear phase

Neither Chebychev nor Butterworth filters are ideal for digital modes because they delay each part of the signal by a different amount of time. This is the origin of what we call "ringing" in a CW filter. RTTY and AMTOR also need to have reasonably constant delay to preserve proper timing in these signals. If you think a garden-variety filter is "only" irritating on CW, you should listen to the difference with a linear-phase filter!

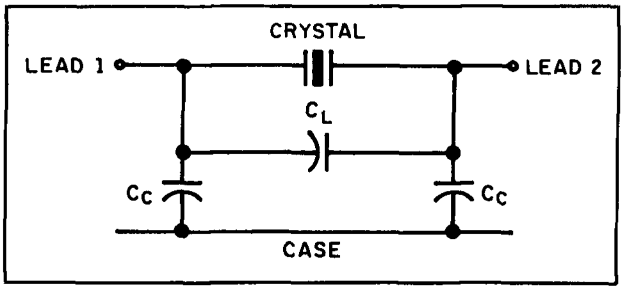

Figure 1. A more complete crystal model with three capacitors; the capacitance between the two crystal leads, C_L, and two capacitances, C_C, from each lead to the case.

HC-6	1.4 pF
HC-18	1.0 pF
glass HC-6	0.5 pF

Table 1. Measured average C_c for a variety of crystals.

Gaussian, Gaussian-to-6 dB, Gaussian-to-12 dB, and the equiripple phase families of filters approximate constant delay with slightly different compromises. They all give up some sharpness in frequency response to obtain the constant delay.

Choosing a lossless prototype filter

LADPAC has built-in tables for lossless Butterworth or Chebychev filters. Lossless 6, 8, and 10-pole, 0.5-degree equiripple phase and Gaussian-to-6 dB prototype low-pass filters are tabulated in **Table 2**, but must be entered manually. For SSB, the Chebychev shape is common, while for CW, RTTY, or AMTOR modes the equiripple phase approximation filters have the least ringing, and Gaussian-to-6 dB has better selectivity and little ringing.

While we don't really have lossless crystals (that is, crystals with infinite Q), we can often assume so. The approximate minimum crystal Q required in a lossless design depends on the kind of filter being built. Compute the average crystal Q for the batch. If filter Q is defined as center frequency/bandwidth, then the approximate values desired for crystal Q for 6 and 8-pole filters are as shown in **Table 3**.

For instance, an SSB filter with bandwidth of 2 kHz at 4 MHz has a filter Q of $4000/2 = 2000$. Crystal Q of about $2000 \times 90 = 180{,}000$ is fine for a 6-pole 0.1 Chebychev filter, while a crystal Q of 2000×230

n	C1	L2	C3	L4	C5	L6	C7	L8	C9	L10
6	0.3313	0.5984	0.8390	0.7964	1.2734	2.0111				
8	0.2718	0.4999	0.6800	0.6312	0.8498	0.7447	1.3174	1.9626		
10	0.2359	0.4369	0.5887	0.5428	0.7034	0.5827	0.8720	0.6869	1.4317	1.8431

Gaussian response to 6dB. Load resistance is always 1 ohm and source is 1 ohm for n = 6, but source resistance for n = 8 is 1.0502 ohms and source resistance for n = 10 is 1.1372 ohms.

n	C1	L2	C3	L4	C5	L6	C7	L8	C9	L10
6	0.5041	0.9032	1.2159	1.0433	1.4212	2.0917				
8	0.5031	0.9699	1.2319	1.1324	1.4262	1.0449	1.6000	1.9285		
10	0.4682	1.0839	1.1516	1.2991	1.3293	1.2748	1.4216	1.1730	1.5040	2.1225

L = henries
C = farads
All L and C are lossless (infinite Q).

Table 2. Linear phase with equiripple error: Phase error = 0.5 degree. (Information taken from Zverev.[4])

= 460,000 is required for an 8-pole 0.5 dB Chebychev filter.

"Linear phase" type filters will accept lower crystal Q as being nearly "lossless." A 400-Hz Gaussian-to-12 dB RTTY filter at 4 MHz will be happy with a crystal Q of 250,000 in a 6-pole filter.

These aren't hard-and-fast rules. Values down to half of these can be used without getting into too much trouble, but when you assume infinite Q and don't meet the multipliers indicated above, you should ask for a slight wider filter during design.

The 14-pole, 0.1 Chebychev filter described later uses crystals having filter Q × 72, about half of what could readily be considered "lossless." For that filter the −3 dB bandwidth came out fifteen percent narrower than the design, and the ripples of the ideal filer virtually disappear at the edges of the passband.

LADPAC can design these other types of crystal filters when the crystals meet (or nearly meet) these minimum Q values. **Table 2**, using information from **Reference 4** gives values for 6, 8, and 10-pole, *0.5-degree equiripple approximation to linear phase* and *Gaussian-to-6 dB* low-pass filters. There are additional low-pass tables in **Reference 4** for other filter shapes with 3 to 10 poles. LADPAC can convert these low-pass filters to bandpass crystal filters.

Filter type	8-pole	6-pole
0.5° error equiripple	filter Q × 25	filter Q × 20
Gaussian-to-6 dB	filter Q × 45	filter Q × 35
Butterworth	filter Q × 50	filter Q × 32
0.01 dB Chebychev	filter Q × 120	filter Q × 65
0.1 dB Chebychev	filter Q × 160	filter Q × 90
0.5 dB Chebychev	filter Q × 230	filter Q × 130

Table 3. Approximate values desired for crystal Q for 6 and 8-pole filters.

From table low-pass values to crystal bandpass filter

To use the tables, start LADPAC's **L** (low-pass filter) program by typing **L ENTER** at the DOS prompt, then **3. Generate k and q values**. Enter **6, 8,** or **10** for order of filter, −1 to insert g[k] values from the table, then enter those values from left to right. After the last entry has been made, press **S** to save the computed values, and exit the **L** program by typing **99**.

Next start the crystal filter program by typing **X ENTER** at the DOS prompt. Press **K** to load the values previously computed by **L. X** will already know how many "meshes" are in the filter, so press **ENTER** in response to this question. The program will then prompt for the crystal frequency and average inductance. Type in the average values of the chosen crystals. Press **ENTER** to accept the first overtone default, then enter the value of holder capacitance and the average crystal Q. When the program prompts for each k value, the value will automatically be from the table-generated filter, so you can press **ENTER** for each k value prompt.

You then get to choose source and load resistances and see how the filter values look. If the capacitances are impractically small (say below 15 pF), you can change the resistance and the program will recompute the capacitors. When you are satisfied with a design, you exit with **D**, another **D**, and **escape** to exit the **X** program.

From the DOS prompt type **G ENTER** to start the general-purpose analysis program and load the crystal filter design by pressing **D**, then **B**. Press **D** to find insertion loss and bandwidth, **P** to draw pictures of the filter response, or **E** to edit the component values. At this point you can change capacitor values to see how critical each will be.

After you go through this process a few times, you can evaluate alternative filter designs very quickly, then pick up the soldering iron knowing exactly what to expect. Rest assured there's a good chance that your design will work the first time.

Prototypes with losses

To use the lossless tables for a 100-Hz phase filter for Clover-I, **Table 3** says you'll need crystals having Qs on the order of at least one million at 4 MHz. Using crystals with a Q of 150,000 will *not* produce the desired filter! That doesn't mean that you can't make the filter with the crystals; it just means that you need to take the finite crystal Q into account. You can't use the lossless values of **Table 2**, or LADPAC's internal tables, which are also lossless. The solution is to use *predistorted* tables. Information included in **Table 4** is taken from such tables found on page 374 of Zvevrev.

Zverev's predistorted tables assume various amounts of loss in the crystals. These tables are tabulated for different values of q_o where:

q_o = crystal Q × filter bandwidth/filter center frequency

If you want a 6-pole, 100-Hz width Gaussian-to-12 dB filter with the 4434 kHz crystals previously calculated to have Q = 133,026, then:

$q_o = 133{,}000 \times 100/4{,}434{,}220 = 2.99$

For this example, the nearest table value on page 374 of Zverev (included in **Table 4**) has $q_o = 2.791$, which gives the insertion loss of 9.77 dB for the filter. This signal loss is the price you must pay for the finite crystal Q. The table lists **input Q, output Q**, and the **coupling coefficients** required to produce the desired filter with those crystals. Instead of using **L** to first compute k_{ij} values from low-pass filter components, those coupling coefficients are typed directly into the **X** program, then LADPAC will compute the coupling capacitors between each crystal.

A different set of tables is required for every type of filter and every number of poles, and every value of q_o. Pages 342 to 379 of Zverev (37 pages!) are necessary to list a reasonable range of possibilities from 3 to 8 poles. While it requires access to these tables, the job is no more difficult than designing a filter assuming lossless crystals. It's too bad the tables are too extensive to list here; but using Zverev in a library, you can design very narrow filters up to 8 poles with crystals that don't have enough Q for a lossless design.

For instance, a 15-meter receiver breadboard has eight DigiKey crystals in an 8-pole, 0.5-degree approximation filter with 120 cycle bandwidth. It matches the predicted response almost perfectly, has a wonderful "transparent" sound to it, doesn't ring at all, and can be operated for hours without fatigue. The insertion loss is 6 dB.

Selecting coupling capacitors

Coupling capacitors can be as low as 10 to 20 pF for SSB width filters, to several hundred pF for a narrow filter. To obtain the desired filter, you must use the specified capacitor value. While using LADPAC's **G** program to simulate the filter, it is possible to edit each capacitor value and see how critical it'll be in obtaining the desired filter.

Gaussian Response to 12-dB

q_0	I.L.	q_1	q_n	k_{12}	k_{23}	k_{34}	k_{45}	k_{56}
Inf.	0.000	0.5427	0.5585	1.8394	1.4416	0.6857	0.7069	1.4676
22.327	1.125	0.5869	0.5714	1.7858	1.4334	0.6786	0.7196	1.4318
11.164	2.255	0.6464	0.5788	1.7399	1.4180	0.6682	0.7420	1.3982
7.442	3.390	0.7394	0.5737	1.7156	1.3776	0.6567	0.7796	1.3693
5.582	4.557	0.7896	0.6061	1.6631	1.3933	0.6787	0.7705	1.3232
4.465	5.768	0.8476	0.6420	1.6048	1.4148	0.7044	0.7631	1.2801
3.721	7.031	0.9157	0.6821	1.5384	1.4436	0.7363	0.7581	1.2406
3.190	8.359	0.9969	0.7268	1.4496	1.4818	0.7804	0.7570	1.2050
2.791	9.770	1.0962	0.7766	1.3247	1.5302	0.8525	0.7639	1.1748
2.481	11.290	1.2257	0.8300	1.0924	1.5633	1.0233	0.8024	1.1578

Table 4. Values for 6-pole Gaussian-to-12 dB filters with different crystal Q. (Information taken from Zverev.[4])

A large junkbox full of NPO or dipped mica capacitors is useful. Putting two capacitors in parallel reduces the number of capacitors you need in the junkbox, and gives considerably more flexibility. For example, a 92-pF coupling capacitor might be built from two 47-pF capacitors in parallel. Ten 47-pF capacitors can be paired up in 45 different ways, making it more likely you'll find two that produce 92 pF, or very close to it.

If you have access to an accurate capacitance bridge, select capacitors until you find one, or a pair in parallel, very close to the calculated value. You can build a capacitor tester and calibrate it to measure small capacitors within 1 to 2 percent.[5] Such a tester can also measure the lead-holder and lead-lead capacitance of your crystals.

The tuning concept

Hayward stated that each crystal, when put in series with the coupling capacitors on each side of it, should resonate at the same *loop* frequency. LADPAC gives you a "head start" by computing the frequency offset of each crystal that will produce this result. If your coupling capacitors have the correct values and the relative series-resonant frequency of the crystals have the specified offsets from the "zero-frequency offset" crystal, no tuning is required and soldering these parts will produce exactly the filter you designed.

However, it's highly unlikely your crystals will have exactly the specified offset. Your capacitors will also display some deviation from the theoretical values. But you can compensate for minor deviations in components by tuning each loop of the crystal filter, using the actual parts.

Tuning cookbook

Choose the lowest frequency crystal of the group as the zero-frequency offset crystal. Connect this zero offset crystal *in series* with the two coupling capacitors that will be on either side of the crystal in the filter. Measure the series-resonant frequency of this crystal-capacitor-capacitor combination. This is the *loop frequency*; the other loops need to be tuned to this same frequency.

For each other crystal of the filter, add the LADPAC-specified frequency offset to the series-resonant frequency of your zero-offset crystal. If you find a crystal from your set with this frequency, you should be able to use that crystal without any further tuning, although it should be checked, as I'll describe, to be absolutely sure. Otherwise, choose a crystal from your set with a series-resonant frequency slightly *below* that of your zero-offset crystal.

Put that crystal *in series* with the coupling capacitors that will be on either side of it, and add a third tuning capacitor (C_t) *in series*. Put this series combination of crystal and three capacitors into the crystal tester and change C_t until it's resonant at the loop frequency. Smaller C_t moves the frequency up, larger C_t moves it down. If you don't need to move up very much C_t might be as large as several hundred picofarad. If the crystal has the specified offset, C_t becomes "infinite," just a piece of wire, so no C_t is needed for this crystal.

Divide your desired filter bandwidth by 25. This is the maximum tuning error you should allow from the loop frequency. Less is better. For example, if you're making a 300-cycle CW filter, get the resonance of each loop within 12 cycles of loop frequency.

Permanently pair up each crystal with its C_t. Don't mix them up; they form a matched set that *tunes* the crystal to the proper frequency *for its position in the filter.*

Each coupling capacitor is used twice: once while tuning the crystal on its left, and again when tuning the crystal on its right. This procedure works for all crystals except the ones at the end. On one side, they don't have just a capacitor, they also have a load resistance. If the end capacitor happens to be zero, tune the crystal to the loop frequency with just two capacitors in series— C_t and the coupling capacitor on the other side. Otherwise, calculate a temporary capacitor.

First calculate K:

$$K = (2\pi fr_{end} \times C_{end})^2$$

Then calculate the temporary capacitor:

$$C_{Temp} = C_{end}\,(1 + K/K)$$

Find C_t with the end crystal in series with this temporary capacitor. The temporary capacitor isn't used in the filter; it's just for tuning. You haven't tuned with the actual parts that will be used in the filter. However, resonance at the ends of the filter are broadened by the source and load resistances and aren't as critical as the internal loops, so this causes no problem.

After you've "tuned" all the crystals, you can build the filter. Breadboard the filter on a piece of copperclad pc board material and check for the desired passband

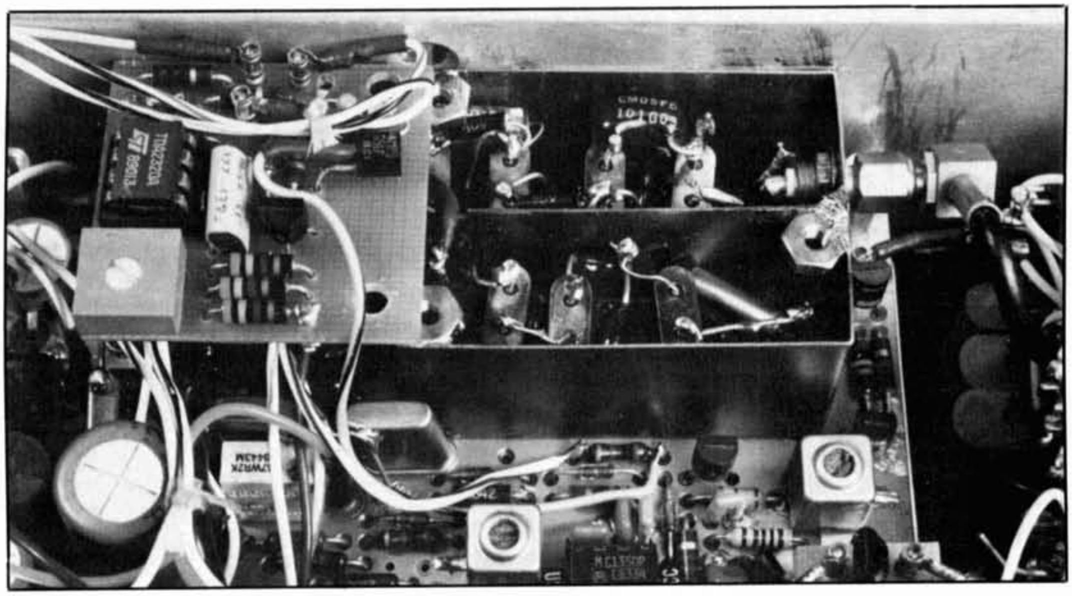

Photo A. Eight-pole, 0.5-degree equiripple phase filter. This filter is 350-Hz wide, CF = 4434 kHz.

shape. Use resistors initially to simulate the impedance level specified by the computer. After you've verified the filter shape, connect L-networks or transformers to match your circuit impedance. Check the shape again after connecting a matching network. Be very methodical, find any mistakes before you build the final filter, and you'll be rewarded with filters that match the computer prediction.

Crystal sources

In three different orders from DigiKey, a total of almost 200 crystals with 3.579, 4.000, and 4.434-MHz frequencies, their *ECS* brand seemed to have the highest average Q and most consistent L for a little over $1 each.

I purchased about 300 4.000-MHz crystals at a swapmeet. Their Q was low; for filter purposes, half were junk and the remainder mediocre. However, their total cost was only $12.

I bought a group of interesting HC-6 style 3.006-MHz crystals in sealed glass cases from a swap table at an ARRL convention. They were excellent crystals with Q over 500,000.

Construction hints

- Ground the crystal case wires.
- It's critical to isolate input and output ends of the filter. Put dividers between input and output leads of *each* crystal. There should not be a line-of-sight path from the shield of one crystal past the shield of the next crystal. The grounded crystal cases can be used as part of the internal shielding.
- Matching network inductors or transformers need to be well shielded or there can be inductive coupling around the filter. You can solder the case of the Amidon slug-tuned coil forms, or adjustable Toko coils, directly to the filter ground. Toroids can be placed inside soldered shield enclosures.
- I've used shields made from pc board material, tinned 0.02-inch sheet steel, and brass strips. All permit you to solder the shields in place, which makes it easy to build and modify. Brass strip can be obtained from almost any model shop. Its precision width makes construction of a rectangular box much easier.

Examples of breadboard and finished filters

Photo A shows the 8-pole, 0.5-degree equiripple phase filter used in my 40-meter mobile rig. The box was built on a base of perforated copperclad Vectorboard, copper side out. Sides are 3/4-inch brass strips, soldered to 5/8-inch high, 1/4-inch diameter nickel-plated brass spacers at the corners, overhanging and soldered to the copperclad all around. Shields are soldered to the brass sides, and connected to the Vectorboard bottom with several heavy tinned wires. Crystal cases are soldered to the bottom with short wires, too.

Notice that the input comes through a miniature SMB coaxial connector on the side wall, and output goes through a hole in the bottom of the filter/IF amplifier board to an L network and MOSFET first IF

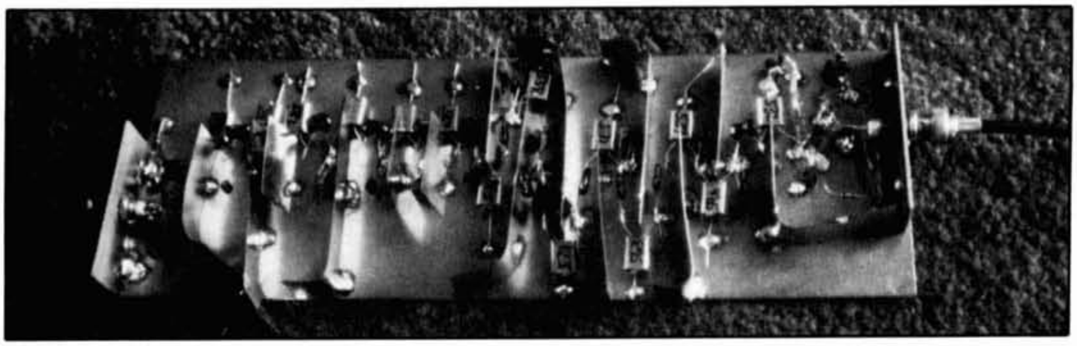

Photo B. Fourteen-pole, 0.1 dB Chebychev breadboard filter, 1.95 kHz at −6 dB, CF = 4344 kHz.

amplifier. Without the top cover in place the input-output isolation is about 70 dB. With it the opposite sideband is down over 120 dB.

Quarter-inch round spacers made of aluminum, brass, or steel are available. I recommend that you avoid aluminum spacers because it's impractical to solder to them. Brass or steel both take solder, and brass won't rust. The 120-degree angle of hex spacers doesn't permit neat 90-degree corners. I clamped the Vectorboard and the aluminum top cover together, then drilled holes through both for the spacers, assuring perfect alignment of the bottom and cover.

Photo B is a 14-pole, 0.1 dB Chebychev SSB-width filter, shown in a breadboard layout to give you a feel for the kind of layout and shielding that are appropriate for filters with this kind of performance. The passband of this filter is very flat, with just a slight 0.5 dB dip at the upper corner. SSB sounds very good through this filter. It is 4 kHz wide at −120 dB, with a 6:120 dB shape factor of just slightly over 2. Without shields, the breadboard had about 70-dB isolation between input and output. Adding a few shields quickly raised attenuation to 100 dB, but kept improving to more than 120 dB with the full complement of shields. To get the full ultimate attenuation from 8-pole filters, consider nothing less than complete shielding.

Acknowledgement

Thanks to Wes Hayward, W7ZOI, for his patient mentoring.

REFERENCES

1. Wes Hayward, W7ZOI, "A Unified Approach to the Design of Crystal Ladder Filters," *QST*, May 1982, page 21.
2. Wes Hayward, W7ZOI, "Designing and Building Simple Crystal Filters," *QST*, July 1987, page 24.
3. Doug DeMaw, W1FB, "A Tester for Crystal F, Q, and R," *QST*, January 1990, page 21.
4. A.I. Zverev, *Handbook of Filter Synthesis*, John Wiley and Sons, New York, 1967.
5. Bill Carver, K6OLG, "An LC Tester," *Communications Quarterly, Winter 1993, page 19.*

PRODUCT INFORMATION

The Major BBS® Version 6

Galacticomm, Inc. has released Version 6 of The Major BBS—a product designed to provide a full-featured, easy-to-use bulletin board system (BBS) for both corporate and private use.

Dynamic Link Libraries (DLLS) automatically "link-in" services to the BBS. The system operator (Sysop) simply types "A:INSTALL" to include a service, such as a database module or text retrieval utility. The Sysop adds the service to a menu, answers a few configuration questions, and the new feature is available to users the next time the BBS is started.

The Major BBS now has the capability to exchange E-mail and Forum messages with MHS applications and gateways. Users can exchange messages with applications like DaVinci E-Mail and other mail networks such as cc:Mail, MCI Mail, CompuServe, X.400 networks, and Internet.

The system runs on an IBM-compatible 286, 386, or 486. It requires a minimum of 2 megabytes of extended memory, MS-DOS or PC-DOS version 3.3 or higher, and a hard disk. Hayes-compatible COM1/2/3/4 modems are supported from 300 to 38,400 bps (hardware performance permitting). For LAN users, a Novell network running NetWare® 2.1 or higher or NetWare Lite 1.0 or higher allows users to log on the BBS through the network. MHS message networking requires MHS version 1.5 or higher.

For additional information about The Major BBS contact Galacticomm, Inc., 4101 SW 47th Avenue, Suite 101, Fort Lauderdale, Florida 33314. BBS: (305) 583-7808. FAX: (305) 583-7846. Voice: (305) 583-5990.

Bill Carver, *K6OLG*
1952 Royal Oak Road
Tustin, California 92680

THE LC TESTER

Measure capacitors, inductors, and coils with this handy piece of test equipment

Sometimes the exact value of small capacitors and inductors used in an RF circuit isn't too important because the circuit can be brought to resonance with the slug in a coil or a trimmer capacitor. However, multipole lowpass and bandpass filters, high-performance crystal filters, or phase shift networks are circuits that can require close tolerance components and there's no slug or trimmer which will compensate for error in a value. My LC Tester (front and back views shown in **Photos A** and **B**) measures capacitors to 2000 pF and inductors to 50 microhenries with 1-percent accuracy.

Theory

The tester measures components by the frequency change they produce in an oscillator. This concept isn't new; the Tektronix model 130 "LC Meter," a '60s instrument, displayed oscillator shift at 140 kHz on an analog meter whose scale was calibrated directly in inductance and capacitance values.

The schematic of **Figure 1** is a JFET Hartley oscillator operating at about 1 MHz, buffered by two transistors to drive an external frequency counter. In use, frequency is measured twice—first without any part connected, then with the unknown inductor or capacitor. The value of the unknown part can then be calculated. The formulas, with examples worked out, appear in the sections headed **Calibration** and **Example**. A simple computer program makes the tedious computations relatively easy.

Calibration of both inductance and capacitance requires one known capacitor; the accuracy will be directly proportional to the

Photo A. Front view of LC tester.

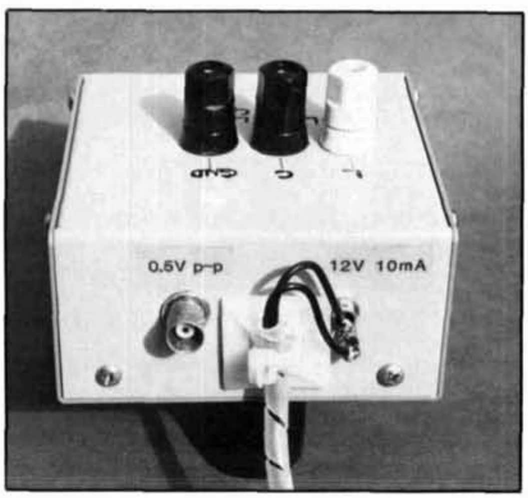

Photo B. Rear view of LC tester.

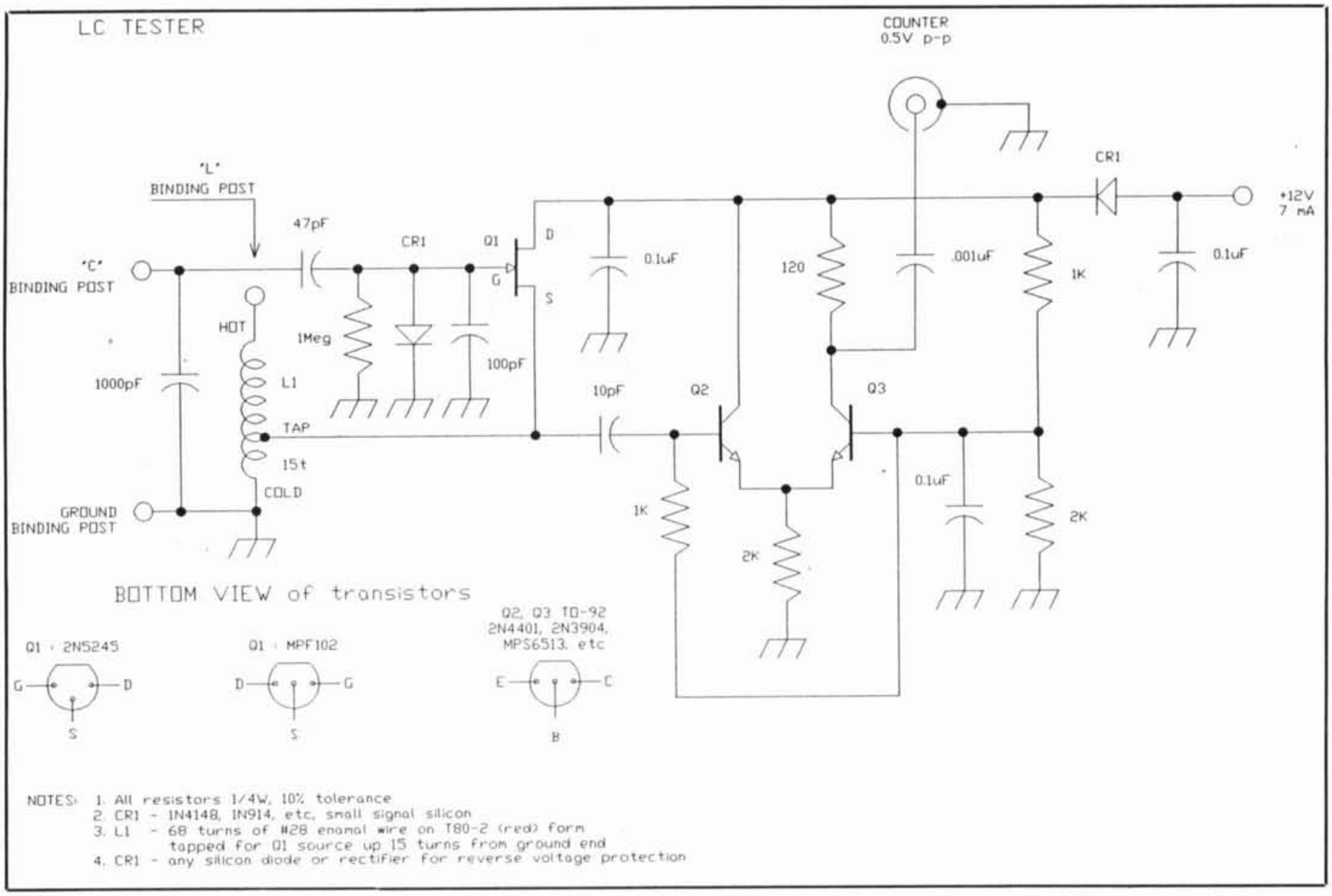

Figure 1. JFET Hartley oscillator operates at approximately 1 MHz and is buffered by two transistors to drive an external frequency counter.

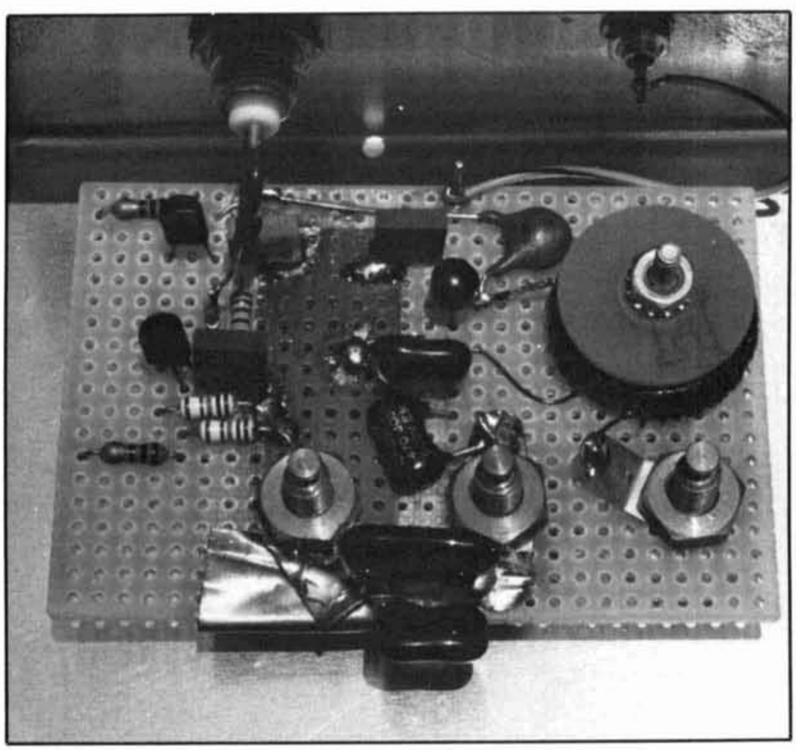

Photo C. The nominal 25-μH tank coil is wound on a T-80-2 (red) powdered iron toriodal from and clamped to the perfboard with a screw and fiber glass washer.

accuracy of that capacitor. I've found one mail order source* of dipped mica capacitors that can provide 1 percent + 0.1 pF accuracy. Swapmeets and surplus stores occasionally yield 1 percent, or even 1/2 percent, dipped mica capacitors. If you have even one-time access to a bridge to accurately measure your calibration capacitor, you'll find that it's easy to maintain 0.25 percent + 0.1 pF accuracy.

Construction

I built the tester in a 4 by 4 by 2-inch aluminum box (LMB CR-442) as if it were a

*All Electronics, P.O. Box 567, Van Nuys, California 91408 (800)826-5432, has a limited supply of the following dipped mica capacitors that can be used for calibrating the tester: DMCP-3106, 20.6 pF; DMCP-3803, 38.3 pF (only a few left); DMCP-4909, 49.9 pF; DMCP-7906, 79.6 pF (only a few left); DMCP-291, 291 pF.

Although they do not have an advertised tolerance, ten DMCP-291 tested in my Boonton bridge (1/4 percent original accuracy) averaged 292.7 pF—less than 0.6 percent higher than the value stamped on them. Three DMCP-291s in parallel would make a good calibration value of 873 pF. While in theory you only need one capacitor for calibration, with several you can see how consistent the tester is and be more confident about its accuracy.

While not precision values, All Electronics also has many 5 percent dipped mica capacitors. The following will work fine as the tank circuit capacitors: DMCP-47, 47 pF; DMCP-100P, 100 pF with pc board leads; DMCP-1K, 1000 pF.

transmitter VFO. A rigid box minimizes frequency changes from the mechanical stress of connecting the component being tested, so as a precaution I strengthened it with two pieces of aluminum angle stock. The oscillator is completely enclosed in order to prevent air drafts from causing short-term frequency changes.

The oscillator used a 2N5245 JFET. A somewhat wider range of gain is possible in a MPF102, but in most cases a MPF102 will work fine. In the unlikely event that a correctly wired oscillator doesn't have enough gain to start, or stops when a 2000-pF test capacitor is connected, measure the power supply current of the non-oscillating oscillator circuit alone (disconnect the buffer from the power supply). If JFET current is less than 3 mA, try another FET or select one with higher zero-bias drain current, I_{dss}.

I wound the nominal 25-μH tank coil on a T80-2 (red) powdered iron toroidal form** and clamped it to the perfboard with a screw and fiber glass washer (see **Photo C**). Exact capacitor values aren't necessary. I used dipped mica tank capacitors, but NPO ce-

**For best stability, I suggest using a slug-tuned ceramic form instead of a toroid core. Wind the coil so a minimal amount of correction (slug insertion into coil) is needed to achieve the desired inductance. Ed.

The author replies: "In this instrument long term stability isn't important, that comes out using the calculations. What's crucial is the SHORT term stability, especially when measuring very small component values. It's particularly crucial to ensure that the oscillator frequency won't change while connecting the part under test . . . while manipulating the binding posts, etc. I ended up using a toroidal coil, tightly clamped to the perfboard with a screw and nonmetallic washer, essentially for mechanical stability."

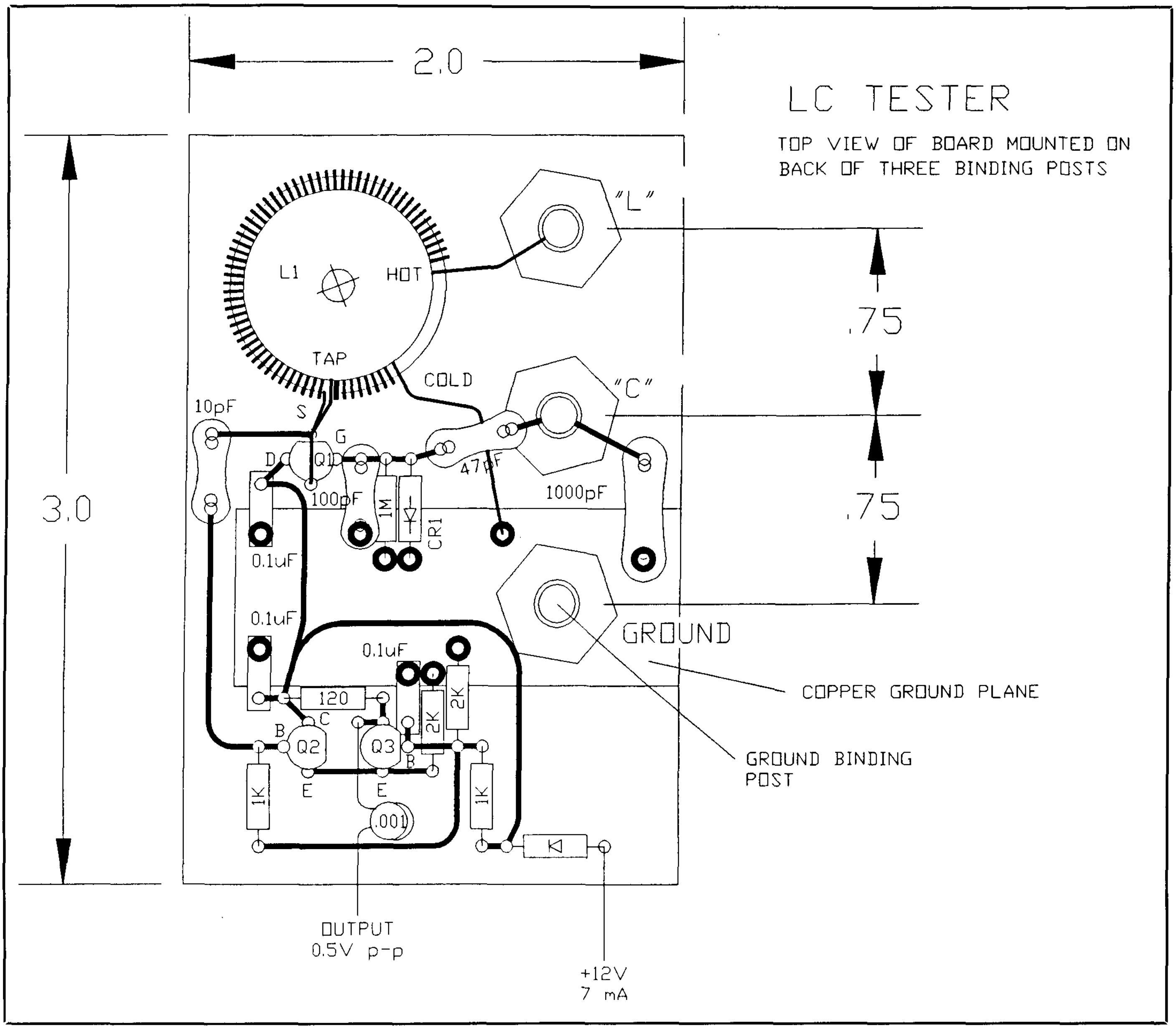

Figure 2. The oscillator and buffer layout on a 2 by 3 inch piece of perforated copperclad board.

ramic or polystyrene will also work. The 1000-pF capacitor can be several capacitors in parallel that add up to about 1000 pF. They should be mounted directly on the binding posts with minimum lead length. Leads of the 47 and 100 pF capacitors should also be short.

Figure 2 shows the oscillator and buffer layout on a 2 by 3-inch piece of perforated copperclad board. Almost all of the copper was pulled off after scoring lines with an X-ACTO® knife, leaving a small patch for grounding. The board is supported on the back of three binding posts having 3/4-inch spacing. Other kinds of connections could serve just as well, but pay attention to their mechanical rigidity and keep the capacitor and ground leads short.

Twelve volts at about 7 mA is required; the frequency changes less than 2 cycles from 9 to 14 volts. The counter output signal is 0.5 volts p-p, well isolated by a two-transistor buffer.

Calibration

Install a shorting wire* between the L and C terminals. Verify that the oscillator is operating at about 1 MHz. Record the oscillator frequency; this is f_1. Now connect a known test capacitor, preferably around 1000 pF, between the C and GND terminals. This calibration capacitor should have leads no longer than 3/4 inch and stand vertically in the binding posts to minimize stray capacitance to ground. Record the new frequency, f_2. Calculate the effective capacitance of the oscillator tank, C_O as:

$$C_O = C_{cal} \frac{f_2^2}{F_1^2 - f_2^2} \qquad (1)$$

$$L_O = \frac{1}{4\pi^2 f_1^2 C_O} \qquad (2)$$

For example, if $f_1 = 1005.984$ kHz, and connecting a 1000 pF, 1 percent capacitor for C_{cal} produces $f_2 = 714.358$ kHz, then the tank capacitance $C_O = 1017.16$ pF and the tank inductance $L_O = 24.607\ \mu$H. These values of L_O and C_O should be stable. Check them each time you begin a group of measurements and record the values in a notebook. When you're confident that your values are stable, you won't need to perform calibrations as often.

The L_O and C_O values are used in measurement calculations that follow.

*The jumper should be a straight tinned wire, like a resistor lead. This has an inductance of about 0.006 μH, which should be subtracted from all inductance measurements.

Originally, I used a carved piece of double-sided copperclad pc board material for the short between the L and C terminals because the self-inductance of a wide, thin strap is lower. However, the wide strap also had a capacitance of about 1/4 pF to the case. Removing that strap to measure a small inductor changed the oscillator capacitance by this 1/4 pF, so instead of improving the accuracy on small inductances, the wide strap resulted in an error of about 40 nH.

Example: measuring an unknown capacitor

After you've calculated the value for C_O, connect an unknown capacitor, C, as shown in **Figure 3**, and record the new lower frequency f_2. Calculate the capacitor value as:

$$C = C_O \frac{f_1^2 - f_2^2}{f_2^2} \qquad (3)$$

For example, if the connection of a capacitor marked 220 pF causes the frequency to drop from 1010 kHz to 910 kHz, it's value is:

$$1017.16 \times \left(\frac{1010^2 - 910^2}{910^2}\right) = 235.84\text{pF}$$

Because a 1-percent calibration capacitor was used, this will be within 1 percent + 0.1 pF, or 2.4 pF; the capacitor is between 233.4 and 238.3 pF.

If you need a specific capacitor value, the frequency it should produce in the LC Tester is:

$$f_2 = f_1 \sqrt{\frac{C_O}{C_O + C}} \qquad (4)$$

If you need a 103-pF capacitor, and intend to try various 100-pF capacitors from your junkbox looking for this value, here's how to proceed. From the previous calculation you know that C_O is 1016.16 pF and f_1 is 1010 kHz, so the frequency you'll be looking for is:

$$f_2 = 1{,}010{,}000 \times \sqrt{\frac{1017.16}{1017.16 + 103}} = 962{,}445\text{Hz}$$

As an alternative to trying every 100-pF capacitor in your junkbox, invest in five 75-pF and five 27-pF capacitors, costing about $2. They will provide 25 combinations with nominal capacitance of 102 pF. Almost certainly, one of those combinations will be your desired 103 pF value, leaving eight capacitors for your junkbox.

Example: measuring a small inductor in series

After calibrating and calculating L_O, record the f_1 frequency with a piece of no. 22 wire shorting the L and C terminals. Then remove the wire and connect the unknown coil in its place (**Figure 4**); the measured frequency drops to f_2. The value of the coil is:

$$L = L_O \frac{f_1^2 - f_2^2}{f_2^2} \qquad (5)$$

For best accuracy with coils less than a few microhenries, subtract 0.006 μH to compensate for the inductance of the shorting wire (see previous footnote for more information).

Alternatively, if you want a coil to have a specific inductance L, the frequency that coil should produce is:

$$f_2 = f_1 \sqrt{\frac{L_O}{L_O + L}} \qquad (6)$$

Suppose you need a 1.97 microhenry inductor for a QRP lowpass filter. *The Amidon Handbook** says 20 turns on a T-50-6 (yellow) core will give 2 microhenries, so wind 20 turns of no. 28 wire on a swapmeet yellow core.

Using the same calibration value of f_1 = 1005.984 kHz with the shorting wire, your toroid produces f_2 = 949.4 kHz. **Equation 5** tells you the inductance is 3.02 microhenries! **Equation 6** tells you 1.97 microhenries should produce a f_2 of 963.982 kHz. It would be more accurate to use 1.97 + 0.006, or 1.976 μH, for L in **Equation 6** to account for the inductance of the shorting wire.

To get up to 963 kHz you removed three turns, and spread the remaining seventeen more evenly over the core. You later realize the swapmeet core is 1/4-inch thick, while the Amidon core is 0.19-inch thick. The filter works fine because you compensated for the different core and have the correct inductance.

Example: measuring a larger inductor in parallel

With the shorting wire between the L and C terminals in place, record f_1. Then connect the coil being measured between the C and GND binding posts. The frequency will increase to f_2. The calculation for the unknown inductance is:

$$L = L_O \frac{f_1^2}{f_2^2 - f_1^2} \qquad (7)$$

*Amidon Associates, 2216 East Gladwick Street, Dominguez Hills, California 90220. (310)763-5770. Ask for free "Tech-Data" flyer, which shows inductance and Q produced by winding wire on a wide variety of their cores.

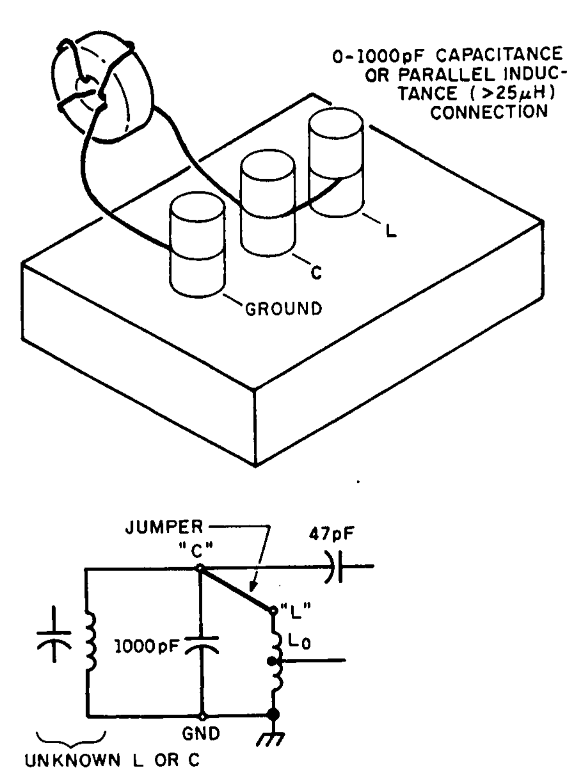

Figure 3. Connection for coils greater than 25 μH (L_p, "parallel" connection) and capacitors.

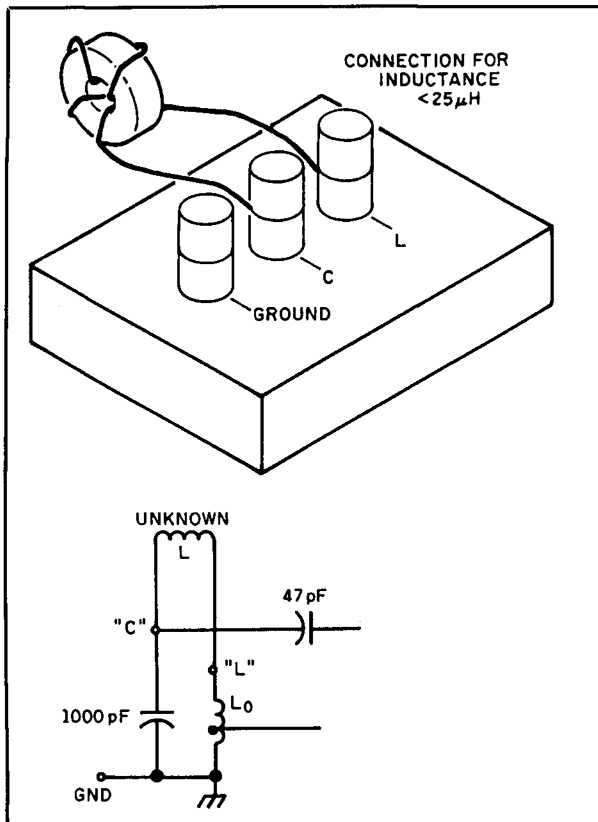

Figure 4. Connections for coils less than 25 μH (L_s, "series" connection). Ground post is not used, unknown L replaces jumper between L and C posts.

```
program LC_TESTER;
uses crt;
var
  L, Lo, Lx, C, Co, Ct, f2, f1 : real; todo : char;

procedure CAL;
begin
  writeln('CALIBRATE');
{enter calibration entries}
  write('ENTER the freq without CAL capacitor  (Hz) : '); readln(f1);
  write('ENTER the freq with the CAL capacitor (Hz) : '); readln(f2);
  write('ENTER VALUE of the CAL capacitor      (pF) : '); readln(Ct);
{convert to picofards, calculate and print L and C of oscillator tank}
  Ct := Ct*1e-12; Co := Ct/(sqr(f1/f2)-1); Lo := 1/(Co*sqr(2*pi*f1));
  writeln('the tank capacitance is ',Co*1E12:4:2,' pF');
  writeln('the tank inductance  is ',Lo*1E6:4:3,' uH'); writeln; writeln;
end;

procedure CAP;
{calculate unknown CAP from frequency measurements}
begin
  f2 := f1; while f2 >= f1 do
  begin
    {enter measured frequencies}
    write('ENTER the frequency without any  capacitor (Hz) : '); readln(f1);
    write('ENTER the frequency with UNKNOWN capacitor (Hz) : '); readln(f2);
    if f2 >= f1 then writeln('second freq must be lower!');
  end;
  C := Co*(sqr(f1/f2)-1); writeln('UNKNOWN capacitor = ',C*1E12:4:2,' pF');
end;

procedure CFREQ;
{calculate the frequency that would be produced by a certain capacitance}
begin
  write('ENTER the free running frequency (Hz) : '); readln(f1);
  write('ENTER the capacitor value        (pF) : '); readln(C); C:= C*1E-12;
  f2 := f1*sqrt(Co/(Co+C));
  writeln('the frequency from ',C*1E12:4:2,' pF is ',f2*1E-3:4:3,' KHz');
 end;

procedure INDUCT;
{calculate the inductance from frequency measurements}
begin
  write('ENTER the frequency WITH JUMPER       (Hz) : '); readln(f1);
  write('ENTER the frequency with the inductor (Hz) : '); readln(f2);
  if f2>f1 then L := Lo*sqr(f1)/(sqr(f2)-sqr(f1)) else L := Lo*(sqr(f1/f2)-1);
  writeln('UNKNOWN inductor = ',L*1E6:4:3,' uH');
end;

procedure LSFREQ;
{calculate the frequency that would be produced by an inductance in series}
begin
  write('LSFREQ: ENTER the free running freq (Hz) : '); readln(f1);
  write('ENTER the inductor value (uH) : '); readln(L); L := L*1E-6;

  f2 := f1*sqrt(Lo/(Lo+L));
  writeln('the frequency from ',L*1E6:4:3,' uH = ',f2*1E-3:4:3,' KHz');
end;
```

The frequency a desired parallel inductor, L, will produce is:

$$f_2 = f_1 \sqrt{\frac{L + L_0}{L}} \qquad (8)$$

Software: mechanizing the calculations

The calculations are error-prone and terminally tedious to do by hand, but a programmable calculator or personal computer on the bench makes the process practical.

Listing 1 is a Turbo Pascal listing of a simple program for calibrating, then calculating component values from frequency measurements.**

**Microcomputers and older software can have small maximum number sizes and accuracy limitations. Four "sanity checks" for the calculations are suggested:

1) "Calibrate" by entering f_1 = 1,000,000, f_2 = 707,071, and C = 1000 pF. The program should respond with C_0 = 1000 pF, L_0 = 25.33 μH or something very, very close to these values.

2) Compute a "C" with f_1 = 1,000,000 and f_2 = 900,000. The response should be C = 234.6 pF.

3) Compute "L_s" using f_1 = 1,000,000, f_2 = 900,000. The response should be L_s = 5.942 μH.

4) Compute "L_p" using f_1 = 1,000,000, f_2 = 130,000. The response should be L_p = 36.71 μH

```
procedure LPFREQ;
{calculate the frequency that would be produced by an inductance in parallel}
begin
  write('LPFREQ: ENTER the free running freq (Hz) : '); readln(f1);
  write('ENTER the inductor value (uH)            : '); readln(L); L := L*1E-6;
  f2 := f1*sqrt(1+Lo/L);
  writeln('the frequency from ',L*1E6:4:3,' uH = ',f2*1E-3:4:3,' KHz');
end;

procedure get_cmd;
begin
  {get single character from keyboard and convert to upper case}
  readln(todo); todo := upcase(todo);
end;

begin
  clrscr; writeln('{ 1.0 - 11/02/92 - K6OLG }'); writeln;
{Here's the program that gets keyboard entries, and calls the various
 calculating and value-printing procedures shown above}
  CAL;
  repeat
    writeln; writeln;
    writeln('PRESS U  to find the value of an unknown ');
    writeln('PRESS F  to find the Frequency produced by a desired componant');
    writeln('PRESS Q  to QUIT');
    get_cmd;
    case todo of
      'U' : begin
              clrscr;
              writeln('PRESS C  to find the value of an unknown Capacitor');
              writeln('PRESS L  to find the value of an unknown Inductor');
              get_cmd;
              case todo of
                'C' : CAP;
                                                   'L' : INDUCT;
                end;
              end;
      'F' : begin
              clrscr;
              writeln('PRESS C to find the Frequency produced by a desired capac
              writeln('PRESS L to find the Frequency produced by a desired induc
              get_cmd;
              case todo of
                'C' : CFREQ;
                                                   'L' : begin
                         writeln('S for the Frequency produced with a SERIES indu
                         writeln('P for the Frequency produced with a PARALLEL in
                          get_cmd;
                          case todo of
                            'S' : LSFREQ;
                            'P' : LPFREQ; end;
                        end;
              end;
            end;
      end;
    writeln;
  until todo = 'Q';
end.
```

Accuracy

With a few precautions, the accuracy of the instrument is determined by one calibration capacitor. *Note that accuracy will be undermined if the oscillator frequency changes while you connect the part to be measured.* The beefed-up sheet metal box is very sturdy, a small die cast box would be ideal. Avoid any temptation to put this in a plastic box; durability is important!

Oscillator stability isn't difficult to achieve at 1 MHz, and drift error can easily be made negligible. My oscillator drifts less than 10 Hz in ten minutes, which will cause only 0.02 pF error in the value of a 10-pF capacitor. Still, don't allow too much time to elapse between measurement of f_1 and f_2, or accuracy may suffer.

I checked a number of parts on a surplus Boonton 63H inductance bridge, 75B capacitance bridge, and my LC Tester calibrated with a 0.001-μF 1/2-percent silvered mica capacitor:

Small coils. A molded inductor with "0.15" color code measured 0.1412 μH on the Boonton bridge. The calculated induc-

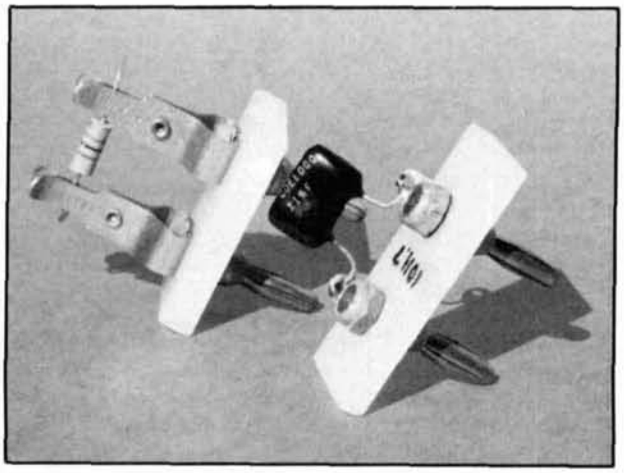

Photo D. A spring clip attachment holds the capacitor to be measured in place.

tance was 0.1422 μH—0.7 percent higher than the bridge.

Larger coils. A molded inductor with "18" color code measured 17.754 μH on the bridge. The calculated inductance was 17.603 μH—0.9 percent lower than the bridge.

Even larger coils: The parallel coil connection. I measured molded chokes up to 100 microhenries with a few percent deviation from the bridge reading, but be aware that larger inductors frequently have large distributed capacitances. The instrument can't tell how much a frequency change is due to inductance, and how much is due to stray capacitance! Distributed capacitance will make the calculated inductance higher than it really is, so be cautious before staking your life on readings in the parallel connection.

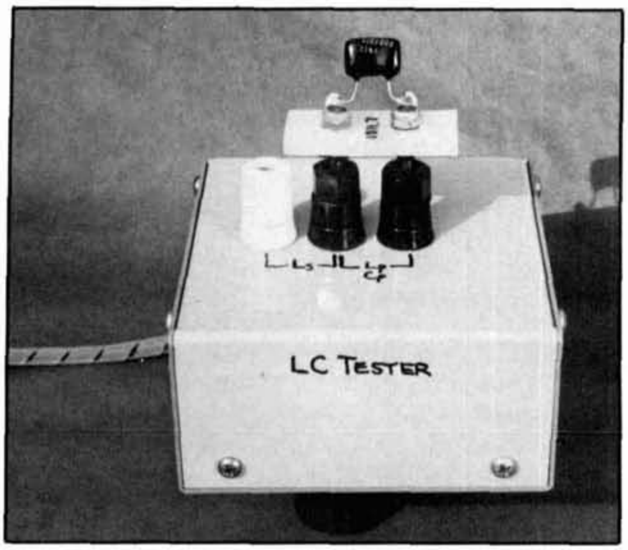

Photo E. Measuring the capacitor when directly attached to the LC tester's binding posts yielded a slight change in frequency.

A 1.5-inch diameter, 4.9-inch long piece of Miniductor measured 25.375 μH on a Boonton inductance bridge. When connected in *series* with the coil of the tester between C and L, the calculated inductance was 25.364 μH—0.02 percent lower than the bridge. When connected in *parallel* with the coil of the tester, between C and GND terminals, it measured 25.518 μH, or 0.56 percent higher. The difference could be attributed to 2.8 pF of distributed capacitance, but I couldn't verify that with any of my test equipment. The accuracy was very good, but it points up one important fact: while this tester is quite accurate for the medium to high Q, low distributed capacitance coils that we normally use, it's not an all-purpose substitute for a laboratory bridge that can measure the secondary parameters of a wide variety of components.

Capacitors. A silvered mica capacitor marked 110 pF, 1 percent measured 109.3 pF on the Boonton bridge. Using the spring clip attachment shown in **Photo D** to hold the capacitor, the tester gave a value of 109.51 pF—0.2 percent higher than the bridge. Although the frequencies changed when the capacitor was directly on the LC Tester's binding posts (see **Photo E**), the second calculated value was 109.59 pF. The small additional capacitance of the spring clips shown didn't compromise accuracy.

Small capacitors. A disk ceramic capacitor marked "2.7 NPO" had a calculated value of 2.38 pF, while the surplus capacitance bridge measured it as 2.432 pF—a difference of 0.05 pF—only 2 percent high for this very small capacitor.

I tested the capacitor by attaching the leads directly to the binding posts. If an exact value or matching a pair is very critical, put the capacitor in the same position relative to the surrounding grounded surfaces at the location where it will be used.

Large capacitors. The 2000-pF limit is arbitrary and conservative. Measurement accuracy is still the same as the calibration capacitor accuracy. At 1 MHz for capacitors above a few hundred pF, the series inductance of wire leads changes the apparent capacitance. Keep leads short when testing *and when using* larger values in circuits operating above 1 MHz requiring close tolerance. Full-length leads on a 1000-pF DM15 mica capacitor change the apparent capacitance by about 1 pF.

A silvered mica capacitor marked 1300 pF, 1 percent measured 1302.9 pF on the bridge. Frequencies from the tester gave a calculated value of 1301.45 pF—0.11 percent lower than the bridge.

A 2096 pF, 1 percent mica capacitor couldn't easily be measured on the bridge. The LC Tester gave a value of 2106.38 pF with 0.5-inch leads, 0.5 percent higher than its nominal value.

When the capacitor gets too large the oscillator simply stops. This oscillator operated at 5000 pF, but a 0.01 μF mica capacitor caused it to stop.

Semiconductor capacitances

The tank circuit can put up to 25 volts p-p on the capacitor being tested. This is too much for semiconductors, making this tester useful only for fixed capacitors.

Next: A self-contained instrument?

If you have a PC or calculator and frequency counter, the LC Tester will provide accurate inductor and capacitor measurement at very little expense. If used frequently, it's possible that the convenience of putting the LC meter circuits, counter, and calculator in one package might be justified. If C_0 is precisely adjusted to some known value, say 1000 pF, the premeasurement calibration step, with its need for a keyboard entry, could be eliminated. I'm currently building a self-contained instrument with built-in microcomputer and LCD display to test its practicality and see how stable the calibration will be with temperature changes and the passage of time.

Acknowledgements

Thanks to Mike Berman, ex-K6RIW, for his photographic expertise.

PRODUCT INFORMATION

Relays and Accessories Guide on Floppy Disk

Philips ECG has released its newly-expanded Relays and Accessories Cross Reference guide on floppy disk for IBM PCs and compatibles.

This program, that contains the same reference data base as the new sixth edition catalog, allows users to access the entire replacement relays data base of over 39,500 industry numbers on their personal computers, crossed to over 530 ECG relays and accessories. CompuCross displays the full ECG relay type description, including relay style, input voltage, contact arrangement and current rating; and a reference to any special note that applies. With an access time less than a second, it also displays a list of manufacturers of the relay type to be replaced.

Requirements for using CompuCross include 512k of RAM, a hard drive and 3-1/2 or 5-1/4" floppy disk drive.

The ECG product line comprising this data base includes replacements for electromechanical relays, definite purpose magnetic contactors, reed, solid state, DIP and time delay, as well as an array of cube timers and standard and slim line I/O modules.

For more information contact Philips ECG, 1025 Westminster Drive, Williamsport, PA 17701, (800) 526-9354.

Jensen's 1993 Master Catalog Available

Jensen Tools has a new 284-page master catalog that includes OSHA-required insulated tool sets (VDE certified), magnetic screwdrivers, and other hard-to-find tools for electrical and electronic installation and repair. For a free copy of the catalog write Jensen Tools Inc., 7815 S. 46th Street, Phoenix, Arizona 85044, or call (602) 968-6231 or FAX (800) 366-9662.

Application note on Microsoft® Windows DDE protocols available

A new application note, "Utilizing DDE for Test and Measurement Applications," is available from Hewlett-Packard Company. The note (Literature 5091-2950E, Application Note 1219-1) explains the Dynamic Data Exchange (DDE) protocol feature of Microsoft Windows 3.0, and provides the information you need to use it in test-and-measurement applications.

To obtain a free copy of this application note, contact Hewlett-Packard Company Inquiries, 19310 Pruneridge Avenue, Cupertino, California, 95014.

Bob Brown, *NM7M*
504 Channel View Drive
Anacortes, Washington 98221
Condensed for publication by:
Ward Silver, *N0AX*
P.O. Box 927
Vashon, Washington 98070

LONG-PATH PROPAGATION

Data from two ionospheric seasons, factors affecting LP, and a quantitative summary.

This is the conclusion of a two-part article reviewing the results of a year-long study of long-path propagation performed by Bob Brown, NM7M. Part 1 covered the basics of long-path, gave details about how the study was performed, and presented some practical guidelines for long-path DXing. Part 2 concludes the review with a look at the data, discussion of factors affecting long-path, and a quantitative summary of the results. de N0AX.

Data from the two ionospheric seasons

In examining the effects of geomagnetic disturbances on LP propagation, I would first like to summarize the results for the various paths and seasons. During the spring/summer season, I made a total of 669 LP contacts: 309 on auroral zone paths (including 64 to Crozet Island), 137 on polar paths, and 223 on extreme long paths. **Table 1** gives a breakdown of these contacts. For a given type of path, there was the possibility of one or more contacts during an LP session—depending on propagation and the usual competition for DX contacts. Consequently, some days went by without a single contact on a given type of path while, as was more often the case, other days yielded at least one and maybe more contacts.

Spring/Summer Path	Contacts/session 0	1	>1
Auroral Zone	35	47	86
Polar	96	37	35
Extreme Polar	77	36	55

Table 1. LP contacts for the spring/summer season.

The fraction of days with one or more contacts on an auroral zone path is given by the ratio (47 + 86)/168, corresponding to 79 percent of the days. By the same token, on 43 percent of the days, I made one or more contacts on polar paths and 54 percent of the days included one or more extreme long-path contact.

Fall/Winter Path	Contacts/Session 0	1	>1
Auroral Zone	97	43	31
Polar	123	42	6
Extreme Polar	15	8	148

Table 2. LP contacts for the fall/winter season.

Ap	Days	Auroral Zone 0	1	>1	Polar 0	1	>1	Extreme Polar 0	1	>1
0-10	51	7	13	31	15	16	20	18	17	16
11-20	39	6	11	22	22	11	6	16	5	18
21-30	31	3	11	17	21	4	6	16	7	8
31-40	16	4	4	8	12	2	2	6	4	6
41-50	10	1	4	5	6	3	1	5	1	4
51-60	7	4	1	2	7	0	0	5	1	1
>60	14	10	3	1	12	2	0	10	2	2

(Contacts/Session)

Table 3. Long-path sessions, April through September.

Ap	Days	Auroral Zone 0	1	>1	Polar 0	1	>1	Extreme Polar 0	1	>1
0-10	47	26	10	11	34	11	2	0	0	47
11-20	57	31	15	11	35	18	4	0	1	56
21-30	31	16	10	5	23	8	0	0	4	27
31-40	12	8	2	2	10	2	0	2	2	8
41-50	5	2	2	1	5	0	0	2	0	3
51-60	7	5	1	1	5	2	0	3	1	3
>60	12	8	4	0	12	0	0	9	0	3

(Contacts/Session)

Table 4. Long-path sessions, October through March.

In the second half of the LP study, I made a total of 1,009 contacts: 125 contacts on auroral zone paths, 56 on polar paths, and 828 on extreme long paths. The percentages of days for one or more contacts on the various paths were markedly different from the spring/summer season, now 12, 6, and 82 percent, respectively.

On a daily basis, there were 171 active days in the second part of the study and the LP contacts were distributed among the various paths as shown in **Table 2.**

As **Table 2** shows, the percentage of days with one or more contacts on the various paths are: 43, 28, and 91 percent, respectively. But from the distribution of days shown, it is clear that a very significant shift took place in the second part of the study. Contacts on the polar paths were far fewer in number, while the percentage of days with multiple contacts on extreme polar paths reached a high of 87 percent, as compared to the earlier value of 33 percent.

Of the 339 days, there were 256 days of non-storm conditions. I made no LP contacts on three of those days, only one LP contact on 15 days, and more than one LP contact on 238 days. This means I made at least one LP contact on 253 of the 256 days, or on 99 percent of the non-storm days!

On the 43 days with minor storm conditions, I made at least one LP contact on 39 of these days, or 91 percent of the minor storm time. For the 40 days of major storm conditions, I made at least one contact on 20 of the days, or 50 percent of the major storm time. This last point is rather amazing when you consider the havoc that storm conditions wreak on the HF bands.

The next step in the analysis was to see if the ability to make LP contacts was affected by geomagnetic activity. Thus, for the first part of the study, **Table 3** shows a breakdown of the days when I made LP contacts according to paths and levels of magnetic activity, ranging from quiet to major storm. The second part of the study is given in the same format in **Table 4.**

Inspection of the two tables shows a distinct change in the character of LP propagation between the two ionospheric seasons. But before discussing those observations, it is important to consider the magnetic conditions which prevailed when the data were obtained. As I noted in the discussion following **Table 1**, the spring/summer season was the stormier of the two seasons with minor and major magnetic storm conditions on 28 percent of its days as compared to 21 percent for the fall/winter season. Further, examination of the extreme values of Ap during the study shows that not only were storm conditions more prevalent in the spring/summer, but they also involved higher values of Ap than in the fall/winter.

Turning now to **Tables 3** and **4**, you can see a striking difference when you compare the results for the two seasons. Despite the decreased disturbance level of the fall/winter season, there was a marked change in the effectiveness of LP propagation; the auroral zone and polar paths deteriorated even with non-storm conditions. At the same time, however, LP propagation improved greatly on the extreme long paths.

The spring/summer results in **Table 3** show a negative correlation with magnetic activity; propagation deteriorated, particularly with high values of Ap. In itself, that is nothing new. But the fall/winter season is different because of another factor—ionospheric absorption on the paths. Thus, propagation on extreme long paths improved because with the Northern Hemisphere experiencing winter, the sun was at a lower angle in the sky when LP opened. Indeed, the "reach" of ELP signals into Europe increased, shifting from the Crimea, the Ukraine, and the Balkans in the spring/summer season into Western and Northern Europe—say west to the British Isles and north into Scandinavia.

During the fall/winter season, ionospheric absorption increased—particularly on paths across the Indian Ocean. Thus, while I made contacts with Mauritius (3B8), Reunion Island (FR5), and the like in the first month after the autumnal equinox, they soon came to a halt and did not resume until a month before the spring equinox. Those paths are in the polar category and I had the same experience with paths to India and Sri Lanka, in the auroral zone cateory. The reason, of course, is that with the start of the spring/summer season in the Southern Hemisphere, the paths from the Northwest United States to those regions were illuminated and signal strengths dropped to a vanishing level because of the ionospheric absorption.

The statistics in **Table 4** also suggest a deterioration of propagation on paths in the auroral zone category. With the exception of the paths to India and Sri Lanka just discussed, the remainder of the paths are to Crozet Island and locations in Southern Africa. Crozet Island is a special case, especially with the frequent presence of FT4WC on the band, followed by the cessation of his operations in November 1991.

A review of my log shows contacts with Southern Africa did decrease during the fall/winter season, but did not cease altogether as they did with stations in the Indian Ocean area. More specifically, I made contacts with Southern Africa at an average rate of one per day in the first and last months of the fall/winter season, and at about half that rate during the intervening four months. But the contacts were not marginal, as there seemed to be no significant decrease in signal strength over the entire period. That being the case, one must look for other reasons than the onset of ionospheric absorption, particularly during that period, because paths from the northwest to Africa were in darkness except at either end.

Several factors come to mind when looking for explanations for the decrease of contacts to Southern Africa; some are the result of occurrences in the natural world, others are of human origin. From the standpoint of the natural world there is the question of the extent to which summer weather conditions affect amateur activity in the southern parts of Africa. That region, along with South America and the East Indies, has an extremely high seasonal rate of thunderstorm occurrence. If nothing else, electrical storms at the rate of one or two every day would surely be intimidating—particularly with regard to the safety of electronic equipment connected to ungrounded antennas or the power lines.

That aspect is local to particular times, regions, and topographies. Of a broader nature, is the radio noise generated by electrical storms. In that regard, global studies of the distribution of noise have divided areas of the earth according to zones, 1 through 5. The regions most distant from thunderstorm areas, which receive little atmospheric radio noise by skywave propagation are classified as zone 1. Using this classification scheme, regions where thunderstorm activity is most frequent are located in zones 4 and 5. Southern Africa lies within zone 4 during the months of December, January, and February.

In addition to the zone in which a receiving station is located, another important factor is the relationship of radio frequency distribution of atmospheric noise[1] to the time of day. The general features of the distribution distinguish between daytime and nighttime, and there are finer differences according to zone and local times. But the essential features show a high level of noise around 14 MHz, day or night, for zone 4 regions. As a result, it may be possible to explain the smaller number of contacts with stations in Southern Africa in terms of thunderstorm activity and the radio noise or

		Contacts							
		Sub-Auroral		Auroral		Polar		Extreme Polar	
Ap	Days	0	≥1	0	≥1	0	≥1	0	≥1
0-10	51	(2)	49	7	44	15	36	18	33
11-20	39	(4)	35	6	33	22	17	16	23
21-30	31	(1)	30	3	28	21	10	16	15
31-40	16	(3)	13	4	12	12	4	6	10
41-50	10	(2)	8	1	9	6	4	5	5
51-60	7	(1)	6	4	3	7	0	5	2
>60	10	(4)	10	10	4	12	2	10	4

Table 5. Data collected from 13 operators.

static crashes that are propagated in from surrounding regions. Indeed, this is attested to by recent accounts (*DX Magazine*, April 1992) of DXpeditions to Southern African regions like Malawi.

As for human factors, note that the distribution of LP contacts shown shifts to later times in UTC with the onset of the fall/winter season. I have a suspicion that not all DX operators are aware of the shift and do not adjust their operating hours accordingly. I say that because, in the course of this study, I had occasion to be called frequently, almost on a schedule, by an operator in Africa. He always called me just when LP began to open up here, and signals were growing in strength. It was with some difficulty that I got him to shift to a later time. If operators do not understand the need to shift operating times with season, they will find LP propagation deteriorating at the same time of day and come to the erroneous conclusion that LP propagation is closing for the season.

Also the shift of LP to later times in the fall/winter season brings the time of LP openings closer to the dinner hour in Africa. In addition, there is the matter of personal comfort in the hot, humid climate along the coastal regions near the Tropic of Capricorn. While I do not have any first-hand experience in the matter, I would think that sitting on the veranda, sipping a glass of iced tea would present a greater attraction in the late afternoon than operating on 20-meter CW looking for contacts into North America.

All in all, I can find no plausible explanation in pure ionospheric terms for the smaller number of contacts with Southern Africa during the period from November to February. I have to leave it there, leaning toward the thunderstorm explanation, but would be interested in learning the views of others on the matter. For me the effect is real, but puzzling.

To bring this section to a conclusion, I have mentioned that there was a negative correlation between LP and magnetic activity. However, the data in **Tables 3** and **4** show that ionospheric absorption can be a factor, depending on the paths involved. Thus, in examining the question of a negative correlation, one should look at specific paths that are as free of absorption effects as possible, using a large data sample. I did this with auroral zone paths in the spring/summer and extreme long paths in the fall/winter season. Of course, the results obtained apply only to paths from the Pacific Northwest.

Change in origin for great-circle paths

Having made the point that seasonal variations may be somewhat different at lower latitudes, say in the Los Angeles area, one can examine whether similar results might be expected for disturbances due to solar outbursts. To that end, I calculated details of great-circle paths again for an origin at Los Angeles. In contrast to the seasonal effects, where the shift in origin would have a small effect on the time when signal paths are lost, a southern shift in origin has a large effect on the categories of paths when viewed using geomagnetic coordinates.

Using Los Angeles as the point of origin, many great-circle paths are shifted into the sub-auroral category. The only exceptions are 4S7 and VU2, which still remain as auroral zone stations. Great-circle paths for 3B8, FR5, FR5/T, and 3B9 remain in the polar category, while others (FH, D6, and 5R) change to the auroral zone category.

While the distances are not particularly different using Los Angeles as the origin, perhaps 1,500 km shorter on the average, the extreme geomagnetic latitudes are quite different. A sample of auroral and sub-au-

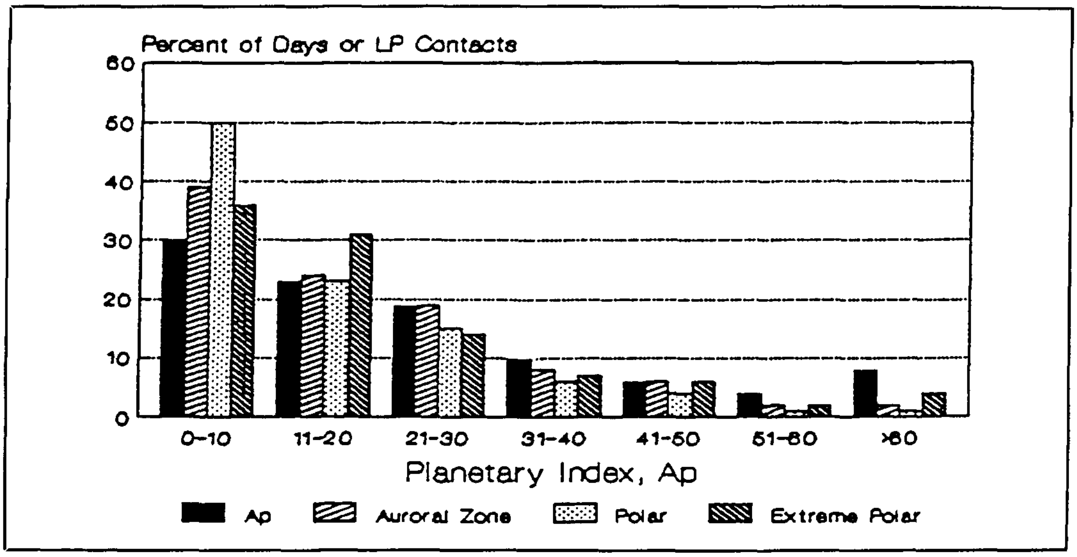

Figure 1. Distribution of magnetic activity and long-path contacts: April 1, 1991 through September 21, 1991.

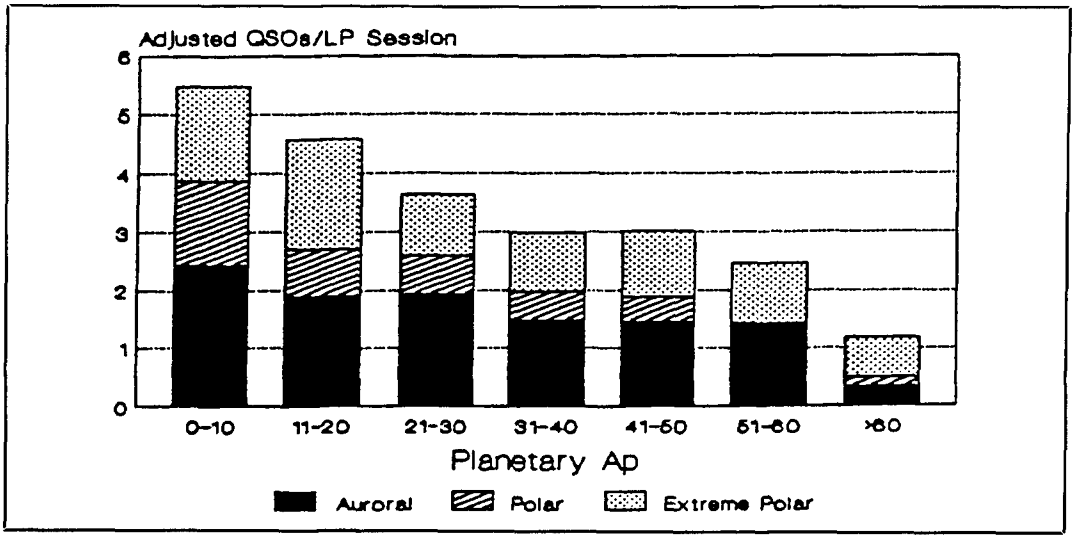

Figure 2. Adjusted LP QSO/LP session versus AP index ranges: April 1, 1991 through September 21, 1992.

roral great-circle paths average nearly 20 degrees lower in latitude, while polar paths average 12 degrees lower.

I sent out a call to long-path operators in the Los Angeles-San Diego area and South Africa for log data (date, time, and call) for contacts made during the spring/summer season. The selection criterion was quite simple, I required just one or more contacts on a sub-auroral path in the same time interval of UTC as the study. The response was quite gratifying and, when the data was finally collected from thirteen operators, four in Southern California and nine in Southern Africa, I combined it in **Table 5**.

The result provides a quantitative indication that lower latitude paths are less susceptible to disruption than other paths that reach into higher magnetic latitudes. Previously, the only information that was available on this topic was of an anecdotal nature so, to that extent, the present results do represent an improvement.

As for its physical basis, the difference is due to the fact that the ionosphere on sub-auroral paths lies at the feet of magnetic field lines that only go out 2 to 3 earth radii, while the ionosphere for auroral paths involves field lines going out 6 to 7 earth radii. The latter are more vulnerable to the effects of the impact of solar plasma on the magnetosphere.

Let's look at the database from some different perspectives. First consider **Figure 1**, which gives the percentage of days of different levels of magnetic disturbance and the percentage of contacts in the spring/summer season on the three different types of paths. You can see that during quiet conditions (Ap 10 or less), the percentage (39 percent) of QSOs completed on auroral zone paths is out of proportion to the percentage (28 percent) of days of magnetic quiet. At the other extreme, for storm conditions (Ap greater than 50), one sees the percentage (2 percent) of QSOs completed is considerably less than the percentage (8 percent) of days with those conditions.

From that, one can conclude that there is some cross-over point or level of magnetic activity at which propagation begins to suffer. But that approach only deals with apparent success and ignores failure as well as real success, the complement of failure.

Having used both simple and complicated methods to explore the correlation between magnetic activity and propagation, we could take a less than conservative approach and use QSOs/session instead of the success/failure approach to the data. The success/failure approach is more appropriate to a study of HF propagation, but the use of QSO data relates more closely to amateur radio experience. However, it should be understood that the results will be more subjective with the QSO approach because differences in operating style may influence them. Be that as it may, the adjusted QSO rates for LP sessions in the spring/summer season are given in **Figure 2**.

I leave it to the reader to suggest factors other than operating style, which are not related to the forces of nature, yet contribute to the changes in QSO rates as Ap increases or decreases. Certainly, there is the matter of persistence, previous low values of the A-index bringing on more of the same, and DXers out in droves. Similarly, high values of the A-index don't decay away at once and have a rather discouraging effect. These are obvious factors, but certainly there are others.

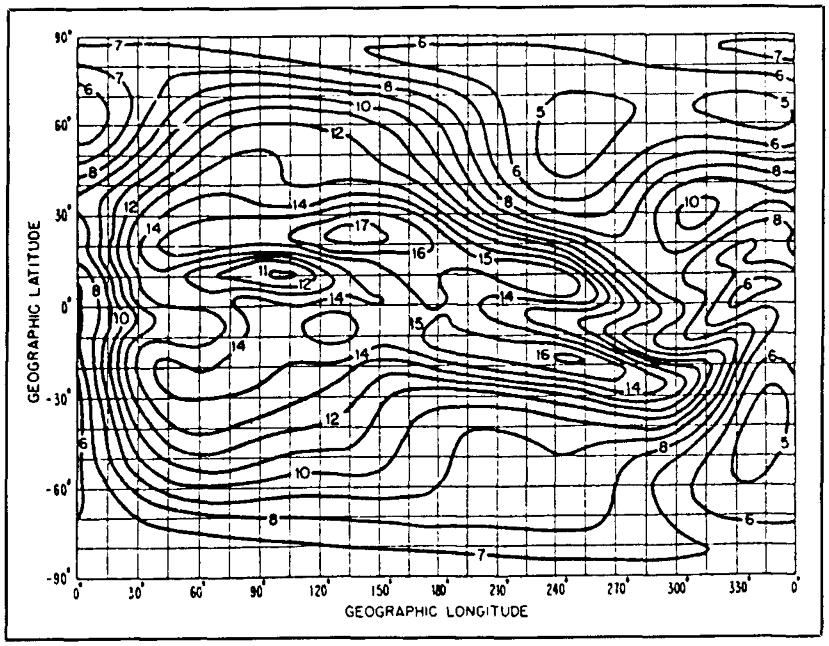

Figure 3. Contour map (in MHz) of the global representation of the median value of FoF2 for March 1979 at 0600 hours universal time.

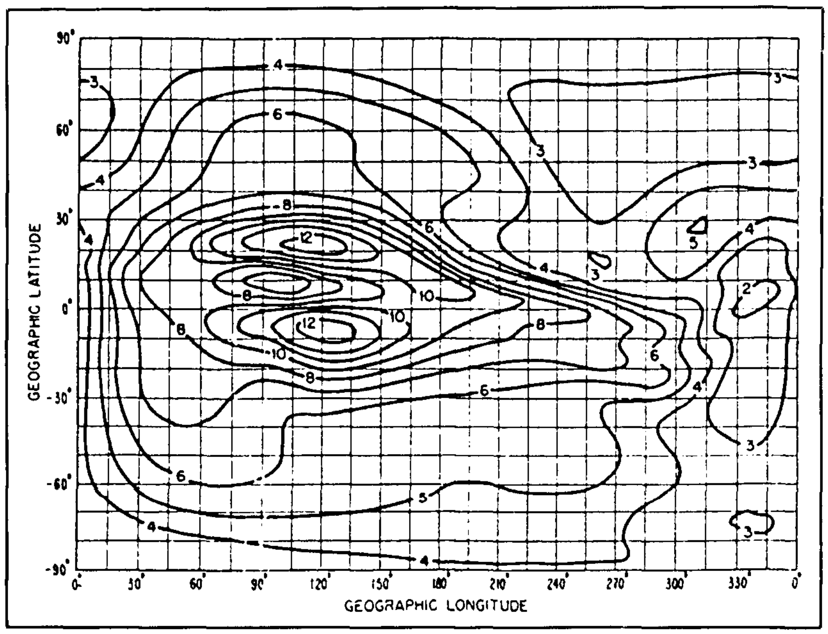

Figure 4. Contour map (in MHz) of the global representation of the median value of FoF2 for March 1976 at 0600 hours universal time.

FoF2 maps and long-path propagation

One cannot discuss propagation, either short or long path, without considering the properties of the ionosphere at a given time of day, month, and sunspot number. After all, successful propagation depends on wave refraction back to earth, time and again, along a path, and adequate signal strength depends on the solar illumination along the path. A knowledge of the state of the upper and lower regions of the ionosphere along a proposed path is essential in order to see whether a viable situation presents itself or not. To that end, one needs ionospheric maps for the critical frequencies of the F-layer for the upper reaches. The lower reaches, on the other hand, are dealt with using the spatial relationship of the terminator and the path.

Readers who were active DXers before propagation programs on computers became so readily available know well what I

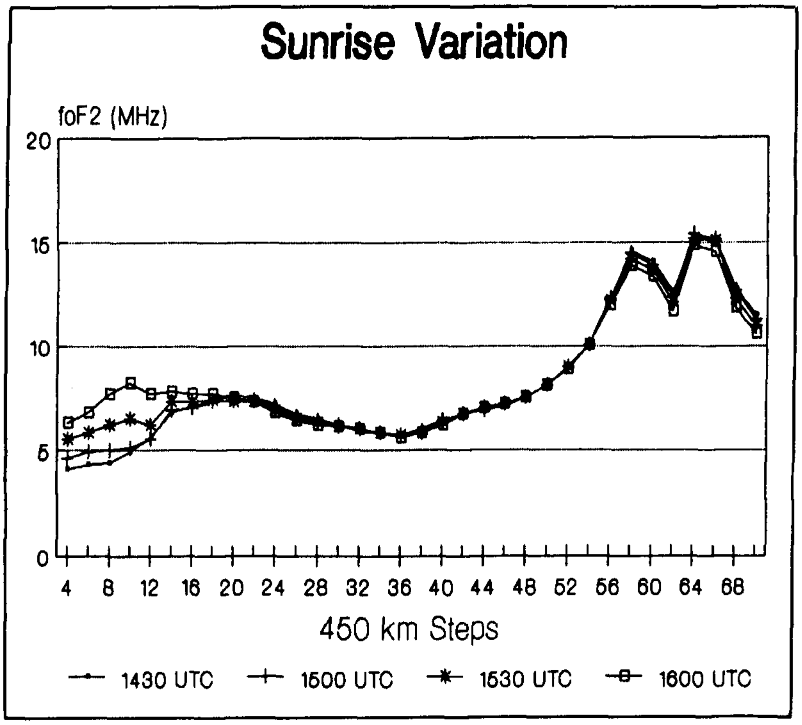

Figure 5. Long path to HB-land.

am talking about when I refer to ionospheric maps—those MUF (ZERO)F2 and MUF (4000)F2 maps prepared from years of ionospheric soundings and then published by the Department of Commerce back in the '60s and '70s. They provided a mapping of the monthly median critical frequencies over the world in two-hour intervals.

To illustrate the matter, I have chosen two FoF2 maps from a paper by Davies and Rush (1985),[2] shown in **Figures 3** and **4**. They give global representations of the monthly median value of FoF2 for the month of March and the years 1979 and 1976, respectively. These choices highlight the differences in FoF2 values and their spatial distributions between times of solar maximum in Cycle 21 in 1979 when the SSN was 137, and solar minimum, earlier when the sunspot number (SSN) was a mere 12.

I'd like to call attention to the striking differences between the FoF2 maps in **Figures 3** and **4**. In **Figure 4** for solar minimum, conditions can best be described as "bleak," showing how low the critical frequencies are around solar minimum as compared to solar maximum, (shown in **Figure 3**). In addition, you can see how small and limited the ionosphere is at solar minimum as compared to its larger extent around solar maximum. Now, in 1993, when we're past solar maximum and facing the prospect of a gradual descent toward minimum, one can see that propagation based on earth-ionosphere hops will suffer—at least on the higher HF bands.

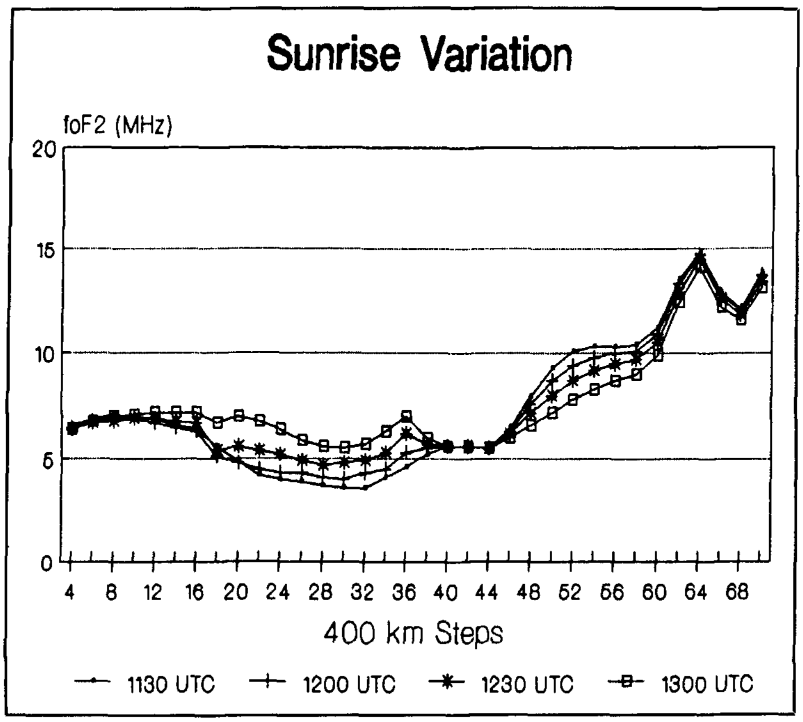

Figure 6. Long path to VU-land.

More on the gray line

One cannot leave the previous discussion about the equatorial anomaly without revisiting the matter of gray line DXing. This is the case as the method of following the variation of the critical frequencies along a path has direct application to that question. To illustrate the matter, consider LP DXing in the fall/winter season. I've already mentioned that signals from the Indian Ocean area disappear after the paths become illuminated with the change of seasons. Also, the time-distribution of LP contacts has shifted to later times, as shown in part 1 of this article. Recalling the DX Edge picture for December (*Communications Quarterly*, Fall 1992, page 37), one would conclude that gray-line considerations are important for DXing into Africa and Europe in December.

What are "gray-line considerations?" According to the literature, these factors are generally "static" in nature and involve the geometry of the terminator, something which changes regularly, year in and year out—without any relation to solar activity. The appeal of matters that are ionospheric in character is only related to the extent that D-region absorption is minimal along the gray line. For my part, I would argue that

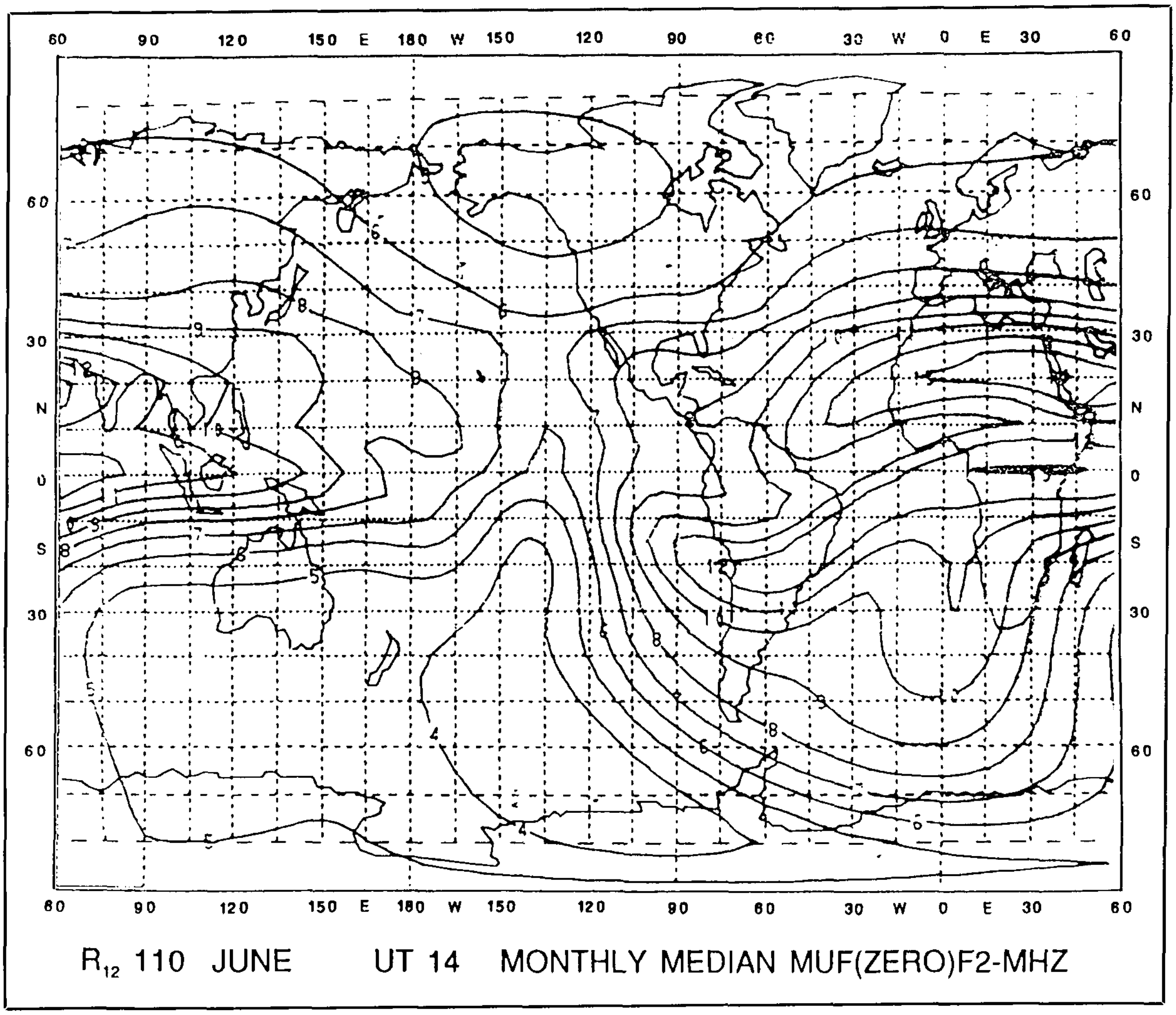

Figure 7. Global FoF2 map for 1400 UTC, June (SSN = 110). From *Leftin* (1971).

gray-line considerations are "dynamic" in nature, frequency sensitive, and even localized to some extent—rather than distributed ALL along a path. Here are some examples.

Consider a path into Europe, say to HB-land in December. From the DX EDGE, you would think that D-region absorption is the story. But if one looks at how critical frequencies change with time along the path as shown in **Figure 5**, it becomes apparent that the opening really develops because of changes in the F-region here along the West Coast. Thus, for success in the first refraction of 14-MHz signals heading toward Europe, one needs a minimum critical frequency of about 5 MHz in the F-region at the apex of the first hop. This is around step 4 or 5 in the diagram. That situation develops as the sun rises out over the Pacific, about 1,400 km west of Los Angeles.

The ionization and critical frequencies along the rest of the path are more than adequate, and the path to HB-land opens after 1500 UTC. But that is a dynamic F-region process, something which one can actually hear by following the enhancement of a signal for 10 to 15 minutes. The path closes more slowly as D-region absorption changes, increasing more on the sunrise part of the path over the Pacific than it decreases on the part of the path that goes into darkness along East Africa and Europe.

Similar considerations apply for the path to South Africa. The main difference is due to the fact that the path is shallower, moving to 55 S as compared to 70 S latitude for the path to Europe. Thus, the opening and closing of the path are due to F and D-region processes closer to the point of origin than in the other case.

Finally, one cannot conclude this discussion of the gray line without referring back to the original instance mentioned—the summer paths to India and Sri Lanka, as shown for June on the DX Edge (*Communications Quarterly*, Fall 1992, page 36). There, the paths appeared to be sheltered from solar illumination. But what makes

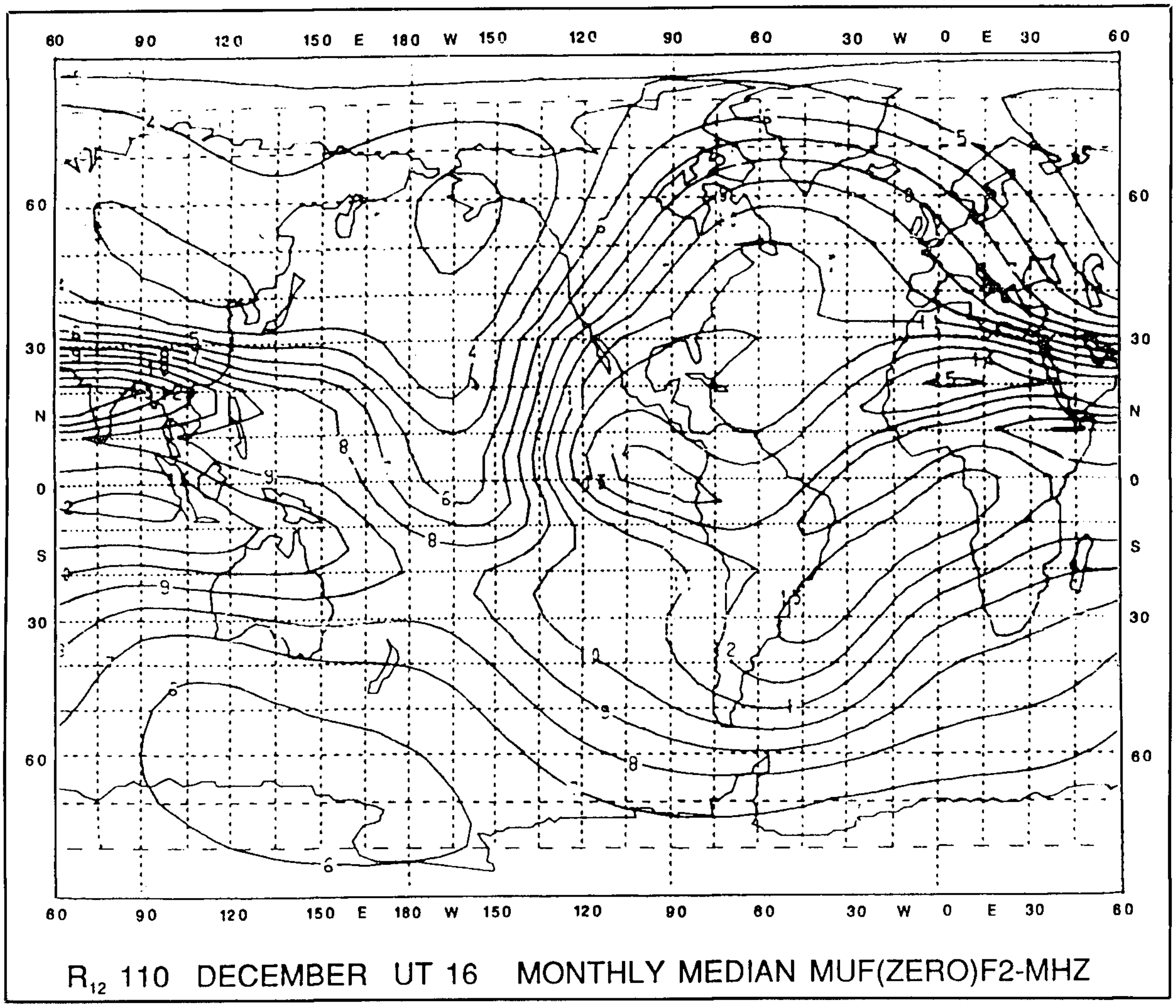

Figure 8. Global FoF2 map for 1600 UTC, December (SSN = 110). From *Leftin* (1971).

them open? What makes them close?

To understand the mechanics of path openings and closings, go to **Figure 6**, which shows the critical frequency variations along a path to India. One can see that the opening to India develops because of a rise in the critical frequencies with sunrise along the path in the Southern Hemisphere, from about step 18 (13 S, 103 W) to the deepest winter part of the path at step 38 (76 S, 37 W). Again, the critical frequencies along the rest of the path are sufficient to support propagation and, as expected, the path closes because of the growth of D-region absorption on the western portion of the path where the sun is rising.

If you want to look deeper into the difference between the cases of propagation to HB-land and VU-land, refer to **Figures 7** and **8**. You'll find that the significant rise in critical frequency with sunrise in the northern Pacific area in December is a result of the relatively long period of darkness after sunset (up to 16 hours at this latitude) and the decay of ionization at F-region heights. For June, the long period of illumination during the northern Pacific area spring/summer season (up to 16 hours) means that less decay in ionization occurs in this area after sunset, and the F-region variations important on the path to India are now found in the Southern Hemisphere during its winter season.

Given these remarks, it should be clear that the earlier discussions of the gray line miss the essence of the matter in the present cases—the dawn enhancement of critical frequencies in the winter portion of the F-region. This would also apply at higher frequencies, say on the 21 and 28-MHz bands. At lower frequencies, where maximum usable frequency (MUF) considerations are less important, say 7 MHz, ionospheric absorption plays the greater role.

An example of extreme long-path propagation

The most distant contact made, indeed

verified, in this study was with Oistein, LA9EF, in Vadso, Norway (70.15 N, 29.85 E); the date was October 26, 1991 and the time of contact was 1428 UTC. The LP great-circle distance from Guemes Island to Vadso is 33,368 km and the beam heading from Guemes Island is 191 degrees east of north—very close to the gray line at the time. In its extremes in the Southern Hemisphere, the path reached 82.0 S geographic latitude and 86.2 S geomagnetic latitude.

Let's consider the ELP contact with Vadso, Norway. The variation of F-region critical frequency along the great circle was obtained by dividing it into 40 segments of about 850 km each, and then calculating the value of FoF2 at each of those geographic locations using the MAXIMUF algorithm. The results are shown in **Figure 9**. Here you see that critical frequency varies somewhat in the first half of the path, from 5 to 8 MHz, then increases steadily after step 24, and goes through two peaks—17.6 and 17.4 MHz—which are separated by a valley where the critical frequency is 14.1 MHz.

The geomagnetic dip equator is located close to the valley around step 32, and the two peaks in critical frequency represent the regions of peak electron density associated with the equatorial anomaly in the early evening hours. While this variation of critical frequency along the path clearly points to a strong horizontal gradient in the electron density, that quantity must be calculated in two dimensions—not just in the dimension that is direction along the path. When the calculation has been performed, albeit in an approximate fashion, it shows that the gradient of the equatorial anomaly, as obtained using MAXIMUF, was mainly along the direction of propagation.

The double peak in FoF2 on the approach to Vadso points to a long chordal hop toward the final location on the path. As for the initial portion of the path, that presumably involved a conventional multi-hop mode between the earth and the ionosphere—as no comparable gradient structure is found in **Figure 9**.

Of the other common paths in the present study, only the ones to Sri Lanka and India come close to the equatorial anomaly. In that regard, **Figure 10** shows the FoF2 variation along a path to Sri Lanka. Here, the critical frequency begins to rise significantly in the last 2 to 3 steps before the terminus. That variation probably affected the last downward refraction on the path, but would not have given rise to a chordal hop. Judging by the slow variation in critical frequency observed earlier, the other portions

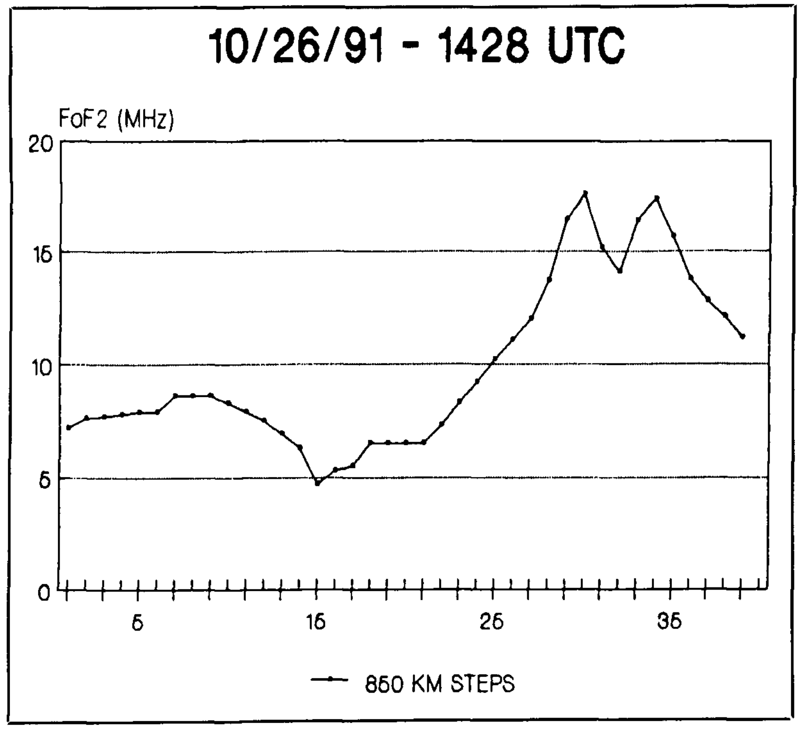

Figure 9. FoF2: NM7M to LA9EF.

would have involved only earth-ionosphere reflections.

Simultaneous short and long-path propagation

There are occasions in the morning hours around the equinoxes and during the fall/winter season when both short and long-path propagation are in effect at the same time. One's ability to notice this circumstance depends on the antenna systems used. For example, I have found both SP and LP to be open when listening to a European station that used a dipole or a vertical antenna. Thus, one hears multi-pathing from the two signals, but the details depend on how one's beam is oriented.

A case in point was ES1RA, who uses "200 watts into a gp." I've contacted him both SP and LP within a period of 5 minutes. But when my beam was pointed north, his CW was muddled by the overlapping of the prompt SP signal and the delayed LP signal, a "trailing ghost." On that occasion, LP propagation was the better of the two and, when my beam was rotated to the south, the effects of multi-pathing were not as severe. Moreover, since my QTH is on an island, a true low-noise site, I could even hear his weak SP signal first, a "leading ghost" coming in the back lobe of my beam, and then the louder, delayed LP sig-

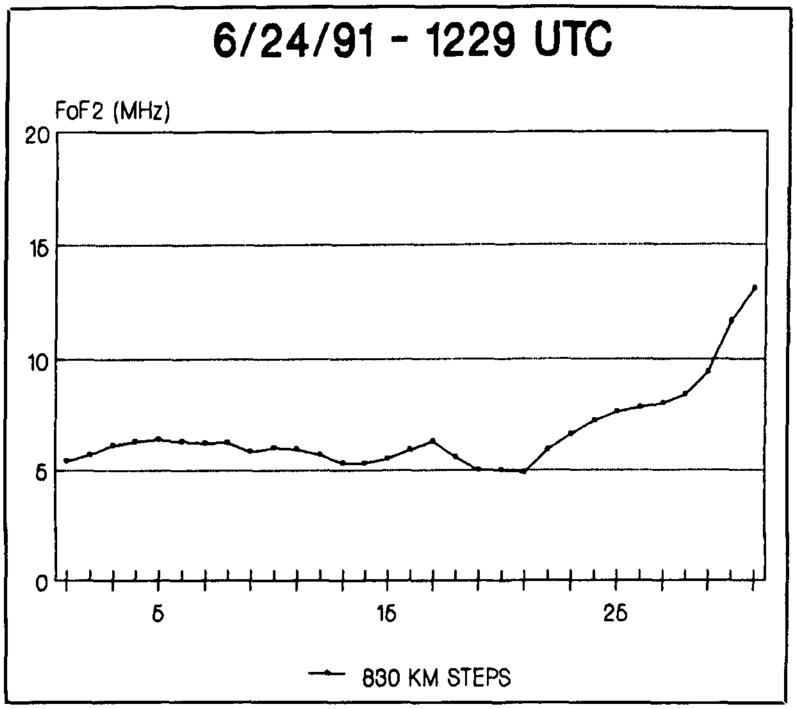

Figure 10. FoF2: NM7M to 4S7CF.

nal via the front lobe—now with a sharp, crisp termination on every dot and dash.

With high power, multi-path effects can be quite pronounced and one does not need a low-noise site to get a sense of what is going on. By listening carefully to the sound at the end of dots and dashes for a crisp termination, one can recognize when the multi-path effect is due to the early arrival of the short-path signals. If local noise is too great a problem and does not permit the use of "ghosts," one must rely on signal strength variations with antenna rotation to establish the reality of an LP contact or, if the other person speaks English, it can be confirmed by rotating both beams to SP. Indeed, such an occasion, when Peter, SM7BAU, and I spent some time checking both LP and SP propagation on April 1, 1991, was the actual stimulus that led to the present study.

Off great-circle signals

On one occasion just before the autumnal equinox, I found signals from my antipodal friend, FT4WC, were weak in the usual direction, and remembering my earlier experience with back lobes, I swung the beam more to the west. Sure enough, his signals peaked about 35 degrees farther to the west. To be sure it was not due to a side spur of the back lobe, I swung the beam farther north, looking to see how his signals were in the short-path directions. To my surprise, they were weaker in the SP direction—not what I had expected. I went back to double-check and found that the best signal came from about 35 degrees westward from his usual position. So, I had a real case of an "OGC" signal, one coming in from a direction that was off the great-circle path.

But that wasn't the end of it. My initial observations were made about an hour before dawn at this longitude. As dawn approached, the signals from FT4WC became stronger on his usual heading and by the time the sun was up, it was clear that his signal had swung around toward his usual long-path direction. Interesting! That was on September 19 and Ap was only 10.

By way of interpretation, this had to be an example of the influence of a transverse ionospheric tilt—primarily in the dawn sector. There have been other occasions when I heard off great-circle signals from LP, but not more than 20 in the whole period—far less than one would expect from the remarks that surface in the literature from time to time. I heard other OGC signals during the study, but they were not LP signals. Here, I have in mind signals from the Indian Ocean area, say VU and 4S7, which are not heard via LP during winter months when their paths in the Southern Hemisphere are fully illuminated. Short path can be open to that region in late December and early January and, on at least four occasions, I made contacts into the area around the Arabian Sea, with N9NN/MM and AP/WA2WYR, as well as the Indian Ocean, with VU2KOJ and 4S7WP, when the geomagnetic field was relatively quiet.

Discussion of factors affecting LP propagation

In discussing long path propagation, we must first recognize that LP propagation is in effect on almost 100 percent of the days when the earth's magnetic field is without disturbance, for hours at a time. In a sense, LP propagation amounts to a shorter version of around-the world (RTW) propagation.

In essence, the ionization conditions for LP propagation are created along, and continue to exist, well behind the terminator as it moves from east to west. Put another way, like a boat, the moving terminator leaves a wake or a wave behind it as it goes across the sky, a crest of rapidly increasing ionization with sunrise on the morning side and a trough of slowly decreasing ionization with sunset on the evening side. Of course, at lower altitudes along the exposed portion of the great-circle path D-region absorption starts to increase with sunrise, while the absorption decreases on the dusk side as it moves into darkness.

Were it not for the increasing absorption of signals on the sunlit portion of the path, LP propagation would continue for a much longer period, until the decay of ionization somewhere along the dusk portion reached a level which no longer supported ionospheric refraction. As it is, however, D-region absorption dominates and ultimately closes the path for the day. The path then reopens when the required levels of ionization are "refreshed" at the next sunrise—about the same time on the following day.

Having made the point that LP propagation is really "the rule," not requiring any sort of ionospheric circumstances beyond the rising and setting of the sun, we should next deal with the exceptions. These are unusual solar/terrestrial circumstances that may disrupt LP propagation.

Polar cap absorption events

We begin at the high energy end of the spectrum, considering the polar cap absorption (PCA) events due to energetic solar protons. As is well known, those particles are accelerated to tens and hundreds of MeV of energy during some solar flares and sent out into the interplanetary magnetic field—some finally reaching our polar ionosphere.

The ideas and understanding of PCA events that apply to short-path propagation also apply to the long-path situation. But it is important to note that the particle influx into the two polar regions may not be the same, depending on how the particles gain access to a particular polar cap. Access varies according to season, as one polar cap may be more inclined toward the advancing solar protons than the other.

There may also be differences in conditions on signal paths in the two hemispheres, namely the amount of sunlight they receive. This has an effect on the D-region absorption on the paths—leading to greater absorption by as much as 5 to 10 times that found in the sunlit polar cap during a PCA event.

Auroral absorption events

Proceeding down the energy scale, but still in the disturbance regime, we come to auroral absorption (AA) events caused by energetic electrons, now accelerated to tens and even hundreds of keV of energy by processes within the earth's magnetosphere. These particles are known mainly for the optical emissions they produce in the nighttime hours, but because of their high fluxes, they can also create significant ionization at E-layer heights, and may give rise to ionospheric absorption of radio signals passing through the regions.

While both PCA and AA events are sporadic rather than regular in appearance, they differ in details of frequency of occurrence, duration, and times of incidence. Solar protons can produce PCA events of long duration, lasting for several days, after some large solar flares; but auroral electrons produce AA events more often, and with durations measured in hours. And, instead of being slowly varying and continuous as with PCA events, AA events generally show rapid time variations in absorption (in hours or less), and are most often limited to certain times of the day. Moreover, PCA events extend broadly over the two polar caps, while AA events are quite limited in latitude and longitude in the auroral zones.

Long-path propagation and auroral disturbances

In connection with LP study, it is necessary to look in some detail at how AA events develop, particularly with regard to the auroral zone as a whole. First, note that AA events occur mainly around local (magnetic) midnight when auroral forms become active and involve only modest ionospheric absorption.

It becomes clear that the paths in this study are not out of harm's way as far as times of minor to modest auroral activity. However with more intense auroral activity, say during those geomagnetic storms that produce strong auroral currents, auroral absorption of more than 4 dB at 30 MHz would be expected for signals passing through the auroral E-region.

As for the polar paths, they cross through the auroral zone twice. For paths toward the dark hemisphere (to 9J2, ZE, and 7Q7), the crossing into the auroral zone is closer to the region of auroral activity (around 180 degrees east longitude) than where it emerges from the polar cap and crosses the auroral zone again going on toward the terminus involved. Thus, auroral activity could affect LP propagation by absorption processes in that particular region.

Other paths go deep into the southern polar cap and follow steep trajectories, entering the auroral zone around 122 to 164 west longitude and emerging around 50 to 60 east longitude. In essence, they too would be fairly immune to effects from auroral absorption.

Magnetic storm disturbances

Electrons and protons with energies well below those of solar protons and auroral electrons are also able to influence, indeed disrupt, HF radio propagation. These particles, called solar plasma, originate on the sun and affect the shape and dynamics of the geomagnetic field for a day or two during geomagnetic storms.

Geomagnetic storms either begin suddenly or gradually, the components of the geomagnetic field departing significantly from their typical daily variations. Storms with a sudden commencement (SC) originate with solar flares and bursts of plasma that leave the vicinity of the flare site—sometimes arriving at the outer reaches of the earth's field anywhere from 20 to 40 hours after the flare.

The main effect of geomagnetic storms on the HF bands is the lowering of the maximum useable frequency (MUF) on paths of interest. This results from a reduction of the electron density at F-region heights; however, as a geomagnetic storm wanes, the critical frequencies of the F-region return to their normal values and HF propagation is gradually restored to its pre-storm condition.

In this study of LP propagation, the presence of a magnetic storm would reveal itself by the band being dead at the start of an LP session, with no signals heard in the predawn hours from low-latitude stations out in the Pacific Ocean area. If the storm was of major proportions, say induced by flare outbursts as in June and July of 1991, that situation would continue throughout the first and possibly the second and third LP sessions, and the sessions would prove barren with regard to LP contacts.

But if the storm were minor, as is more typical of those due to coronal holes, or in a recovery phase at the time of an LP session, propagation would begin to return with sunrise at F-region heights on regions in the nearby area. Thus, the nocturnal ionization levels to the west would begin to recover from their depleted condition by the incidence of solar ultra-violet radiation. That restoration of the electron density in the ionosphere would serve to produce the final refraction of signals necessary to complete LP links to this location, particularly from Europe and Africa.

Ionospheric modes in long-path propagation

Let's turn our attention to modes and how they would be related in LP propagation. To begin, chordal hops or the whispering gallery mode are thought to involve consecutive wave reflections off the ionosphere, without the adverse effects of D-region absorption and ground losses associated with intermediate earth reflections. The chordal hop is the fundamental unit in such discussions, and the whispering gallery mode is the result of a series of shorter chordal hops. But in the last analysis, for successful communication, any ray path must start and end with a multi-hop type of refraction that touches the earth's surface.

Chordal hops

Apparently, the idea of chordal hops began with a suggestion by Albrecht (1957).[3] He found the strength of LP signals from Europe to Australia was just too great—inconsistent with the calculated losses expected from intermediate ground reflections and ionospheric absorption in the usual earth-ionosphere hop mode. His suggestion may have been a good one, but for the wrong reasons, as the relation for field strength and distance in use at the time proved to be less than satisfactory. In any event, in order to have chordal hops, ionospheric tilts are required.

But if one looks at the ionospheric maps along these paths, there are no unique ionospheric gradients or features—not even the equatorial anomaly—that would support the idea of a chordal hop along any path from here to South Africa. In short, it would appear that salt water and antipodal focussing, to whatever degree present, are the only things going for auroral zone paths from this QTH into South Africa.

While chordal hops are attractive in aiding discussions of propagation over great distances, if one is going to invoke them, it is necessary to identify a suitable set of ionospheric gradients to support the proposal. While the gradients around dawn and dusk are regular parts of the ionosphere, they do not come up to the degree or extent of the equatorial anomaly—already a proven part of transequatorial propagation on short paths from one hemisphere to another.

The equatorial anomaly

As indicated earlier, the equatorial anomaly of the ionosphere is two parts of the F-region, having higher than normal electron densities as well as heights, which are located about 15 degrees on either side of the magnetic dip equator. Those regions are most notable during the daytime hours, reaching the extreme values around early evening. In amateur radio circles, it is credited for transequatorial propagation (TEP) at frequencies higher than conventional MUF calculations would predict.

The winter anomaly and stratwarms

At this point, I've considered the various forms of disturbance that can affect LP propagation, as well as the factors that contribute to their success. There is still one more disturbance or effect to consider, not so much for its reality as its mythical proportions. I am referring to the "winter anomaly" in D-region absorption and its purported relation to increases in ionospheric absorption with stratospheric warming, "stratwarms" for short.

The current understanding of these anomalies is that they start with a reservoir of nitric oxide in the winter polar cap or vortex. This reservoir is created by the dissociation of molecular nitrogen at auroral latitudes by electron bombardment, and then followed by the association of N and O atoms to form the NO molecule. The atmospheric circulation in vertical-meridional planes would carry the NO from auroral altitudes at around 120 km, toward the pole and then downward into the D-region (70 to 90 km). It would then cycle equatorward and, finally, upward again.

The "stratwarm" condition announced on WWV broadcasts involves a warming in the high-latitude regions of the winter hemisphere and leads to distortions of circulation in the winter atmosphere. This transports the NO-rich air to mid-latitudes where it can be ionized during the sunlit hours, increasing attenuation of HF signals. Because this phenomenon affects the winter polar cap, it can be discounted as affecting LP from the Northern Hemisphere during the fall/winter season.

Quantitative summary of the long-path study

In discussing any matter of technical or scientific interest, one must always touch base with those who have gone before, making reference to their work lest one be accused of not giving them their due or, even worse yet, the cardinal sin of "reinventing the wheel." So let me say right here and now that long-path propagation had its foundations in the early work on around-the-world (RTW) echoes. As best I can tell, that dates back to the work of Quaeck and Moegel (Germany), in 1926, as cited in the article by Hess (1948).[4]

Now, having paid homage to the ancients, let's turn to the present, reiterating some features from earlier work and adding others from the present effort. As noted at the outset, the present study shows that long-path propagation is an integral part of HF propagation during undisturbed conditions. Except for major storm conditions, when both short and long-path propagation are severely disrupted, it is something that can be expected on a regular basis. It is not a brief, fleeting condition that comes and goes. When present, long-path propagation provides a means of communication over a wide range of distances, latitudes, and longitudes, simultaneously. Thus, in the present study, it was not uncommon to hear LP signals from as close as Crozet Island and Africa, or as far as Europe at approximately the same time.

In the summer/spring season, I reported 669 LP contacts in my log. Given the number of active days, that number corresponded to an average of 4.0 LP contacts/day. The contacts in that season reached from Crozet Island (20,465 km) to Enkopping, Sweden (32,558 km).

In the fall/winter season, I recorded 1009 LP contacts in my log--ranging this time from Crozet Island to Vadso, Norway (33,368 km). But the openings were much shorter, starting in the hour before local sunrise and lasting about 90 minutes or so. The stations in the Indian Ocean area, from 4S7 and VU to 3B8 and FR5, gradually disappeared from the bands as their paths passed through regions in the Southern Hemisphere which were increasingly illuminated.

Turning to the geophysical conditions during the study, it is fair to say that they consisted mainly of magnetic disturbance. Beyond that, NOAA's "Monthly Activity Summary and Solar Cycle Outlook" released in September 1991 pointed out that since late March 1991 there had been a near-record or greater number of days of major geomagnetic storm levels. Indeed, there had not been such a high level of activity since 1960. Thus, while geomagnetic coordinates and disturbance are relevant to any discussion of LP propagation, the high level of magnetic activity during the study made them all the more important.

The other potential source of disturbance for long-path propagation, polar cap absorption (PCA) events, never really played a significant role in this study. Solar proton events were most numerous and intense during the spring/summer portion of the study. However, PCA effects are the strongest in the sunlit polar cap, and that was the northern polar cap during the spring/summer season—a hemisphere away from all the paths in this study.

If one were to make a value judgement about which of the two seasons was the most rewarding, it would depend on the personal point of interest. In terms of variety of DX signals heard during LP sessions, the spring/summer season would be the best, by far, when it comes to working "New Ones." This is simply due to the fact that the Indian Ocean and East African stations would be available then and, curiously enough, the fact that it would be the cooler season on the African continent.

In our fall/winter season, the opposite is the case and it was not uncommon to hear complaints from African stations about high temperatures (about 30 °C) in the radio shacks over there. In addition, the shift of the LP openings to later times, came into conflict with their dinner hour! But those complaints were minor; the real problem was the thunderstorm activity that develops during their summer.

While this was alluded to in personal correspondence, a search of the literature revealed the magnitude of the problem. Thus, Campen et al. (1960) provide information on the frequency of occurrence of thunderstorms over the entire globe, month by month. Starting in September, thunderstorm activity in Africa spreads eastward from Central Africa into the southern end of the Continent. By January, it fully engulfs the southern part of Africa and Madagascar, showing the highest rate of thunderstorm activity (more than 25 days per month) on the entire earth—peaking in the area around Madagascar as well as Zimbabwe and Malawi. Then, as summer turns to fall, the thunderstorm activity retreats northward toward equatorial latitudes, so there's little wonder that African stations aren't found on LP at these times. It's more of a matter of self-preservation than anything else.

If one enjoys the idea of working stations at great distances, say three-quarters of the way around the world, then the fall/winter season comes in first as the most rewarding experience. I wouldn't think that one could work WAC on LP with any ease, but if you're an oblast hunter, you should be able to earn an LP endorsement for the R-100-O Award by contacting 100 Russian oblasts using the "back door." In 1992 alone, I managed to work more than 70 oblasts with the UB prefix, then UA9, UA3, UA4, and UA6 in a descending order, followed by Byelorussia, the Baltics, and the lower part Russia from Azerbaijan (UD) to Takzikistan (UL).

This brings us to the end of this "short course" in long-path propagation. Readers who want to know more may be interested in obtaining a copy of the full study from NM7M. You may purchase a nicely bound copy of the study for $10 by writing to Bob at the address listed at the beginning of the article. Having heard long path discussed over my 20-year ham career, and having worked some LP DX, this report has answered a void in propagation literature available to the DXer. See you on the bands! de N0AX

REFERENCES

1. K. Davies, *Ionospheric Radio*, Peter Peregrinus Ltd., London, 1990.
2. K. Davies and C.M. Rush, "High-Frequency Ray Paths in Ionospheric Layers with Horizontal Gradients," *Radio Science*, 20, 95-110, 1985.
3. H.J. Albrecht, "Investigations on Great-Circle Propagation Between Eastern Australia and Western Europe," *Geofisica Pura e Applicata*, 38, 169-180, 1957.
4. R.R. Garcia, Susan Soloman, Susan K. Avery, and G.C. Reid, "Transport of Nitric Oxide and the D-Region Winter Anomaly, *Journal of Geophysical Research*, 92, 977-994, 1987.
5. H.A. Hess, "Investigations of High-Frequency Echoes," *Proceedings of the I.R.E.*, 36, 981-992, 1948.
6. C.F. Campen, W.S. Ripley, A.E. Cole, N. Sissenwine, T.P. Condoron, and I. Solomon, *Handbook of Geophysics*, Revised Edition, ARDC, MacMillan, New York, 1960.

BIBLIOGRAPHY

1. M. Menvielle and A. Berthelier, "The K-Derived Planetary Indices: Description and Availability," *Re. Geophys.*, 29, 415-432, 1991.

PRODUCT INFORMATION

New Autoranging Digital Multimeter

Philips ECG has a new heavy-duty, autoranging digital multimeter with a large, high-contrast display, and full-function design. Special features include a 0.65-inch high 3-1/2 digit LCD with range indicator, rugged construction, and a high-impact plastic case.

Measurement functions include voltage to 750 volts AC/1000 volts DC, current to 20 amps AC/DC, resistance to 20 megohms, plus audible continuity and diode tests. Basic DC accuracy is 0.5 percent; input impedance is 10 megs.

All ECG products are available from authorized Philips ECG distributors. To locate the nearest distributor, consult the "Electronic Equipment and Supplies" section in the telephone directory yellow pages or call toll free, 1-800-526-9354.

Jerry Sevick, *W2FMI*
32 Granville Way
Basking Ridge, New Jersey 07920

6:1 AND 9:1 BALUNS

Although these baluns are more difficult to construct, they have many applications

Many radio amateurs associate the use of the 6:1 and 9:1 baluns with 300-ohm twin lead feeding folded dipoles or 450-ohm "ladder" line feeding single or multi-band antenna systems. But what is neglected (in some cases) is the effect of the height of these antennas above earth and the length of the transmission lines feeding them.

Broadband 6:1 and 9:1 baluns are considerably more difficult to construct than the more common 1:1 and 4:1 baluns. This is especially true when matching 50-ohm cable to impedances of 300 and 450 ohms. Furthermore, there are some important trade-offs in low-frequency response for efficiency.

From what I could gather "on-the-air" or talking to radio clubs, here are probably two of the most common misconceptions regarding the use of these baluns:

- **6:1 baluns.** In free-space, the folded dipole has a resonant impedance close to 300 ohms. It also has this value at a height of about 0.225 wavelength above ground. But at a height of about 0.17 wavelength it is only 200 ohms and at 0.35 wavelength it is 400 ohms (the maximum). In many cases, the 4:1 balun would actually do a better job of matching.
- **9:1 baluns.** Some are unaware of the relationship between the impedance at the input of a transmission line, the characteristic impedance of the line, and the impedance at the end of the line. Because a transmission line has a characteristic impedance of 450 ohms doesn't necessarily mean that a 9:1 balun will perform a satisfactory match to 50-ohm cable. Far from it. For example, if the line is terminated by a halfwave dipole with an impedance of 50 ohms, the 9:1 balun would see 50 ohms when the line is a halfwave long and 4050 ohms when it's a quarterwave long! Broadband baluns cannot be designed to handle impedances as high as 4050 ohms. It's very likely that a well-designed 50:450-ohm balun would experience (particularly on 80 and 160 meters) harmful flux in the core *and* excessive heating because of the large voltage drop along the length of its transmission lines. This problem of presenting very high (and harmful) impedances to baluns is quite prevalent with multi-band antenna systems.

But clearly, there are many applications for 6:1 and 9:1 baluns. They not only include matching 50-ohm cable to balanced loads of 300 and 450 ohms, but also to balanced loads of 8 and 5.6 ohms as well. Furthermore, many of the designs in this article will perform almost as well in unun (unbalanced-to-unbalanced) applications. The trade-off (which is usually very small) is in low-frequency response. Additionally, these baluns could be used to exploit the low-loss properties of 300 and 450 twin-lead where very long transmission lines are used. This is especially important at 14 MHz and above.

In the pages that follow, I'll present a variety of baluns* matching 50-ohm cable to 300 ohms (actually to 312.5 ohms, a 6.25:1 ratio) and to 450 ohms as well as 50-ohm cable to 8 ohms and 5.6 ohms. Also included are two different versions of 6.25:1 baluns. One is a series-type using a 1.56:1 unun in series with a 4:1 Guanella balun and the other a series-parallel arrangement using two 4:1 Guanella baluns. Since the series-parallel balun adds voltages of equal

*Kits and finished units available from Amidon Associates, Inc., 2216 East Gladwick Street, Dominguez Hills, California 90220.

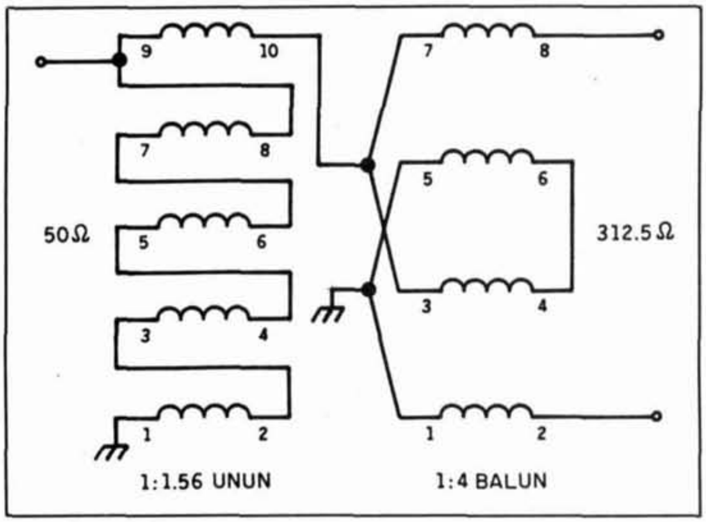

Figure 1. Schematic diagram of the series-type balun with a 1:6.25 ratio designed to match 50 ohms to 312.5 ohms.

delays, you'll find its high-frequency capability is much greater.

The 9:1 balun is a conventional Guanella balun with three transmission lines connected in series at the high-impedance side and in parallel at the low-impedance side. Therefore, it also sums voltages of equal delays. Some of the comparisons and analyses of these 6.25:1 and 9:1 baluns are probably published for the first time in this article.

6.25:1 series-type baluns

Figure 1 shows the schematic diagram of a series-type balun designed to match 50-ohm cable to a balanced load of 312.5 ohms. It consists of a 1:1.56 unun in series with a 1:4 Guanella balun. The overall ratio of 1:6.25 should satisfy most of the 1:6 requirements. **Photo A** shows three examples. All three baluns use the same step-up unun consisting of four quintufilar turns on a 1.5-inch OD ferrite toroid with a permeability of 250. Winding 9-10 is no. 14 H Thermaleze wire and the other four are no. 16 H Thermaleze wire. Because this unun sums only one direct voltage with four equally delayed voltages, it has an excellent high-frequency response.[1]

The balun on the left in **Photo A** has eight bifilar turns of no. 18 hook-up wire on each transmission line of its 1:4 balun. The wires are further spaced with no. 18 Teflon® tubing giving a characteristic impedance close to 150 ohms (the optimum value). The ferrite toroid has a 2.4-inch OD and a permeability of 250. When matching 50-ohm cable to a floating load of 312.5 ohms, the response is essentially flat from 1.7 to 30 MHz. A conservative power rating, under matched conditions, is 500 watts of continuous power and 1 kW of peak power. Since the 1:4 balun in this series-type 1:6.25 balun uses only one core instead of two, this transformer should never be used when the load is grounded at its center. This series-type balun presents balanced currents and not balanced voltages.

The balun in the center of **Photo A** has seven bifilar turns of no. 16 SF Formvar wire on each transmission line on its 1:4 balun. The wires are covered with Teflon sleeving and further separated by no. 16 Teflon tubing. The characteristic impedance is also close to the objective of 150 ohms. The toroid also has a 2.4-inch OD and a permeability of 250. When matching 50-ohm cable to a floating load of 312.5 ohms, the response is essentially flat from 3.5 to 30 MHz. Over this frequency range, this balun can easily handle the full legal limit of amateur radio power. Because this

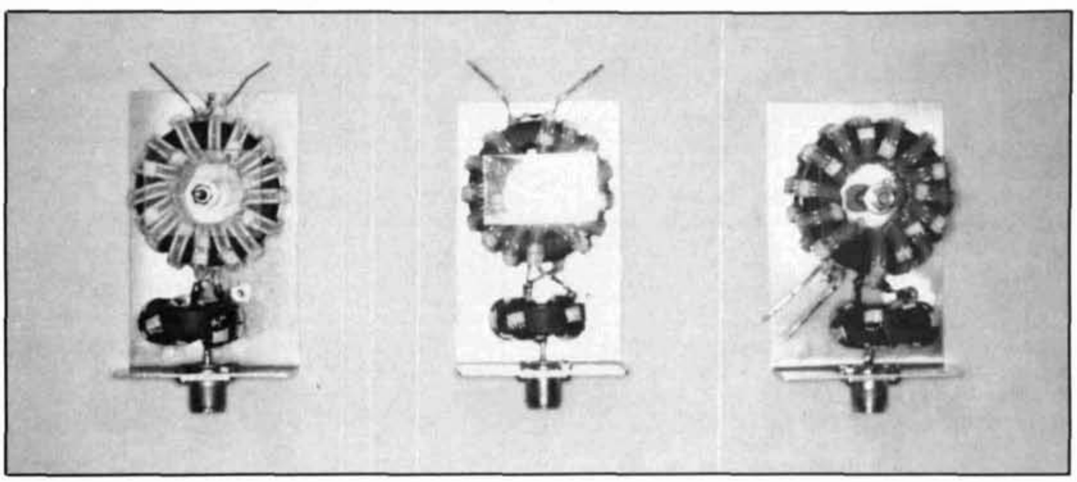

Photo A. Three examples of series-type 1:6.25 baluns. The balun on the right, with a double-core 1:4 balun, has both a balanced voltage and current output. The other two only have balanced-current outputs.

balun also presents balanced currents and not balanced voltages, it should not be used when the load is grounded at its center.

The balun on the right in **Photo A** has fourteen bifilar turns of no. 16 SF Formvar wire on each of the two toroids of the 1:4 balun. The wires are also covered with Teflon sleeving and further separated by no. 16 Teflon tubing. For ease of connection, one core is wound clockwise and the other counter- clockwise. When matching 50-ohm cable to a 312.5 load that is either floating, grounded at its center, or grounded at its bottom (a broadband unun), the response is essentially flat from 1.7 to 30 MHz. Under this matched condition, it can easily handle the full legal limit of amateur radio power. Furthermore, this is a true balun because it presents equal currents and equal voltages. If one were to measure the voltages-to-ground, when matching into a balanced load, one would find them to be equal and opposite. The other two 1:6.25 baluns using single-core 1:4 baluns, would have equal currents but not equal voltages.[2] Since they are easier to construct, they should be tried.

Figure 2 shows the schematic diagram of a series-type balun designed to match 50-ohm cable to a balanced load of 8 ohms (perhaps a short-boom Yagi). It consists of a 1.56:1 step-down unun in series with a Guanella 4:1 step-down balun. The over-all ratio is 6.25:1. **Photo B** shows two examples. Both baluns use the same step-down unun which has four quintufilar turns on a 1.5-inch OD ferrite toroid with a permeability of 250. Winding 5-6 is no. 14 H Thermaleze wire and the other four are no. 16 H Thermaleze wire. The interleaving of the wires is such that the performance is optimized for matching 50 ohms to 32 ohms.

The balun shown on the left in **Photo B** has four turns of low-impedance coaxial cable on each transmission line on the single-core 4:1 balun. The inner conductor is no. 14 H Thermaleze wire and it has two layers of Scotch no. 92 polyimide tape. The outer braid is from a small coax (or 1/8 inch tubular braid) and is tightly wrapped with Scotch no. 92 tape to achieve the 17 ohm characteristic impedance (the optimum value). The ferrite toroid has a 1.5-inch OD and a permeability of 250. When matching 50-ohm cable to a floating load of 8 ohms, the response is flat from 1 to 40 MHz. In a matched condition, this balun can easily handle the full legal limit of amateur radio power.

The balun on the right in **Photo B** has six turns of the same coaxial cable on each of the two cores of the Guanella step-down balun. The cores also have a 1.5-inch OD and a permeability of 250. The performance of this balun is practically the same as the balun above with the single-core 4:1 balun. The main differences are that this 6.25:1 balun also performs as well whether the load is center-tapped-to-ground or grounded at the bottom (a broadband unun).

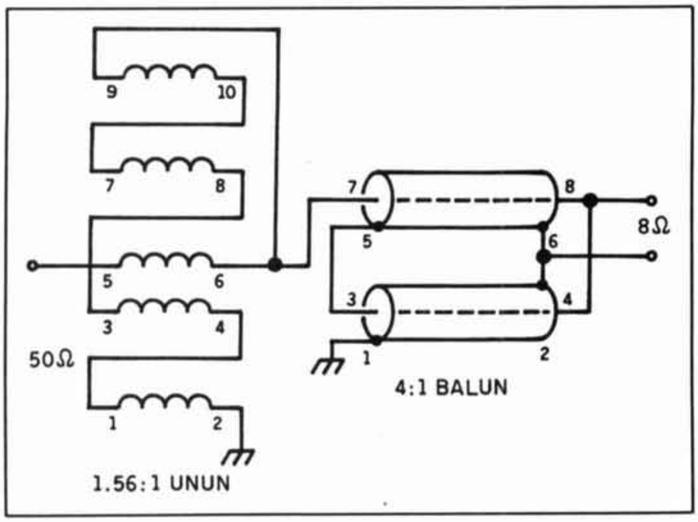

Figure 2. Schematic diagram of the series-type balun with a 6.25:1 ratio designed to match 50 ohms to 8 ohms.

6.25:1 parallel-type baluns

The 6.25:1 series-type baluns described in the previous section actually consisted of a 1.56:1 unun, which is an extension of Ruthroff's "bootstrap" approach for ununs,[1] and a Guanella 4:1 balun.[2] The upper-fre-

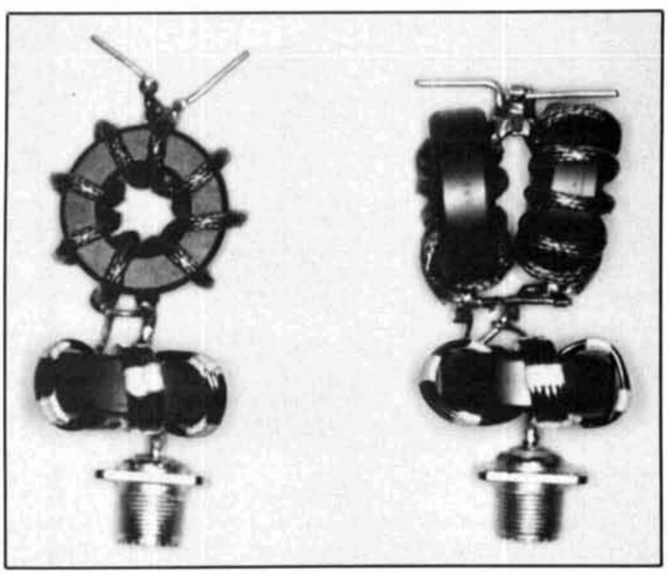

Photo B. Two examples of the series-type 6.25:1 balun optimized at the 50:8-ohm level. The balun on the left is designed to match into a floating 8-ohm load. The balun on the right is designed to match into an 8-ohm floating, center-tapped-to-ground or grounded load and (unun).

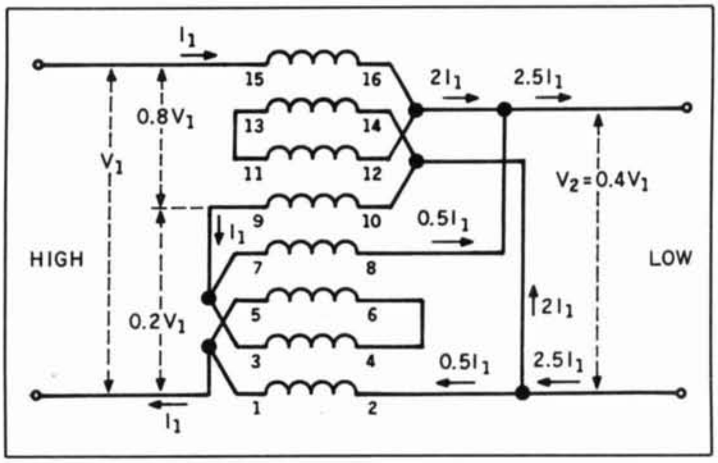

Figure 3. Schematic diagram of the parallel-type balun (and unun) with a 6.25:1 ratio. The currents and voltages are shown for analysis purposes (see text).

quency limit for this combination is really set by the unun, which sums a direct voltage with four delayed voltages. The parallel-type 6.25:1 baluns described in this section are really extensions of Guanella's approach, which sums voltages of equal delays. Therefore, the upper-frequency limit is mainly dependent upon the parasitics in the interconnections.

The 6.25:1 parallel-type balun uses two 4:1 Guanella baluns connected in parallel on the low-impedance side and in series on the high-impedance side. As you will see, one of the baluns is reversed giving the desired ratio of 6.25:1. Other combinations can produce different fractional-ratios (other than $1{:}n^2$ where n is 1, 2, 3,. . .) like 2.25:1 and 1.78:1. Since very little practical design information is available[3,4] on this family of very broadband baluns, this section also includes my high-frequency analysis of the 6.25:1 parallel-type balun. It should also be pointed out that very little sacrifice in performance occurs whether the load is grounded at its center or at the bottom (as an unun).

Figure 3 shows the coiled-wire version of the 6.25:1 parallel-type balun. For analysis purposes, the voltages and currents are also shown. As can be seen, the top 4:1 balun is connected as a step-down balun while the bottom 4:1 balun is connected as a step-up balun. The baluns are in series on the high-impedance side (on the left) and in parallel on the low-impedance side (on the right). As **Figure 3** illustrates, the lower 1:4 balun adds a current of $0.5\ I_1$ to the load resulting in a total current of $2.5I_1$. Thus the impedance transformation ratio is 2.5^2 or 6.25:1.

For maximum high-frequency response, each transmission line should see a load equal to its characteristic impedance. In other words, they should be "flat" lines. If the high side on the left is 50 ohms, then 40 ohms appears on the input of the top balun and 10 ohms on the input of the bottom balun. Thus the optimum characteristic impedance for *all* transmission lines is 20 ohms. On the low-impedance side on the right, the top balun wants to see 10 ohms while the bottom balun wants to see 40 ohms. Since 10 ohms in parallel with 40 ohms equals 8 ohms, each balun conveniently sees its ideal load and a broadband ratio of 6.25:1 is obtained.

If the balun is required to match 50-ohm cable (on the right side) to a balanced load of 312.5 ohms (on the left side), the same analysis shows that the optimum characteristic impedance of all the transmission lines is 125 ohms.

Because the parallel-type balun (or unun)

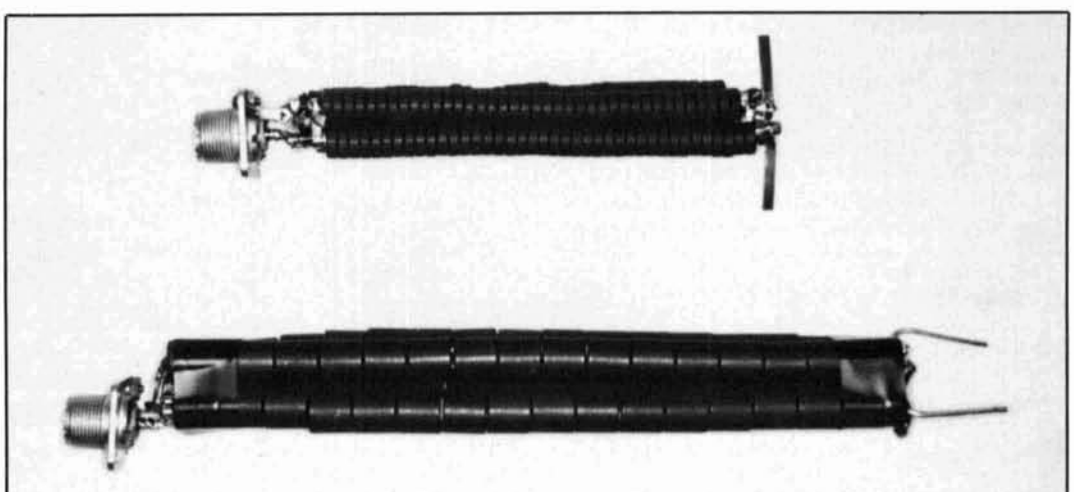

Photo C. Two beaded-line versions of the parallel-type 6.25:1 balun (and unun). The top transformer is designed to match 50-ohm cable to 8 ohms. The bottom transformer is designed to match 50-ohm cable to 312.5 ohms.

sums voltages of equal delays and therefore has no built-in high-frequency cut-off, it has a real advantage over the series-type balun in the VHF band and above. Furthermore, beaded transmission lines with low-permeability ferrite beads (125 and less) can be used resulting in high efficiencies. In the HF band where coiled windings are generally used, the series-type balun is preferred because of its simplicity.

Photo C shows two beaded-line 6.25:1 transformers. The top balun, designed to match 50-ohm cable (on the left) to 8 ohms (on the right), uses low-impedance coaxial cable lines. The schematic diagram is shown in **Figure 4**. It has 5 inches of 0.375 inch OD beads (permeability 125) on four coaxial cables with characteristic impedances of 20 ohms. The inner-conductors of no. 12 H Thermaleze wire have two layers of Scotch no. 92 polyimide tape. The outer braids, from small coaxial cable or 1/8-inch tubular braid, are also wrapped tightly with the same tape in order to preserve the 20-ohm characteristic impedance. When matching 50 ohms to 8 ohms, the response is essentially flat from 10 MHz to beyond 100 MHz (the limit of my simple bridge). Under this matched condition, this balun can easily handle the full legal limit of amateur radio power. Furthermore, it has practically the same performance when operating as an unun (both terminals 1 and 2 grounded). In the unun application, the bottom transmission line has no voltage along it and therefore requires no beads.

The bottom balun in **Photo C**, which is designed to match 50-ohm cable to a balanced load of 312.5 ohms, has 8 inches of 0.5-inch OD beads on 125-ohm twin lead transmission lines. The ferrite beads also have a permeability of 125. The wires are no. 14 H Thermaleze wire and are covered with Teflon sleeving. They are further separated by no. 18 Teflon tubing. When matching 50-ohm cable (on the right side) to 312.5 ohms (on the left side), the response is essentially flat from 20 MHz to over 100 MHz. Under this matched condition, this balun can also easily handle the full legal limit of amateur radio power. Additionally, this transformer performs practically as well when used as an unun.

9:1 baluns

The broadband 9:1 balun, matching 50-ohm cable to a balanced load of 450 ohms, is one of the most difficult ones to construct because high-impedance transmission lines (150 ohms) are required for maximum high-frequency response and greater

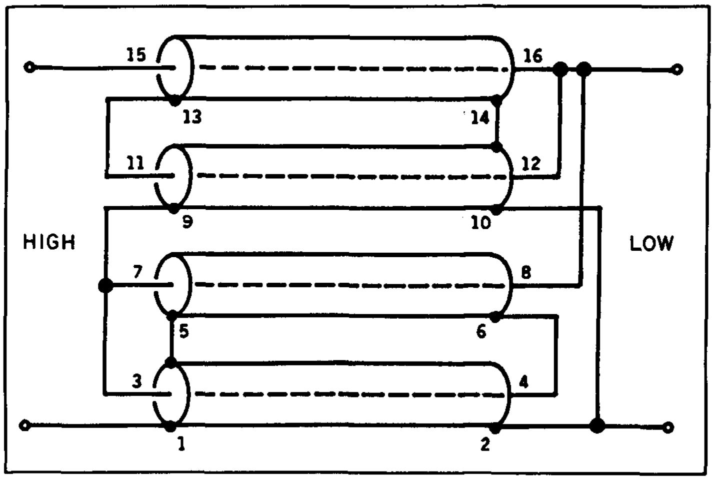

Figure 4. Schematic diagram of the coaxial-cable version of the parallel-type 6.25:1 balun (and unun).

reactances are needed in order to isolate the input from the output. In order to appreciate the task at hand, this section also provides a brief review of the theory of these devices.[1]

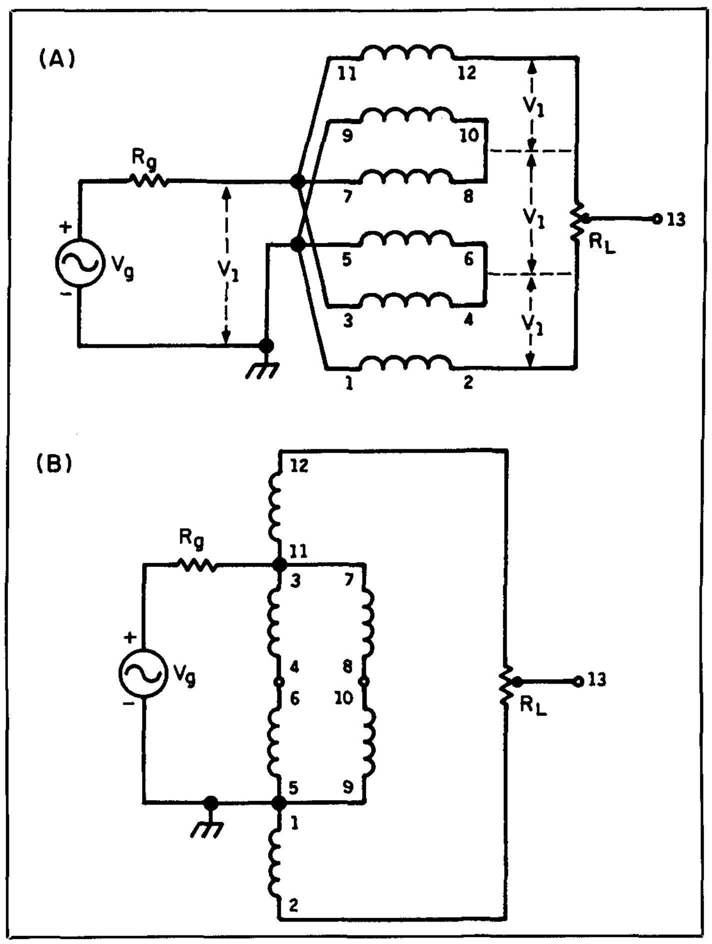

Figure 5. Models of Guanella's 1:9 balun: (A) high-frequency model. It assumes that $Z_0 - R_L/3$, and therefore V_2, the output of each transmission line equals V_1; and (B) low-frequency model. It assumes no energy is transmitted to the load, R_L, by a transmission line mode.

Figure 5 shows the high and low-frequency models of the Guanella 9:1 balun which connects three transmission lines in series at the high impedance side and in parallel at the low-impedance side. Since Guanella's baluns (which can be easily converted to ununs) sum voltages of equal delays, they offer the highest frequency capability.

The high-frequency model (**Figure 5A**) assumes that there is sufficient choking reactance in the coiled (or beaded) transmission lines to isolate the input from the output and only allow transmission line currents to flow. Under this condition the analysis is rather straightforward, since it only involves transmission line theory. Simply stated—the maximum high-frequency response occurs when each transmission line is terminated in a load equal to its characteristic impedance, Z_0. Thus the transmission lines in the 9:1 balun have no standing waves. Because each transmission line sees one-third of the load, the optimum value of Z_0 is $R_L/3$. Except for parasitics in the interconnections and self-resonances in coiled windings, Guanella's approach is literally "frequency independent."

On the other hand, the low-frequency analysis of the Guanella 9:1 balun is most important because it reveals the major difficulty in designing them for low-loss, wideband operation. **Figure 5B** is the model for determining the low-frequency response. It assumes that no energy is transmitted to the load by a transmission line mode. Although the terminology and analysis is the same as that used for conventional autotransformers, the similarity ends when there is sufficient choking reactance to only allow for the efficient transmission line mode.

As with conventional transformers, one can analyze the low-frequency response of the 9:1 balun from either the low or high-impedance side. By putting the generator on the low-impedance side in **Figure 5B**, I've chosen to analyze it from the low-impedance side. With the output open-circuited, the generator sees four coiled (or beaded) lines connected in series-parallel. The net result is that the generator sees the reactance of only *one* coiled (or beaded) line. In order to prevent a shunting current to ground (and/or autotransformer operation), the reactance the generator sees should be much greater than R_g (at least by a factor of 10 at the lowest frequency of interest). The inductance of the coiled or beaded line that prevents the unwanted currents is still known as the magnetizing inductance, L_M.

But what is important to point out here is that the low-frequency model of the Guanella 4:1 balun does not have the series-parallel combination of coiled or beaded lines.[1,2] Only two lines, which are in series, exist in its model. Therefore, for a two-core Guanella balun having the same number of turns (and same cores) as a 9:1 Guanella balun, its low-frequency response is better by a factor of two.

Another advantage that goes to the Guanella 4:1 balun lies in the number of turns that can be wound on the same cores. Because 4:1 baluns require characteristic impedances of 100 ohms (instead of 150), the width of the transmission lines is considerably less, allowing for more turns. Also, as will be shown later, the efficiency of the 4:1 balun is greater because the potential drops along the transmission lines are less (less dielectric loss). And finally, as you can see in **Figure 5B**, by also grounding terminal 2 (unun operation), windings 1-2 and 3-4 are both shorted, thus degrading the low-frequency response because L_M is reduced by one-third.

Another interesting analysis of baluns and ununs concerns the potential gradients (voltage drops) along the transmission lines. Since the loss with these transformers, when transferring the energy by a transmission line mode, is a dielectric-type (that is, voltage-dependent), the higher the gradient, the greater the loss. The interesting cases are when the load is: a) floating, b) grounded at the center, and c) grounded at the bottom (an unun).

Floating load. With terminal 13 in **Figure 5A** ungrounded, the top transmission line has a gradient of $+V_1$ and the bottom transmission line has a gradient of $-V_1$. The center transmission line has a gradient of zero. Therefore, the center transmission line only acts as a delay line and doesn't require a magnetic core or beads. As a result, the top and bottom cores (or beads) account for the dielectric loss.

Load grounded at the center. With terminal 13 grounded at the center of the load, the top transmission line has a gradient of $+V_1$, the bottom transmission line has a gradient of $-V_1$, and the center transmission line has a gradient of $-V_1/2$. This configuration results in about 25 percent more loss because of the extra gradient along the center transmission line. Incidentally, this condition exists when matching into balanced systems like 450-ohm transmission lines or antennas because they have virtual grounds at the center of the loads they present.

Load grounded at the bottom. With terminal 13 grounded at the bottom of the

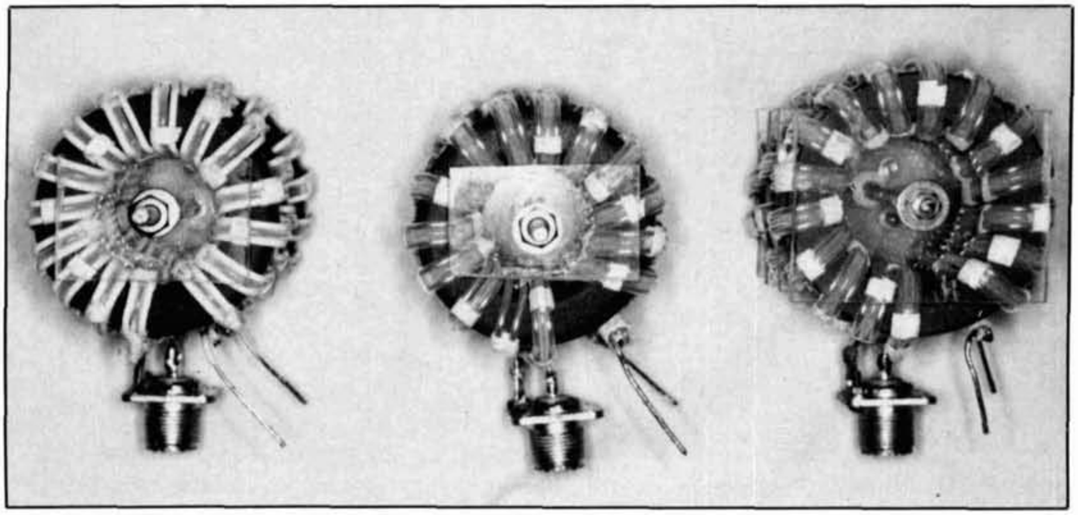

Photo D. Three broadband Guanella 9:1 baluns designed to match 50-ohm cable to 450 ohms. The transformer on the left, using no. 18 hook-up wire, can handle 500 watts from 1.7 to 45 MHz. The transformer in the center, using no. 16 wire, can handle 1 kW from 3.5 to 45 MHz. The transformer on the right (with larger cores) using no. 16 wire, can handle 1 kW from 1.7 to 45 MHz.

load (an unun), the top and center transmission lines have gradients of $+V_1$. The bottom transmission line has no gradient and therefore no loss. It only acts as a delay line and consequently requires no magnetic core or beads.

Some practical 9:1 balun designs

Photo D shows three versions of the broadband Guanella 9:1 balun designed to match 50-ohm cable to 450-ohm loads. The transformer on the left has 15 bifilar turns of no. 18 hook-up wire on each of the three ferrite toroids with a 2.4-inch OD and permeability of 250. The wires are further separated by no. 16 Teflon tubing resulting in a characteristic impedance close to 150 ohms (the optimum value). In matching 50 ohms to 450 ohms, the response is essentially flat from 1.7 to 45 MHz. In this matched condition, this transformer can easily handle 500 watts of continuous power and 1 kW of peak power.

The transformer in the center of **Photo D** has 14 bifilar turns of no. 16 SF Formvar wire on each of the three ferrite toroids with a 2.4-inch OD and permeability of 250. The wires are covered with Teflon sleeving and further separated by no. 16 Teflon tubing. The characteristic impedance is also close to the optimum value of 150 ohms. In matching 50 ohms to 450 ohms, the response is essentially flat from 3.5 to 45 MHz. In this matched condition, this transformer can easily handle 1 kW of continuous power and 2 kW of peak power.

The transformer on the right in **Photo D** is designed to handle 1 kW of continuous power and 2 kW of peak power from 1.7 to 45 MHz. Because this transformer uses larger cores with slightly higher permeabilities (2.68-inch OD and 290 permeability), which are not as popular as those used in the other two baluns, it's much more expensive to construct. It has 16 bifilar turns of no. 16 SF Formvar wire on each toroid. The wires are covered with no. 16 Teflon sleeving and further separated with no. 16 Teflon tubing. In matching 50 ohms to 450 ohms, the response is flat from 1.7 to 45 MHz.

And finally, **Figure 6** shows the schematic diagram of a 9:1 balun (or unun) using coaxial cables wound about ferrite cores or threaded through ferrite beads. This form of the transformer is especially useful when matching 50-ohm cable to 5.6 ohms since the choking reactance of the magnetizing in-

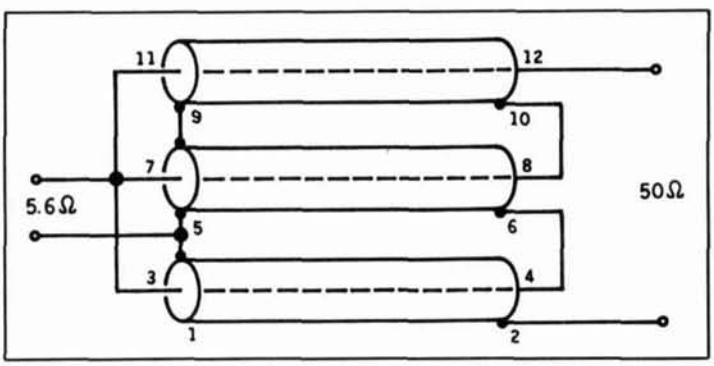

Figure 6. Schematic diagram of a coaxial cable (beaded or coiled) 9:1 Guanella balun (or unun). This design is especially useful in matching 50-ohm cable to 5.6 ohms over a very wide bandwidth.

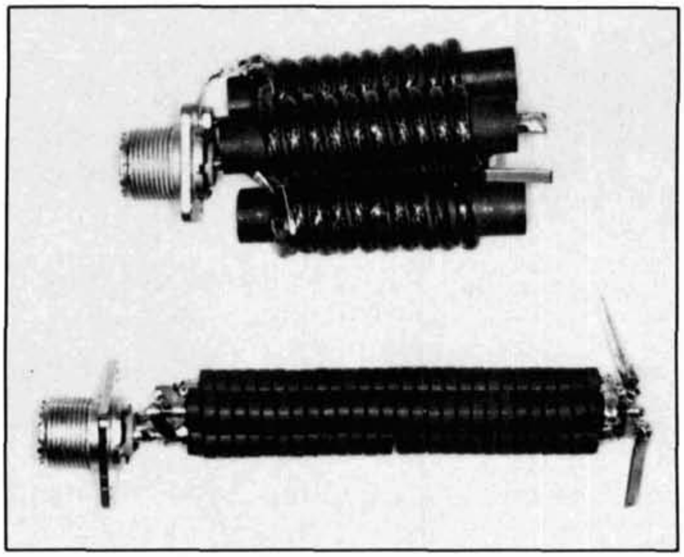

Photo E. Two versions of the coaxial cable 9:1 Guanella balun (or unun) designed to match 50-ohm cable to 5.6 ohms.

ductance, L_M, only has to be much greater than 5.6 ohms. **Photo E** shows two different designs.

The transformer on the top has 9-1/2 turns of low-impedance coaxial cable on each rod. The rods are 1/2 inch in diameter, 2-1/2 inches long, and have a permeability of 125. The low-frequency response of this balun is quite insensitive to the length and permeability of the rods.[1] The inner conductors of the coaxial cables are no. 12 H Thermaleze wire with two layers of Scotch no. 92 tape. The outer braids are from small coax (or 1/8-inch tubular braid). They are also further wrapped with Scotch no. 92 tape in order to preserve the low-impedance of 17 ohms. When matching 50-ohm cable to 5.6 ohms, the response is essentially flat from 1.7 to 30 MHz. The optimum impedance level was found when matching 40 to 4.45 ohms. Adding another layer of Scotch no. 92 tape would optimize this transformer at the 50:56-ohm level. Then the high-frequency response would exceed 100 MHz. This transformer is very efficient and should easily handle the full legal limit of amateur radio power.

The bottom transformer in **Photo E** is designed to match 50-ohm cable to a load of 5.6 ohms in the VHF band. It uses 3-1/2 inches of beads on three low-impedance coaxial cables. The ferrite beads have an OD of 3/8 inch and a permeability of 125. The inner conductors of the coaxes are no. 12 H Thermaleze wire with one layer of Scotch no. 92 tape. The outer conductors are from small coaxes or 1/8-inch tubular braid, and are also tightly wrapped with Scotch no. 92 tape in order to preserve the low characteristic impedance. In matching 50-ohm cable to 5.6 ohms, the response is essentially flat from 7 MHz to over 100 MHz (the limit of my test equipment). This 9:1 balun (or as an unun) can handle the full legal limit of amateur radio power, under matched conditions, because of the low-permeability beads and the low voltage gradients along the lengths of its transmission lines.

Concluding remarks

One of the most important properties of broadband baluns and ununs (which all use ferrites) is their capability of having extremely high efficiencies. Knowing the loss mechanism in these transformers and the trade-off in low-frequency for efficiency, allows one to optimize their applications. In the paragraphs that follow, I'll discuss the losses and trade-offs with the transformers presented in this article. The approach used here should be applicable to all forms of transmission line transformers. This section ends with a review of two recent articles which contained 9:1 baluns. As you'll see, I have some rather different views on the claims made in these articles.

Accurate measurements on many broadband ununs have found the losses to be related to the permeability and the impedance level.[1] Permeabilities greater than 300 resulted in excessive losses. Because these losses are unlike that of the conventional transformer whose losses are current-dependent, it can only be assumed that their losses are voltage dependent—a dielectric-type loss. Therefore, higher-impedance transformers have higher voltage gradients along their transmission line and thus have greater losses. Additionally, it was found that the higher the permeability, the greater the loss with frequency. Taking into account the accurate measurements and the factors noted above, I offer these values of losses for the transformers in this article:

1.56:1 ununs. The 1.56:1 ununs (either step-up or step-down) used in series with Guanella 4:1 baluns to form 6.25:1 baluns have the lowest potential gradients along their transmission lines. Voltage drops of only about 0.2 V_1, where V_1 is the input voltage, exist along their transmission lines. Accurate measurements have shown losses, in a matched condition, of only 0.04 dB. If the cores, which have a permeability of 250, were replaced with cores having 125, the losses could be as low as 0.02 dB over much of the passband. The low-frequency response would still be acceptable at 1.7 MHz. This unun is a natural for matching into 75-ohm hard line when long transmission lines are required.

6.25:1 and 9:1 low-impedance baluns. Baluns matching 50-ohm cable to 8 ohms or to 5.6 ohms, also have very low voltage drops along their transmission lines. Generally, they are about twice that of the 1.56:1 unun. Therefore, the losses with these baluns should be of the order of 0.1 dB in their passbands.

6.25:1 high-impedance baluns. The losses in the series-type baluns are mainly in the 1:4 Guanella baluns which have potential gradients of about 1.25 V_1, where V_1 is the input voltage. From previous measurements at this impedance level, it suggests that the losses (with ferrites of 250 permeability) should be about 0.1 dB at 7 MHz and 0.2 dB at 30 MHz. By using toroids with permeabilities of 125, the losses could be 0.07 dB and 0.15 dB, respectively. But with a permeability of 40, the losses could be as low as 0.05 dB within the passband. However, one must consider the sacrifice in low-frequency response incurred when using these lower-permeability ferrites. With a permeability of 125, it is poorer by a factor of 2. With a permeability of 40, it is poorer by a factor of 8! The 6.25:1 parallel-type balun in this article uses ferrite beads with a permeability of 125 and therefore should have similar losses to its series-type counterpart.

9:1 high-impedance baluns. As was shown in this article, the potential gradient along two of the transmission lines is V_1, where V_1 is the input voltage. The third transmission line, with a balanced load (or as an unun), has no potential gradient and therefore, no loss in its core. Since the loss with the series-type balun mainly exists in one core, the loss with the 1:9 balun should be a little less than twice as great. With ferrite cores of 250 permeability, the suggested losses are 0.2 dB at 7 MHz and 0.4 dB at 30 MHz. With cores of 125 permeability, the losses are about 0.14 dB and 0.28 dB, respectively. Again by using cores with permeabilities of 40, the losses are practically negligible—only about 0.1 dB within its passband.

As in the case of the 1:6.25 baluns above, similar trade-offs occur in the low-frequency response. That is, by using 125 permeability cores, the low-frequency response is poorer by a factor of 2 and with 40 permeability cores, it is poorer by a factor of 8. But the major difference here is that the low-frequency performance of the 9:1 balun, as seen by its low-frequency model, is not as good as the 4:1 balun that controls the low-frequency response of the series-type 1:6.25 balun. Additionally, it should be pointed out that all of the suggested losses for the transformers in this article are for matched conditions—that is with VSWRs of 1:1. If the VSWR is 2:1 due to a load twice as large as the objective, the input voltage to the balun increases by about 40 percent. Therefore, the losses should increase by about the same percentage.

In closing, I would like to report my findings on two recent articles in amateur radio journals that also described 9:1 baluns matching 50-ohm cable to 450 ohms. One[5] advocated using three 150-ohm coaxial cables threaded through high-permeability ferrite beads—a 9:1 Guanella balun. Because of the low voltage-breakdown capability of the coaxial cable and the high loss found by accurate measurements on ununs using these high-permeability ferrites, the design was suspect. A design was constructed and found to be, as expected, unable to handle any appreciable power. The second article[6] advocated using 14 trifilar turns of "magnet wire" on a 2-inch OD powdered-iron core (permeability of 10). This balun was also constructed and tested. Again, as was expected, when matching 50-ohm cable to a floating load of 450 ohms, the 9:1 balun barely reached a true 9:1 ratio at 7 MHz. Above 7 MHz, the ratio became greater than 9:1 and also introduced a reactive component. Below 7 MHz, there was insufficient choking reactance to prevent flux in the core. The three objections to this design are 1) a trifilar design has a poor high-frequency response because it sums a direct voltage with a delayed voltage that traversed a single transmission line and a delayed voltage that traversed two transmission lines, 2) the characteristic impedances of the transmission lines are only 50 ohms (the objective is 150 ohms), and 3) the low-frequency response is poor because of the low-permeability powdered-iron core. Neither of the designs in the two articles are recommended.

REFERENCES

1. Jerry Sevick, W2FMI, *"Transmission Line Transformers,"* 2nd edition, Amateur Radio Relay League, Newington, Connecticut, 1990.
2. Jerry Sevick, W2FMI, "The 4:1 Balun," *Communications Quarterly*, Fall 1992, pages 23-29.
3. S.E. London and S. V. Tomeshevich, "Line Transformers with Fractional Transformation Factor," *Telecommunications and Radio Engineering*, Volume 28/29, April 1974.
4. D. Meyer, "Equal-Delay Networks Match Impedances Over Wide Bandwidths," *MICROWAVES & RF*, April 1990, pages 179-188.
5. John S. Belrose, VE2CU, "Transforming the Balun," *QST*, June 1991, pages 30-33.
6. Carl Markle, K8IHQ, "Wideband RF Baluns," *73 Amateur Radio Today*, September 1992, pages 20-23.

Joseph J. Carr, *K4IPV*
P.O. Box 1099
Falls Church, Virginia 22041

SMALL LOOP ANTENNAS: PART 1

Design and construction notes on an often overlooked receiving antenna

Virtually everyone who studies radio communications soon learns about antenna reciprocity; that is, the well-known fact that an antenna will work exactly alike on both receive and transmit.* An antenna azimuthal pattern, for example, is insensitive to whether the signal is being transmitted or received. Perhaps overlooked, however, is a certain nonreciprocity of applications: some antennas work better for receive applications, others work better for transmitting. However, this statement doesn't contradict well-established antenna theory for we are not talking about electromagnetic reciprocity, which holds true nonetheless, but simple usefulness.

Amateur radio operators in the 160-meter (1800-2000 kHz) and 75/80-meter (3500-4000 kHz) bands sometimes prefer to use two different antennas, one each for receive and transmit functions, because each type of antenna has unique characteristics. The transmit antenna is often a full-size dipole or vertical, where practical, or some loaded variant. The receive antenna is often a small directional loop antenna.

There are two principal uses for small loop antennas in the amateur radio bands. First, there is the traditional radio direction finding (RDF) role. Hidden transmitter hunting, tracking down pirates and interlopers, and finding noise or QRM sources are practical uses for RDF in the amateur bands. The other use, as a main receiver antenna, is perhaps a little less well known, but is nonetheless quite viable. The idea is to use a loop's sharp nulling capability to eliminate interfering cochannel and adjacent channel signals. **Figure 1** shows this use. The small loop has a "figure-eight" pattern with its nulls orthogonal to the plane of the loop.[1] If signals "A" and "B" are on or near the same frequency, such that they will interfere in the receiver, then ordinary reception will be difficult, or even impossible; in any event, it will at least be uncomfortable. According to Villard, around 20 dB of discrimination between the two signals provides generally acceptable results.[2] Even though the desired signal ("B") is not in the highest sensitivity region of the loop's pattern, the null is placed in the approximate direction of the undesired interfering signal ("A"), so the ratio of the two signals at the receiver is sufficient to provide acceptable reception of one signal versus the other.

---

*According to Terman's *Radio Engineering Handbook* page 787, "The reciprocal relation between transmitting and receiving properties of an antenna are incorporated in several theorems, the most important of which was discovered by Rayleigh and extended to include radio communication by John R. Carson, It is to the effect that if an electromotive force E inserted in antenna 1 causes a current I to flow at a certain point in a second antenna 2, then the voltage E applied at this point in the second antenna will produce the same current I (both in magnitude and phase) at the point in antenna 1 where the voltage E was originally applied. *The Rayleigh-Carson theorem fails to be true only when the propagation of the radio waves is appreciably affected by an ionized medium in the presence of a magnetic field, and so holds for all conditions except short-wave transmission over long distances.*"

The ending statement is confusing to hams because of the beginning which is widely quoted and so seemingly self-evident. But a lot of us hams do use short-wave transmission over long distances and we do encounter nonreciprocity.

If one has ever listened, on the east coast, to 75 meters at about 3:00 p.m. of a winter's afternoon, he'd often hear European signals quite strongly, but attempts to work them are nearly always futile—they don't hear us at all. The problem is that signals arrive from Europe over far different paths and conditions than our signals are offered in an attempt to return.

It's worth mentioning that the theorem doesn't hold for all situations, particularly since for many amateurs short-wave transmission over long distances is their main experience. Ed.

The author replies: "I object to the technical editor's note 'disproving' antenna reciprocity on the shortwave bands. This aroument is an old one, and is not correct because it hinges on the fact that the propagation medium between transmit and receive sites is nonlinear. If the same antenna were tested in a chamber, or at a frequency where this propagation doesn't occur, then reciprocity is retained. The editor's argument doesn't disprove reciprocity, but merely proves that thing's can happen to radio waves differently in different directions of transmission.

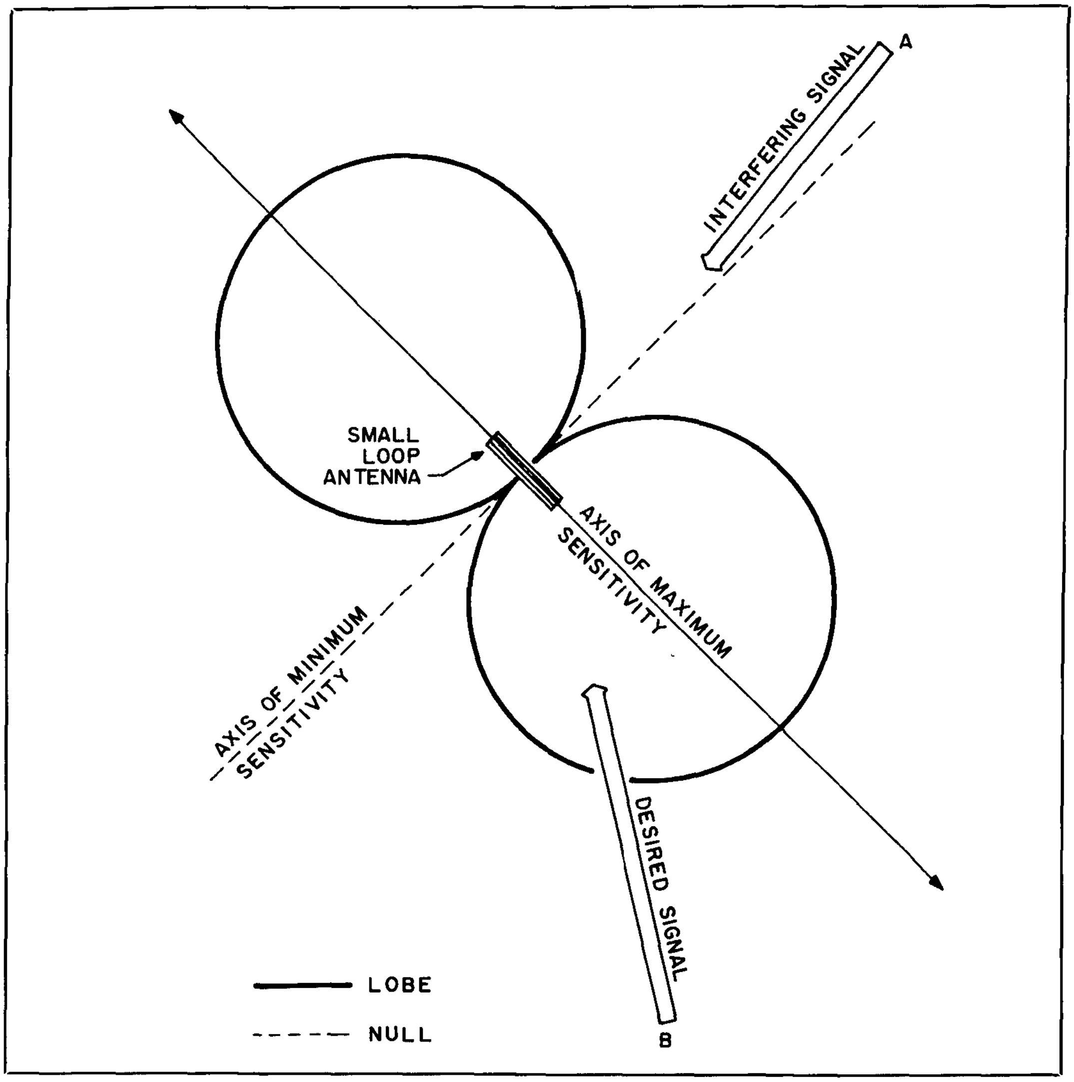

Figure 1. The loop antenna's sharp null can help with rejection of cochannel or adjacent channel interference.

Loop antennas are well represented in the radio literature, although most articles I located in my literature search dealt with the RDF aspects of loops. One article that dealt with the receiving applications was written by W2IMB and appeared in *Ham Radio* in 1975.[3] In this present article, we'll take a look at the design and construction of loops suitable for either RDF or reception in crowded bands.

Small loops versus large loops

Although large loops (like one element of a quad beam) and small loops are superficially similar to each other, they are fundamentally different. Large loop antennas have total wire lengths of 0.5λ or greater, while the length of small loops is $<<\lambda$. The standard square large loop antennas seen in most amateur literature, including the elements of typical quad beams, are full wave (1λ); that is $\lambda/4$ per side. The "Bi-square" loop antenna is typically 2λ, or $\lambda/2$ per side.[4]

Small loop antennas, both circular and square (**Figure 2**), have been defined variously, but in all cases it is agreed that the radius of a circular loop (r), or the side of a square loop (a), is very small compared with one wavelength (a or r $<< 1\lambda$). One World War II United States Navy training manual suggested that RDF loops are $<0.22\lambda$; Jasik used $\leq 0.17\lambda$;[5] Kraus used $\leq 0.1\lambda$;[6] and the ARRL recommends $\leq 0.085\lambda$.[7] It's interesting to note that the far fields of circular and square small loop antennas are approximately equal—provided that $A^2 \leq \lambda/100$, where A is the area.[8]

A defining characteristic of the small loop versus the large loop is that the small loop has a uniform current in all portions of the loop, while the current in a large loop varies along the length of the conductor.[9] The small

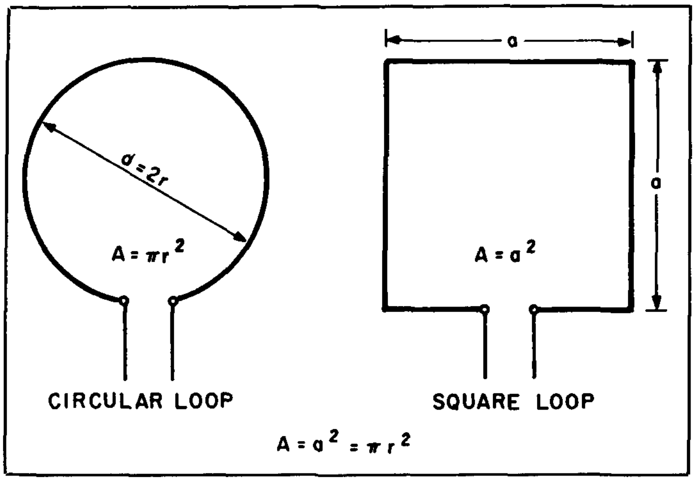

Figure 2. Loop antennas may be made in either circular or square configurations.

loop responds to the magnetic component of the electromagnetic wave radio signal, while the large loop responds to the voltage component of the wave.

The basic form of the square loop is shown in **Figure 3**. This loop is square, with sides the same length "a" all around. The width of the loop ("b") is the distance from the first turn to the last turn in the loop, or, if only one turn is used, the diameter of the wire. The turns of the loop in **Figure 3** are *depth wound*; that is, each turn of the loop is spaced in a slightly different plane, but all planes are parallel. The turns are spaced evenly across distance "b." Alternatively, the loop can be *planar wound*; that is, wound so the turns are in the same plane. In either case, the sides of the loop ("a") should be no less than about five times the width ("b").

The reason why a small loop has a null when its broadest aspect is facing the signal is simple, even though it seems counterintuitive. In **Figure 4**, we have two identical small loop antennas at right angles to each other. Antenna "A" is in line with the advancing radio wave, while antenna "B" is broadside to the wave. Each line in the wave represents a line where the signal strength is the same; i.e., an "isopotential line." When the loop is in line with the signal (antenna "A"), there is a difference of potential from one end of the loop to the other, so current can be induced in the wires. But when the loop is turned broadside, all points on the loop are on the same potential line, so there is no difference of potential between segments of the conductor; thus little signal is induced (and the an-

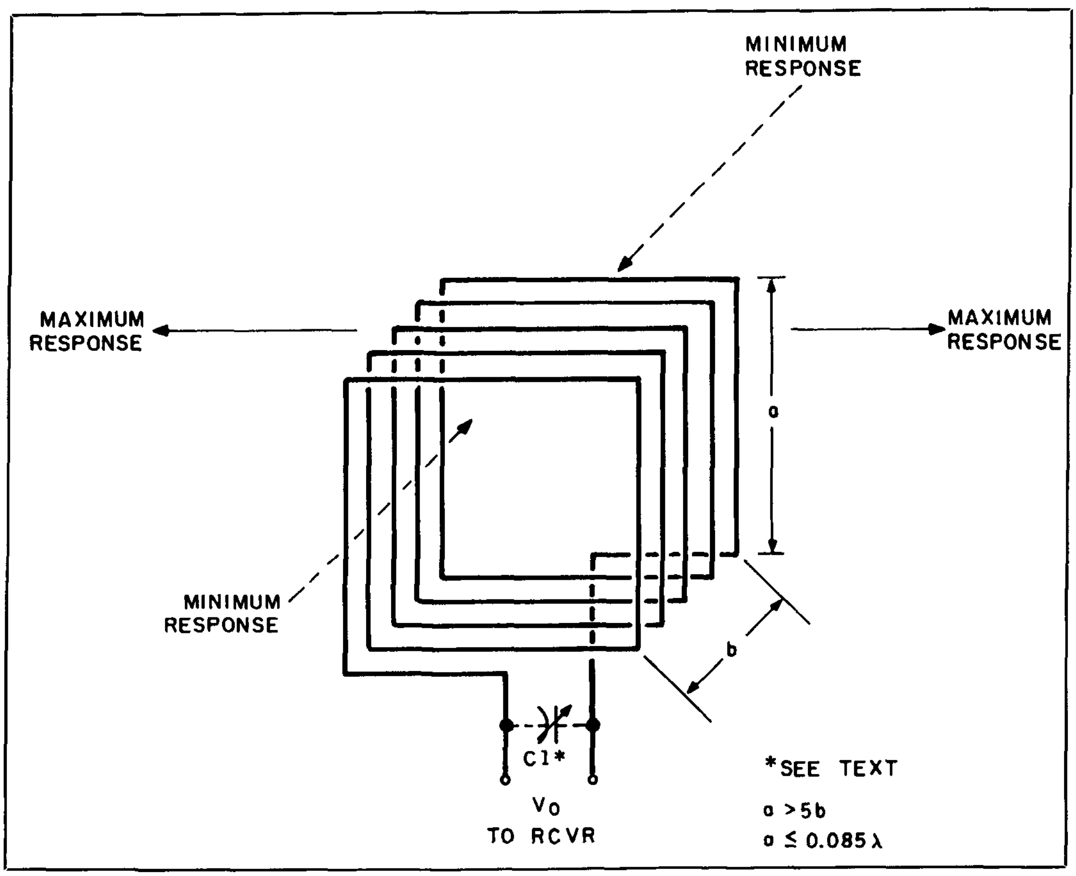

Figure 3. Basic square loop antenna using a "depth wound winding."

tenna therefore sees a null).

The actual voltage across the output terminals of an untuned loop is a function of the angle of arrival of the signal α (see **Figure 5**), as well as the strength of the signal and the design of the loop. The voltage V_0 is given by:

$$V_o = \frac{2\pi ANE_f \cos\alpha}{\lambda}$$

Where:

V_0 is the output voltage of the loop
A is the area of the loop in square meters (m^2)
N is the number of turns of wire in the loop
E_f is the strength of the signal in volts per meter (V/m)
α is the angle of arrival of the signal
λ is the wavelength of the arriving signal

Loops are sometimes described in terms of *effective height* of the antenna. This number is a theoretical construct that compares the output voltage of a small loop with a vertical piece of the same kind of wire that has a height of:

$$H_{eff} = \frac{2\pi NA}{\lambda}$$

If a capacitor (for example, C1 in **Figure 3**) is used to tune the loop, the output voltage V_0 will rise substantially. The output voltage found in **Equation 1** is multiplied by the loaded Q of the tuned circuit, which can be from 10 to 100 (if the antenna is well constructed):

$$V_o = \frac{2\pi ANE_f Q \cos\alpha}{\lambda}$$

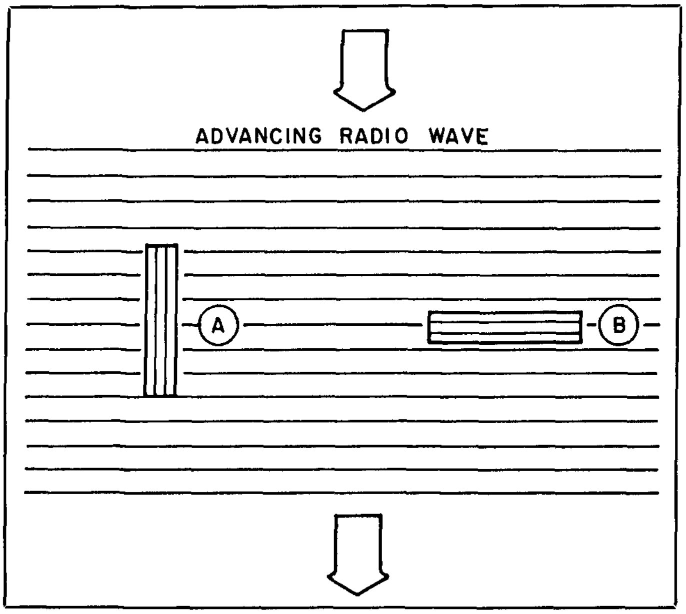

Figure 4. With its broadest aspect facing the signal, small loop antenna is in a deep null.

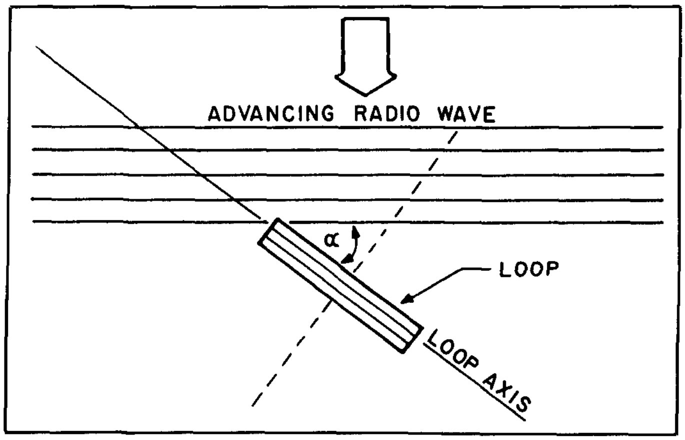

Figure 5. The actual signal voltage developed across the loop antenna windings is a function of the angle of the arriving signal.

Transformer loops

It's common practice to make a small loop antenna with two loops rather than just one. **Figure 6** shows such a *transformer loop* antenna. The main loop is built exactly as discussed above: several turns of wire on a large frame, with a tuning capacitor to resonate it to the frequency of choice. The other loop is a one or two turn *coupling loop*. This loop is installed in very close proximity to the main loop, usually (but not necessarily) on the inside edge and not more than a couple centimeters away. The purpose of this loop is to couple signals induced from the main loop to the receiver at a more reasonable impedance match.

The coupling loop is usually untuned, but in some designs a tuning capacitor (C2) is placed in series with the coupling loop. Because there are far fewer turns on the coupling loop than the main loop, its inductance is considerably smaller. As a result, the capacitance to resonate is usually much larger. In several loop antennas constructed for purposes of researching this article, I found that a fifteen-turn main loop resonated in the AM broadcast band* with a standard 365-pF capacitor that was barely meshed, but the two-turn coupling loop required three sections of a ganged 3 × 365 pF capacitor connected in parallel to resonate at the same frequencies.

In several experiments, I used computer ribbon cable to make the loop turns. This type of cable consists of anywhere from 8 to 64 parallel insulated conductors arranged in a flat ribbon. Properly interconnected

*The AM broadcast band was used because its propagation characteristics are similar to 160 meters, but the stations are always there and local stations have reasonably constant signal strength.

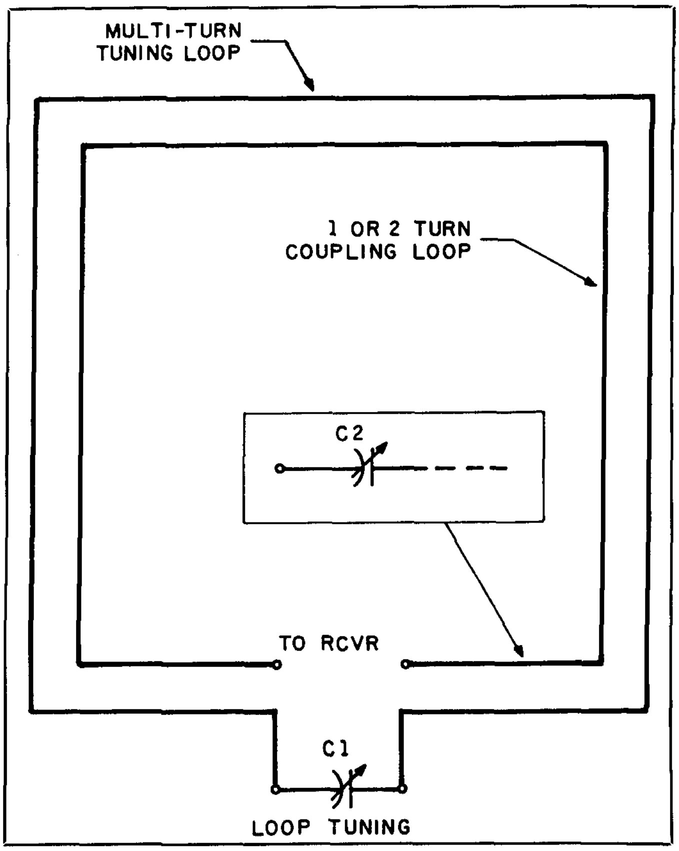

Figure 6. A transformer loop antenna. The primary antenna winding is tunable and resonated at the operating frequency. A small one or two turn coupling loop provides a reasonable impedance match to the receiver.

(more later), the conductors of the ribbon cable form a continuous loop. It's no problem to take the outermost one or two conductors on one side of the wire array and use it for a coupling loop. In a couple of the projects found in Part 2, you'll see the use of both coupling loops and ribbon cable.

Loop inductance

Before a loop antenna can be tuned to resonance, it's necessary to know the loop's inductance. The inductances of typical amateur band loops are surprisingly high for so few turns of wire. There seems to be two different sets of equations in the literature for square loop antenna inductance. Somerfield[10] uses:

$$L = \frac{2 a \mu_o N^2}{\pi} Ln\left(\frac{16 a}{b}\right)$$

Where $\mu_o = 4\pi \times 10^{-7}$, and the turns are spaced on width b, a distance of $b/(N-1)$ apart (that is, close-wound). The Somerfield equations seem to work within an expected error, but Grover's equations[11] seemed closer to the actual inductance in empirical tests that I performed recently:

$$L_{\mu H} = K_1 N^2 a \left(Ln\left(\frac{K_2 a N}{(N+1) b}\right) + K_3 + \left(\frac{K_4 (N+1) b}{a N}\right)\right)$$

Where:

$L_{\mu H}$ is the inductance in microhenrys (μH)
a is the length of a loop side in centimeters (cm)
b is the loop width in centimeters (cm)
N is the number of turns in the loop
K1 through K4 are given in **Table 1**

It didn't seem to make much difference whether the square loop antennas I built were depth wound or planar wound. When the inductance was calculated and the resonating capacitance determined, the calculated results were consistent with the experimental results. The Grover equations are calculated in the MS-DOS BASIC program in **Table 2**. This program is part of a larger program called "ANTLERS" that I wrote for a new book, the *Receiving Antenna Handbook*.*

Tuning schemes for loop antennas

Loop performance is greatly enhanced by tuning the inductance of the loop to the desired frequency. Not only is the bandwidth of the loop reduced, which reduces front-end overload and is in general quite desirable, tuning also increases the signal level available to the receiver by a factor of 10 to 100 times. Although tuning can be a bother if the loop is installed remotely from the receiver, as is sometimes the case, the benefits are well worth it in most instances.

*Available from HighText Publications, 7128 Miramar Road, Suite 15, San Diego, California 92121. Phone: (619) 693-5900.

Shape	K1	K2	K3	K4
Triangle	0.006	1.1547	0.65533	0.1348
Square	0.008	1.4142	0.37942	0.3333
Hexagon	0.012	2	0.65533	0.1348
Octagon	0.016	2.613	0.75143	0.07153

Table 1. Values of K1 through K4 from Equation 5.

Table II
MS-DOS Program For Calculating Loop Inductance

```
1000 'MS-DOS BASIC PROGRAM FOR LOOP ANTENNAS
1010 'Color monitor required. Delete "SCREEN 9" and "LINE..."
1020 'statments to convert to monochrome computers.
1030 'INITIALIZATION
1040    CLS : KEY OFF: SCREEN 9: PI = 22 / 7
1050 'SUBROUTINE FOR RDF LOOP ANTENNAS
1060    CLS : LINE (380, 198)-(148, 137), 3, BF
1070    LOCATE 11, 20: PRINT "                           "
1080    LOCATE 12, 20: PRINT " Radio Direction Finding    "
1090    LOCATE 13, 20: PRINT " Small Loop Option Selected "
1100    LOCATE 14, 20: PRINT "                           "
1110    TIMELOOP = TIMER: WHILE TIMER < TIMELOOP + 2.5: WEND
1120  CLS : 'Draw Loop Antenna Picture
1130    LINE (316, 300)-(165, 300)
1140    LINE (315, 300)-(315, 330)
1150    LINE (165, 300)-(165, 110)
1160    LINE (475, 110)-(165, 110)
1170    LINE (475, 290)-(475, 110)
1180    LINE (475, 290)-(180, 290)
1190    LINE (180, 290)-(180, 120)
1200    LINE (460, 120)-(180, 120)
1210    LINE (460, 280)-(460, 120)
1220    LINE (460, 280)-(195, 280)
1230    LINE (195, 280)-(195, 130)
1240    LINE (445, 130)-(197, 130)
1250    LINE (445, 270)-(445, 130)
1260    LINE (445, 270)-(350, 270)
1270    LINE (350, 270)-(350, 330)
1280    LINE (165, 245)-(120, 245)
1290    LINE (165, 245)-(160, 240)
1300    LINE (165, 245)-(160, 250)
1310    LINE (195, 245)-(235, 245)
1320    LINE (195, 245)-(200, 240)
1330    LINE (195, 245)-(200, 250)
1340    LINE (474, 90)-(166, 90)
1350    LINE (474, 90)-(469, 85)
1360    LINE (474, 90)-(469, 95)
1370    LINE (165, 90)-(170, 95)
1380    LINE (165, 90)-(170, 85)
1390    LINE (165, 107)-(165, 70)
1400    LINE (475, 107)-(475, 70)
1410      LOCATE 12, 30: PRINT " FORM OF THE WIRE LOOP "
1420      LOCATE 14, 30: PRINT " Shape: Square "
1430      LOCATE 16, 30: PRINT " A/B > 5 "
1440      LOCATE 24, 38: PRINT "To Receiver"
1450      LOCATE 17, 14: PRINT "B"
1460      LOCATE 6, 40: PRINT " A "
1470    TIMELOOP = TIMER: WHILE TIMER < TIMELOOP + 7: WEND
1480      CLS : 'Clear screen
1490  GOSUB 2760: 'Get operating frequency
1500  F = FKHZ * 1000
1510 'LOOP INDUCTANCE PROGRAM
1520 'Initialization Routine
1530    CLS : 'Clear screen if not already clear.
1540 'Execution Routine
1550      GOSUB 1750
1560      ON TYPER GOSUB 2030, 2060, 2090, 2120: 'Get constants
1570      GOSUB 2150: 'Determine loop dimensions
1580        IF TYPER = 1 THEN GOSUB 2440: 'Calculation for other
loops
1590        IF TYPER = 2 THEN GOSUB 2440
1600        IF TYPER = 3 THEN GOSUB 2440
1610        IF TYPER = 4 THEN GOSUB 2440
1620      GOSUB 2510: 'Calculate capacitance needed for resonance
1630      CLS : LINE (493, 250)-(100, 145), 3, BF
1640        LOCATE 12, 16: PRINT "                                 "
1650        LOCATE 13, 16: PRINT " Loop Type: "; A$; ""
1660        LOCATE 14, 16: PRINT "                              "
1670        LOCATE 15, 16: PRINT " Inductance: "; : PRINT USING
"####.#"; L;
1680        PRINT " uH       "
```

```
1690        LOCATE 16, 16: PRINT "                              "
1700        LOCATE 17, 16: PRINT " Capacitance to Resonate "; FKHZ;
" KHz: ";
1710     PRINT USING "#####.#"; C; : PRINT " pF"
1720       LOCATE 20, 16: GOSUB 2720: 'Press any key...
1730       GOSUB 2540: 'Determine next step
1740 GOTO 2710: 'Skip to end of program
1750 'Opening Screen
1760     LINE (450, 250)-(100, 100), 3, BF
1770     LOCATE 9, 25: PRINT "                    "
1780     LOCATE 10, 25: PRINT " SELECT TYPE OF LOOP "
1790     LOCATE 11, 25: PRINT "                    "
1800     LOCATE 12, 25: PRINT "      (T)riangle     "
1810     LOCATE 13, 25: PRINT "      (S)quare       "
1820     LOCATE 14, 25: PRINT "      (H)exagon      "
1830     LOCATE 15, 25: PRINT "      (O)ctagon      "
1840     LOCATE 16, 25: PRINT "                    "
1850     LOCATE 17, 25: PRINT "   Make Selection:   ";
1860     TYPE$ = INPUT$(1)
1870     'Test TYPE$ variable
1880        IF TYPE$ = "T" THEN TYPER = 1
1890        IF TYPE$ = "t" THEN TYPER = 1
1900        IF TYPE$ = "s" THEN TYPER = 2
1910        IF TYPE$ = "H" THEN TYPER = 3
1920        IF TYPE$ = "h" THEN TYPER = 3
1930        IF TYPE$ = "O" THEN TYPER = 4
1940        IF TYPE$ = "o" THEN TYPER = 4
1950          IF TYPER < 1 THEN 1750 ELSE 1960
1960          IF TYPER > 4 THEN 1750 ELSE 1970
1970          IF INT(TYPER) = TYPER THEN 1980 ELSE 1750
1980        IF TYPER = 1 THEN A$ = "Triangle "
1990        IF TYPER = 2 THEN A$ = "Square "
2000        IF TYPER = 3 THEN A$ = "Hexagon "
2010        IF TYPER = 4 THEN A$ = "Octagon "
2020 CLS : RETURN: 'End of subroutine
2030 'Subroutine for Triangle Antennas
2040     K1 = .006: K2 = 1.1547: K3 = .65533: K4 = .1348
2050 RETURN
2060 'Subroutine for Square Antennas
2070     K1 = 8.000001E-03: K2 = 1.4142: K3 = .37942: K4 = .3333
2080 RETURN
2090 'Subroutine for Hexagon Antennas
2100     K1 = .012: K2 = 2: K3 = .65533: K4 = .1348
2110 RETURN
2120 'Subroutine for Octagon Antennas
2130     K1 = .016: K2 = 2.613: K3 = .75143: K4 = .07153
2140 RETURN
2150 'Subroutine to determine loop size
2160     CLS : LINE (458, 211)-(149, 152), 3, BF
2170     LOCATE 12, 20: PRINT "
  "
2180     LOCATE 13, 20: PRINT " What is the length of each loop
SIDE "
2190     LOCATE 14, 20: PRINT " in centimeters (cm)?
  "
2200     LOCATE 15, 20: PRINT "
  ";
2210        INPUT A
2220     CLS : 'Now go get depth
2230     CLS : LINE (403, 211)-(149, 152), 3, BF
2240     LOCATE 12, 20: PRINT "                            "
2250     LOCATE 13, 20: PRINT " What is the WIDTH of the loop "
2260     LOCATE 14, 20: PRINT " in centimeters (cm)?          "
2270     LOCATE 15, 20: PRINT "                            ";
2280        INPUT B
2290     CLS
2300     CLS : LINE (394, 211)-(149, 152), 3, BF
2310     LOCATE 12, 20: PRINT "                           "
2320     LOCATE 13, 20: PRINT " Enter the number of turns in "
2330     LOCATE 14, 20: PRINT " the loop                    "
2340     LOCATE 15, 20: PRINT "                           ";
2350        INPUT N
2360     CLS
2370 RETURN: 'End of subroutine
2380 'Calculation for flat wound square loops
2390     A = A / 100: B = B / 100
```

```
2400      XA = 2 * A * 4 * PI * 10 ^ -7 * N ^ 2 / PI
2410      XB = LOG((16 * A) / B)
2420      L = XA * XB: L = L * 10 ^ 6
2430 RETURN: ' End of subroutine
2440 'Subroutine for other types of antenna
2450      NN = N + 1: XA = K1 * N ^ 2 * A
2460      XB = ((K2 * A * N) / (NN * B))
2470      XB = LOG(XB)
2480      XB = XB + K3 + (K4 * NN * B) / (A * N)
2490      L = XA * XB
2500 RETURN: 'End of subroutine
2510 'Calculate resonance
2520      LA = L / 10 ^ 6: C = (1) / (4 * PI ^ 2 * F ^ 2 * LA): C =
C * 10 ^ 12
2530 RETURN: 'End of subroutine
2540 'Subroutine for determing what's next
2550      CLS : LINE (450, 250)-(100, 100), 3, BF
2560      LOCATE 10, 20: PRINT "                          "
2570      LOCATE 11, 20: PRINT " (D)o Another?            "
2580      LOCATE 12, 20: PRINT " (F)inished?              "
2590      LOCATE 13, 20: PRINT "                          "
2600      LOCATE 14, 20: PRINT "  Make Selection:         ";
2610      BB$ = INPUT$(1)
2620         IF BB$ = "D" THEN BB = 1
2630         IF BB$ = "d" THEN BB = 1
2640         IF BB$ = "F" THEN BB = 2
2650         IF BB$ = "f" THEN BB = 2
2660           IF BB < 1 THEN 2540 ELSE 2670
2670           IF BB > 2 THEN 2540 ELSE 2680
2680           IF INT(BB) = BB THEN 2690 ELSE 2540
2690      CLS
2700      ON BB GOTO 1540, 1740
2710 END
2720 'Press Any Key... Subroutine
2730 LOCATE 23, 20: PRINT "Press Any Key To Continue..."
2740 A$ = INKEY$: IF A$ = "" THEN 2740 ELSE 2750
2750 RETURN
2760 'Determine Operating Frequency Subroutine
2770 CLS : LINE (435, 212)-(147, 151), 3, BF
2780 LOCATE 12, 20: PRINT "                                   "
2790 LOCATE 13, 20: PRINT " Enter Desired Operating Frequency "
2800 LOCATE 14, 20: PRINT " in kilohertz (KHz):               "
2810 LOCATE 15, 20: PRINT "                                   ";
2820 INPUT FKHZ
2830 CLS : RETURN
```

The resonant frequency of an inductor/capacitor (LC) tuned circuit is given by:

$$f = \frac{1}{2\pi\sqrt{LC}}$$

Where:

f is the frequency in hertz (Hz)
L is the inductance in henrys (H)
C is the capacitance in farads (F)

Note that these units aren't the normal radio units, e.g., microhenrys (μH) and picofarads (pF), but the root units. Be sure to convert the actual units to farads and henrys (1 F = 10^{12} pF and 1 H = 10^{6} μH).

Equation 6 can be solved for the unknown capacitance needed to resonate the inductance of the loop coil at a desired frequency. The terms are rearranged in the flowing form in order to make that calculation:

$$C = \frac{1}{4\pi^2 f^2 L}$$

There are several different schemes available for tuning; these are detailed in **Figure 7**. The parallel tuning scheme, by far the most popular, is shown in **Figure 7A**. In this type of circuit, the capacitor (C1) is connected in parallel with the inductor, which in this case is the loop. Parallel resonant circuits have a very high impedance to signals on their resonant frequency, and a very low impedance to other frequencies. As a result, the voltage level of resonant signals is much larger than the voltage level of off-frequency signals.

The series resonant scheme is shown in **Figure 7B**. In this circuit, the loop is connected in series with the capacitor. Series resonant circuits offer a high impedance to all frequencies except the resonant frequency (exactly the opposite of the case of parallel resonant circuits). As a result, current from the signal will pass through the series resonant circuit at the resonant frequency, but off-frequency signals are blocked by the high impedance.

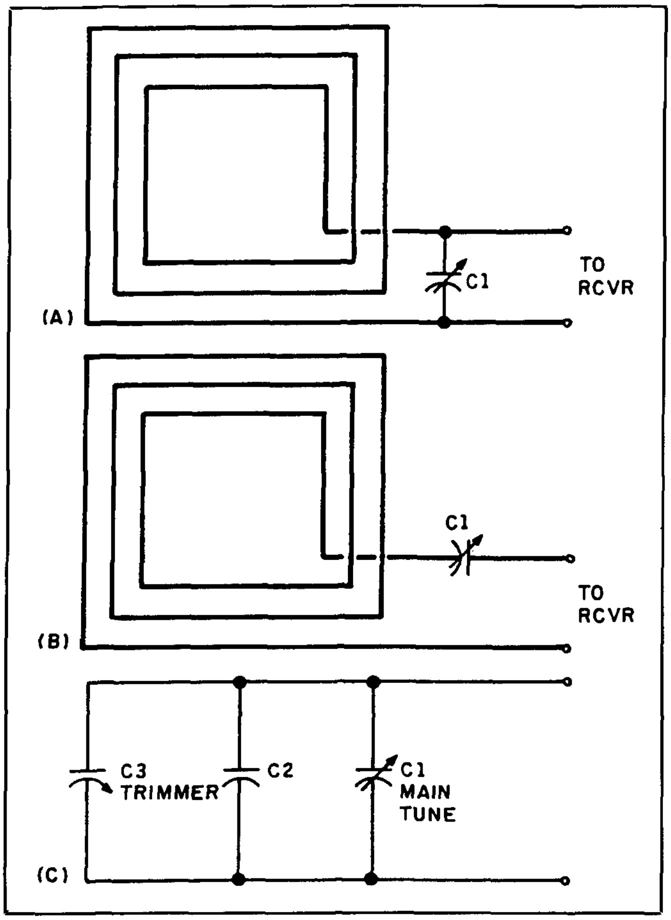

Figure 7. Two forms of loop tuning. Loop 7A is parallel tuned, while loop 7B is series tuned. Fixed padding capacitors may be added across the tuning capacitor if more capacitance is needed (7C).

There's a wide margin for error in the inductance of loop antennas. Even the very precise looking equations are actually estimations. The exact geometry of the loop as built determines the actual inductance in each particular case. Consequently, what often happens is that the tuning provided by the capacitor isn't as exact as desired, so some form of compensation is needed. Alternatively, the capacitance required for resonance isn't easily available in a standard variable capacitor, so some means must be provided for changing the capacitance. **Figure 7C** shows how this is done. The main tuning capacitor can be connected in either series or parallel with other capacitors to change the value. If the additional capacitors are connected in parallel, then the total capacitance is increased (all capacitances are added together). But if the extra capacitor is connected in series, then the total capacitance is reduced to:

$$C_t = \frac{1}{\frac{1}{C1} + \frac{1}{C2} + \ldots \frac{1}{C_n}}$$

The extra capacitors can be switched in and out of a circuit to change frequency bands. I know one fellow who fancies listening to only two distant AM stations, one at 650 kHz and another at 780 kHz, so he used screwdriver adjustable trimmer capacitors to tune the loop to these fixed frequencies. A switch lets him select which capacitor is in the circuit at any given time.

Tuning of the remote loop can be a bother if done by hand, so one needs to find a way to do it from the receiver location (unless you fancy standing on ladders, or climbing into the attic). Traditional tuning methods called for the use of a low RPM DC motor to turn the tuning capacitor. A very popular combination included the little 1 to 12 RPM motors used to drive rotating displays in retail store show windows. That approach isn't really needed today. We can use *varactor* voltage variable capacitance diodes to tune the circuit.

A varactor works because the junction capacitance of the diode is a function of the applied reverse bias voltage. A high voltage (for example, 30 volts) drops the capacitance, while a low voltage increases it. Varactors are available with maximum capacitances of 22, 33, 60, 100 and 400 pF. The latter are of greatest interest because they have the same range as the tuning capacitors normally used with loops. Look for service shop replacement diodes intended for use in AM broadcast band radios. A good selection, which I have used, is the NTE-618 device. It produces a high capacitance >400 pF, and a low of only a few picofarads over a range of 0 to 15 volts.

Figure 8 shows how a remote tuning scheme can work with loop antennas. The tuning capacitor is a combination of a varactor diode (CR1) and two optional capacitors: a fixed capacitor (C1) and a trimmer (C2). The DC tuning voltage (V_t) is provided from the receiver end from a fixed DC power supply (V+). A potentiometer (R1) sets the voltage to the varactor, and also tunes the loop. A DC blocking capacitor (C3) keeps the DC tuning voltage from being shorted out by the receiver input circuitry.

Shielded loop antennas

The loop antennas discussed thus far have all been unshielded types. Unshielded loops work well under most circumstances, but in some cases their pattern is distorted by interaction with the ground and nearby structures (trees, buildings, etc.). In my own tests, trips to a nearby field proved necessary to measure the depth of the null because of interaction with the aluminum sid-

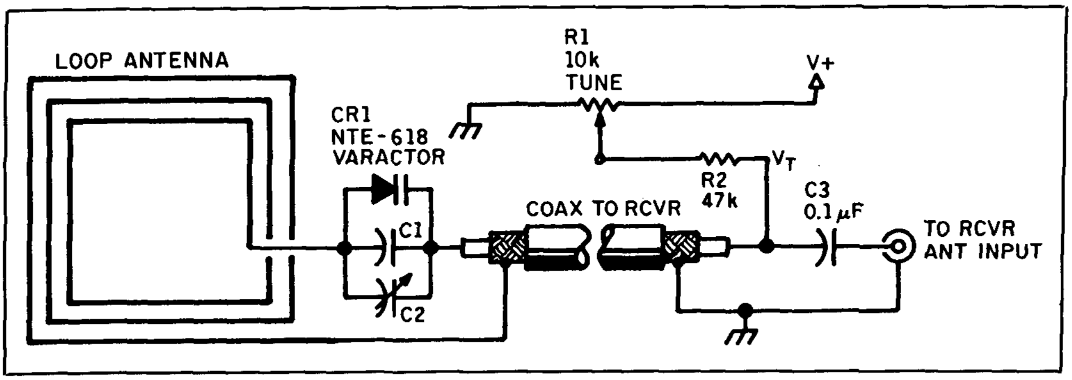

Figure 8. Remote tuning scheme allows the antenna to be mounted some distance from the operating position.

ing on my house. **Figure 9** shows two interaction situations. In **Figure 9A** we see the pattern of the normal "free-space" loop; that is, a perfect figure-eight pattern. But when the loop interacts with the nearby environment, the pattern distorts. In **Figure 9B**, we see some filling of the notch for a moderately distorted pattern. Some interactions are so severe that the pattern is distorted beyond all recognition. The distortion of **Figure 9B** is actually quite small compared to what is possible.

The solution to the problem is to reduce interaction by shielding the loop, as in **Figure 10A**. Loop antennas operate on the magnetic component of the electromagnetic wave, so the loop can be shielded against *voltage* signals and electrostatic interactions. A gap is left in the shield at one point to preserve the ability to pick up the magnetic field.

There are several ways to shield a loop. One can, for example, wrap the loop in adhesive backed copper foil tape. Or, alternatively, one can wrap the loop in aluminum foil and hold it together with tape. Still another technique is to insert the loop inside a copper or aluminum tubing frame. Or. . .the list seems endless. Perhaps one of the most popular methods is to use coaxial cable to make a large single-turn loop. **Figure 10B** shows this type of loop made with RG-8/U or RG-11/U coaxial cable. The cable is normally supported by wooden cross arms, as in the other forms of loop, but they are not shown here for sake of simplicity. Note that, at the upper end, the coaxial cable shields aren't connected.

Twin-loop directional antenna

So what do you do if the offending station and the desired station are in a direct line with each other, and your receiving location is between them, as in **Figure 11**? Both nulls and lobes on a loop antenna are bidirectional, so a null on the offending station will also null the desired station in the opposite direction. You could use a small whip "sense" antenna to spoil the pattern of the loop into a cardioid shape.[12]

It's also possible to use a spoiler loop to null the undesired signal. The spoiler loop is a large box loop placed one to three feet (found experimentally) behind the reception loop; i.e., in the direction of the offending signal. This method was first described by Levintow, and is detailed in **Figure 11**.[13] The small loopstick may be the antenna inside the receiver, while the large loop is a box loop like the Sports Fan's Loop anten-

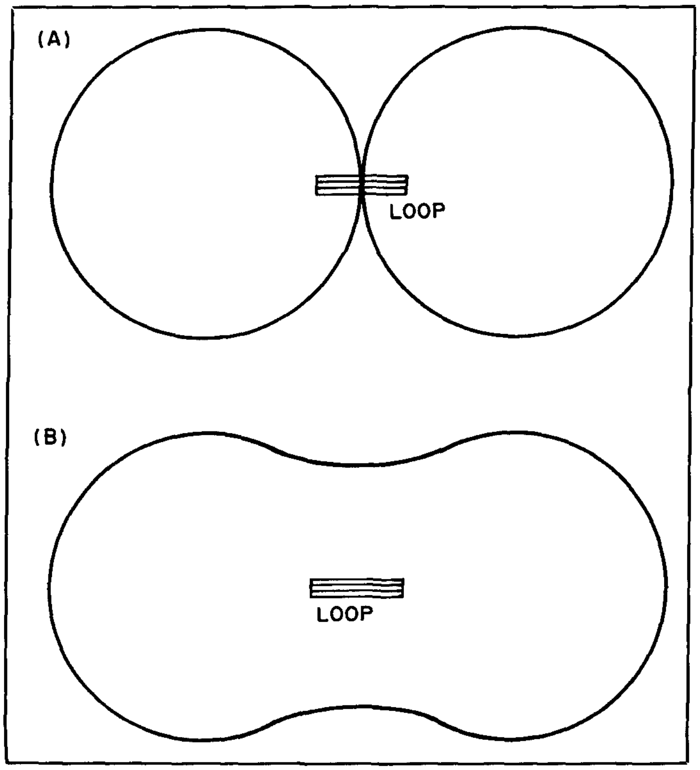

Figure 9. *Ideal text figure-eight pattern for the free space loop is shown* in 9A. Figure 9B shows a real-world pattern that can occur when the antenna interacts with the nearby environment.

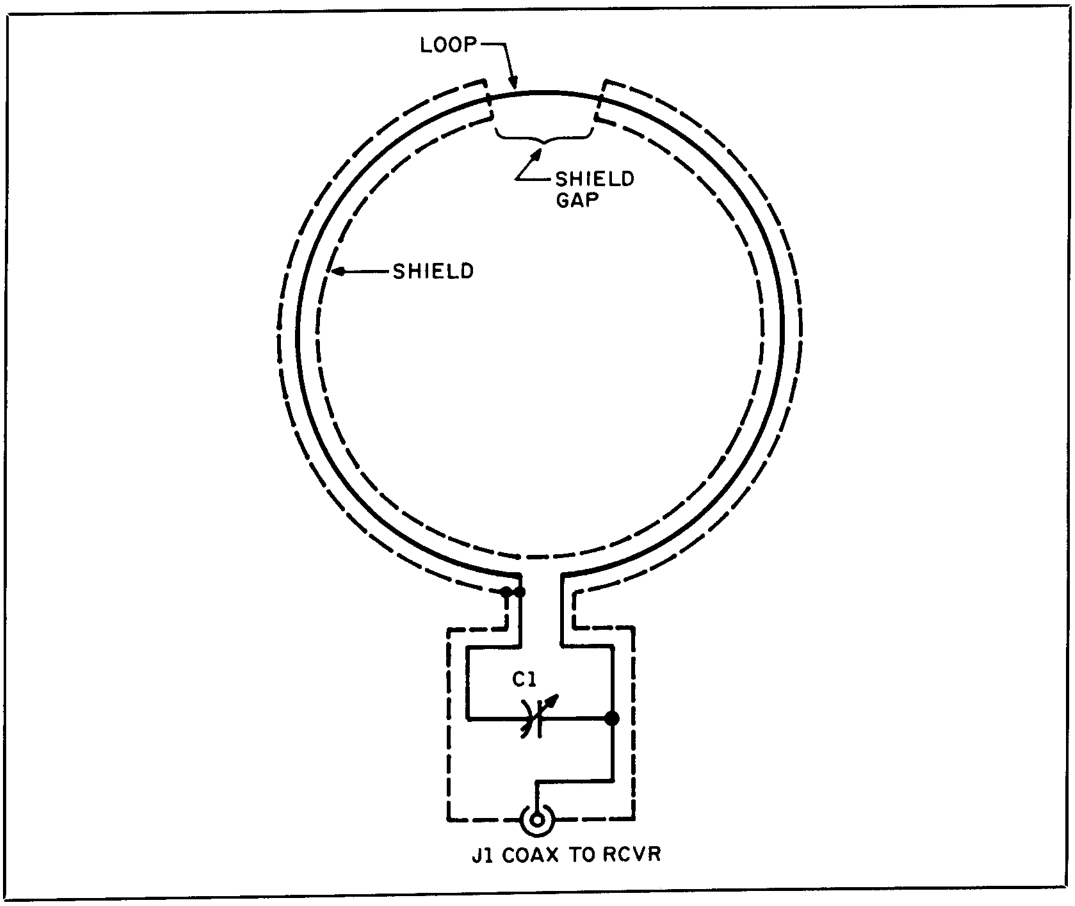

Figure 10A. Shielding the loop antenna against voltage signals and electrostatic interaction allows the antenna to respond only to the magnetic component of the signal.

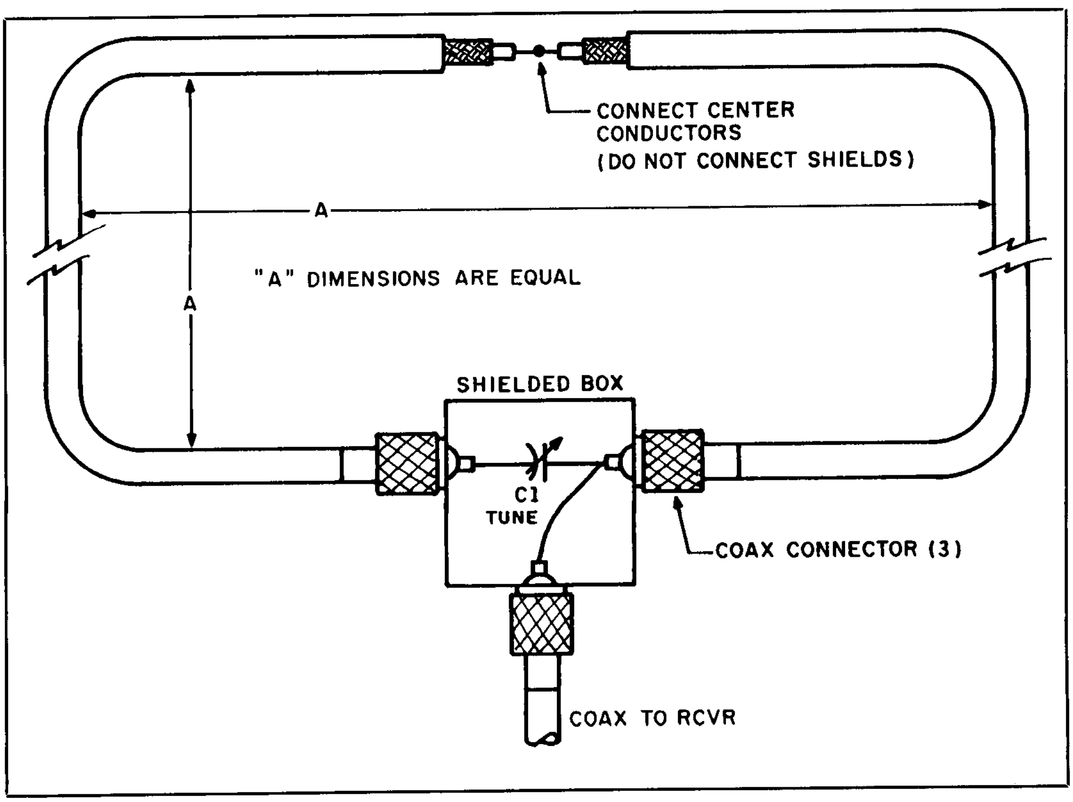

Figure 10B. A practical shielded loop antenna constructed from a large turn of coaxial cable.

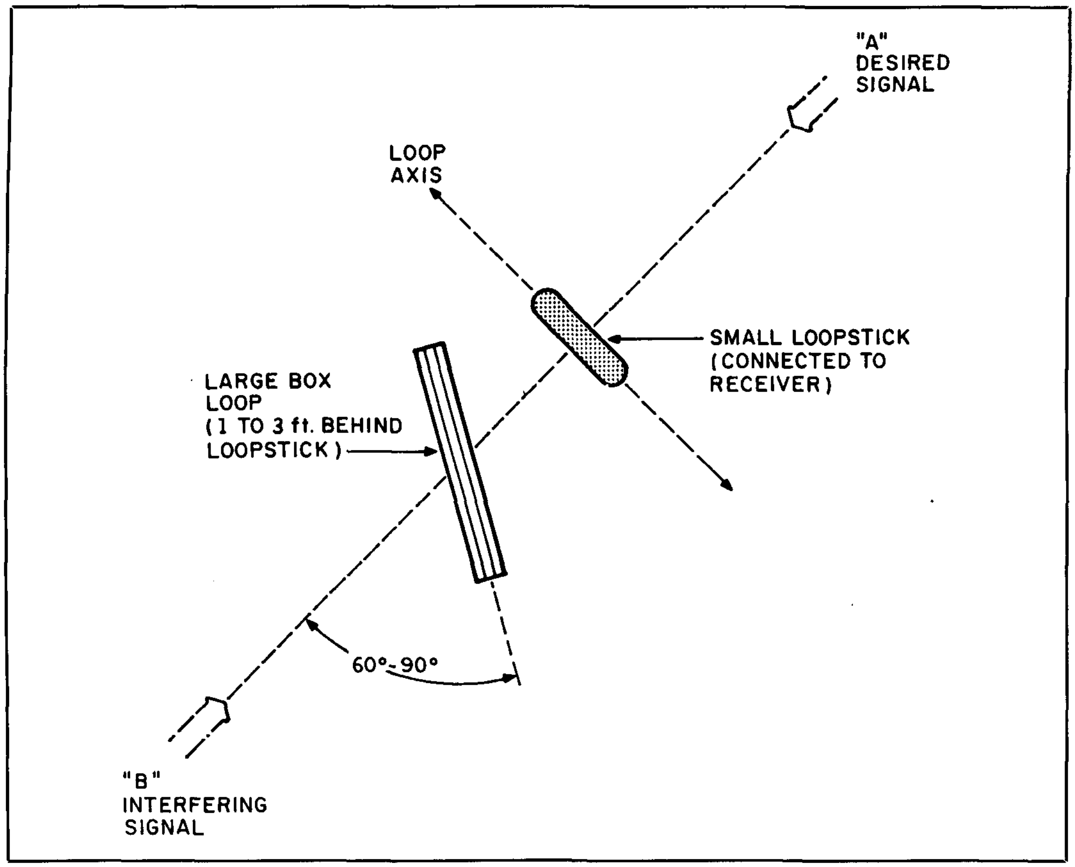

Figure 11. The figure-eight pattern may be distorted into a cardioid pattern by using a small whip "sense" antenna or by using a second "spoiler" loop in conjunction with the loop antenna.

na. The large box loop is found about 1 to 3 feet (exact distance found experimentally) behind the loopstick, in the direction of the offending station. The angle with respect to the line of centers should be 60 to 90 degrees, which is also found experimentally.

Next, in Part 2. . . .

In Part 2 we'll take a look at loop preamplifier circuits, and at some practical loops I built while researching this article.

REFERENCES

1. *The ARRL Antenna Book*, Amateur Radio Relay League, Newington, Connecticut, 1988, page 5-1ff.
2. O.G. Villard, Jr., "Combatting Interference in Shortwave Reception with Compact Indoor Antennas," SRI International, Menlo Park, California. Draft copy of an article intended for *World Radio Television Handbook*, dated October 24, 1989.
3. Ken Cornell, W2IMB, "Loop Antenna Receiving Aid," *Ham Radio*, May 1975, pages 66-70. See also any recent edition of *The ARRL Antenna Book*.
4. John D. Heys, G3BDQ, *Practical Wire Antennas: Effective Designs for the Radio Amateur*, Radio Society of Great Britain, Potters Bar, Herts., England, 1990, 1991.
5. Henry Jasik, Editor, *Antenna Engineering Handbook, McGraw-Hill Book Company, New York, 1961.*
6. *John D. Kraus, Antennas*, McGraw-Hill Book Company, New York, 1950.
7. *The ARRL Antenna Book* (op cit).
8. Kraus (op cit).
9. Kraus (op cit) and ARRL (op cit).
10. A. Somerfield, *Electrodynamics*, Academic Press, New York, 1952, page 111; cited in T.H. O'Dell, "Resonant-Loop Antenna for Medium Waves," *Electronics World* + Wireless World, March 1992, page 235.
11. F.W. Grover, *Inductance Calculation-Working Formulas and Tables*, D. VanNorstrand Co., Inc., New York, 1946. Cited in ARRL (op-cit).
12. Joseph J. Carr, K4IPV, Ham Radio Column, *Popular Electronics*, June 1992.
13. Mike Levintow, "Using Two Loop Antennas to Generate Asymmetrical Receiving Patterns," National Radio Club reprint no. A13. National Radio Club Publications Center, P.O. Box 164, Mannsville, New York, 13661; catalog of reprints in $1.

PRODUCT INFORMATION

E.E. Public Domain Library Operates BBS

The E.E. Public Domain Library's bulletin board service (BBS) is operational 24 hours a day. The BBS supports forums on a number of topics of interest to engineers. It provides for downloading of all 32 disks in the library plus many other public domain programs. For additional information call the BBS at (516) 681-1612, write: E.E. Public Domain Library, 36 Irene Lane East, Plainview, New York 11803, or phone (516) 938-6769 between the hours of 10 a.m. and 8 p.m. Eastern time.

Rick Littlefield, *K1BQT*
109A McDaniel Shore Drive
Barrington, New Hampshire 03825

QUARTERLY DEVICES

The Collins Mechanical Filter: "Back to the Future"

Old-timers licensed in 1952 will no doubt recall the best ham band receiver money could buy back then—the Collins 75A-2. This radio provided switchable IF selectivity and razor-sharp adjacent-channel rejection thanks to a new device called the Collins Mechanical Filter. Shortly thereafter, the now famous 51J and R390 general-coverage receivers appeared on commercial and military markets using the same filter technology. The rest is history. During the '50s and '60s, Collins mechanical filters dominated HF radio production as the industry standard of excellence. Collins Radio and scores of other manufacturers gobbled them up by the tens-of-thousands, as fast as the factory could turn them out.

A few years later, high-frequency crystal filters and high-tech imported transceivers would take a giant bite out of Collins' domination of the amateur radio market. But, as any seasoned KWM-2 buff knows, when it's contest time on Kilowatt Alley, the venerable old mechanical filter can still hold court with the best. And, given this distinguished record of performance, it should be no surprise that a Collins Division of Rockwell International still makes them—some 40 years and 3.5 million pieces later.

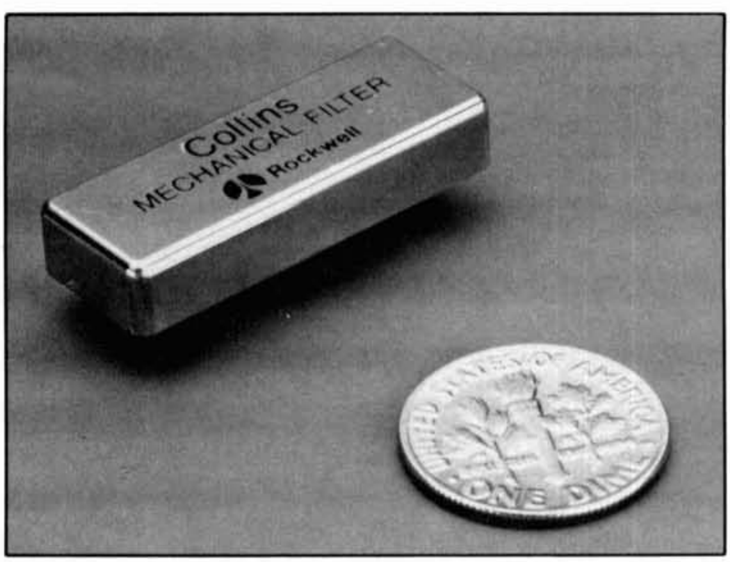

She ain't what she used to be

Although the mechanical filter has been around for a long time, there's been a lot of change in these devices over the years. Walk through any flea market, and you're likely to find an interesting cross-section of aging government-surplus Collins filters representing early offerings. S-Line and KWM-2 owners will no doubt recognize the familiar shape of the case shown in **Photo A**. This "classic" 455-kHz package was manufactured in huge quantities and many bandwidths. Collins owners often hunted down and installed wider or narrower versions to customize their radios especially for rag-chewing or chasing DX.

Today's Collins filter is a whole new breed of cat. While maintaining traditionally impressive performance, the latest packaging is much smaller (see **Photo B**). In relative terms, today's mechanical filters are also smaller in price. But, before I get into specifics, let's review how the mechanical filter works—and how Collins was able to take an industry standard and improve upon it.

How mechanical filters work

The mechanical filter is an acoustic device. At one end, a resonant piezoelectric transducer converts 455-kHz electrical energy into mechanical vibrations (see **Figure 1**). These minute vibrations propagate down a series of precision-tuned metal resonators tied together by stiff coupling wires to form

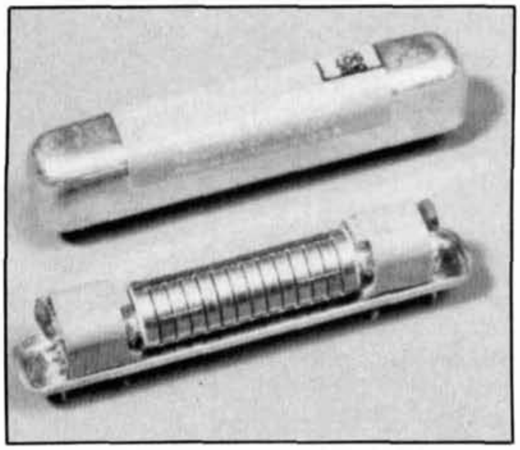

Photo A. Disc-Wire mechanical filter.

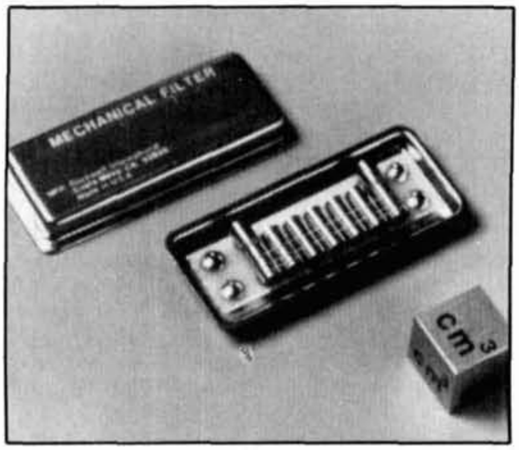

Photo B. Torsional mechanical filter.

a ladder network. Acoustical energy falling within the frequency window of the network will excite the resonators and pass to the far end of the ladder with little energy loss. However, acoustical energy falling outside the frequency window does not pass, but is reflected back to the source. At the far end of the ladder, the surviving vibrations are converted back into an electrical waveform by a second piezoelectric transducer.

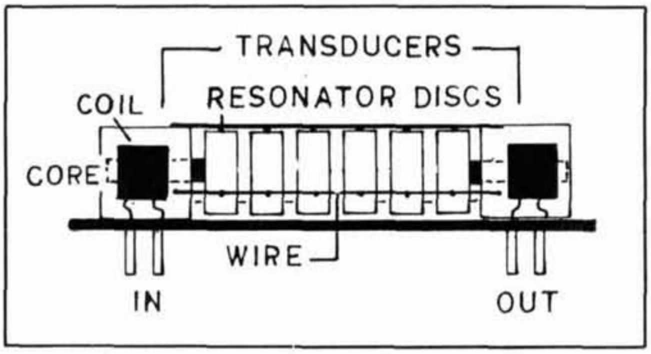

Figure 1. Input transducer converts 455-kHz waveform to acoustic vibrations. Metallic resonators suspended on wire propagate in-band vibrations to far end. Output transducer converts vibrations back to electrical signal.

A new mousetrap

All mechanical filters work on the basic principle outlined above. However, designs like the one depicted in **Figure 1** and **Photo A** are called Disc-Wire devices. A series of tablet-shaped metallic resonators make up the frequency-critical elements of the filter ladder, and these vibrate in "flexure" when excited by the input transducer. While this style filter is still being manufactured, its mechanical structure does not lend itself well to further miniaturization.

In 1985, responding to demand for miniaturized filters, Collins introduced a newer design called a Torsion-Resonator device. This was adapted from frequency division multiplex (FDM) telephone transmission technology, and uses special nickel-iron alloy cylindrical-shaped rods that vibrate in a twisting motion rather than in flexure. Torsion resonator rods are considerably smaller in diameter than the older-style discs—and reasonably short (a second-mode resonator for 455 kHz is about 1/4 inch long). As shown in **Figure 2**, this particular rod shape lends itself to compact "flat-pack" packaging.

New low-cost, low-profile AM, SSB, and CW filters

Until recently, torsional filters were quite expensive to build. Then, in 1990, Collins began to implement a new High-tech production capability that enabled them to produce a new line of inexpensive 455-kHz torsional filters for use in competitively priced consumer and commercial products. This

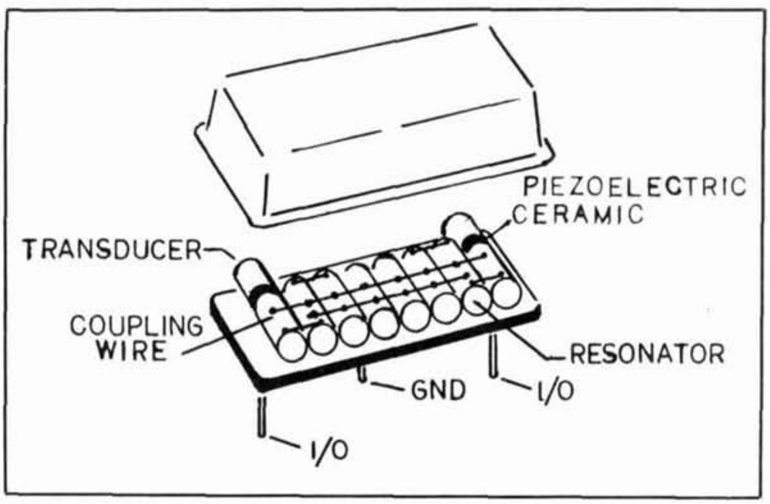

Figure 2. Nickel-iron alloy torsional resonators are smaller, permitting miniaturized "flat-pack" packaging.

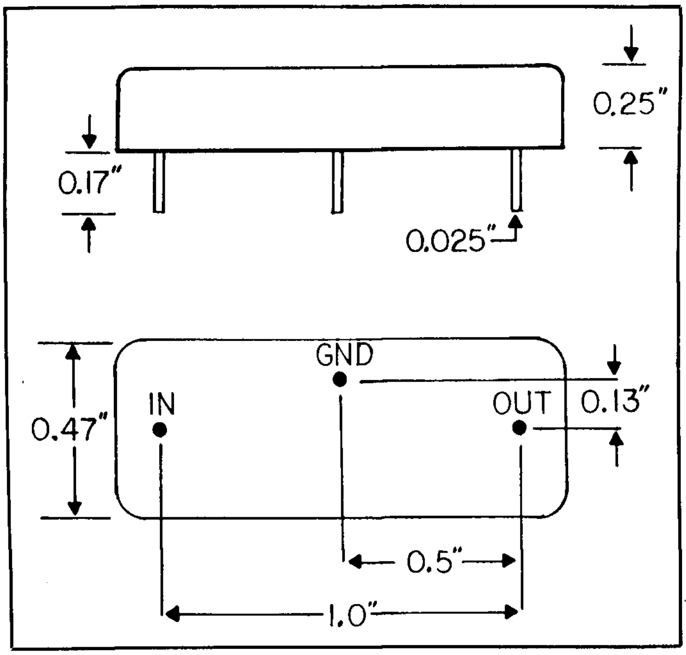

Figure 3. Package dimensions for SP-style filter case.

production capability includes automated tuning using computer-controlled robotic handling and laser tuning.

The new line of Collins filters is available in AM, CW, and SSB bandwidths. Each comes in a low-profile "SP" package, which is a miniature 3-pin metal case designed to complement high-density pc-board layouts (see **Figure 3** for precise dimensions). General filter specifications—plus a complete rundown of AM, SSB, and CW specifications—are given in **Table 1**. An accompanying frequency response graph visually depicts the passband characteristics for each filter type.

According to Collins applications engineers, the new filters are especially well-suited for establishing AM, SSB, or CW passband selectivity in any receiver or transceiver employing double or triple conversion. In addition, 455-kHz filters may be used in some HF single-conversion applications where extreme simplicity and high-perform-

Specifications (0 °C to 60 °C)

	CW 526-8634-010	SSB 526-8635-010	AM 526-8636-010
Center frequency (kHz)	455 ± 0.15	455 ± 0.15	455 ± 0.3
3 (dB) bandwidth (kHz)	0.5 ± 0.1	2.5 ± 0.1	5.5 Min
60 dB bandwidth (kHz)	2 Max	5.2 Max	11 Max
No. of resonators	7	8	8
Passband variation (dB)	3 Max	3 Max	3 Max
Insertion loss (dB)	6 Max	5 Max	5 Max
Spurious rejection (± 100 kHz) (dB)	60 Min	60 Min	50 Min

Common Specifications

Shock	100 Gs ll ms
Vibration	MIL STD 202
Storage temperature	− 30 °C to + 85 °C
Source & load impedance	2-k/30 pF
Max input level	1 volt RMS

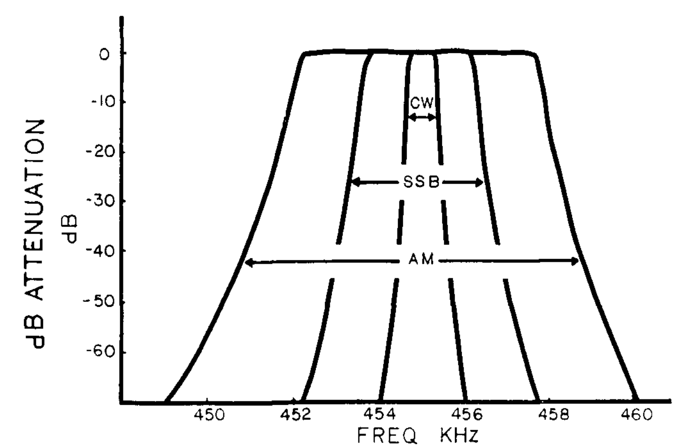

Table 1. General filter specifications with frequency response graph.

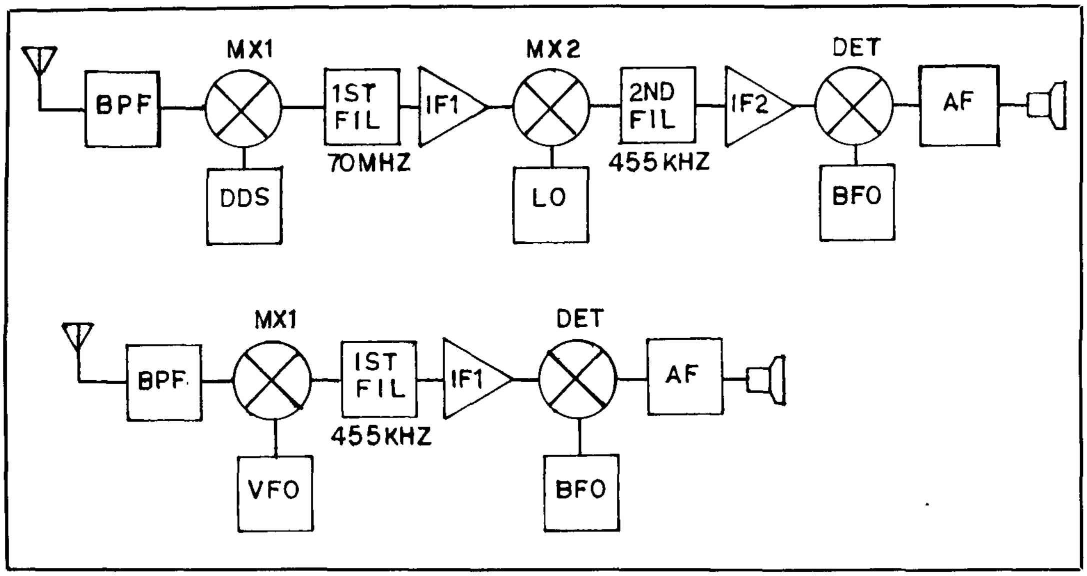

Figure 4. Typical receiver configurations using a 455-kHz filter to determine passband response.

ance are needed (see **Figure 4** for typical receiver circuit configurations).

Collins mechanical filters, which are well known for steep skirt selectivity and symmetrical passband response, can benefit SSB transmitter designs by improving carrier suppression and by ensuring equal passband cutoff on both USB and LSB (crystal ladder filters are often less symmetrical). The favorable shape factor of mechanical filters also provides excellent rejection of adjacent channel interference in receivers. All three filters have a 2-k input and output impedance that provide a direct match to popular Gilbert-cell mixers like the NE602 and LM1496. **Figure 5** illustrates the recommended termination for lowest insertion loss and best passband response. From a practical standpoint, there can be a secondary cost benefit derived from using 455-kHz filters. Inexpensive 455-kHz ceramic resonators, which are easily pulled in frequency for USB, LSB, or LO injection, are easily substituted for expensive custom-ground crystals.

In addition to performing well, torsional filters are unusually temperature-stable and rugged. As the temperature versus frequency plot shows in **Figure 6**, little frequency drift occurred at extremes of temperature. Data for repetitive shock-testing at 100-Gs also showed little change in center-frequency performance. This data suggests that these filters will hold up well in rough-service applications.

Advanced applications

Mechanical filters have traditionally been used for establishing the final message-channel bandwidth in communications equipment. With the advent of DSP for this purpose, one might question the future role of mechanical filters in advanced receiver design. However, according to Rockwell applications engineers, employing DSP does not automatically eliminate the need for tight IF filtering. Even DSP-enhanced receivers require rigorous IF bandwidth limiting to prevent aliasing during analog-to-digital conversion. The excellent selectivity, low passband ripple, and temperature stable group-delay characteristics of torsional filters also make them especially attractive for both DSP and narrow-band data transmission applications.

Where and how to get them

Whether your goal is to build a data-compatible commercial SSB transceiver, a handheld global-positioning receiver, or simply the ultimate miniature QRP backpacking rig, the new low-cost line of Collins mechanical filters may be your best bet for top performance and rugged reliability. Product literature and samples are available directly

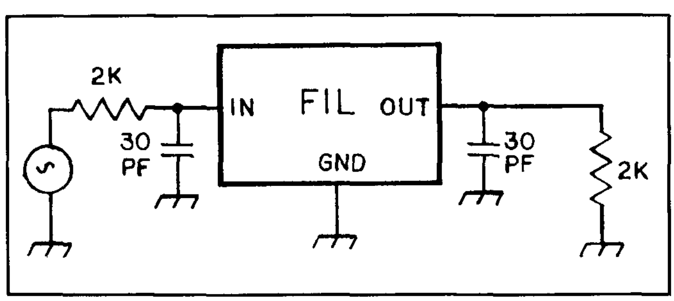

Figure 5. Termination circuit for Collins 455-kHz torsional filters.

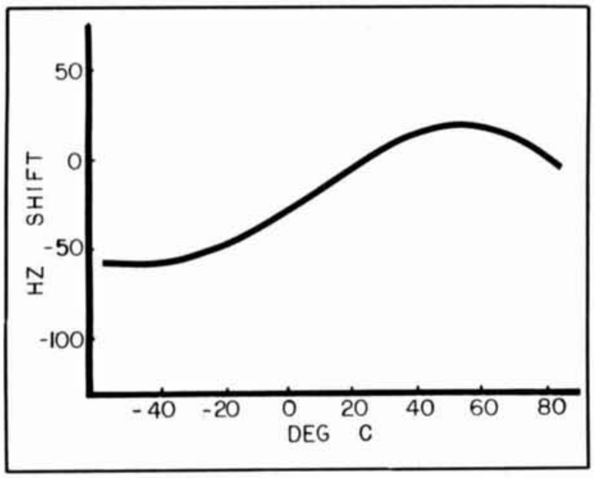

Figure 6. Center frequency shift versus temperature change in degrees Celsius for 455-kHz torsional filter.

from Rockwell International, 2990 Airway Avenue, Costa Mesa, California 92626. Literature is free. Experimenter samples are $69.83 each for quantities of 1 to 4 plus $10.00 for processing, shipping, and handling. OEM pricing for a quantity of 100 or more is considerably less—$30.90 per unit, FOB the plant.

MMIC postscript

In the last issue, we discussed how to apply Mini-Circuits monolithic amplifiers to practical construction projects. Since then, Avantek has announced the new low-cost MagIC™ line of plastic MMICs that includes a 31-dB gain, 500-MHz device with a maximum noise figure of only 2.0 dB. As far as I know, this is the lowest-NF, low-cost plastic MMIC available at this time. The part number is INA-02184, and 100-lot price is given as $3.40. If you have application for this device, you may request samples—plus Avantek applications note AN-S012, "MagIC Low Noise Amplifiers"—by contacting Avantek directly at (408) 970-3142; or by FAXing (408)970-6070, attention Dennis Moy.

PRODUCT INFORMATION

New Sprague-Goodman dielectric trimmer capacitors

Sprague-Goodman Electronics has announced the addition of military type 5.8 x 5.2 mm models to its line of ceramic dielectric trimmer capacitors.

Designed and constructed to meet the environmental requirements of MIL-C-81, these new devices are offered in six capacitance ranges (from 1.3 to 3.0 pF to 5.0 to 40.0 pF), have an operating temperature rang of -55 °C to 125 °C, voltage ratings of 250 volts DC at 85 °C and 200 volts DC at 125 °C, and insulation resistance of 10^4 Megohms min. In addition, the stator terminal's construction is of brass with silver plating and the rotor terminal's composition is of phosphor bronze and silver plating resulting in maximum durability.

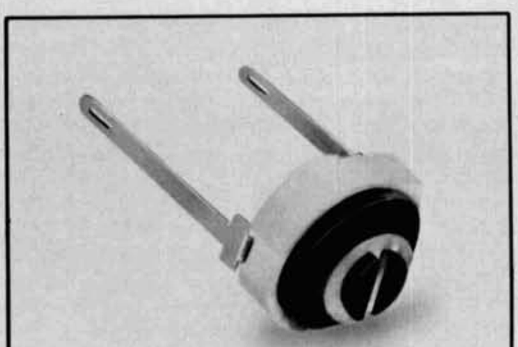

For more information contact Sprague-Goodman Electronics, Inc., 134 Fulton Avenue, Garden City Park, NY 11040-5395. Phone: (516) 746-1385, FAX: (516) 746-1396.

Motorola Note Looks at High-Power Audio Amplifiers

Motorola has a new application note describing both 100 and 200-watt single-channel high-fidelity amplifiers using plastic package bipolar transistors as outputs and drivers. Application Note AN1308, "100 and 200 Watt High Fidelity Audio Amplifiers Utilizing a Wideband-Low Feedback Design," explains design philosophies for both the amplifiers and their power supplies.

The amplifiers described in this note are designed for use in high-end and professional audio applications; however, the concepts presented could be applied to other audio amplifier designs.

To obtain a free copy of the new high-power audio amplifier application note, call Motorola Literature Distribution at (800) 441-2447, or write: Motorola Inc., Literature Distribution Center, P.O. Box 20924, Phoenix, Arizona, 85063. Ask for AN1308/D.

John Osborne, *G3HMO*
Reprinted with permission
from *Radio Communications*
June and July 1992

A REMOTE READING RF AMMETER

This handy gadget has a variety of uses.

The electromagnetic radiation at a distant point from an antenna depends on several factors, such as the RF current flowing in each element multiplied by the length of that element. But the current usually varies along the length, as normally we have standing waves (as well as resistive losses).

To get an idea of the power radiated we need to know what the current is over each section of the antenna.

Traditionally, the best that can be done to check the antenna current is to put an ammeter in series with the antenna as it leaves the shack. The bigger the reading, the bigger should be all the components up there in the air—though we still have no indication of the current at some fixed point along the antenna.

It is theoretically possible to calculate the current at one point knowing it at another, but this usually involves assumptions and approximations, ignoring local conditions such as trees and buildings and capacitance to ground. Likewise, we seldom know if the currents in the two arms of a dipole are really equal; nor do we know how much current flows on, and radiates from, the outside of a coax feeder and whether a balun has reduced it to zero. Unfortunately, it is not practical to put our RF ammeter up there to see what the current really is; nor can we use an ammeter shunt or current transformer and run a lead down to the meter—the meter would become part of the antenna system and invalidate the reading. But maybe we can...

A ray of light

When demonstrating optic fibers to students, I had an idea that here might be a solution. Light from an LED is coupled into an optic fiber that conducts the light to a detecting photodiode. The diode is connected through a meter to a battery; the brighter the LED, the greater the meter reading. If the LED could be driven by a current transformer energized by the antenna current, then the meter reading could be related to RF in the antenna. The optic fiber of glass or plastic contains no conducting metal and so does not influence the antenna. If the idea works, we have the makings of the ideal antenna ammeter.

To explore the possibility, I took the standard design of a current transformer as used in VSWR meters and shown in **Figure 1**. A ferrite ring has a secondary of typically ten or twelve turns. The primary is formed by taking the wire carrying the antenna current straight through the ring forming a

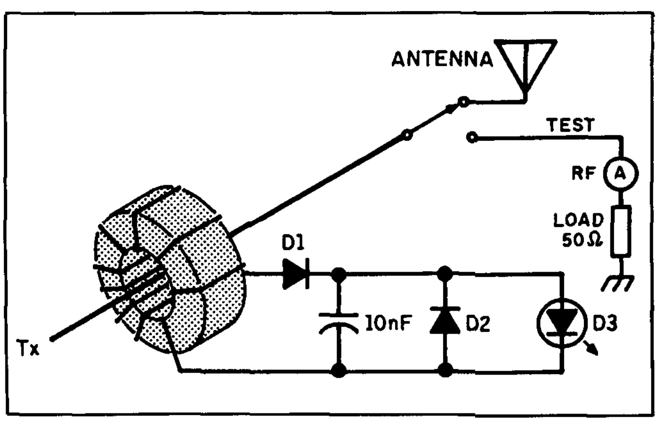

Figure 1. the test setup of the remote reading ammeter. The light output from the LED D3 is approximately proportional to the RF current through the ferrite ring.

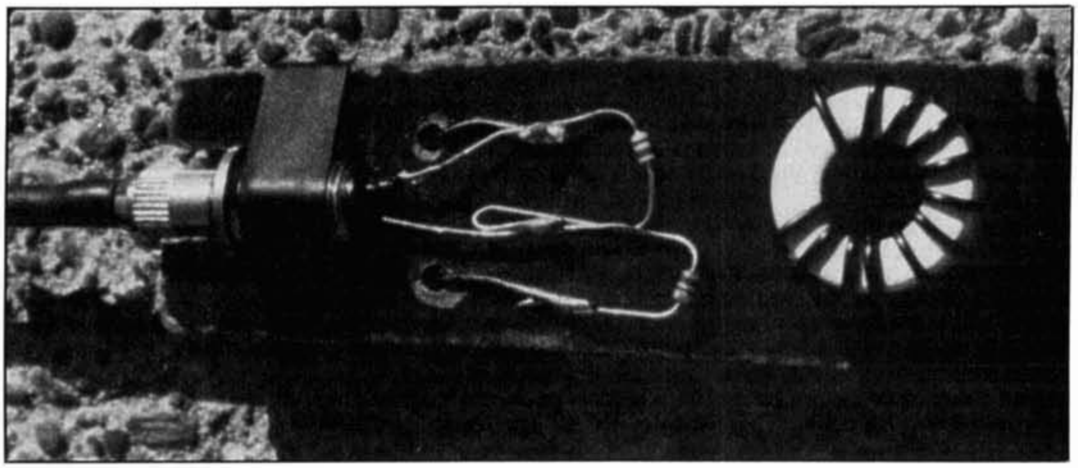

Photo A. The probe or "business end" of the remote reading ammeter on the ground ready for threading onto the antenna wire. The fiber is coupled onto the LED emitter.

12:1 transformer. An RF detector and an LED replace the usual resistor.

A low-capacitance signal diode in series is used to rectify the RF; the LED lights convincingly with half an amp of RF in the antenna. In fact, the transformer ratio does not predict the LED current accurately owing to flux leakage and losses. These are not serious, however, and the LED current is typically around 20 mA with half an amp of RF in the primary.

This ferrite ring and LED assembly can be used alone as a current indicator just as a neon lamp can be used to indicate RF volts. The protective diode across the LED may not be necessary, but it is inexpensive enough not to omit as LEDs have a low reverse rating. A small capacitor, say 10 nF, acts as an RF bypass.

Having confirmed that the theory thus far worked, I took the plunge and spent around 50 pounds on fiber optic components. It is possible to economize with inexpensive DIY alternatives, but to test this new venture I wished to remove as many unknowns as possible. The components had full-performance specifications. It was clear that a meter amplifier would be required, so a bread-board was set up to establish a suitable, very simple design. I was now ready to construct the prototype.

Prototype system

The system consists of three components: the probe, the fiber, and the meter unit.

The probe is shown in **Figure 1** and **Photo A**. The ferrite ring is attached to a small piece of insulating board and is located over a hole through which the current-carrying wire with be threaded. Twelve turns of 20 SWG enamelled copper wire are wound on the ring and the ends threaded through holes in the board to retain them. The high-output LED is taped to the board with its threaded front conveniently exposed for coupling to the optic fiber. The diodes used in the original were BAT85 silicon Schottky barrier type, but the earlier germanium types would probably do equally well. The circuit is soldered together using the wire ended diodes for connections.

The optic fiber is of the relatively inexpensive polymer variety, supplied on a cardboard drum in a 20-meter length. The fiber is carefully unwound, a procedure best done out of doors in a straight line. A small hole is made in the cardboard flank of the drum and one end of the fiber is threaded through the hole before winding the fiber carefully back on the drum. Both ends are now accessible and special ferrules are fitted following the supplier's instructions for terminating the fiber.

The meter unit is based on an educational (classroom) meter. Optional shunts for different ranges in standard boxes plug into the side of a large-scale 100-μA movement. The photodiode that matches the LED is mounted on the outer side of a box with the threaded part protruding for connection to the optic fiber. The box should be large enough to contain a small (PP9) 9-volt battery and the two transistors for the amplifier. The circuit is shown in **Figure 2** and the general layout in **Photo B**. Two transistors such as BC108 in a Darlington configuration make a suitable high-gain amplifier. They are soldered to a small piece of Veroboard that is supported on stiff wire leads. No switch is needed; plugging the box into the meter serves that function. The meter reads over full scale in daylight until the fiber is connected and cuts out stray light.

When connected up, a current of half an amp RF results in a meter reading of about 80 μA. Note that the meter can be up to 20 meters from the probe, the drum of fiber being unwound as required. It matters not if the fiber is wound on the drum, as there is no inductance in a coil of fiber!

For calibration I used my FT77 transceiver which has a variable drive, an old RCA thermocouple ammeter, reading to 1 amp, set up with a dummy load as in **Figure 1**. The thermocouple ammeter had a nonlinear scale and only currents over 0.2 amp gave a useful deflection. **Table 1** shows the calibration of the prototype for the 7-MHz band. Other HF bands gave similar, but not identical, results.

It is convenient to store the unused fiber on the drum for several reasons; it protects the fiber which might otherwise be tripped over and damaged, it avoids having to cut lengths and provide new terminations, it avoids the need to join fiber which can introduce serious losses, and most important, only one calibration table need be made.

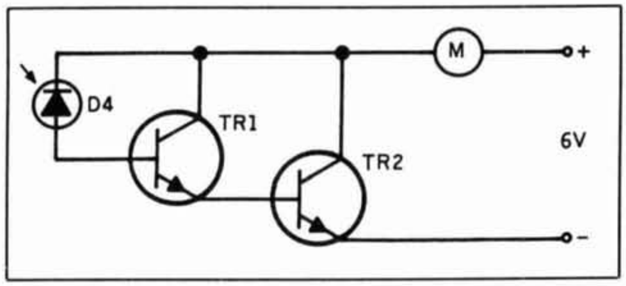

Figure 2. Circuit of the photodiode and simple amplifier to measure the light coming down an optic fiber from D3 in *Figure 1*.

RF current A (amps)
Meter reading M (microamps)

A	0	0.2	0.3	0.4	0.5	0.6	0.7
M	0	20	35	50	65	80	100

Table 1. Calibration

Testing the performance

Although this project was developed to test the feasibility of the idea, I had no specific application in mind. As it seems to work according to predictions, I offer this description for the benefit of other antenna experimenters who might find the remote reading ammeter a useful tool.

For my own satisfaction, I decided to test the performance in a typical application. At my holiday QTH, I have a long-wire antenna, about 40 meters long and about 5 meters high, used on all HF bands. It is the conventional inverted-L, supported by a chimney at the house with downlead to a ground floor window, and by a guyed aluminum pole at the other end **(Photo C)**.

I lowered the antenna, threaded on the probe, and moved it to the house end. Leaving the fiber dangling down, I raised the antenna, loaded up the FT77 on 7 MHz with an SEM transmatch and, with key down, adjusted the drive to give 0.5 amp of antenna current into the downlead. A temporary extension lead for the key was contrived, passing through the window to the ground under the antenna. The meter unit was connected to the fiber and placed alongside the key.

By pressing the key I could take a current reading in two seconds, without causing significant QRM. I had chosen a clear frequency when the band was quiet to avoid

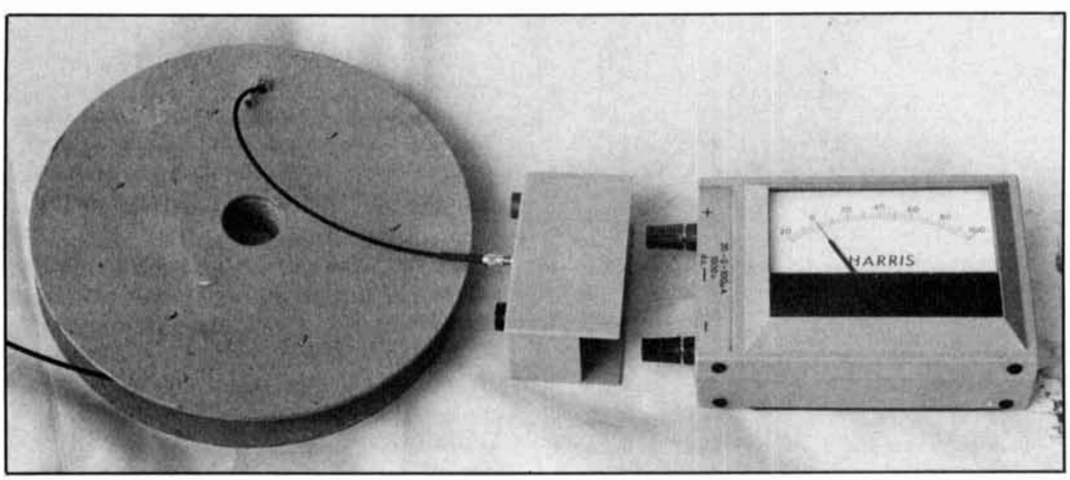

Photo B. The reel of optic fiber, amplifier, and meter. The fiber is coupled to the photodiode, which protrudes from the amplifier. The amplifier box plugs into the side of the meter.

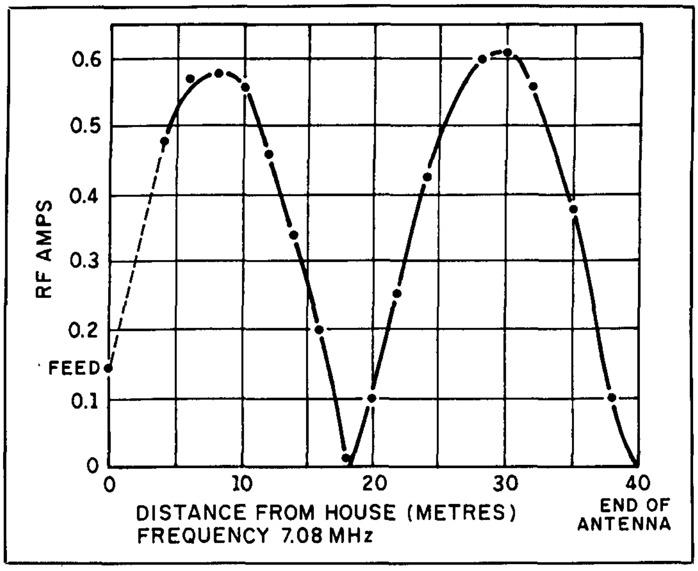

Figure 3. Variation of RF current at 7 MHz along a wire antenna as measured with the remote ammeter.

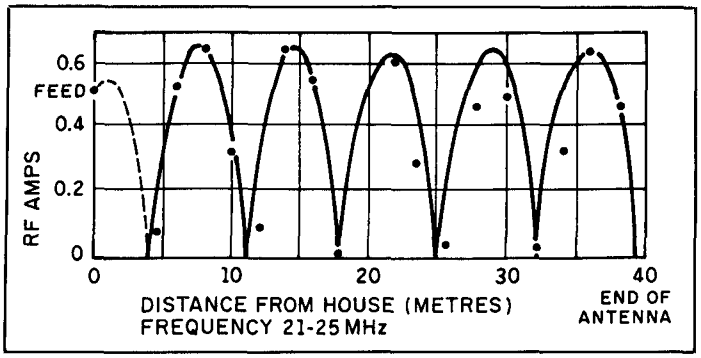

Figure 4. Variation of current as in *Figure 3* but at 21 MHz in the same 40-meter long-wire antenna.

causing interference. A tape measure was laid out under the antenna and, with the aid of two long bamboo sticks taped together, I pushed the probe along at 2-meter intervals—taking readings at each point. I soon discovered that the readings were going off scale, so I reset the drive to 0.15 amp and started again.

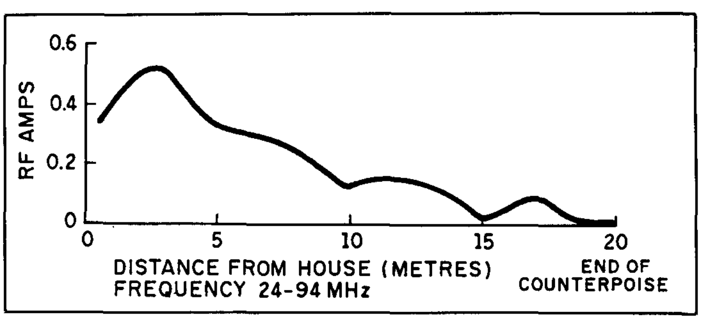

Figure 5. The decline of current in a counterpoise lying on the ground under the antenna at 25 MHz. The troughs and crests are spaced approximately 5 meters apart. In free space at 25 MHz a half-wave is 6 meters.

The readings are shown in **Figure 3**. Although the results show nothing surprising, they do emphasize the possible differences between the current at the feed and the current "up there." I then tuned to 21 MHz and repeated the experiment. These readings are shown in **Figure 4**. For precision the antenna could have been marked with a dab of white paint at 2-meter intervals, but judging distance by eye from ground level seems adequate enough to show that the system works.

Another experiment was to investigate the distribution of the current in a counterpoise consisting of 20 meters of insulated wire laid on the surface under the antenna. **Figure 5** shows the result, on this occasion at 24 MHz.

Continuing with other possibilities, I substituted a large-diameter ferrite ring for the original—again with twelve turns, with little change in sensitivity. I then used this successfully to probe the current along the arms of a rigid aluminum tube dipole on 25 MHz. This suggests that the technique might be useful in probing currents in the parasitic elements of beams, for which no simple alternative exists.

Other experiments

Various experiments are outlined in **Figure 6**. These have not been tried and raise the possibility of designing different probes for different jobs. If, due to a lack of access, a probe cannot be threaded onto the wire, can the ring be split? I have used a broken ring with the secondary winding on one half and the other half taped into position. It seems to light the LED normally and might prove a solution to this problem. A coil on a short ferrite rod held at right angles and close to the wire will also light an LED, but in this case calibration would be meaningless as displacement of the rod would alter the reading. With the ring, no change of reading occurs wherever the ring is moved or angled—provided that the (primary) wire passes through the ring. Ferrite is not essential and my *Admiralty Handbook of Wireless Telegraphy* (1940 pre-ferrite) shows an air-wound toroid around an antenna wire used with a hot-wire ammeter for monitoring antenna current.

It is axiomatic that one cannot measure anything without in some degree modifying the quantity measured. In the case of a ferrite-ring/LED configuration, the effect on the antenna current is not easy to predict with confidence. However, it should be insignificant in practice.

When the ferrite ring transformer is driving the LED, the power for the LED is obviously provided by RF from the transmitter. As nothing gets hot, the power drawn from the system is little more than that to light the LED. The LED has a forward voltage drop of 2 volts and a current of 20 to 40 mA maximum—less than 0.1 watt. If we take a typical case of 0.5 amp in an antenna of 70 ohms, the radiated power would be around 20 watts; i.e., the ring/LED is probably absorbing less than 2 percent of the power. The ring will also introduce a small inductance into the circuit. A test of the effect of the meter was contrived as follows: a second ferrite ring/LED assembly (as in **Figure 1**) was threaded over the antenna wire. This was pushed along the wire while monitoring the antenna current at a fixed point with the remote reading instrument. Fluctuations always less that 5 percent were observed, implying that the ring/LED had a very small effect on the antenna and its radiating performance.

Another point to be remembered is that if RF current is rectified, harmonics will be generated; and although these may be weak, they are happening up there in the antenna itself. The probe is a manmade "rusty bolt" and could cause QRN. It may be advisable to remove the probe when it is not in use, as a precaution.

Optic fibers are commonly available at reasonable cost, but it is necessary that the three components, LED fiber, and photodetector are compatible. Quite apart from terminating the fiber to interface with the solid-state devices at each end, it is vital that the wavelength of the light (or infrared) emitted by the LED is transmitted by the fiber with acceptably low loss and is within the range to which the photodiode is sensitive. In practice, this means choosing a matched set. The originals used in the above were the emitter, fiber, and photodiode of the polymer system by RS Components. This matched group operated at 665 nm, which falls in the visible spectrum. The red glow of the emitter can be easily seen when testing before connecting up the fiber. A much cheaper alternative, the emitter, fiber, and detector set from Maplin has now been tested with a full length of fiber and appears equally satisfactory from initial tests. The wavelength in this case is in the infrared (820 nm), so the advantage of "seeing" the emitted radiation is lost. For test purposes a visible-light LED can be substituted when setting up, and the infrared emitter put in when ready to go.

The connection of the fiber to the devices at each end is critical if one is to avoid big losses. The protective outer sheath must be stripped back by half-an-inch or so to expose the fiber. It is important not to damage the inner core at this stage. The end is then cut to length for the end connector, according to the maker's instructions. The cut must be made with a sharp knife (Stanley or scalpel) on a hard surface to give a clean face to the end. Press very hard vertically; do not saw. If the fiber has an uneven end (from saw marks) then light will be lost at the interface. It is possible to polish the end with a fine polish such as jeweler's rouge.

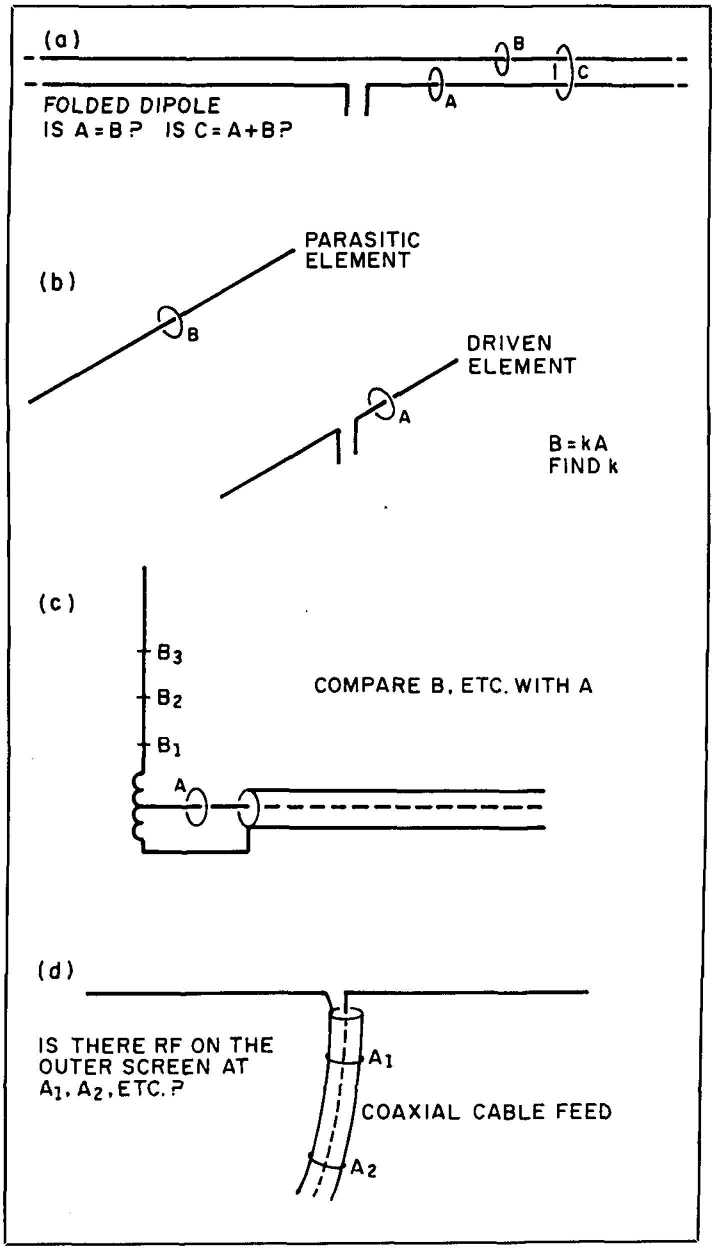

Figure 6. Some different experiments in which the remote reading ammeter could be used. (a) Does a folded dipole check with theory? (b) What is the current induced in a parasitic element of a Yagi? (c) What are the currents at different points in a vertical whip, compared with the feed current? (d) Are the currents flowing on the outside of a coax feeder serious? How essential is a balun?

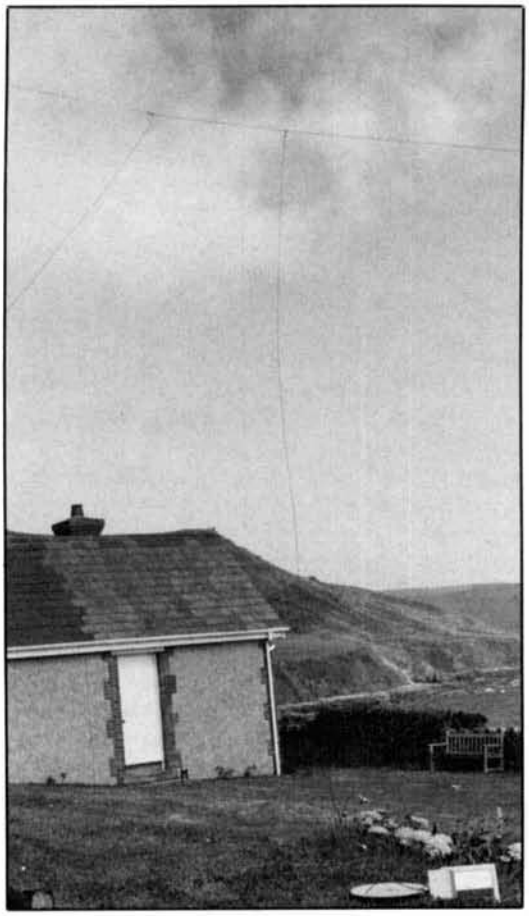

Photo C. The probe is just visible on the antenna. The fiber from it hangs down to the drum, seen here in the foreground alongside the meter and amplifier.

Conclusions

As I said at the start, the project is ready for further development. How sensitive can one make the system? Can one work at very low powers? Putting a 1.5-volt cell on the probe to forward-bias the LED gives a big increase in sensitivity; however, dependence on battery voltage would compromise accuracy and reliability. Maybe a precision op amp could be integrated into the probe. What is the cheapest source of optic fiber and associated components? Could a pulley system be devised to move the probe along an antenna wire from the ground?

All sorts of experimental possibilities exist; with a little imagination you could probably come up with more new ideas. Quite routine possibilities may also crop up such as "How does the current vary as the antenna is raised to different heights?" I look forward to hearing from those who find new uses for the ammeter.

Parts List

Probe
Ferrite ring: OD 5/8 inch (16 mm)
ID 5/16 inch (8 mm)
Height 5/16 inch (8mm)
Winding: 12 turns 20 SWG enamelled
Diodes (D1,D2): BAT85 (or 1N34 probably okay)
Set 1: Emitter LED (D3) RS type 301-561 GaAsP
(Peak wavelength at 50 mA, 665 nm)
Set 2: Sender LED (D3) Maplin FD14Q (MFOE71 F/optc Emittr) (Wavelength 820 nm)

Fiber
Set 1: Polymer RS type 368-047
Attenuation 200 dB/km at 665 nm
End termination connectors RS type 456-396
Set 2: Polymethyl methacrylate fiber Maplin XR56L
3 dB from 385 to 880 nm, attenuation 1.2 dBm
No connectors required; couplers integral with devices.

Meter Unit
Set 1: Detector (D4) PIN Photodiode RS type 655-032
Set 2: Detector (D4) Maplin FD12N (MFOD71 F/optc Dtctr)
Transistors (Q1,Q2) SiNPN BC108 or equivalent

Cost of optoelectronics:
RS Components (Set 1 visible light) approximately 50 pounds
Maplin (Set 2 infrared) approximately 25 pounds

RS Components Ltd., P.O. Box 99, Corby, Northants NN17 9RS, UK
Maplin Electronics Supplies Ltd., P.O. Box 3, Rayleigh, Essex SS6 2BR

None of the components used for the remote reading RF ammeter are critical except for the matched sets of fiber optic parts.

R.P. Haviland, *W4MB*
1035 Green Acres Circle, North
Daytona Beach, Florida 32119

INSULATED ANTENNAS

The effect of insulating coatings on antennas

Although technical literature refers to antennas with enough thickness of insulation on their surfaces to affect their characteristics as "dielectric coated antennas," I like to call them "insulated antennas."

There isn't much about insulated antennas in the amateur literature. I found nothing in the bibliography in the 1988 edition of *The ARRL Antenna Handbook*.[1] Rosen's cross-referenced bibliography, *From Beverage to Oscar*,[2] produced no search matches. I do remember a short note in one of Bill Orr's columns to the effect that use of insulated wire in quads caused detuning, but I haven't been able to find the exact column. There's a little more in the technical literature, but we'll get to that later.

Conceptual approach to insulation effects

You can get a general idea of the effect of an insulating coating on an antenna by taking a simple dipole and considering only major (first-order) effects. As sketched in **Figure 1**, let Rw be the radius of the conductor of an antenna and Rd be the radius of a surrounding insulation, a dielectric, where Rd is always greater than Rw. The dielectric constant of the insulation is K times that of the surrounding air. For simplicity, assume that the magnetic permeability of the wire and insulation are the same as for air, and that the losses in the insulation can be neglected.

A short length of such insulated conductor will have resistance, inductance, and capacitance. To the first order, we can write:

$$Z = XL - XC + R + A \times f \times f + (\ ) + (\ ) \qquad \textbf{(1)}$$

Where:

- Z is a per-unit impedance
- f is the operating frequency
- XL is the reactance due to inductance of the wire
- XC is the reactance due to capacitance of the wire
- R is the RF resistance of the wire
- A is a resistance representing energy loss by radiation from the wire
- ( ) represents smaller, neglected terms.

Because the simplifying assumption is that there are no inductive or resistive effects, the presence or absence of the insulation can only affect the C term, and possibly the A term. Let's concentrate on the first.

If the insulation were essentially absent, the C term must be the same as for a bare wire. And if the insulation extended to infinity, the unit capacity would be increased by the amount of the dielectric constant. With practical amounts of insulation, the C term will be greater than for a bare wire, but by a small amount.

The square root of the quantity L•C is the reciprocal of a frequency and, taken over the entire length of the wire, gives the resonant frequency of the antenna. Since the effect of the insulation is to increase C, what results is a decrease in the resonant frequency. The amount of change is small for a thin layer of insulation. The ratio of no-insulation frequency to coated frequency

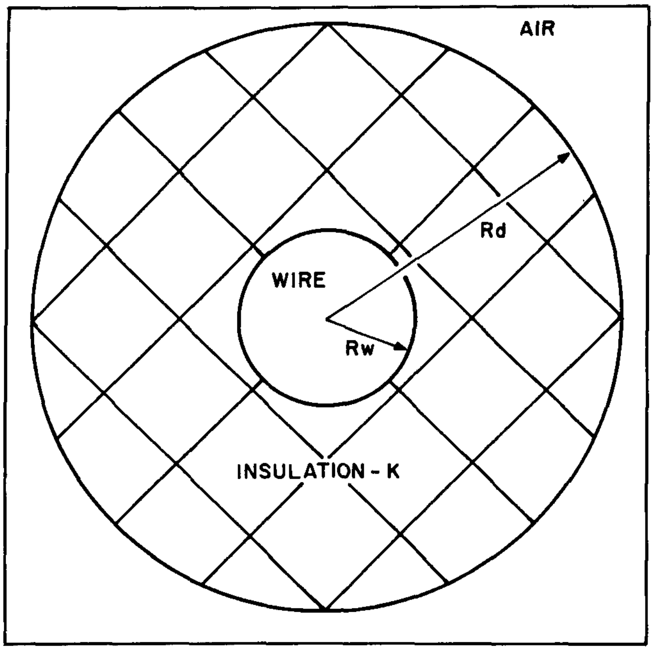

Figure 1. Cross section of an insulated antenna. Rw is the radius of the wire, Rd is the radius of the dielectric, K is the dielectric constant of insulation. The diameter ratio may be used.

is always less than the square root of the dielectric constant, K.

You can get an idea of the way the resonant frequency varies by further simplifying assumptions. Let the capacitance be composed of two capacitors in series. C1 is that of a coaxial capacitor formed of the wire and a conductive cylinder of radius

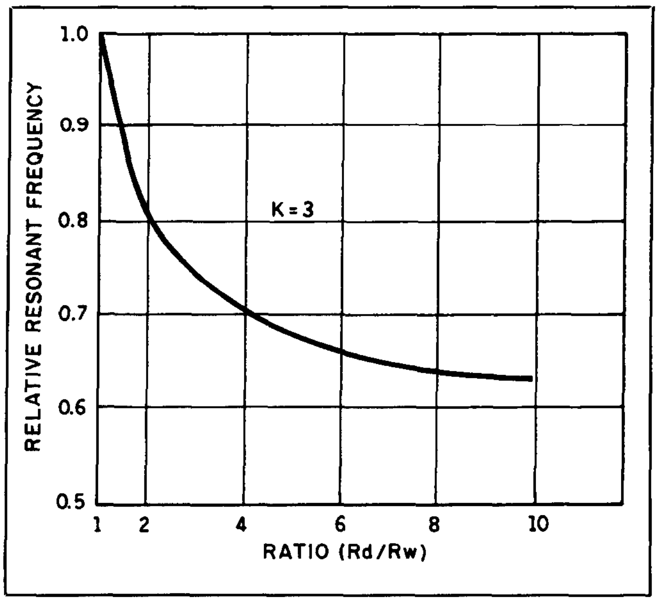

Figure 2. Very approximate results of insulation with dielectric constant of 3 on a spherical antenna, showing reduction of resonant frequency as insulation thickness increases. The limit of reduction is 1 over the square root of the dielectric constant.

Rd, with the space between filled with the dielectric. C2 is the capacitance between the conductive cylinder and infinite space, with air as the dielectric.

A look at the equations in Terman's *Radio Engineer's Handbook*[3] quickly shows that a lot of "number shoving" can be avoided if one assumes that the antenna is spherical rather than cylindrical, as the resulting symmetry simplifies the equations for C. While this changes the details somewhat, the principle is exactly the same.

The equations needed are:

$$C1 = 1.412 \times K \times (Dw \times Dd)/(Dw - Dd) \quad \textbf{(2)}$$

$$C2 = 1.412 \times Dd \quad \textbf{(3)}$$

Diameter is used rather than radius. Combining these by the series capacitance formula and taking the square root of the result gives the relative variation in frequency as the amount of insulation (Dd/Dw or Rd/Rw ratio) is changed. This quantity is plotted in **Figure 2** for a dielectric constant of 3.

With no insulation, the resonant frequency is that of an isolated wire. As the insulation thickness increases, the frequency decreases linearly with the thickness ratio for a time. When the thickness is equal to the wire size, the rate of change is about half the initial. With insulation of ten times wire size, the relative resonant frequency has reduced to nearly the limiting value, the reciprocal of the square root of the dielectric constant, 0.58 times the free space value in this case.

Method of moments analysis

The analysis done thus far is an approximation, but it shows the overall trend to be expected and some of the intermediate details. More accurate results need a much more complex analysis.

One approach to a more accurate analysis can be developed from the Method of Moments, widely used in antenna study. You'll recall that this technique divides the antenna into segments, establishes an impedance matrix Zmn of the self and mutual impedances of the segments, and calculates the matrix values from the fields generated. The matrix is then inverted to calculate the currents in the segments, the pattern, and the drive conditions.

J.H. Richmond of Ohio State University followed this approach in a study for NASA.[4] He found that adequate accuracy was obtainable if the impedance matrix was considered to be composed of two parts,

$$Z = Zmn + Z'mn \quad (4)$$

where Zmn is the matrix for the antenna with no insulation present. The additive matrix Z'mn contains all of the effects of the insulation.

The elements of this add-on matrix are of the form:

$$Z'mn = P \times F(l) \quad (5)$$

where P is a function of the insulation dielectric constant and dimension, and its multiplier F(l) is solely a function of segment length factors multiplied by constants.

The complete expression for P is:

$$P = (K - 1)/K \times LN(Rd/Rc) \quad (6)$$

where the LN term is the natural logarithm of the radii ratio.

Richmond has taken the relations involved in obtaining the impedance matrices and their solutions and written them as a Fortran computer program. This, as a well-documented paper copy, is available in a NASA Contractors report[5] or alternatively from the NTIS.[6] (While well documented, it's not always easy to follow the translation from the equations to the computer code.) The program is quite lengthy, about 1000 lines, and uses the complex arithmetic common in Fortran. Input and output are accomplished by the punched cards common in large computer installations of the '70s. I haven't checked, but the source and compiled code should also be available on tape from NTIS.

The Fortran code is standard; anyone with a small computer Fortran compiler, 1977 version, could get the program running at the cost of some typing effort. Alternatively, the 9-line Fortran subprogram which generates the matrix Z'mn could be translated into BASIC and be included in MININEC—adding to its R and X impedance matrices in the same fashion as is done for lumped loads. However, for the purpose of this article, even this seemed to be more work than was justified.

Looking at **Equation 5** again, it's clear that all solutions involving insulation must include, as one endpoint, the corresponding value with no insulation. Further, even though the wire part of one antenna is different from that of another, **Equation 6** shows that the effect of adding insulation to

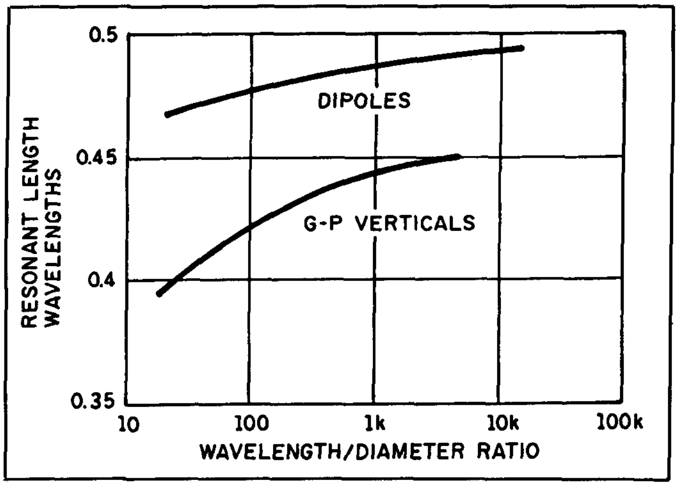

Figure 3. Resonance length factor of dipoles and monopoles as a function of its length to diameter ratio. For quarter-wave verticals over an infinite ground, use the dipole curve with twice the monopole length to diameter ratio. "Half-wave" dipoles are always shorter than the free-space one-half wavelength at resonance.

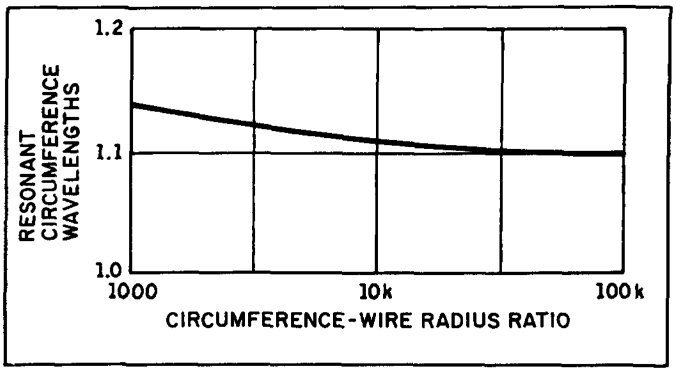

Figure 4. Resonance length factor of a square quad loop as a function of its circumference to radius ratio. Use for equilateral delta loops with negligible error. "One-wavelength" bare conductor loop perimeters are always longer than the free-space wavelength at resonance.

the second will be proportional to that of the first. This means that you can take a particular example solution, and develop from this values for many design situations. Let's do this for resonant frequency, confining our effort to wire antennas.

To perform this operation simply, you'll need three curves. The first is a curve of resonant length with no insulation. As has been shown many times, this is a function of the length to diameter ratio of the antenna conductor, or alternatively, the wavelength to diameter ratio. **Figure 3** shows this as a fraction of free-space wavelength for monopoles and dipoles.[7] **Figure 4** gives the resonant loop circumference for equal-sided quads and for equilateral delta loops.[8] The resonant length can also be determined using one of the available versions of MININEC.

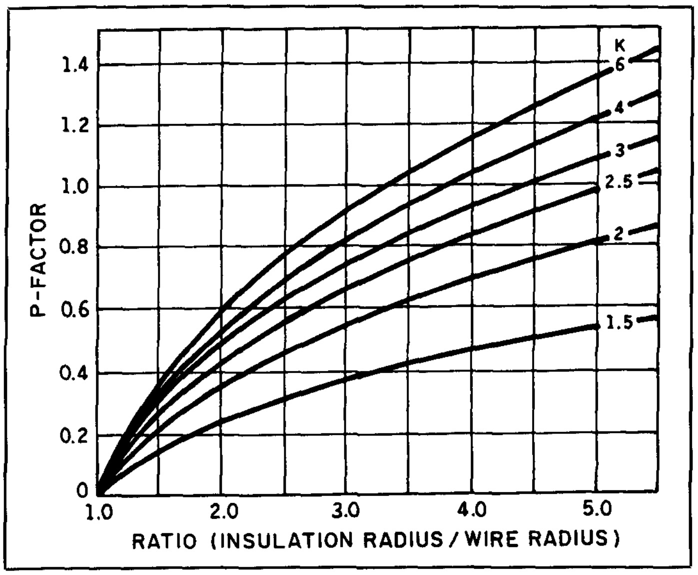

Figure 5. Insulated antenna "P-factor" as a function of the insulation to wire diameters (or radii). Interpolate between curves for the exact dielectric constant. Use *Equation 6* for values outside the curves.

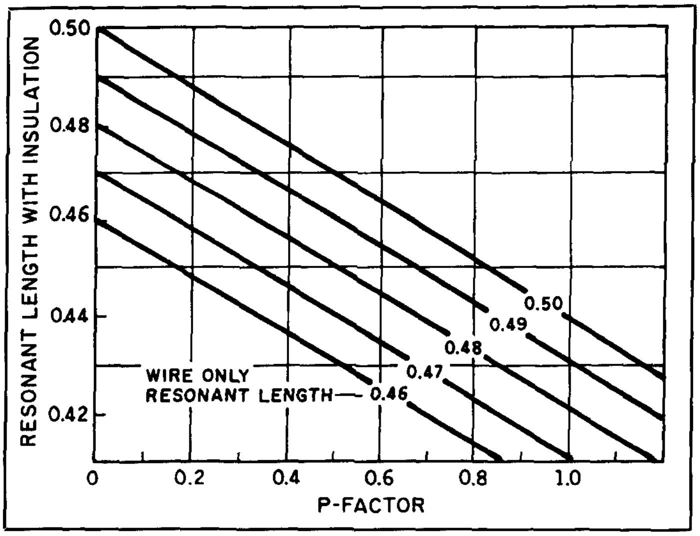

Figure 6. Approximate shortening effect of insulation on dipoles. Select the uninsulated length factor curve using data from *Figure 3*, and for the P-factor from *Figure 5*, interpolating as necessary. For monopoles use one half this indicated length. See text for values beyond the data shown.

The second curve needed is the P-factor, given by **Equation 6**. This curve is plotted in **Figure 5** as a function of the ratio of insulation to wire diameters (or ratio of radii). Dielectric constant is used as a parameter, and intermediate values should be interpolated between the curves. The P-factor can also be determined with a calculator using **Equation 6**.

Finally, the length factor with added insulation is secured from **Figure 6** for dipoles/monopoles, or from **Figure 7** for quads and deltas. The correct curve is selected using the "no-insulation" value from **Figures 3** or **4**, interpolating between curves as necessary. Then the "with insulation" length factor is read off at the intersection of the curve and the P-factor from **Figure 5**. These last curves are developed from a curve in Richmond and Newman,[9] and from the example data given.

The results of using the ensemble of curves will be reasonably accurate for small amounts of low-K insulation, but of lesser accuracy as the insulation size grows. For such situations, Richmond's more exact Fortran program could be used. However, he warns that its calculation accuracy decreases as the insulation becomes large when compared to wire size. In such cases, full-scale measurements of a working prototype are indicated if an application is critical with respect to element length, as it is in parasitic arrays.

Drive resistance and other factors

Returning to the discussion following **Equation 1**, the square root of the quantity L/C is a resistance from which the drive resistance is developed. Because the C term is increased by the addition of insulation, the drive resistance decreases as the thickness of insulation increases. The maximum change is of the same order as for the resonant frequency; i.e., a reduction by the square root of the dielectric constant K.

A three-graph procedure could also be used to develop the drive resistance of the element. This hasn't seemed worthwhile, since it is so variable in arrays, and because any change is easily matched out. The reduction is approximately by the same ratio as for the resonant frequency.

Richmond and Newman[9] state that another factor will appear if the more exact analysis of the computer program is used—specifically, the bandwidth of the antenna decreases. Lammensdorf[10], too, made this statement in his report of experimental measurements on insulated antennas. Both reports refer to the fact that adding insulation narrows the antenna conductance response curve. In amateur terms, the SWR bandwidth will be less for insulated than for bare antennas—even though they both are matched at the center frequency. In most situations, the effect can be ignored.

Some sample situations

Before closing, let's look at a few typical situations. Some use the approximate graphical method described here and others the more exact and measured results of the references.

For the first, assume that a dipole is made of an 8-inch length of RG-59/U coax with the outer cover and the braid outer conductor stripped off. What is the resonant frequency?

For this case, the length/diameter ratio is 8/0.025, or 320. The ratio of insulation to conductor diameter is 0.146/0.025, or 5.8, and the dielectric constant is 2.3. From **Figure 3**, the bare wire length factor is about 0.48. From **Figure 4**, the P-factor is 0.9. The resonant frequency with insulation is 0.425 wavelengths by interpolation. **Reference 9** shows a value of 0.425 for both theoretical and measured resonance.

Suppose the same wire were formed into a quad loop. The perimeter/radius ratio is about 600 and the free space length factor is about 1.18 **(Figure 3)**. With insulation, this reduces to 0.93 **(Figure 4)**. **Reference 7** shows a theoretical value of 0.92, and a measured value of 0.95 for such a loop.

Going outside of the range for which test data is available, suppose that a 10-meter dipole is made from a piece of old RG8/U with the jacket and braid stripped off. Does the antenna need shortening from standard design length?

The insulation ratio for this wire is about 0.285/0.082, or 3.5 average. Dielectric constant is 2.26. Normal length is about 16 feet, for a L/D ratio of 2350, giving a length factor of 0.455. The P-factor is about 0.69. The resonant frequency occurs at a length factor of 0.415. The dipole should be shortened to 15 feet, 2 inches length if the length is critical—as for a Yagi director. Otherwise, the change probably can be ignored, since it is of the same order as changes due to height above ground, or to nearby objects.

In contrast, what is the effect of Formvar insulation of a 40-meter dipole of no. 12 wire? Wire tables show this gives 12 turns per inch, for an insulation diameter of 82.5 mils, compared to 80.8 for bare wire. The diameter ratio is 1.025. By calculation, the P-factor is about 0.06. **Figure 6** shows that this amount of insulation does move the resonant point slightly, but this small change is negligible in practical situations.

Conclusions

The overall conclusions are:

- Adding insulation to the wire does change its performance, especially if the insulation is thick or of high dielectric constant.

- In most real-world situations involving the use of thin layers of insulation on wires, the effect is not likely to be seen because it is about the same as that due to other causes.

- In critical applications, as in Yagi parasitic elements, the effects of insulation require compensation, by the approximate method shown here, or preferably by more exact calculation.

- The state of theory is such that extreme conditions of thickness or high dielectric constant will need full scale measurements for accuracy.

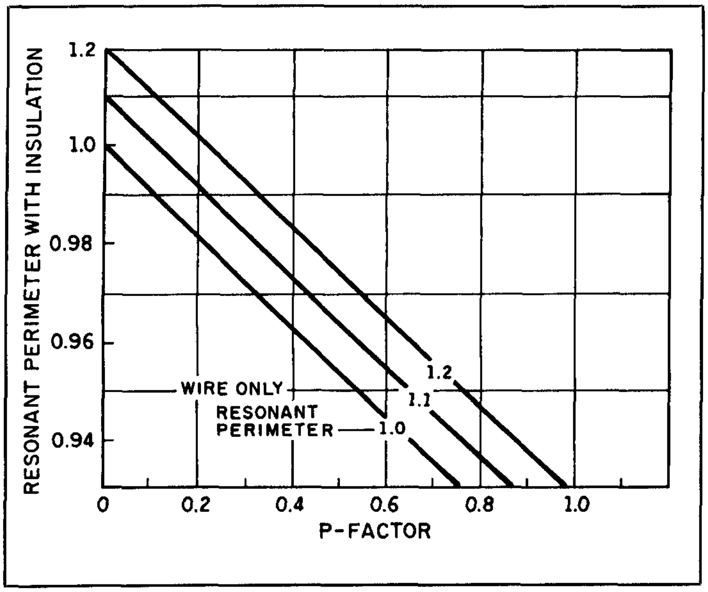

Figure 7. As *Figure 6*, but for loops. Enter with data from *Figures 4* and *5*. Insulated loops may have a perimeter less than one wavelength at resonance.

REFERENCES

1. "Topical Bibliography on Antennas," *The ARRL Antenna Book*, 15th edition, Amateur Radio Relay League, Newington, Connecticut, 1988.
2. *From Beverages thru Oscar—A Bibliography 1908-1988*, Didah Publishing, Nashua, New Hampshire. Available on disk or microfiche.
3. F.E. Terman, *Radio Engineer's Handbook*, McGraw-Hill, New York, 1943.
4. J.H. Richmond, "Radiation and Scattering by Thin-wire Structures in the Complex Frequency Domain," *NASA Report CR-2396*, May 1974. Available from NTSC and from depository libraries.
5. J.H. Richmond, "Computer Program for Thin-wire Structures in a Homogenous Conducting Medium," *NASA Report CR-2399*, June 1974. Available from NTSC and from depository libraries.
6. National Technical Information Service, 5285 Port Royal Road, Springfield, Virginia 22161.
7. *The ARRL Antenna Book*, current edition, Amateur Radio Relay League, Newington, Connecticut.
8. R.P. Haviland, **The Quad Antenna**, CQ Books, Hicksville, New York, in production for publication.
9. J.H. Richmond and E.H. Newman, Dielectric Coated Antennas, *Radio Science*, Volume 11, Number 1, National Bureau of Standards, pages 13-20.
10. David Lammersdorf, "An Experimental Investigation of Dielectric Coated Antennas," *IEEE Transcript on Antenna Properties*, AP-15, N.6, November 1967, pages 767-771.

Peter O. Taylor
AAVSO Solar Division
P.O. Box 5685
Athens, Georgia 30604-5685

THE SOLAR SPECTRUM

Sunspot distribution

Shortly after their first telescopic observations of sunspots in the early seventeenth century, Galileo and his contemporaries realized that the spots are not evenly distributed over the Sun's surface, but are concentrated in 35-degree wide belts that bracket the solar equator. (Small spot groups have appeared briefly at latitudes as high as 70 degrees.) An important property of each solar cycle* concerns the way that groups emerge within these bands.

In 1858, the English amateur astronomer, Richard Carrington, discovered that the onset of each sunspot cycle coincides with the sudden appearance of new spots at a much higher average latitude than those which erupt near the end of the cycle. Carring-

*H. Schwabe is credited with the discovery of the sunspot cycle in 1849.[1] However, others suspected a periodicity in the number of sunspots many *years before Schwabe published his research.*

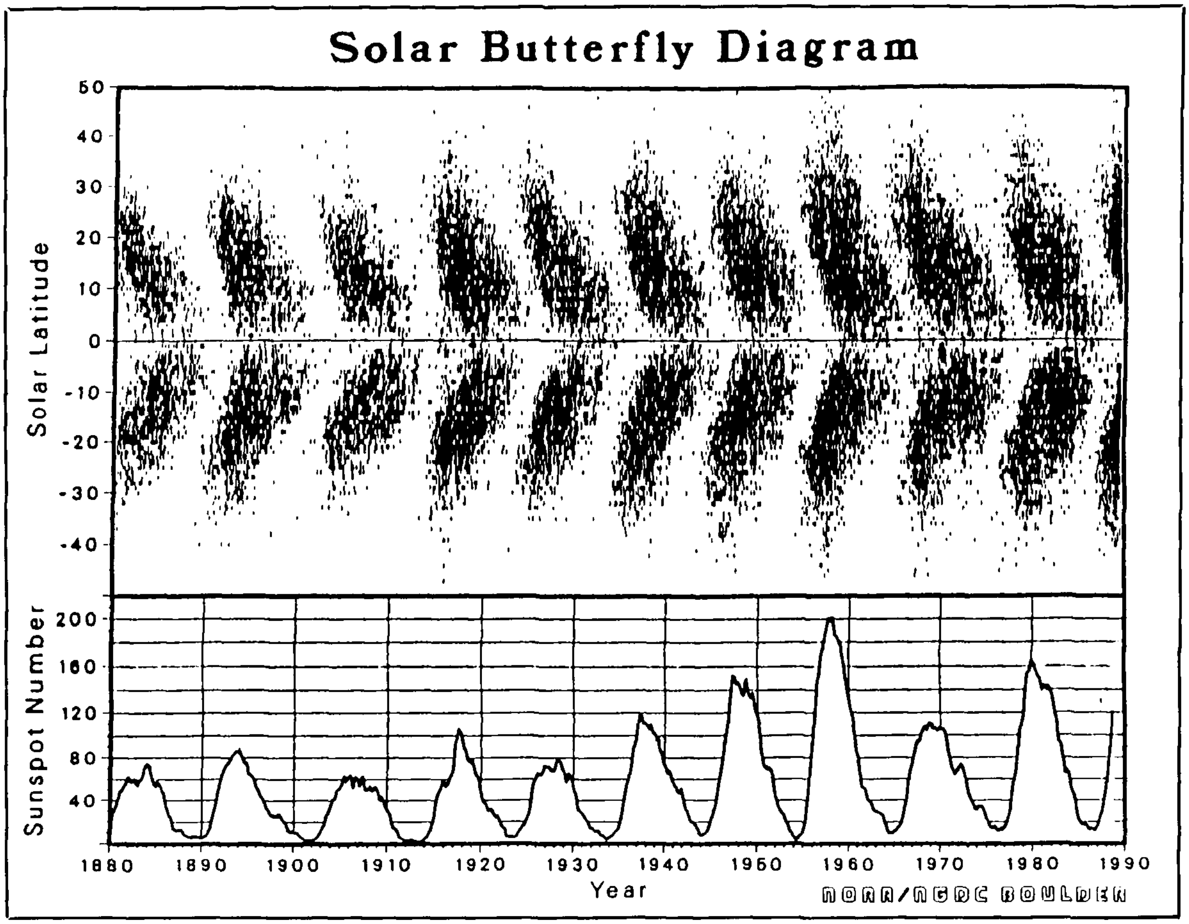

Figure 1. In 1858, Richard Carrington discovered that the first spot groups of a new cycle generally erupt at high sunspot latitudes, while those which follow appear progressively nearer the equator. This plot, prepared by Daniel C. Wilkinson of the National Geophysical Data Center, depicts this activity between 1880 and 1989.

ton's observations were confirmed by Rudolph Wolf and later by Gustav Sporer, who investigated the effect at length. As a result, the process has come to be called "Sporer's Law."

At the beginning of the twentieth century, a second English astronomer, Edward W. Maunder, joined with his wife, Annie, to study this phenomenon. While doing so they developed a graph known as the "Butterfly diagram," which plots the latitudes of emerging spot groups against time. These graphs are so-named because of their distinctive shapes which resemble the outstretched wings of a butterfly. They provide an important link to Maunder's thorough description of this phenomenon.[2] The original figure is displayed in the library of the National Center for Atmospheric Research.

Figure 1, prepared by Daniel C. Wilkinson of the National Geophysical Data Center located in Boulder, Colorado, shows the butterfly effect using data obtained at the Greenwich Observatory until 1978, and compiled by the National Oceanic and Atmospheric Administration thereafter. The sudden change in latitude of sunspot emergence that typically signals the beginning of each new cycle can easily be seen around the time of last cycle minimum (September 1986).

After the publication of Maunder's research, astronomers became aware of an overlap in the sunspot cycle. That is, for several years after the first spots of a new cycle appear, spot groups representing both the old and new cycle frequently exist together. Typically, the first spots from a new cycle emerge about 18 months before the minimum of the cycle in progress, at a latitude near (±) 25 degrees.

Shortly after the old cycle comes to an end, spots from the new cycle make their appearance at an average latitude that is closer to 30 degrees, and the new cycle is officially underway. After cycle maximum, a majority of spots appear at progressively lower latitudes until the end of the cycle when new groups erupt near the equator, at an average latitude of approximately (±) 7 degrees. From their writings, it is apparent that neither Spörer nor Maunder realized that some spots from a coming cycle appear during the active phase of a current cycle. Similarly, it is probable that neither understood that spots from both cycles can be present simultaneously for three or more years.

A cycle often develops unequally in the Sun's Northern and Southern Hemispheres. Consequently, sunspot activity may peak in one hemisphere well before it does in the other (see **Figure 2**). During the present cycle—number 22 according to the Zurich numbering system—the number of spots in the Northern Hemisphere reached a maximum in mid-1989, but the peak in the southern reaches of the Sun was delayed until July 1991.

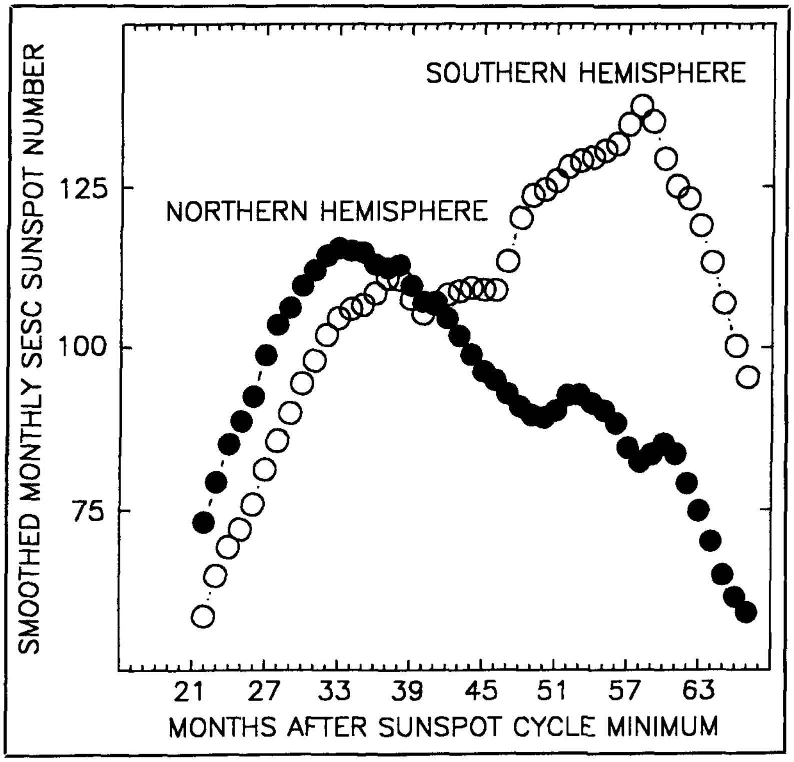

Figure 2. The smoothed monthly relative sunspot number according to hemisphere. This graph was drafted from data obtained by Space Environment Services Center thus far during solar cycle 22 (through October 1992).

Furthermore, a cycle's maximum intensity is often much greater in one hemisphere than in the other. The Southern Hemisphere dominated during cycle 18 and again during the current cycle, but for cycles 19 through 21 sunspot activity was strongest in the North. It is also common for a cycle to alternate between active hemispheres as it develops, which is the case for the present cycle. These factors seem to vary at random and do not appear to follow any set rule.

The situation thus far during cycle 22 is shown in **Figure 3**, a recent version of Maunder's diagram. The figure plots the heliographic latitudes of sunspot groups compiled by the National Oceanic and Atmospheric Administration from April 1985 through November 1992. Again the "leap" in latitude of sunspot emergence that heralded the onset of cycle 22 can be seen around the time of the most recent minimum.

NASA scientist Robert Wilson has shown April 1985 to be the likely date for the first occurrence of a cycle 22 sunspot group.[3] The emergence of this active area is indicated with an arrow shown in **Figure 3**. Based

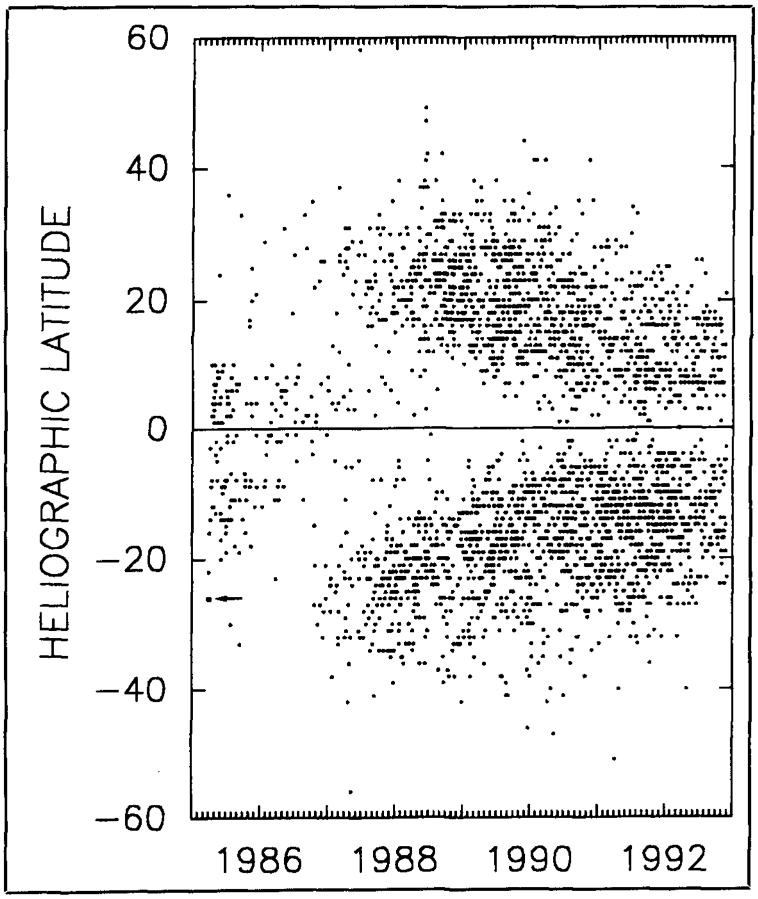

Figure 3. In this version of the Maunder Butterfly diagram, the heliographic latitude of each sunspot group is plotted as a filled circle. The figure includes all groups that made their appearances between April 1985 and November 1992. The single point indicated by the arrow may represent the first spot group of the current cycle, which officially began September 1986. Note the two high-latitude groups that occurred during mid-1987.

on the date of this event and his examination of cycles 11 through 20, Wilson then was able to predict a probable time of first-minimum for cycle 22 of 1986.7, almost exactly on target.

A second interesting quality of the Butterfly diagram may be useful in anticipating the maximum intensity for a new cycle. In 1967 an investigation of the cycle record by Czechoslovakian solar astronomer, M. Kopecki, indicated that high amplitude cycles begin with spot groups that emerge at higher-than-normal latitudes. This work suggests a smoothed relative sunspot number of somewhat less than 150 for the maximum of cycle 22. However, the observed value proved to be a bit higher: 158.1.

What causes this phenomenon? Although it may originate as rising magnetic fields are distorted by the Sun's differential rotation as outlined by H.W. Babcock in 1961,[4] other investigators suspect that the process is actually a product of "torsional oscillation." According to this description, spots emerge when a particular latitudinal zone within the sunspot band reaches a maximum in its rotational velocity. If this is true, a new cycle would not really begin with the emergence of the butterfly pattern, but would be triggered by the onset of a high-latitude torsional wave during the descending branch of the old cycle.

In 1987, a mechanism was proposed that could prove to be the key to this research. H. Snodgrass and P. Wilson[5] suggested that huge waves exist beneath the solar surface which enhance rising magnetic fields by continually forcing them into the Sun's interior so they become compressed and strengthened.

According to this scenario, convective "rolls" originate near the Sun's poles, and then gradually move the magnetic concentrations through a network of currents towards the equator. Presumably, when the material reaches the normal spot latitudes some years later, the magnetic fields are so intensified that they break the solar surface, forming sunspots.

If this is correct, it indicates that two cycles are in progress at the same time; a result that would be incompatible with the model first described by Babcock. Moreover, the phenomenon originally unearthed by Carrington would then be but one manifestation of a more complex process in which sunspots themselves would play only a subordinate role.

Recent activity and short-term outlook[6]

Solar activity generally declined through November, a trend which is expected to continue until a (currently predicted) cycle minimum sometime during 1996. In spite of this tendency, the most intense X-ray solar flare since June 1991 was recorded during the first part of November—a X9.0 Ten-flare that erupted from just behind the Sun's west limb. However, the event caused few consequences in the terrestrial environment. Otherwise, the Sun was relatively quiet, with a majority of days at a low activity level. These conditions are expected to continue during the next several months, although brief intervals of high activity may well occur.

REFERENCES
1. H. Schwabe, *Astronomische Nachrichten*, 21, 1849, page 234.
2. E.W. Maunder, *Monthly Notices of the Royal Astronomical Society*, 64, 1904.
3. R.M. Wilson, *Solar Physics*, 111, 1987, page 255.
4. H.W. Babcock, *Astrophysical Journal*, 133, 1961, page 572.
5. H. Snodgrass and P. Wilson, *Nature*, 328, 1987, page 696.
6. A portion of this information was obtained from the *SELDADS* data base.

Garry Shapiro, *NI6T*
20941 Nez Perce Trail
Los Gatos, California 95030

OPTIMIZING THE PK-232MBX FOR RTTY AND AMTOR

Performance-enhancing modifications for this popular multimode controller

As with many DXers, my first encounter with the digital modes was through VHF packet—more precisely the DX PacketCluster. Watching the DX tide roll in and out on the packet screen was a revelation, and I worked and posted my share of CW and SSB goodies. Yet several modes—the HF digital modes—were not among my station's capabilities and, while observing many intriguing RTTY DX postings, I developed an interest in trying RTTY and AMTOR. I wanted more than RTTY capability, so I considered purchasing a multimode controller (MMC).

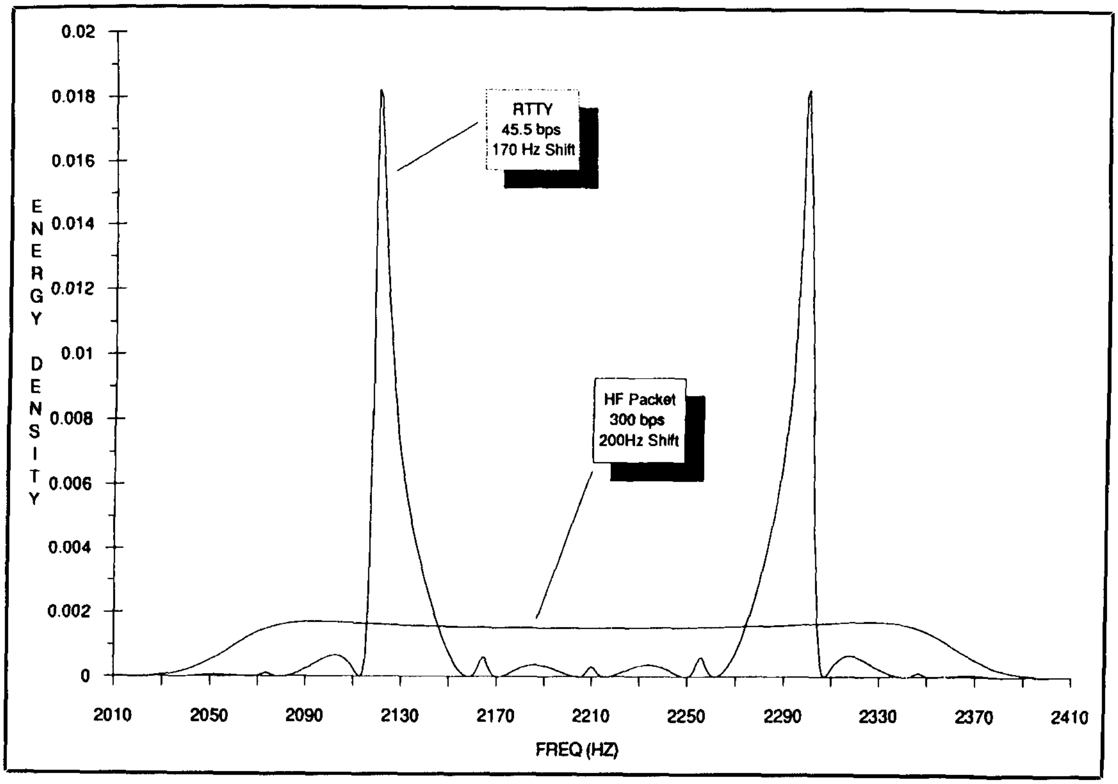

Figure 1. Comparison of RTTY and HF packet spectra.

Multimode data controllers provide two-way operation on many digital modes—VHF and HF packet, RTTY (at various data rates), and AMTOR—as well as the ability to receive additional modes, like WEFAX. Having studied the manuals and the ads of several contending units and speaking with factory customer service engineers, I chose a PK-232.

The AEA PK-232MBX is a popular unit among the read-my-fingers crowd. It contains an analog FSK modem and a microprocessor-based digital controller. Two ports allow selection of different modes and radios (e.g., VHF packet and narrow-shift RTTY)—although not simultaneously, as does the Kantronics KAM, which sports two complete modems. Countless configuration options are keyboard selectable.

I soon fired up on (Baudot) RTTY, using direct FSK with a TS930S. After a number of QSOs, I felt performance was inadequate. Many stations didn't "print" well. Comparing notes with local RTTY veterans, I suspected that the filters weren't quite right. Many RTTY operators seemed to prefer older, specialized RTTY modems and/or preceded their PK-232s with additional switched-capacitor audio filters. It was time to study the circuit schematic more closely. (See the **Sidebar**.)

The schematic[1] discloses that the PK-232 has only *two* analog modes in its analog modem—VHF and HF. The VHF mode selects packet: 1000 Hz shift and 1200 bps. The HF mode is optimized for HF packet: 200 Hz shift and 300 bps. The other HF modes just use the packet settings. **Figure 1** shows the dramatic difference in the transmitted frequency spectra[2,3] between HF packet and standard RTTY (nominal 45.5 bps and 170 Hz shift) in the signal passband. These spectral *calculations* don't precisely model RTTY, ARQ, etc., over short intervals, but are the expected long-term average for random data. The Y-axis values are energy/Hz on a linear scale.* The areas under the curves represent total energy in the signals and are equal.

With its high ratio of frequency shift to data rate, 45.5 bps RTTY concentrates energy near the 2125/2295 Hz shift frequencies and is mostly contained within 200 Hz, while 300 bps packet spreads its energy almost uniformly across about 350 Hz. According to AEA, the bandwidth of the PK-232 receive filter is 450 Hz—but mine measured 500. This is much more than is re-

*Some short-term *measured* of HF data signals, emphasizing passband/stopband relationships are presented by Henry and Petit.[4]

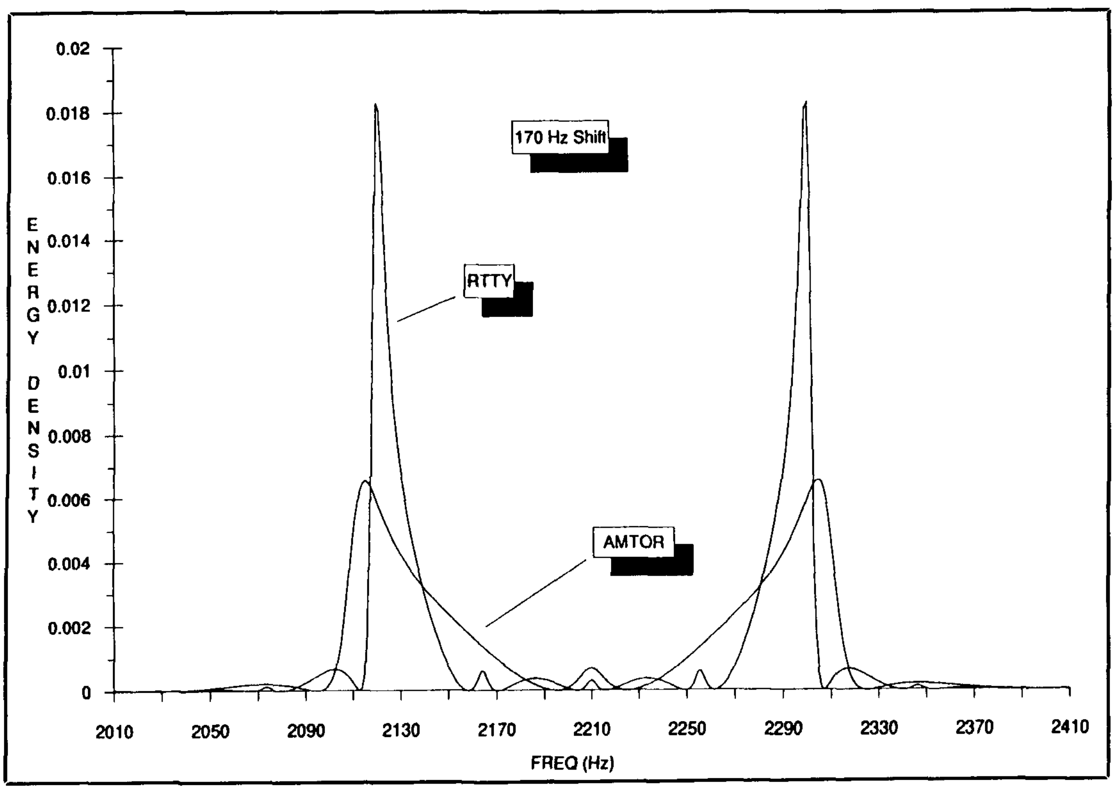

Figure 2. RTTY and AMTOR spectra for 170 Hz shift.

quired for any of the HF modes, and more than twice that required for RTTY!

Excess bandwidth allows more noise and QRM to accompany the signal, degrading performance; doubled bandwidth lowers signal-to-noise ratio by 3 dB. A 3-dB degradation in a binary FSK system can increase bit error rate by several orders of magnitude and render marginal signals unusable.[2,5] Clearly, the PK-232 would benefit from narrowing the bandpass filter for the narrower modes (RTTY and AMTOR), but by how much should the bandwidth be reduced?

Part of the answer lies in the unfortunate situation created by some multimode controllers: the growing use of 200 Hz frequency shift. Although standard RTTY and AMTOR specify 170 Hz shift, many controllers use 200 Hz shift for RTTY/AMTOR, HF packet, and 300 bps ASCII RTTY. This lowers manufacturing cost and wouldn't seem to be a significant difference. AEA's Alan Chandler observed in these pages, "Equipment designed for 200 Hz shift can be used with 170-Hz shift equipment."[6] But **Figures 2** and **3** show considerable differences between the frequency spectra for 170 and 200 Hz shifts. This is especially true for AMTOR, which transmits at 100 bps. Compared to 170 Hz shift, the AMTOR signal with 200 Hz shift dramatically spreads out and develops discrete components at the shift frequencies that reduce the effectiveness of the signal. It seems that 200 Hz is a bad idea, but we appear to be stuck with it unless and until controller manufacturers change their products and amateurs using such controllers in AFSK mode modify their tone generators.

Since some RTTY/AMTOR stations transmit 200 Hz shift, bandpass filter bandwidth must be chosen accordingly. **Figure 3** indicates a minimum bandwidth of ~250 Hz for RTTY only and ~325 Hz for both AMTOR and RTTY. These minima presume that the passband is accurately centered. If you skip the subsequent center frequency tuning procedure, increase the bandwidth 20 to 30 Hz.

Reducing bandwidth raises the Q of each resonator (filter section) and accentuates the effects of resonator frequency errors. The resonance or center frequency is affected by every R and C in **Figure 4** except R1. Even with 1 percent components, substantial errors are possible—errors that result in a distorted passband response, especially at the passband edges. The solution is to tune each resonator to the center frequency of the complete filter by adjusting "R2" of **Figure 4** for each section. Note that the desired

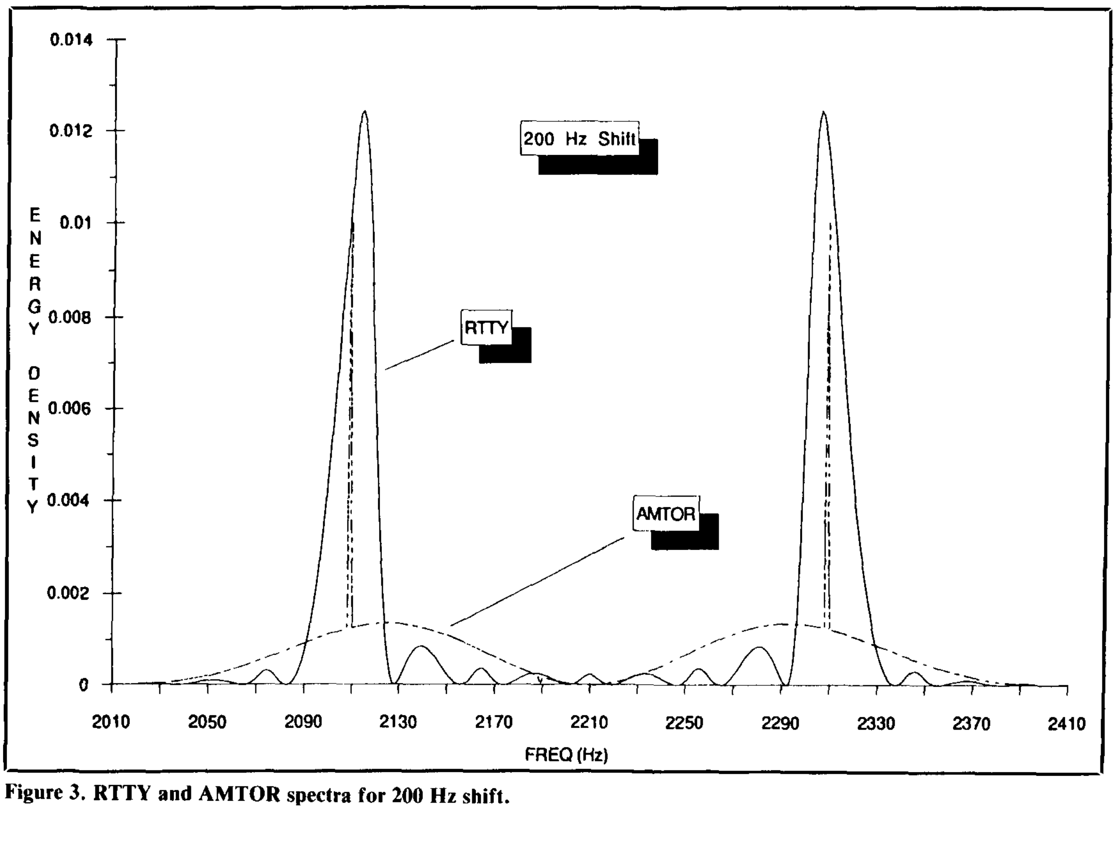

Figure 3. RTTY and AMTOR spectra for 200 Hz shift.

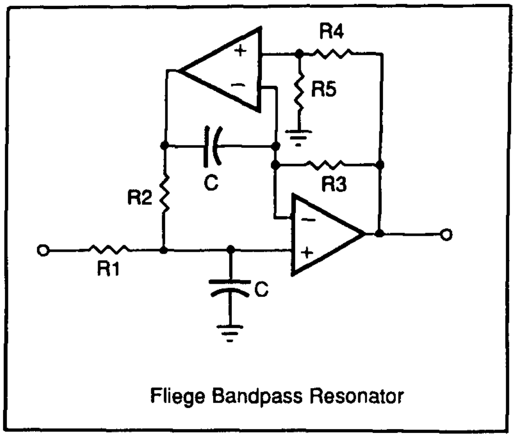

Figure 4. The Fliege bandpass resonator.

center frequency, f_o, is the *geometric* mean, given by:

$$f_o = \sqrt{f_c^2 - (B/2)^2}$$

where f_c is the arithmetic mean (2210 Hz, the average of the mark and space tones) and B is the newly selected bandwidth. The correction isn't large for narrow bandwidths—if $B = 325$, $f_o = 2204$. It's more important that all four resonators have the *same* frequency.

The twin-resonator discriminator (see the **Sidebar**) was originally tuned to the 200-Hz shift frequencies, but can provide adequate RTTY/AMTOR performance over a non-critical range of adjustment of its two filters. The linearity of the center of the discriminator characteristic isn't as essential to RTTY/AMTOR—whose spectra are concentrated around the mark/space frequencies—as it is to packet modes, whose spectra are more evenly distributed across the passband.

The discriminator can be precisely adjusted to enhance the effectiveness of a monitor oscilloscope for tuning incoming signals using the traditional "cross pattern." A cross pattern display results from application of the discriminator filter outputs (available at J7 on the PK-232) to the horizontal (mark) and vertical (space) inputs of an oscilloscope. Ideally, on a properly tuned signal, one would see thin horizontal and vertical lines on the 'scope screen, but in reality ellipses are produced. These are due to the non-zero bandwidth of the discriminator filters: each tone produces output from both filters (see **Figure 5**). Also, because the two outputs are generally not in quadrature (90-degree phase difference), the ellipses will be tilted with respect to the axes and each other.

If the discriminator resonators are tuned so *both* outputs for *each* tone of the pair are in quadrature, the major axes of the ellipses will be at right angles and will lie upon the axes when the incoming signal is properly tuned. Tone pairs with other shifts won't exhibit this symmetry. Use both the cross-pattern display and the PK-232 LED

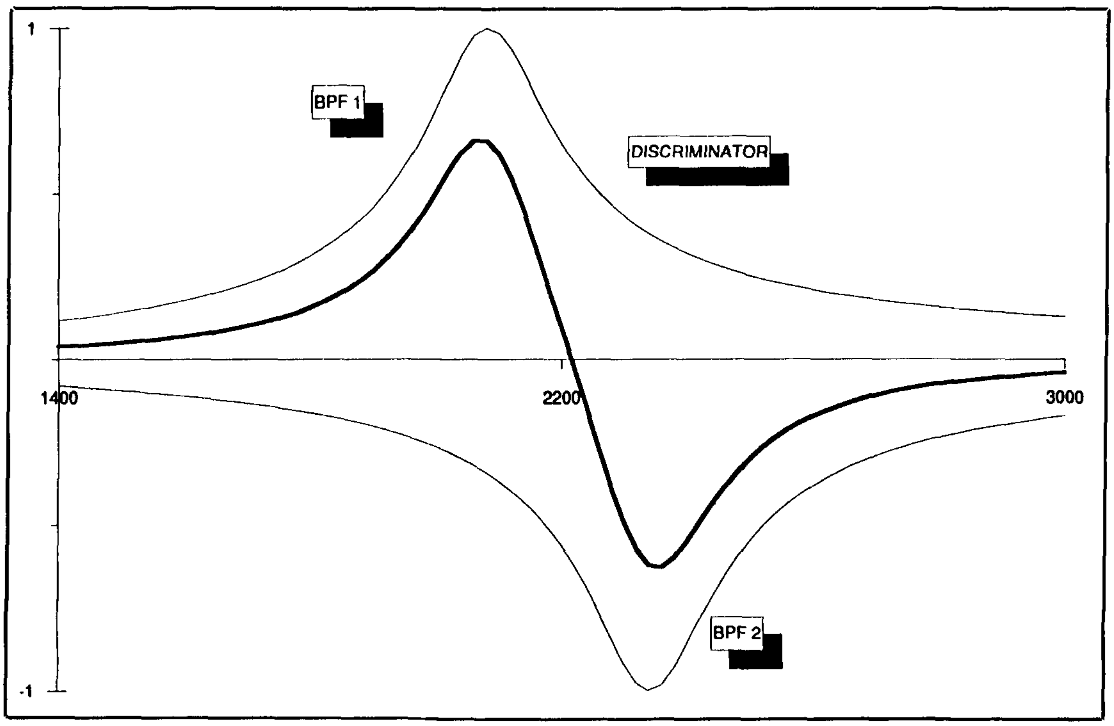

Figure 5. Discriminator frequency response.

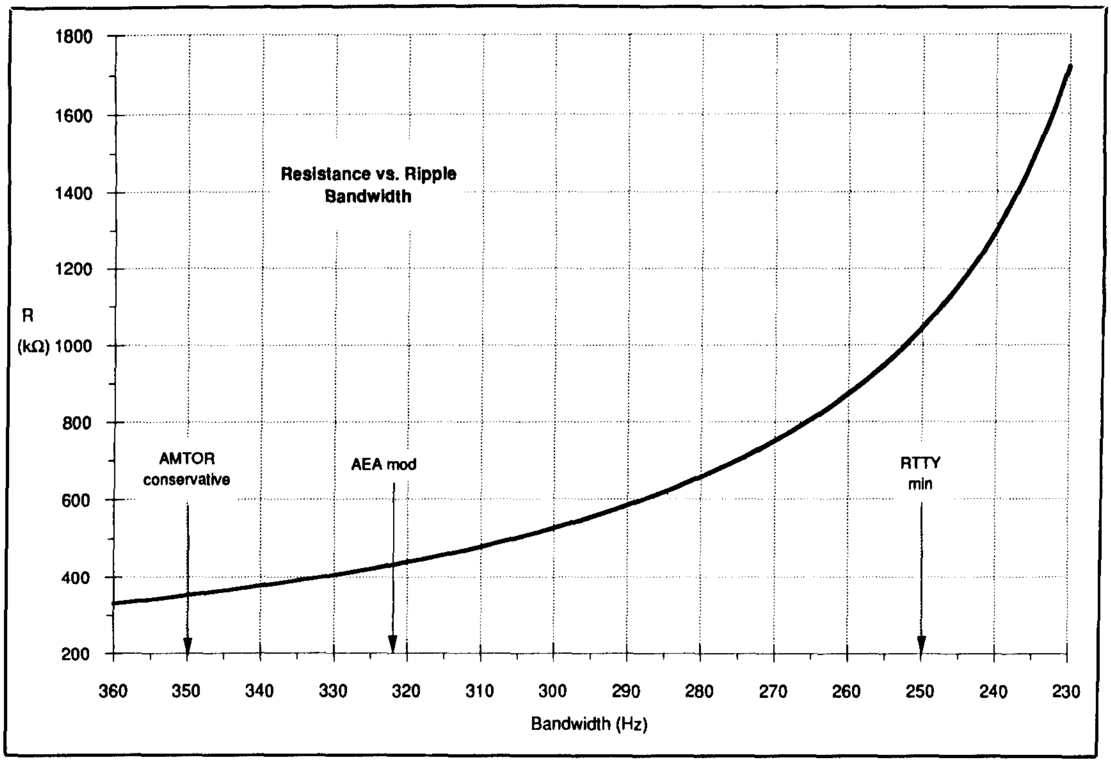

Figure 6. Resistance versus bandwidth.

tuning indicator in RTTY/AMTOR operation.

(The PK-232 resonator frequencies that satisfy the requirement for 170 Hz shift are 2081.9 Hz and 2342.5 Hz. The solution is shown in **Appendix 1**.)

AEA also optimized the post-detection lowpass filter for HF packet. Its passband is much wider than RTTY or AMTOR requires, but its stopband attenuation is satisfactory for all modes. Scaling this filter for RTTY/AMTOR is possible, but has not yet been done.

To counter the spread of 200 Hz shift, I urge PK-232 owners using AFSK to retune the tone generator circuitry for 170 Hz shift; that is, 2125 Hz and 2295 Hz output frequencies.

Tuning procedures

The following procedures implement the modifications and adjustments I've discussed:

a) Reduce the receive filter bandwidth
b) Tune the receive filter resonator center frequencies
c) Readjust the discriminator to optimize RTTY/AMTOR tuning
d) Adjust output tones for 170 Hz shift

a)Reduce the receive filter bandwidth

WARNING: Narrowing the bandwidth will render the PK-232 nonfunctional in the higher data-rate HF modes like HF packet and ASCII RTTY.

This modification requires replacing four resistors—R42, R52, R62, and R72—corresponding to part of R1 in **Figure 4**. Find the replacement value using **Figure 6** by selecting the desired (ripple) bandwidth. Note that the chosen value isn't critical, but that the resistors (use metal film for stability) must match within 1 percent.

AEA provides a free "PK-232 AMTOR Enhancement Modification" kit—432 k, 1 percent metal film resistors—corresponding to ~325 Hz bandwidth, labeled "AEA mod" in **Figure 6**. This a conservative, but satisfactory, value for AMTOR/RTTY—particularly if you also perform modification "b". Serious RTTY operators may prefer a narrower response—as low as 250 Hz ("RTTY min"); in this case, I *strongly* recommend modification b. Locate resistors with the Parts Pictorial in the operating manual.[1] Use 1 percent or better metal film resistors.

b)Tune the receive filter resonator center frequencies

This procedure requires a warmed-up, low-drift, dual-trace oscilloscope (in chopped mode) and an accurate sinewave generator (either synthesized or in conjunction with a counter).

Step 1. Connect the sinewave generator to

```
Unmodified PK-232
WA1  WA1 WA 1  WA1    ???  DE  HC5K NAME TED TED  QTH IS
CUECVA  STUTHERN
BCUUDTR AN  #92 :9,67 .3 74 :-=) 0'3   271  DE  HC5K PSEKKK
.
.
NEXT FEW DAYS FOR SURE IDILSOME THISMORNIVCBUT I LAWWT
REEMBER SEENAQNXOURU
BAAIMGAT PILE.+=VI
 TCU FR CAGT AND  SURE VTOD TO XAE YOU AGIIN    VVVWA1MPB DE
FIHC5=(  5('..
8-89'   '( '(
7SVV=

Modified PK-232
WA1  WA1 WA 1  WA1    ???  DE  HC5K NAME TED TED  QTH IS
CUENCI  SOUTHERN
ECUUDOR AND  HOW COPYU MED UR CAPL PSE   WA1  DE  HC5K PSEKKK
.
.
NEXT FEW DAYS FOR SURE IDND SOME THISMORNIG  BUT I LONBT
REMZMBER SEEN
IYOURU IN THAT PILE...I
 TKU FR CAL AND ISURE GOOD TO SEE YOU AGIIN    VXWA1MPB DE M
HC5K  TKSHN
IADITS   SK SK

Unmodified PK-232
4X6CE
DE 6Y5PH 6YWTPN73 7' TOSCNAND YOURS , MAQ THE GOOD LORD
BLESS AND KEAPIU TILL WE MEET AGN.BEST OF DX MY FRIEND DE
6Y5PJ .Y5PJ

Modified PK-232
4X6C DE 6Y5PH 6Y5PFBKPN 73 TOEC AND YOURS , MAY THE GOOD LORD
BLESS AND KEDP U TILL WE MEET AGN.BEST OF DX MY FRIEND DE
6Y5PJ JMY5PJ
```

Figure 7. On-the-air performance comparisons.

J14, pin 1 and one 'scope probe to U26-14 (the filter output) with AC coupling (the filter operates from a single supply so the DC voltage isn't zero). Power up the PK-232. Using your computer or terminal connected to the RS-232 port, place the PK-232 in either AMTOR or Baudot mode. Tune the sinewave source across the passband, noting the passband width and shape—including the magnitude of the ripple. If the passband is flat within 0.5 dB or so, skip the rest of this procedure. Remove the power and RS-232 cable.

Step 2. Unsolder the summing-junction ends of R66, R68, and R78, leaving the other ends connected. This breaks the feedback loops in the filter. Replace R40, R49, R59, R69 with 8.2 k, 5 percent *metal film* resistors.

Step 3. Solder short bare wires to the wiper and one end of a 100-k *multiturn* linear trimpot. Preset the trimpot for maximum resistance and tack-solder it across R40.

Step 4. Connect the 'scope probes to U18-1 (first resonator input) and U23-1 (first resonator output), using AC coupling. Power up the PK-232. Set the source frequency to f_0 and trigger from either channel. Adjust the generator for 1 volt peak-to-peak at U23-1 and adjust the other channel for similar deflection. Increase the gain of both channels until the waveforms are off-scale and the traces are fairly steep. If the oscilloscope preamp has a "Ch 2 invert," engage it.

Step 5. Set the input coupling on one channel to "ground" and carefully adjust the vertical position to place the trace over the center graticule line. Repeat with the other channel. Make sure both traces are well focused and exactly superimposed. Return both channels to AC coupling.

Step 6. The Fliege resonator (see **Sidebar**) is noninverting, so the input and output are in phase at resonance. (The traces will appear out of phase if "Ch 2 invert" has been engaged). Adjust the trimpot until the traces exactly superimpose (in phase) or cross zero at the same point (out of phase). Remove the trimpot and measure its resistance with a digital ohmmeter.

Step 7. Choose a resistor close to the measured trimpot value and solder it across the 8.2-k resistor at R40. Five percent resistors are sufficient (choose from among several if possible), but 1 percent values are better. When the resistors are cool, check the frequency by varying the source: it should be within 5.5 Hz for 5 percent resistors and 0.5 Hz for 1 percent resistors.

Step 8. Remove power and solder the trimpot across R49. Move the input probe from U18-1 to U23-11 (the output of the second resonator), set the source to f_0, power up the PK-232, and adjust the source level for 1 volt at U23-11. Repeat the procedure as for the first resonator. Then, do the same for the third and fourth resonators. Recheck each resonator before removing power and restoring feedback resistors R66, R68, and R78.

Step 9. Connect one probe to U26-14, power up the PK-232, and repeat the sweep of the passband as in the **Step 1**. The passband should now be uniform and flat within 0.5 dB.

c)Readjust the discriminator

Two trimpots, R81 and R96, adjust the center frequencies of the two bandpass resonators of the discriminator.

The PK-232 Modem Receiver

The PK-232 employs classic FSK receiver design (**Figure 8**).[2] An eight-pole Chebyshev bandpass filter drives a limiter—providing a constant-amplitude signal to the twin-resonator discriminator, or FM detector.

Figure 9 shows the PK-232 bandpass filter configuration; the blocks labeled "T" are identical second-order RC active filters (resonators). While the technique of simply cascading active filter sections works well for many applications, the frequency responses of narrowband, high-order filters suffer greatly from errors due to component tolerances. Multiple-feedback structures like the Hurtig Primary Resource Block (PRB) used in the PK-232 dramatically reduce this sensitivity by use of feedback.[7] The PRB's identical resonators ease scaling of the filter for different modes, because the same component values are switched in each. The poles of the resonators are moved to their proper positions by the feedback.

The resonator is a Fliege bandpass,[8] shown in **Figure 4**. Among its useful properties, R1 independently controls bandwidth, and either R2 or R3 independently controls frequency. In the PK-232, CMOS switches control R1 and R2.

The discriminator employs two bandpass filter resonators tuned to either side of the signal passband; these filter outputs are envelope-detected (rectified and filtered) and the DC outputs subtracted. As represented in **Figure 5**, the discriminator response (heavy line) is the difference between "BPF 1" and "BPF 2." The almost-linear region in the center provides the desired frequency-to-voltage conversion. Signal outputs from the bandpass filter sections are also brought to the rear panel for use with an external monitor 'scope.

The modulation information is recovered by lowpass filtering to remove carrier components, and "slicing"—conversion to a digital signal with a comparator whose trip point is at the center of the discriminator characteristic. The controller's digital circuitry processes the recovered data before sending it to the user terminal or computer.

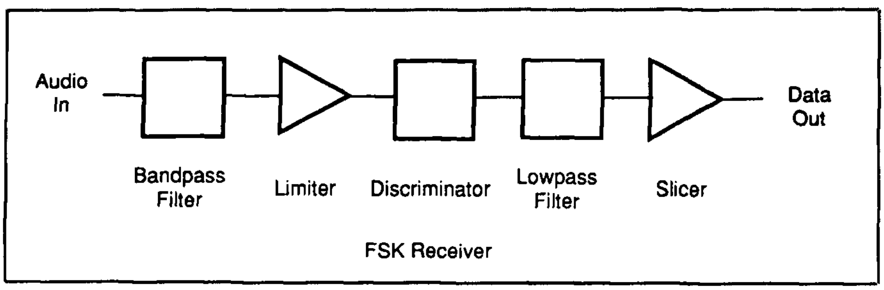

Figure 8. PK-232 modem receiver block diagram.

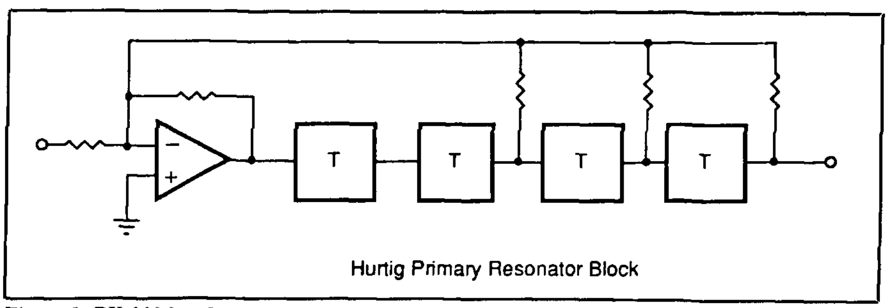

Figure 9. PK-232 bandpass filter block diagram.

Step 1. Ensure that the PK-232 is in Baudot or AMTOR mode. Connect the sinewave source to J14-1. Connect the "Scope Mark" and "Scope Space" outputs to the horizontal and vertical inputs of the oscilloscope. Bypass the 'scope timebase to directly connect the horizontal input.

Step 2. Set the output frequency of the sinewave source to 2125 Hz. Increase the drive from the sinewave source and observe an horizontal ellipse. If the ellipse is not symmetrical about the horizontal axis, adjust R81.

Step 3. Set the signal source to 2295 Hz and observe a vertical ellipse. Adjust R96 if necessary to achieve symmetry about the vertical axis. Repeat **Steps 2** and **3** to converge on the final settings.

d)Adjust output tones for 170 Hz shift

Make this modification only if you use AFSK.

Step 1. Connect a frequency counter to J14-2. Temporarily remove jumper JP8 and ground JP8-B to force the tone generator on in the Mark state. Adjust R168 for a frequency reading of 2125 Hz. Alternatively, connect a synthesized sinewave generator to one channel of a dual-channel 'scope. Set the generator to 2125 Hz and trigger on it. Connect the other channel to J14-2. Adjust R168 until the two waveforms are very close to synchronization.

Step 2. Ground U37-10 or U40-1 to force Space. Adjust R164 to 2295 Hz, as above. Remove the ground lead and restore JP8.

Performance

A group of us compared the performance of modified and unmodified PK-232 units at KN6J on 20-meter RTTY, using separate computers running identical software. The PK-232 units shared the audio output of an ICOM IC-765. We found fading stations and QRM/QRN situations, although we experienced more QRN than adjacent-channel interference. At times, we varied signal-to-noise ratios by rotating the four-element Yagi. We saved, printed, and compared the received data. My observers were KN6J, WU6A, and N6OXR—all experienced RTTY operators.

When signal quality was high, both units performed well. But during fades and with lower signal-to-noise ratios, the modified unit exhibited improved performance: fewer individual character errors and shorter burst error recovery times. Excerpts from the printouts are shown in **Figure 7**. All observers agreed a demonstrable improvement was obtained on marginal signals. And as KN6J noted, a character or two is often the difference between a New One and a lost opportunity.

The tests have not been duplicated in an AMTOR environment. The modifications described here provide improved performance on RTTY/AMTOR compared to an unmodified PK-232. However, one may wish to undo these either to operate the "lost" modes or to sell the unit. To restore the PK-232 to better-than-stock condition, replace the bandwidth resistors R42, R52, R62, and R72 with the original value of 174 k, 1 percent. Then, using the dual-trace oscilloscope technique from procedure b, adjust the discriminator resonators to 2110 Hz with R81 and 2310 Hz with R96. The cross-pattern ellipses will no longer be orthogonal.

Acknowledgement

I am grateful to Dave Barton, AF6S, for the use of his laboratory facilities, and for his editing "evil eye."

Appendix I: Calculation of Discriminator Resonant Frequencies

The transfer function for a second order bandpass filter is:

$$T(jf) = \frac{KjfB}{(f_o^2 - f^2) + jfB}$$

where:

K = gain constant
f = frequency
f_o = resonant frequency
B = bandwidth

The phase function is:

$$\Phi(f) = \arctan \frac{Bf}{(f_o^2 - f^2)}$$

Orthogonal ellipses require 90-degrees phase shift between the two filter outputs at both the mark and space frequencies, or:

$$\arctan \frac{Bf_m}{(f_1^2 - f_m^2)} - \arctan \frac{Bf_m}{(f_2^2 - f_m^2)} = \frac{\pi}{2}$$

$$\arctan \frac{Bf_s}{(f_1^2 - f_s^2)} - \arctan \frac{Bf_s}{(f_2^2 - f_s^2)} = \frac{\pi}{2}$$

where:

f_m, f_s are the mark and space frequencies
f_1, f_2 are the resonant frequencies of the low and high filters.

To find f_1 and f_2, obtain algebraic funcitons by taking the cotangent of both equations, using the identities:

$$\cot(A-B) = \frac{1 + \cot A \cot B}{\cot B - \cot A}$$

$$\cot(\arctan C) = \frac{1}{C}$$

After clearing fractions,

$$(f_1^2 - f_m^2)(f_2^2 - f_m^2) + (Bf_m)^2 = 0$$

$$(f_1^2 - f_s^2)(f_2^2 - f_s^2) + (Bf_s)^2 = 0$$

Solve both expressions for one of the (squared) variables as a function of the other, then set the resultant fuctions equal to each other and order the terms. This will yield a quadratic equation in one squared variable.

$$MX^2 + NX + P = 0$$

where:

$X = f_1^2$
$M = f_m^2 - f_s^2$
$N = f_s^2 (f_s^2 + B^2) - f_m^2 (f_m^2 + B^2)$
$P = f_m^2 f_s^2 (f_m^2 - f_s^2)$
$f_m = 2125$ Hz
$f_s = 2295$ Hz
$B = 197.5$ Hz

Solution of the quadratic equation is straightforward and yields:

$$f_1, f_2 = \begin{cases} 2081.9 \text{ Hz} \\ 2342.5 \text{ Hz} \end{cases}$$

Due to symmetry, *either* variable yields *both* values of filter resonance.

REFERENCES

1. *Operating Manual, Model PK-232MBX Data Controller*, Advanced Electronic Applications, Inc., 1990.
2. R.W. Lucky, J. Salz, E.J. Weldon, Jr., *Principles of Data Communications*, McGraw-Hill, 1968, Chapter 8.
3. W.R. Bennett and J.R. Davey, *Data Transmission*, McGraw-Hill, 1965, pages 327-332.
4. B. Henry and R. Petit, "HF Radio Data Communication: CW to CLOVER," *Communications Quarterly*, Spring 1992, pages 11-24.
5. W.R. Bennett and J.R. Davey, *Data Transmission, McGraw-Hill, 1965, pages 182-190.*
6. *A. Chandler, "HF Modems for Data Transmission," Communications Quarterly*, Spring 1991, pages 74-78.
7. M.S. Ghausi and K.R. Laker, *Modern Filter Design*, Prentice Hall, 1981, pages 331-334.
8. N. Fliege, A New Class of Second-Order RC-Active Filters with Two Operational Amplifiers, *Nachrichtentech.Z, 26(6), 279-282, 1973, reprinted in: L.P. Huelsman, Editor, Active RC Filters: Theory and Application*, Dowden, Hutchinson & Ross, 1976.

CORRECTIONS

Charles Michaels, W7XC, asked that we make the following corrections to his article "How Short Can You Make a Loaded Antenna" (Summer 1992).

The curves in **Figures 2** and **5** were plotted incorrectly. The corrected figures are shown here.

On page 74, delete the last line of the **Figure 2** caption. Also delete the first and second sentences of the second paragraph under **Results**. The text should be revised as follows: The curves of **Figure 2** apply to the no. 10 wire in this 7.15-MHz example. For other frequencies and wire sizes, use the equations in the appendix.

In the appendix on page 79, **Equation 3** *should read:*

$X = 60\{[(\ln(48((A/2) - B)/d) - 1)/\tan\Theta 2] - [(\ln(48B/d) - 1)\tan\Theta 1]\}$

Also, in the definition following **Equation 7**, change R_2 to R_r.

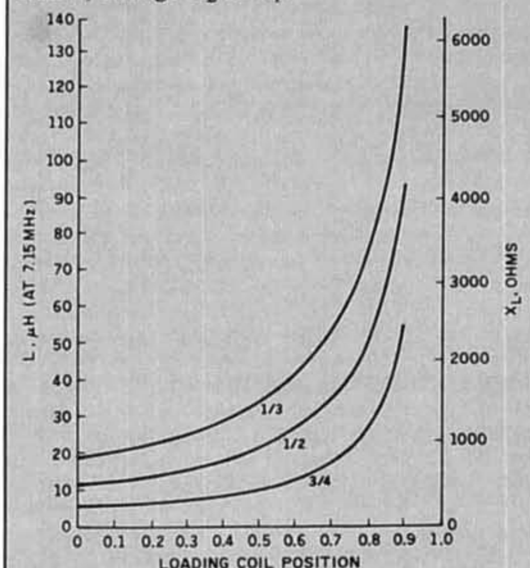

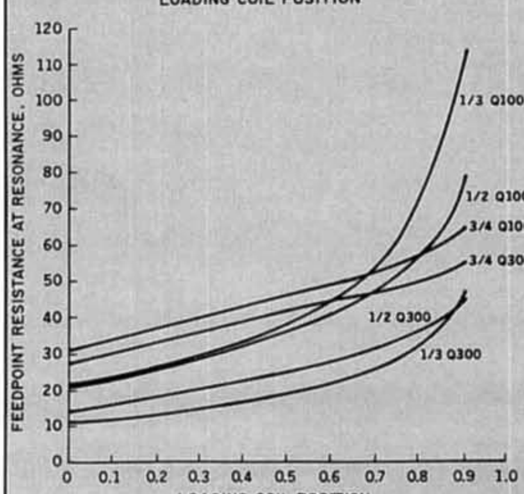

TECHNICAL CONVERSATIONS

Forrest Gehrke, K2BT, had some comments on "A Simple and Accurate Admittance Bridge" (Summer 1992).

Dear Editor:

The article in the Summer issue, "A Simple and Accurate Admittance Bridge," provides no information to a prospective builder concerning the noise source or any discussion of the level of noise signal required. This is a serious omission as insufficient signal will result in wide nulls rendering measurements uncertain or indeterminate. Unfortunately, those unaware of this will unknowingly accept the readings. Having experimented with noise bridges over the past two decades in an attempt to achieve significant accuracy,[1,2,3] I can vouch for the above statements.

Noise signal must be sufficient to make achieving a deep null a quite sensitive procedure as it will be found that the resistance and reactance necessary for a perfect null are quite interdependent. What might appear to be a best null with the resistance dial can be bettered by readjusting the capacitance dial, in turn finding a still better null with the resistance dial, and so on. Having reached an absolute quieting null, the minutest change of either dial will upset it. Insufficient noise signal will significantly reduce this interdependency of finding a null and, consequently, accuracy.

I submit the schematic for a noise source I supplied with my Ham Radio article (see **Figure 1**), with the exception that 2N5179 transistors be substituted for 2N2222. The 2N2222 transistors, though easily and cheaply available, are too variable in characteristics and more seriously, fall off in output too quickly below 20 MHz. This circuit depends for its noise source upon a zener diode which is "starved;" i.e., the current is insufficient to bring it to its stable voltage rating. Builders are advised to try a selection of 5.6 or 6.8-volt zeners for best output over the frequency range with emphasis at the highest end of the range. However, I have seen them fall off at 1.8 MHz as well.

Author Caron has come up with another approach attempting to improve the balance of coupling of the single-ended noise amplifier to the bridge using a transmission line transformer. It is serendipitous that Jerry Sevick's article on transmission line transformers and baluns should appear in the same issue. As Jerry points out, these can have serious limitations depending upon application. In bridge applications, the greatest problem has been lack of balance over the entire frequency range and that they will add a reactance component. These problems are especially noticeable at low resistance loads (under 20 ohms) and with any load having a high reactance.

One of the first published noise bridge articles to use a transmission line transformer was proposed by Pappot in an article in Ham Radio.[4] The advantage of the concept is the very low transmission impedance and the resulting high immunity to strays from high impedance coupling to nearby surroundings. However, this advantage brings with it the ultimate limitation to accuracy by introduction into the two arms of the bridge, reactances that are impossible to keep in perfect balance throughout as wide a frequency as 1.8 MHz to 30 MHz.

Measuring coupling between two antenna elements is an example where accuracy becomes paramount. The resonant self-impedance of two 1/4-wavelength verticals on extensive radial systems will be very

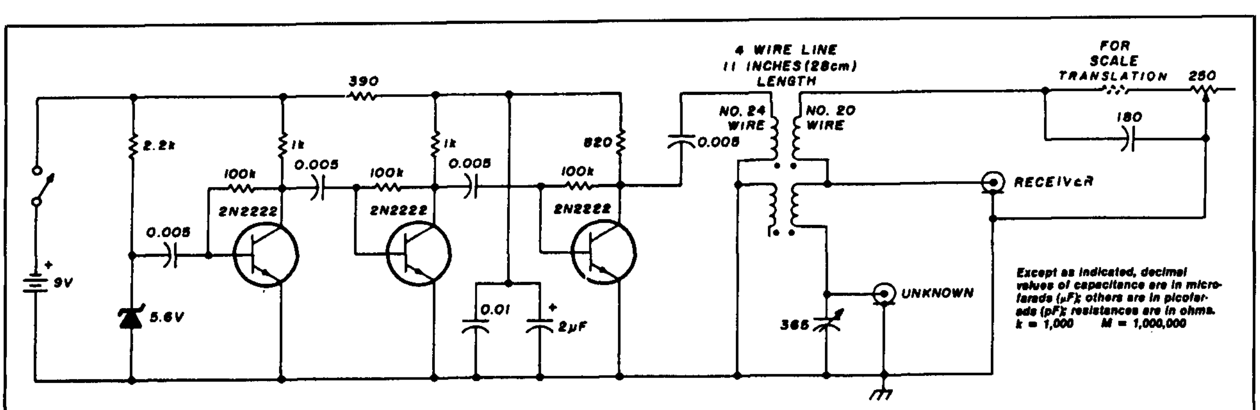

Figure 1. Schematic for noise source. Substitute 2N5179 transistors for the 2N222s.

close to 37 ohms each. If these are spaced 1/4 wavelength, the coupled vertical's resistance will rise to about 40 ohms with a high inductive component of reactance. Bridge measurement accuracy of 5 percent (no mean achievement) can easily introduce an error of 50 percent in the mutual impedance calculation, which would be devastating to the front-to-back ratio of the antenna array because of the errors in the driving network.

I commend Caron for his improvement, but we still need something much more accurate; hopefully, it will be just as economical and as easy to build and calibrate.

Forrest Gehrke, K2BT
Mountain Lakes, New Jersey

REFERENCES

1. Forrest Gehrke, K2BT, "Impedance Bridges" (letter), *Ham Radio*, March 1975, page 60.
2. Forrest Gehrke, K2BT, "Antenna Noise Bridge" (letter), *Ham Radio*, September 1977, page 100.
3. Forrest Gehrke, K2BT, "A Precision Noise Bridge," *Ham Radio*, March 1983, page 50.
4. Gijs Pappot, YA1GJM, "Noise Bridge Impedance Measurement," *Ham Radio*, January 1973, page 62.

Michaels replies to Hansen

I would like to reply to Mr. Hansen's comments in the Fall 1992 issue of *Communications Quarterly* ("Letters," page 8) regarding my use of his work in my article "How Short Can You Make a Loaded Antenna" (Summer 1992), without giving him proper credit.

I found that most libraries do not stock IEEE group transactions. They are, however, available at university science libraries. I found that Hansen's articles are, except for minor wording changes, identical.

Hansen cites a litany of prior work on the problem of loaded monopole (half dipole) efficiency. Only one article made reference to loading point 0.67; another used only the zero order solution of the equations involved. One used long helix, but a discrete inductor is better; another on a UHF laboratory model denigrated because it had caps for the coils. Can't stand that kind of realism can we? These citations appear rather self-serving. They establish that the flatness of the curves is not a new and mysterious phenomenon on which Hansen has some claim of discovery.

Hansen's Method of Moments program (like MININEC apparently) solved the problem for short fat antennas with height to radius ratios, h/a, of 50 and 500. You could "repeat his calculations" for his problem or the problem I posed in my article with a personal computer and a MININEC program. You wouldn't need his article(s), or mine. While the computer-generated data curves in his article solve his problem, *they are absolutely useless for the wire antennas in the lower HF range that I addressed.*

My 40-meter example using no. 10 wire has h/a of upward to 7,000. A ham trying to squeeze a no. 14 wire 80-meter dipole into his yard by some shortening would have h/a of up to above 20,000.

Hansen says his articles "use more accurate impedance formulas, the results should be more useful than those given by Michaels." *There are no impedance formulas in his articles!* His **Figure 7** is a set of curves for coil reactance for antennas with *h/a of 50 and 500*. It is not clear whether these came from a formula or from his computer runs.

I can understand how Hansen seeing the similarity of our efficiency curves would jump to the conclusion that I had simply "repeated his calculations and results." My appendix equations and cookbook directions permit any amateur with a $27.95 handheld calculator to evaluate a planned or existing antenna—equations available to anyone in *QST* and *Ham Radio* articles and *The ARRL Antenna Book*. They are the equations I used in my March 1990 *QST* article, "Evolution of of the Top Loaded Vertical" (see "Feedback," *QST*, November 1991). I used Q of 300 in that article as reasonably achievable and Q of 100 because in an August 1987 *QEX* article I cited a poor coil design having a Q of 110, rounded to 100. His curves are for a *constant h/a*, my curves are for a constant *diameter*. Who measures wire radius? What ham would increase required inductance and loss by using thinner wire in shortening an antenna to keep constant h/a?

On accuracy, my impedance formula (**Equation 3**), is based on Z_0 by Jordan and Balmain, *Electromagnetic Waves and Radiating Systems*, page 387, or Schelkunoff and Friss, page 432. More accurate formulas exist, but I used the simplest approximation. For thin wire $Z_0 = (\ln(2h/a) - 1)$.

Had I used any of Hansen's work, I would have cited him. But under his "credit where credit is due" demand, I should have cited Bulgerin, Walters, Harrison, Fujimoto, Harrington, Czerwinski, Lin, Nyquist, Chen, and Hansen—and any other whom I have offended by omission. How did I miss their appearance in amateur radio literature, if such works were useful to amateurs without computers?

The editor has kindly offered copies of somewhat hurried, but more detailed discussion. (Send an S.A.S.E. to P.O. Box 465, Barrington, New Hampshire 03825.)

Charles Michaels, W7XC
Phoenix, Arizona

Howie Cahn, *WB2CPU*
295 Beacon Street #23
Boston, Massachusetts 02116

THE FINAL TRANSMISSION

Bringing amateur radio into the computer age.

"The Final Transmission" is a forum for our readers and authors. The opinions expressed in this column are those of the writer and not necessarily those of the staff of Communications Quarterly. Ed.

The relationship between hams and our equipment has changed over the last several decades; we're less involved in the technical aspects of communication than we were. We are less likely to be designers, builders, or trouble-shooters of our radios. We're less likely to be technological innovators. While the new operating modes and feature-packed commercial equipment suggest a modern, high-tech activity, the brainpower generated while operating our transceivers isn't that much different from that of other consumers passively using their VCRs and cellular phones. The appeal of amateur radio to us, and our utility to the society at large which authorizes our frequency allocations, is based on many things. Perhaps the primary value to the outside world, though, has been our technical skills. Historically, the amateur radio community has been a important resource in times of war and peace. As our understanding of how our equipment works fades, these skills diminish and the value of our role will be questioned. The question we should be asking ourselves is how can this trend be reversed?

There have been signs that some hams are uncomfortable with this state of affairs. There has been a resurgence of interest in old radio technology and in building and operating QRP equipment. By either going back to circuits that we learned and understood years ago, or by using minimal implementations of more modern components, a sense of connection to and control over the equipment is restored. These attempts, however understandable, are ultimately likely to be unsatisfying and unsatisfactory. It's like a modern army using bows and arrows. A generation of hams used to the performance and convenience of modern transceivers won't be convinced to switch to 6L6 transmitters or direct-conversion receivers. The solution must combine the accessibility of the simpler equipment with the performance of the modern gear.

There is a gap between the commercial and amateur worlds in the acceptance of emerging technologies. Hams were slow to accept the transistor, but the disparity became particularly pronounced with the arrival of the computer and other circuits now based on the integrated circuit. Projects, components, and methods featured in amateur publications often lag those in the professional trade press by a decade or more. Basic proficiency in digital design and programming hasn't become part of the skill set considered necessary to being a technically competent ham. Certainly, computers are found in ham shacks these days—either as stand-alone PCs, with which we run canned programs, or, as fixed-programmed processor chips in our transceivers. But that alone doesn't make us technologists any more than it does the secretaries, accountants, or graphic designers with similar equipment on their desks.

When we do use computers, it's often in ways which don't utilize their full potential or which add complexity to our shacks. They're accessories to our existing stations, used to do things such as logging, packet operation, or satellite tracking. Our attention is divided between two focal points; the computer, where we enter callsigns, get packet spots, or find our satellite, and the radio front panel, where we adjust gains and passbands and read meters. The transceiver manufacturers are perfectly willing to go along with this arrangement and will gladly sell us interface boxes, cables, and software to augment their radios. However, this setup is needlessly costly, confusing, and limiting.

What I would like to see is an equipment architecture where the radio is more directly integrated with the computer. Computer-controlled instruments are becoming standard in the electronics industry. Signal generators, counters, and even oscilloscopes are being built with few, if any, controls on the instrument itself. Instead, control and display functions are represented on the computer screen. These screens are referred to as "virtual instruments."[1] Similarly, a radio front panel could be replaced with a windowed, graphically oriented screen. This would remove a large portion of the radio's cost in meters, fancy tuning knobs, digital displays, pots, and switches.

In addition to reducing cost, users would gain control over how their equipment worked. When you buy a transceiver, you get a box with a fixed set of features and operating characteristics. The ability to change it is pretty much limited to the options the manufacturer will sell you. Of course, you can't use an option from company X if your radio is from company Y. Computers, on the other hand, are inherently more flexible and offer vast possibilities for involvement. On a computer-based system, instead of being wired in hardware or hard-coded into a ROM, operation would be controlled by programs that are accessible in the machine's file structure and therefore modifiable or replaceable. By buying or writing software, you would customize the way you interact with the machine. You could also take advantage of the hardware already in the computer; using the screen as a spectrum analyzer or oscilloscope display, for example, or using the machine's memory for frequency or configuration storage.

The IBM-compatible PC industry provides a model of how ham radio equipment could be built. The PC became the standard, not because of its original processor chip or operating system (arguably, both were inferior to others around then), but because of the weight of the IBM name and the fact that it was modular and followed defined standards that allowed others to participate. Developers around the world stepped in and created the vast amount of hardware and software available today. The result is an efficient, cost-competitive market in PC components. If radio equipment was similarly designed, the monopoly of the few major transceiver manufacturers could be broken.

Present equipment inhibits people from modifying, repairing, or expanding their rigs. If I wanted to experiment with a DSP IF stage, it would be difficult to graft one onto a commercial transceiver; I'd have to build a whole radio from scratch. Few of us have the time or the expertise in all the necessary areas to do this, and some of the things required, like multi-layer boards and custom ASICs, are beyond what you can do in your basement.

If the equipment were divided into modular pieces with defined interfaces, you could work only on those sections you could handle and had time for. I could build my DSP IF stage and buy the rest of a system to plug it into. In addition to encouraging experimenters, a cottage industry would develop with individuals and small companies creating and marketing compatible components; direct digital frequency synthesizers, audio processors, or my IF stage, all of which would fit together into unified systems. Someone who had no interest in building would still be more involved by being able to configure the system they wanted from the products available. You could repair your equipment by swapping modules. Adding a new feature wouldn't require buying a whole new rig; just replacing a board. Many of us complain about how we wish we could change our equipment. With modular hardware and user-accessible software we'd have the opportunity to do so.

There is another benefit to making radio equipment more computer-based: attracting a new generation of technically oriented hams. One of the reasons that there is so much interest in old radio equipment is that as a group we're getting older. The age of the average ham is well over 50. It's widely recognized that we're not drawing young newcomers like we did in the post-war years. Back then, the best and brightest kids with technical interests gravitated to ham radio; now, they're more likely to become active in computer-related hobbies. The energy and intelligence of these kids are needed to sustain the us in the future. Having grown up with video games, Apple computers, and DOS, they can provide a perspective that we desperately need. If we can narrow the perceived gap between computers and radio, we can attract some of them. I think we provide many opportunities they'd find very appealing: high-speed data networks, satellite communication, image and video transmission, etc. The first step has been taken with the creation of the code-free license. The next is making radios that are seen as extensions of the computer, like a modem. If amateur radio was viewed as a natural partner to their computer technology and culture, I believe that many would join us.

About twenty years ago a major shift took place in amateur radio. The gulf between the technology in traditional ham gear and the new microprocessors and other integrated circuits grew so wide that the American ham equipment manufacturers were quickly swept away. The familiar names disappeared, replaced by Japanese makers of synthesized transceivers who did take advantage of the new technologies. I believe that we have again deviated sufficiently from the mainstream of electronics that a similar transition will follow soon. This time it is the new establishment who will try to maintain the status quo. The computer-integrated radios I described would be a threat to these manufacturers because they would open up the market and be based on a computer technology not under Japanese control. The whole radio market would again be available to domestic producers who currently are limited to selling add-on peripherals. What we need to do is define the standards for this new kind of radio equipment and encourage their use. I'd like to talk to and work with anyone who has similar feelings.

REFERENCES
1. Bryan P. Bergeron, NU1N, "Micro-Computer-Based Instrumentation Systems," *Communications Quarterly*, Winter 1992, page 36.

PRODUCT INFORMATION

A New Family of DSOs

John Fluke Mfg. Co., Inc. and Phillips have introduced a series of 100 and 200-MHz analog/digital oscilloscopes which feature true four-channel operation. There are also models with 2 + 2 input channel configuration.

The four oscilloscopes in the PM 3382/84 and PM 3392/94 family combine the ease of operation and realtime 100 or 200-MHz bandwidth of an analog instrument, with digital sampling rates of 200 million samples per second. The units also provide additional features like triggering, automatic pass/fail testing, signal math and analysis, signal averaging and peak detect mode for HDTV tri-level sync. A serial interface for printer/plotter is standard on all scopes; a GPIB/IEEE 488.2 interface option is available.

The PM 3384 and PM3394 offer 4-channel operation providing full sensitivity with complete attenuation ranges on each channel. The PM 3382 and PM 3392 offer 2 + 2 channel operation, as a cost-effective alternative to four fully featured inputs.

For more information contact John Fluke Mfg. Co., Inc. P.O. Box 9090, Everett, Washington, 98206-9090.

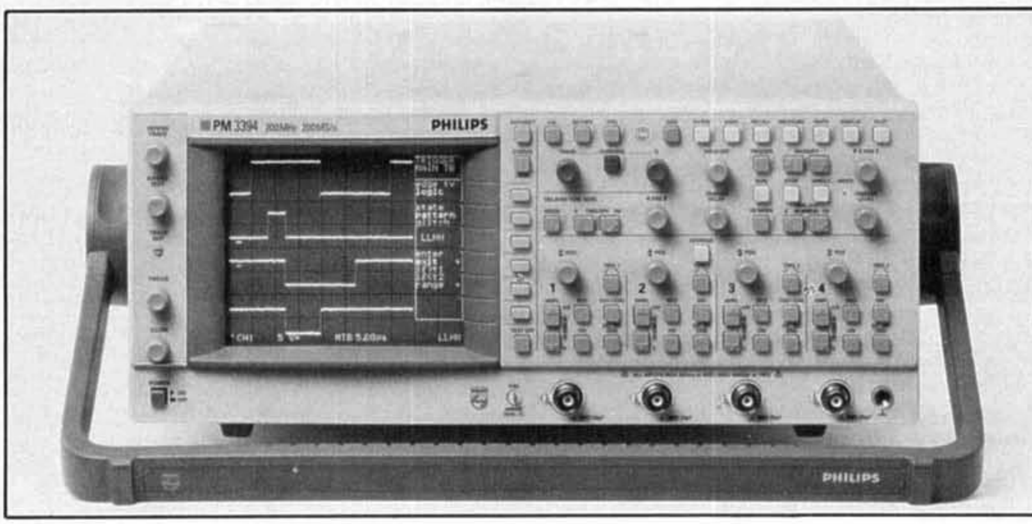

A note from down under

This tech note was written by Lloyd Butler, VK5BR, of Panorama, Australia. It is reprinted with permission from the July 1992 issue of Amateur Radio magazine. I want to thank Jerry Sevick, W2FMI, for his assistance and comments.
Peter Bertini, K1ZJH, Senior Technical Editor

Measurements on Balanced Lines Using the Noise Bridge and SWR Meter

Lloyd Butler, VK5BR

I have often been asked how test instruments common to the radio shack could be used to measure the performance of balanced transmission lines. This is a good question considering that instruments such as the noise bridge and the SWR meter, in their usual form, are made for unbalanced lines with a ground common. Furthermore, the usual SWR meter is made for a balance at 50 ohms, and sometimes 75 ohms, whereas balanced lines, such as TV ribbon and open wire pairs, have a higher characteristic impedance such as 300 ohms.* There seems to be little in the amateur radio handbooks addressing this problem, so I decided to experiment with a few ideas aimed at using these instruments on balanced lines operating in the HF region.

Initial discussion follows around the use of special balancing circuits which connect to the usual amateur radio noise bridge. The discussion leads on to the SWR meter. In the process of experiment, I constructed a special SWR meter for balanced lines and this instrument will be described. To lead up to this subject, the operation of a typical SWR meter for unbalanced lines is discussed. Whilst there is plenty of available construction information on these instruments, basic theory is often just assumed. Most radio amateurs use these instruments, but I often wonder how many understand the significance of what they measure.

Measurements through balun transformers

Measurements into balanced lines can be made through a 1:1 RF transformer with primary and secondary tightly coupled. This is easily achieved with the primary and secondary twisted together and wound on a suitable toroidal ferrite or iron dust core. The method shown in **Figure 1A** is not satisfactory for measurement purposes because there is a capacitance unbalance reflected to the secondary from the unbalanced primary. An electrostatic shield between primary and secondary would solve this problem, but be difficult to apply whilst still maintaining tight coupling.

A more satisfactory connection is shown in **Figure 1B**, in which each leg of the line is fed through one of the two windings. For the balanced load, the current Ib in each winding is equal but opposite in phase to each other, and the magnetic field is balanced out, resulting in zero inductance. For any common mode signal, the currents IC1 and IC2 through the two windings are in phase, hence the device acts as an inductive choke. If there is an unbalance in the load currents IB1 and Ib2 through the windings due to an unbalance of impedance in the load to ground, the device acts as a choke to the differential value of the current (Ib1-Ib2) or (Ib2-Ib1). In effect, the transformer acts as an inductive choke to all but the balanced load current.

The noise bridge

The noise bridge is inherently a device for measuring the reactance and resistance of an RF load with one side grounded. The rotor of its tuning capacitor is grounded and the output to the receiver has one side grounded. I did consider the possibility of a new circuit with the whole bridge floating above ground, but this would have presented some real design problems. However, I found that quite reasonable results could be achieved by connecting the balanced load under test via the choke circuit of **Figure 1B** and as shown in **Figure 2**. For frequencies below 10 MHz, I used 12 bifilar turns on an

*Amateurs using any bridge should remember that unless the bridge is placed directly at the antenna feedpoint, measurements made at the end of a random length of feedline will produce erroneous readings. For example, a 300-ohm line terminated to a 50-ohm half-wave dipole could give readings from as low as 50 ohms to as high as 1800 ohms. For a full-wave dipole the scenario is even worse—readings from as low as 5 to as high as 10,000 ohms are possible. The impedance of the transmission line may not be the impedance seen by the bridge. Ed.

Amidon FT50-72 toroidal ferrite core. The method of winding does introduce some shunt capacitance across the circuit, and five turns were found to be more suitable above 10 MHz to reduce error caused by this capacitance.*

One problem with the common form of noise bridge is that maximum resistance measurable is limited to 250 ohms or less. The characteristic impedance of ribbon cable and open wire line is usually much higher than this. In my own home-constructed noise bridge I can switch in extra fixed resistance to allow measurement up to 800 ohms.

An alternative method of measurement is to connect the balanced line via a candelabrum connected balun as shown in **Figure 3**. Two separate transformers, each similar to that of **Figure 1B** are used and an impedance transformation of 4 to 1 is achieved. The circuit is an extension of the **Figure 1B** 1:1 ratio with the inputs of the two transformers in parallel and the outputs in series. Resistance and reactance measurements are indicated on the bridge as a quarter of the real value. For example, 300 ohms resistance would be read as 75 ohms.

I found the two methods of measurement to be satisfactory on a transmission line provided the line was well balanced, such as when terminated in a centre-fed antenna. If some degree of unbalance exists, such as when the line is matched into the end of an antenna, the measured results are in question. In this case, reversing the connecting leads to the line gives a different impedance reading. I suspect the true impedance in the balanced mode is some form of mathematical mean between the two readings, but I am not sure about this.

I found that the out-of-balance component could be essentially eliminated by using the candelabrum divide by four circuit, but further isolating its input via another balun choke of **Figure 1B**. The complete system is shown in **Figure 4**. Using this system, the transmission line leads could be reversed without change of reading, even if the line was a little out of balance. I recommend this as the preferred measurement system.

Concerning the toriodal transformer design, the inductive reactance of a winding should be sufficient to act as a choke at the impedance being measured (say 10 times the impedance). On the other hand, as few turns as possible should be used to minimize capacitance between the windings. To achieve high inductance with few turns, a high permeability ferrite core is desirable. The Amidon FT50-72 cores which I used have a permeability of 2000.

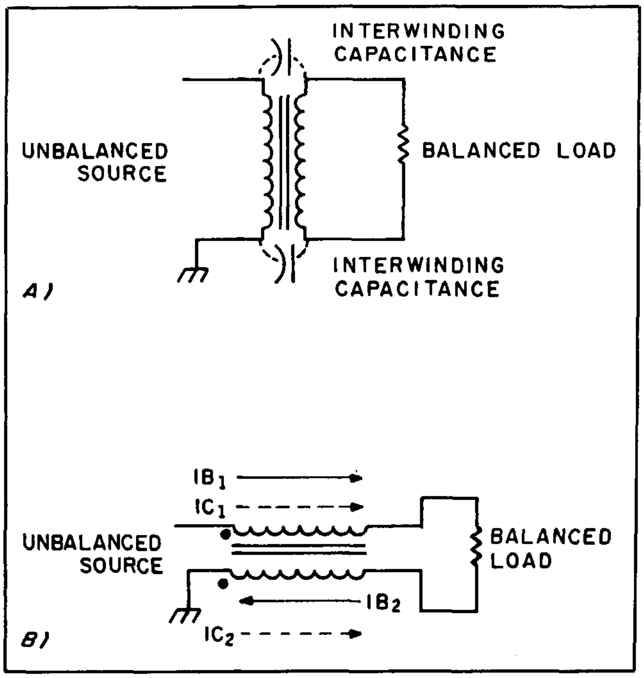

Figure 1. Two forms of 1:1 unbalanced-to-balanced circuit transformer.

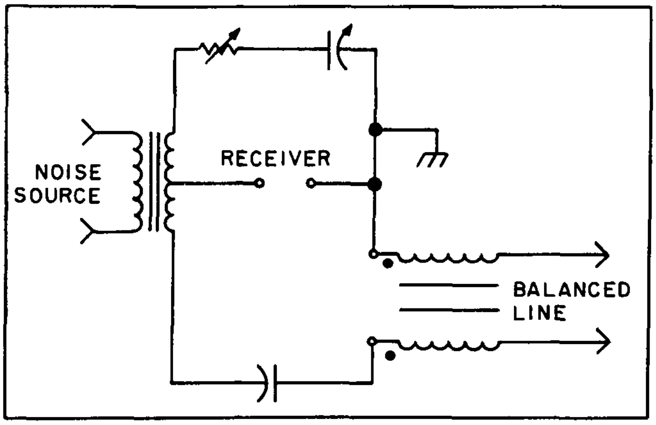

Figure 2. The noise bridge connected to read impedance of a balanced line via balun choke.

Before making any measurement on an actual transmission line, the circuit can be checked out using a resistor of value equal to the characteristic impedance of the line. This will give an indication of the accuracy of the system and whether any appreciable reactance is introduced by the balancing network. This is most important towards 30 MHz where the result can be most affected by a small amount of shunt capacity and lead inductance.

The SWR meter

Before introducing SWR measurement on balanced lines, I thought it would be help-

* Standing waves, not the shunt capacitance of the turns on the balun, limit the high frequency response. Using fewer turns only results in shorter transmission lines and hence less effect from standing waves. Ed.

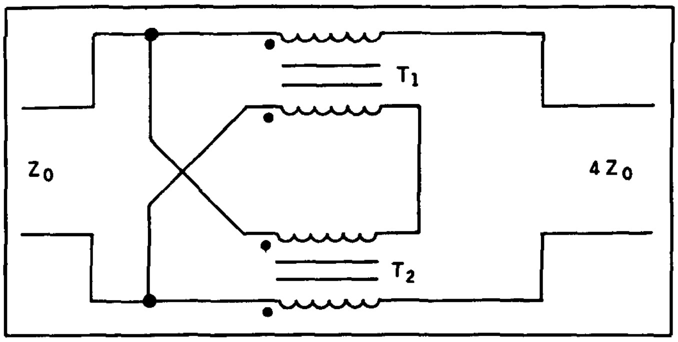

Figure 3. The candelabrum balun arrangement provides a 4:1 impedance transformation.

ful if I first discussed the operating principle of the standing wave ratio (SWR) bridge. Most radio amateurs could explain that the instrument somehow measures forward wave power and reflected wave power, and that it derives a ratio between maximum and minimum of standing wave voltage or current on the transmission line. Let us examine the operation of the instrument in a little more depth.

The instrument operates by comparing two voltages. One voltage is derived from the voltage across the line and is proportional to and in phase with that voltage. The other is derived from the current through the line and is proportional to and in phase with that current. One type of instrument uses a loop run along in parallel with a length of the line to inductively couple the current component. The voltage component is capacity coupled into the loop. Most SWR meters are also calibrated in power, and this particular instrument, more often used at VHF/UHF, gives a power reading which varies with frequency. Hence it requires a power versus frequency calibration chart.

An SWR meter, which is often assembled by the home constructor, makes use of a toroidal current transformer to derive the current sourced voltage component and a resistive voltage divider for the voltage component. A typical circuit taken from *Amateur Radio*[1] is shown in **Figure 5**. Because of the methods used to couple each component, the developed voltages are constant with frequency, and a calibration chart is not required. For this particular circuit, operation to 70 MHz is claimed. For further explanation of the SWR meter, we will make use of this circuit.

The voltage derived from current in the line is developed across either of the two 27-ohm resistors marked R. The voltage VI is calculated as follows:

$$VI = I_L R/T$$

where I_L is the line current and T is the turns on the secondary of the current transformer. (The primary is, in effect, one turn.)

The voltage Vv developed from that across the line is equal to the voltage divider ratio formed by VR1 in parallel with R2 and connected in series with R1. The values of T, R, R1, and R2 in parallel with RV1 are carefully selected so that VI = Vv when the load resistance is equal to the nominated line impedance (50 or 75 ohms).

Two detector circuits record the summed voltage of Vv and VI. One, which we will call Forward, adds them directly. The other, which we will call Reverse, adds them, but with VI reversed in phase. We now refer to the vector diagrams of **Figure 6**. If the load is resistive and equal to line impedance, then for Forward, (Vv = VI and the resultant Vr = 2Vv = 2VI (**Figure 6A**). For

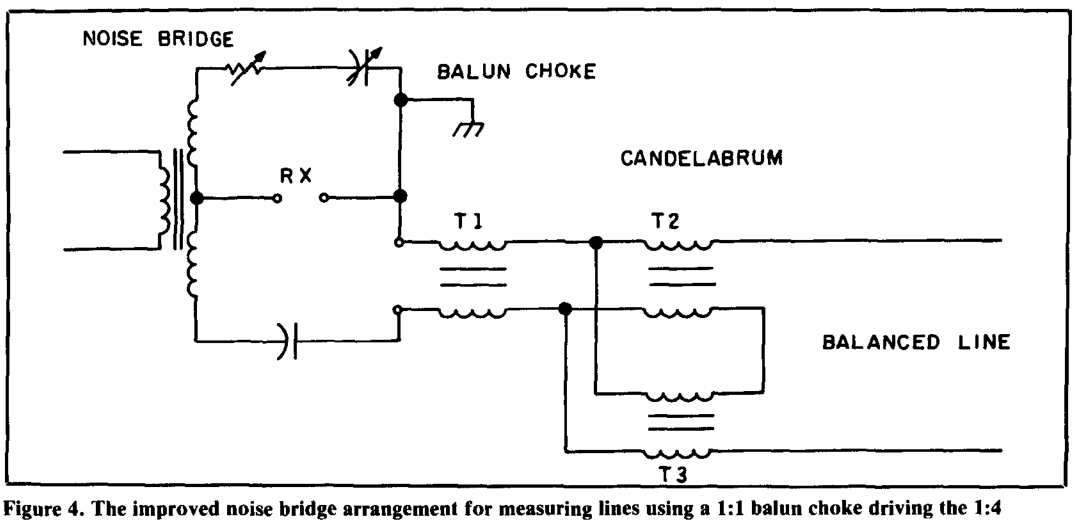

Figure 4. The improved noise bridge arrangement for measuring lines using a 1:1 balun choke driving the 1:4 candelabrum circuit.

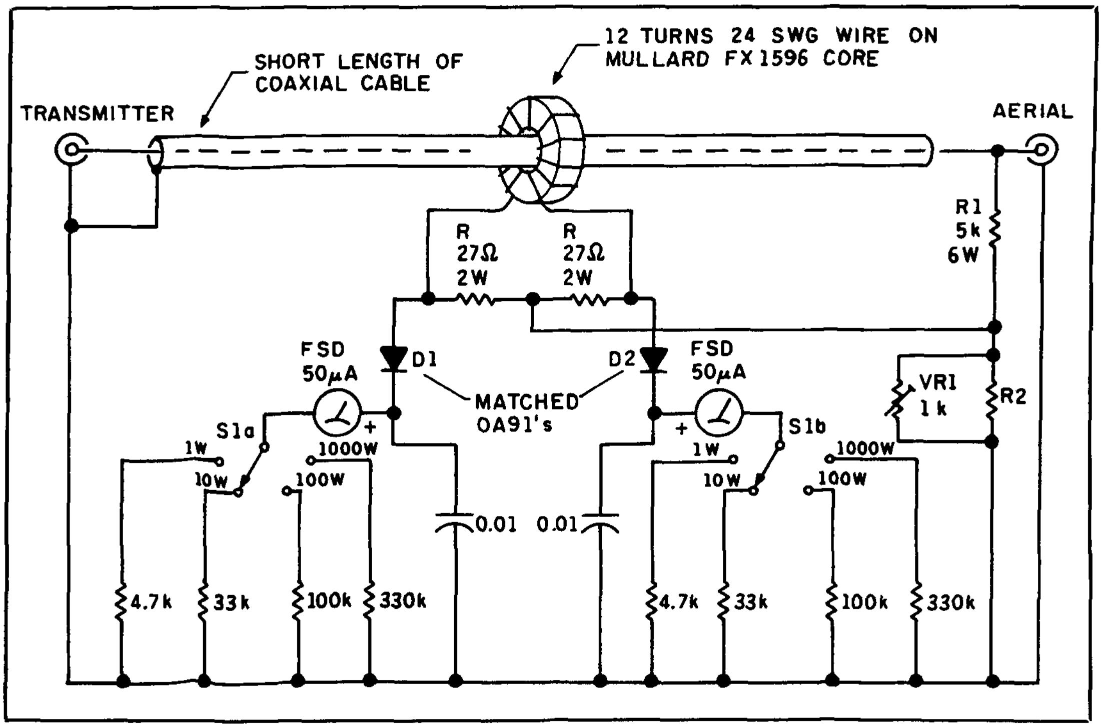

Figure 5. Typical SWR/power meter for HF frequencies (from *Amateur Radio*, November 1969). The sensitivity ranges given in S1a and S1b are double the correct figure. Those in the caption are correct. Circuit of the basic Frequency-Independent Directional Wattmeter, with four ranges corresponding to full-scale deflections of 0.5, 5, 50, and 500 watts in 50-ohm lines, when the value of R2 (including VR1, if fitted) should be 220 ohms. For 75-ohm systems R2 equals 150 ohms, and the calibration is different. The coaxial cable acts as an electrostatic screen between its centre conductor and the secondary winding of the toroidal transformer; the cable length is unimportant.

Reverse, the resultant is zero (**Figure 6B**), hence the ratio R between Reverse and Forward values of Vr is zero.

If the load resistance is not equal to Zo, as shown in **Figures 6C** and **D**, a finite value of resultant voltage Vr is developed for Reverse, and the ratio R between Reverse and Forward values of Vr is finite.

A third case (**Figure 6E** and **F**) shows a load impedance equal to Zo, but reactive, hence the load current is out of phase with the load voltage. Again a finite value of resultant voltage Vr is developed for Reverse, and the ratio R between Reverse and forward values of Vr is finite.

It can be seen that the instrument is a bridge circuit which balances when there is a resistive load equal to Zo and records by ratio R the degree by which the load deviates in impedance from that resistive value. When connected to a transmission line, ratio R also equals the ratio between the reflected wave voltage and the incident or forward wave voltage on the line. In operation, transmitted power is set (or meter sensitivity is set) so that the Forward meter reads full scale representing forward wave voltage down the line. The Reverse meter, representing reflected wave voltage, then reads the ratio R between Reverse and Forward values of Vr, hence representing the ratio between reflected and forward wave voltage. The relationship between standing wave ratio (SWR) and ratio R is given by the formula:

$$SWR = (1 + R)/(1 - R)$$

The normal practice is to calibrate the Reverse meter scale in SWR as defined by the formula. The Forward meter scale in SWR as defined by the formula. The Forward meter is calibrated in power based on E squared divided by Zo where E is the line voltage for an SWR = 1.

Most amateur radio operators of today use an SWR meter, but I venture to say they are used more to ensure that a 50-ohm load is presented to their transmitter than to check SWR on their transmission line. If some form of tuning or matching device is connected between the SWR meter and the transmission, there is no relationship between what is read on the meter and what standing waves are actually on the line.

How often do we hear on the air someone quoting his SWR = 1:1 to indicate how well his antenna system is adjusted, when in fact he is really telling us how well his transmitter is loaded to its correct load impedance? In the next breath, he tells us that he is using a Z match or transmatch or whatever and, in reality, has no idea of what standing waves exist on his transmission line, or what power loss these waves might be causing.

We can use the SWR meter to check the performance of a dummy RF load. We often see a dummy load quoted as having a standing wave ratio of some value at a given frequency. This, of course, is an anomalous declaration. The path length through the core of the dummy load can be considered as but a fraction of a wavelength, hence there are virtually no standing waves. What they really mean is that using an SWR bridge to check deviation in impedance from the nominal value of dummy load resistance R, a given value on the SWR scale is recorded. It means the impedance load produces a SWR reading similar to a transmission line of Zo = R and operated with that SWR.

So the SWR meter is not really some device which, by some form of magic, separately plucks out the forward wave and the reflected wave to calculate standing wave ratio. It is a bridge circuit which records impedance deviation from a given nominal resistance and is calibrated in terms of transmission line SWR.

If it is not obvious, to measure SWR on the transmission, the meter must face the line. If the line is balanced, or is a different Zo from that for which the meter is designed, some form of transformer is required. As will be discussed in later paragraphs, this addition in itself can produce some questionable readings on the meter.

Owing to loss in the transmission line, the SWR reading will always be higher at the far or antenna end of the line. It is good to check out the far end, but somewhat difficult if located high out in space. If the line is balanced, a balanced SWR meter would seem to be the order of the day. As you will see in the following paragraphs, I have made an effort to design one. I must admit that, up to now, I have stayed at ground level and have not attempted to use it aloft.

Concerning **Figure 5**, I built a unit based on this type of circuit some years ago. For the record, I added a small capacitor across R2 to make the unit balance properly at the upper end of the HF band. This seemed to be necessary to correct for a few picofarads

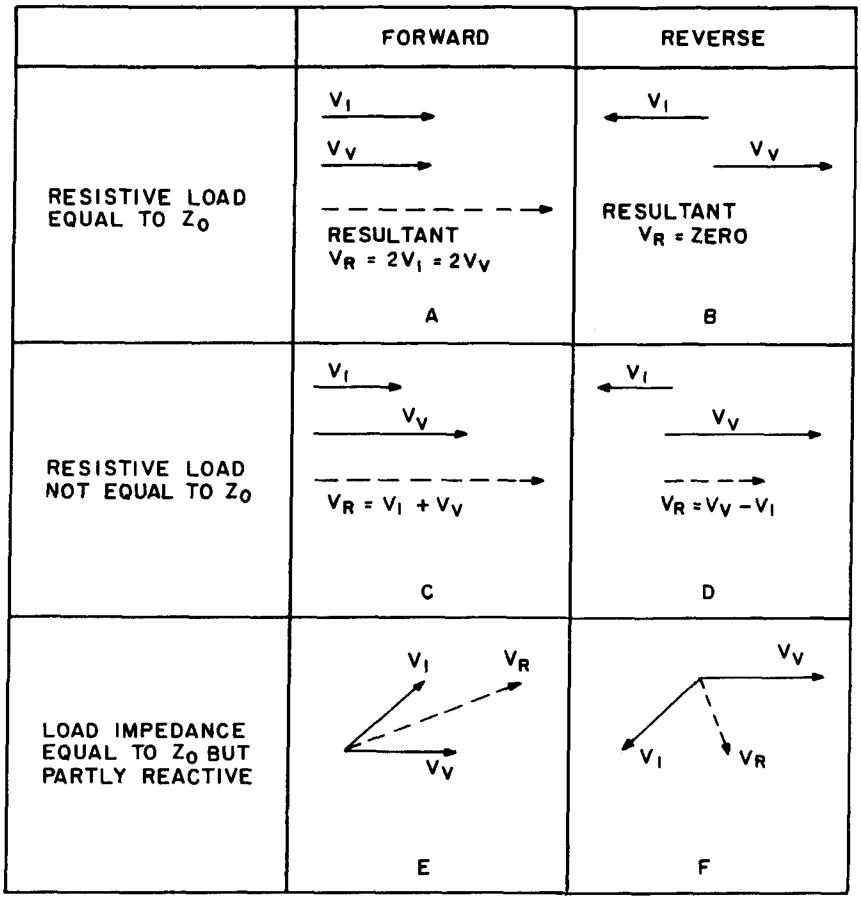

Figure 6. Vector diagrams for the SWR meter (see text).

of stray capacity in parallel with R1. This might be a useful tip for someone else building such a unit.

An SWR meter for balanced lines

As part of the balanced line exercise, I set out to build an SWR meter for balanced lines. It seemed a simple matter to base the design on the circuit of **Figure 5**, but with a toroidal current transformer in each leg and a balanced voltage sensing circuit. The outer cover and braid were stripped off some coax cable leaving the centre conductor insulated by the coax dielectric. A length of this was slipped through each toroidal core to form the two legs of the metered transmission line. A short length of braid was ultimately put back over the dielectric where it went through the toroidal core to form an electrostatic shield. I found this was necessary to correct a balance error caused by capacitance coupling into the winding around the core. (Of course, the unbalanced versions such as **Figure 5** all used the braid shield, so this was not unexpected.)

The circuit of the balanced meter is shown in **Figure 7**. The circuit constants have been worked out for a balance with 300 ohms resistance, which suits common forms of TV ribbon and open wire line. The secondaries of the two 12:1 current transformers (T2, T3) are connected in series. (They also work quite well when connected in parallel.) The voltage divider network (R10 in series with R6//R7 and R8//R9) is coupled into the signal combining and detector/metering circuit via transformer T4.

It all seemed straightforward, but I experienced a lot of trouble with circuit balance and common mode currents. I found it necessary to isolate the transmitter source with balun choke T1 to improve the balance at the instrument input. (I should point out that the source was already fed via a standard 4:1 transmitting balun.) For T1, a 30-mm diameter ferrite core was used to accommodate the transmitter power. This was a high-permeability Philips type which I happened to have on hand.

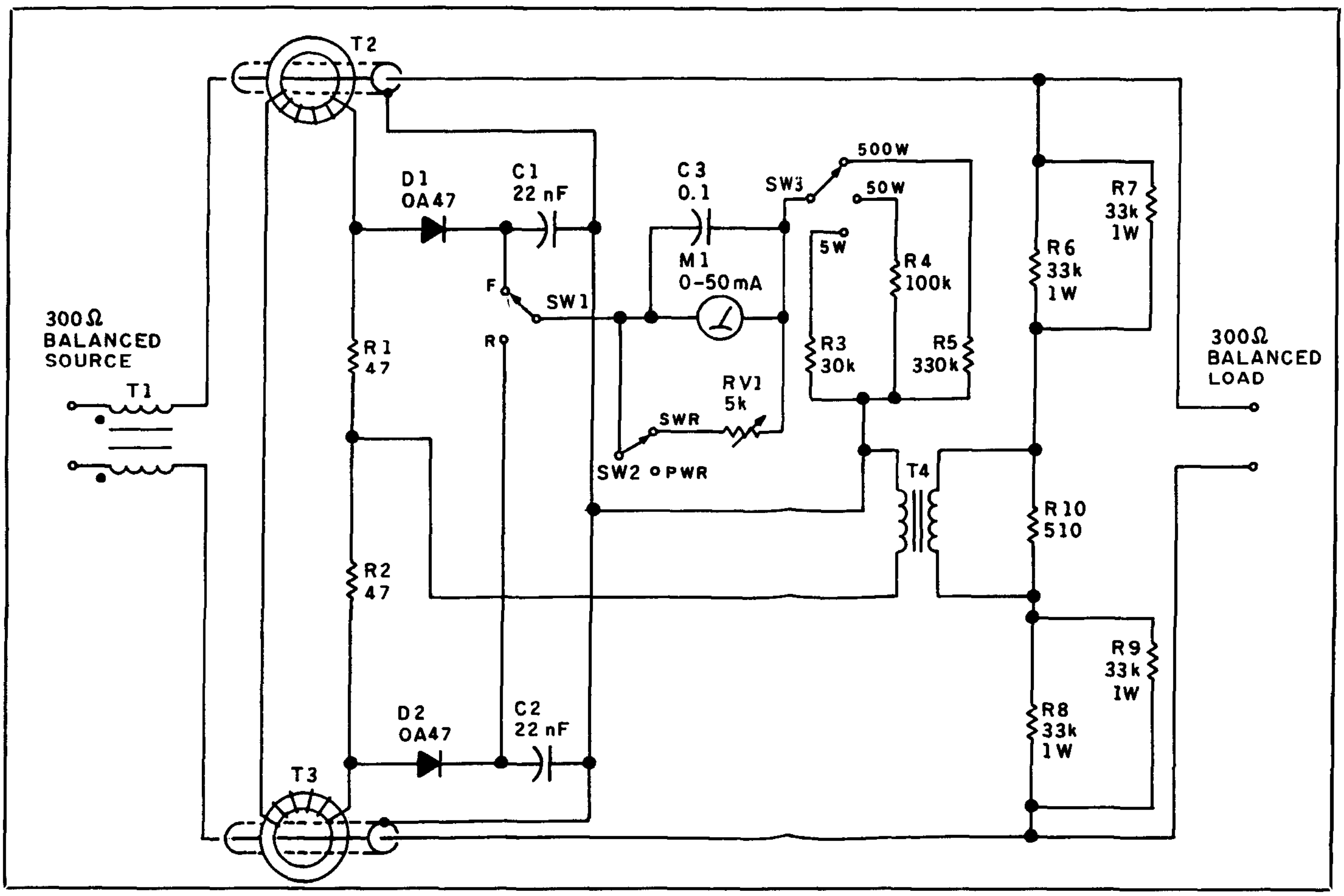

Figure 7. VK5BR SWR/power meter for 300-ohm balanced lines. T1 is 6 bifilar turns on Philips TDK2609 30-mm diameter toroidal core, μ = 800. T2 and T3 are 10 turns on Amidon FT50-72 toroidal core, μ = 2000. T4 is 10 bifilar turns on Amidon FT50-72 toroidal core.

A problem of line balance on some of the lines showed up as a different SWR value when the line pair legs were reversed. (This was a similar problem to that experienced when using the noise bridge.) The problem was compounded by unbalance in the source circuit and hence the reason for the input choke.

Isolating transformer T4 plays an important part in minimizing the effects discussed. A conventional transformer connection as in **Figure 1A** seemed more effective for this particular circuit than the choke connection in **Figure 1B**.

I tried all sorts of balancing arrangements, but finished with the circuit as shown. The measures taken did not completely eliminate the response to out-of-balance signal, but the level of this response was reduced enough to be tolerated.

Other impedances

The balanced SWR meter is designed for a balance at Zo = 300 ohms, but other impedances could be used by changing the value of resistor of R10. The value of R10 is inversely proportional to Zo. For example, for Zo = 600 ohms, halve the value of R10. I haven't tried any other impedances, but that is how it can be worked out. For correct power calibration, the meter resistors must also be changed. These are changed in inverse proportion to the square root of the impedance change. For Zo = 600 ohms, divide the meter resistors by root 2.

Checking the balance

High power 300-ohm non-inductive loads are not easily obtained, but the balance is easily checked by using low transmitter power and loading the SWR meter with a few one or two watt resistors to make up 300 ohms. Five watts on the lowest power select meter position gives full-scale forward reading, and this is applied for just long enough to carry out the test without burning out the resistors. When the meter is selected for reverse or reflected power, the 300-ohm load should give a low meter reading (near 1:1 SWR) at all HF frequencies.

SWR	μA	Power	μA
1	0	0	0
1.5	10	2	10
2	17	5	16
3	25	10	22
5	33	20	32
7	38	30	39
20	46	50	50
INF	50		

Table 1. Data to use when calibrating the meter scale.

Meter calibration

The information in **Table 1** can be used to calibrate the meter scale.

75-ohm SWR meter with candelabrum balun

Although 50 ohms is the most common operating impedance for SWR meters, many have a switch to select either 50 or 75 ohms. The type of meter which uses resistive voltage division (as in **Figure 5**) can also be converted to 75 ohms by shunting the lower resistance arm of the voltage divider.

Another method I used for checking SWR on a 300-ohm line was to couple a 75-ohm SWR meter into the line via a 4:1 candelabrum balun pair as shown in **Figure 8**. The toroidal cores of the balun pair needed to be large enough to handle the full RF power which passes through their windings. I used Amidon FC500 FT114 ferrite cores which are 29 mm in diameter. The windings were bifilar wound with 19 turns on each, which gave a calculated inductance of 29 microhenries. This seemed to be a good compromise between sufficient reactance over most of the HF band without too much capacitance.

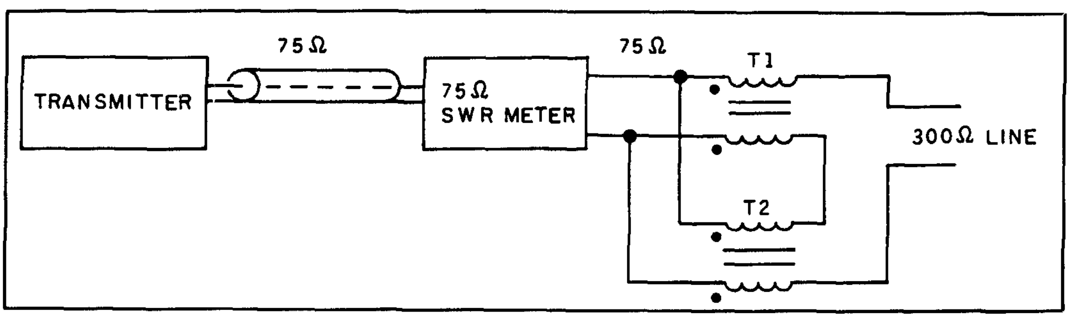

Figure 8. Measurement of SWR on a 300-ohm balanced line with a 75-ohm SWR meter and candelabrum circuit. T1 and T2 are 19 bifilar turns on Amidon FC500 29-mm ferrite core, μ = 125.

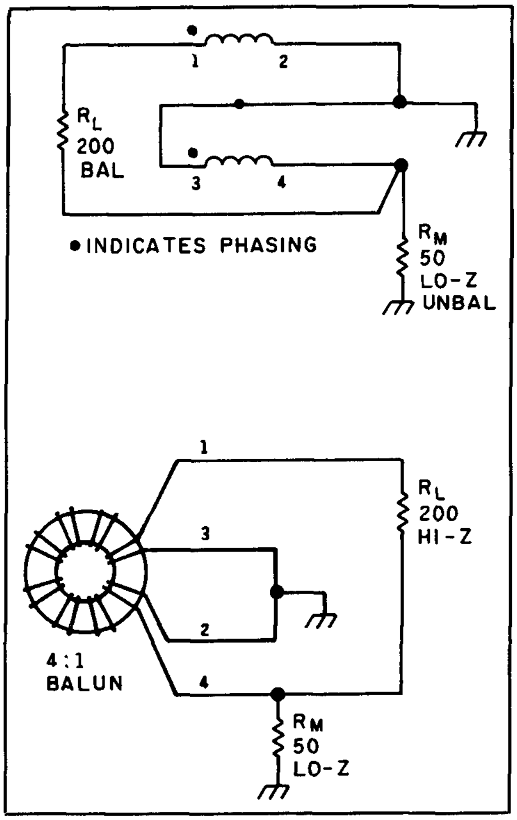

Figure 9. The usual 1:4 balun circuit—poor common mode rejection.

I found this measuring system worked like a charm. None of the problems I experienced with my balanced SWR meter (**Figure 7**) was apparent, and the transmission line legs could be transposed at will. This seemed to be the best system of measurement, its only limitation being it could be used only at the transmitter end of the line. For measurements at the load or antenna end, the balanced meter would have to be used.

I did try adding a further 1:1 balun choke at the candelabrum input as I had found to be necessary with the noise bridge. However, this did not enhance the performance in any way and, in fact, tended to modify the impedance reflected at the highest frequencies.

One might well ask how the normally used 4:1 impedance ratio balun connection (*Figure 9*) performs as compared with the candelabrum circuit. This connection is a type of auto transformer and probably does little to reject common mode signals. Anyway, when using this type of transformer, I again experienced the problems of a different answer when the line leg pairs were reversed.

The balun transformer used for the **Figure 9** type balun was the one that can be bought as a 1 kW kit with an Amidon T200 iron powder core. Fourteen bifilar turns were placed on the core. When terminated in a 300-ohm resistance, this balun reflected a considerable reactive component at the lower HF frequencies. (This was verified with the noise bridge.) Using the 75-ohm SWR meter, the SWR at 21 and 28 MHz was 1.2:1, but increased to 1.8:1 at 7 MHz, and 2.8:1 at 3.5 MHz. This compared poorly with my candelabrum circuit, which gave a reading with 1.1:1 over the whole range of 3.5 to 28 MHz.

This is an interesting result. Suppose you use this typical broadband balun at, say, 3.5 MHz to couple to a transmission line and then adjust your matching at the antenna end by stub or whatever. You adjust for a 1:1 SWR on the meter, but actually achieve a mismatch and standing waves on the line. Of course, the core needs more turns for the lower frequencies. Some time ago, I did some tests with this core using the 1:1 ratio winding connection and a 50-ohm load. I came to the conclusion that, for better performance, the number of turns should be increased to around 20 for frequencies below 5 MHz and reduced to around six turns for frequencies above 10 MHz. Anyway, there is a message here. Do not take your balun transformer for granted. Check it out at the frequency of operation using the SWR meter and with its secondary terminated in a dummy resistance equal to the working load impedance. Fortunately, even if mismatched, line losses at the lower HF frequencies are small, hence we are usually able to tolerate the effect I have discussed ithout recourse to rewinding the transformer.

REFERENCE
1. *Amateur Radio*, Wireless Institute of Australia, November 1969.

PRODUCT INFORMATION

Audio Power Meter

Harbin Test System's HTS-83C audio power meter is designed to test and troubleshoot power amplifiers. The meter can be used to measure audio power output from 0.1 mW to 200 watts over the frequency response range of 20 Hz to 40 kHz ±0.5 dB.

For more information about the HTS-83C write to Harbin Test Systems, 3826 Old Getwell Road, Memphis, Tennessee 38118, or call (901)794-1667. FAX: (901)794-2515.

LETTERS

An excellent article, but...

Mr. Mork's excellent article, "A User's View of Charge Coupled Device Imaging" (Spring 1992), contained an unfortunate factual error, which was then compounded by a mathematical error. I refer to his report on page 66 of the frequency of the world's record laser QSO as "7.5×10^{14} Hz (7.5 teraHertz)." Since Tera (and yes, it should be capitalized) represents 10^{12}, the frequency listed should, of course, have been 750 THz.

Only that was not the frequency KY7B and WA7LYI actually used for their record shot. Seven-hundred and fifty THz is just at the boundary of visible and ultraviolet light (see **Figure 1**), and the contact used visible light. I know, because I've seen the videotape, and the signal was surely visible to my eye, which doesn't respond to 750 THz. Besides, "they observed a beam spread of 250 feet at the detector," so the signal must have been visible.

Helium Cadmium lasers can operate in several modes, and can produce both visible and ultraviolet outputs. The most common of these devices (produced by Omnichrome, Liconics, and Nihon Dempa Kojyo Co. Ltd., among others) produce signals at 325 nm (a frequency of 923.1 THz) and 441.6 nm (which corresponds to 679.3 THz). This latter frequency corresponds to blue visible light, and since the laser beam in the videotape appeared blue to my eye, I suspect this mode was being utilized.

I am aware of no HeCd laser which operates at or near 750 THz, although that's close to the answer you get if you calculate the geometric mean of the blue and μV HeCd modes. There is an interesting "white light laser" produced by Nihon Dempa Kojyo, which produces 40 mW of output distributed between the wavelengths of 533.7 nm, 537.8 nm, and 635.nm. Taken together, these spectral components appear quite white. The highest ouput power HeCd of which I am aware comes from Omnichrome, and puts out 150 mW of decidedly blue light. I'd like to get my hands on two of those for a record attempt!

Dr. H. Paul Schuch, N6TX
Professor of Electronics
Pennsylvania College of Technology
Williamsport, Pennsylvania

K.V.G. CRYSTAL PRODUCTS

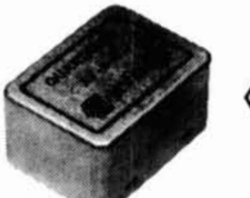

9 MHz CRYSTAL FILTERS

MODEL	Application	Bandwidth	Poles	Price
XF-9A	SSB	2.4 kHz	5	$ 75.00
XF-9B	SSB	2.4 kHz	8	105.00
XF-9B-01	LSB	2.4 kHz	8	145.00
XF-9B-02	USB	2.4 kHz	8	145.00
XF-9B-10	SSB	2.4 kHz	10	185.00
XF-9C	AM	3.75 kHz	8	110.00
XF-9D	AM	5.0 kHz	8	110.00
XF-9E	FM	12.0 kHz	8	120.00
XF-9M	CW	500 Hz	4	80.00
XF-9NB	CW	500 Hz	8	165.00
XF-9P	CW	250 Hz	8	199.00
XF-910	IF noise	15 kHz	2	20.00

10.7 MHz CRYSTAL FILTERS

XF-107A	12 kHz	$105.00
XF-107B	15 kHz	105.00
XF-107C	30 kHz	105.00
XF-107D	36 kHz	120.00
XF-107E	40 kHz	125.00
XF-107S139	100 kHz	175.00

41 MHz CRYSTAL FILTER

XF-410S02	$199.00

Write for full details of crystals and filters. Shipping: $7.00 Shipping: FOB Concord, MA Prices subject to change without notice.

VISA MasterCard

si

Spectrum International, Inc.
P.O. Box 1084 Dept. Q
Concord, MA 01742 U.S.A.
Phone: 508-263-2145
FAX: 508-263-7008

W2FMI BALUNS AND UNUNS

How to put MORE power into your antenna and get better and higher signal strength ???

– Use the all new MOST OUTSTANDING, HIGHEST EFFICIENCY (97% TO 99%), and the BEST BROADBAND UNUN (unbalanced to unbalanced) and BALUN (balanced to unbalanced) TRANSFORMERS exclusively designed and optimized by DR. JERRY SEVICK (W2FMI). Amidon Associates, Inc. now offers the widest selection of the W2FMI Baluns and Ununs to meet all your requirements for better and more consistent communication. Also available in do-it-yourself kits.

Use UNUN transformers for matching 50-ohm cable to:
(1) Vertical antennas, inverted L's and ground fed slopers (all over good ground systems),
(2) 75-OHM cable,
(3) A junction of two 50-OHM cables,
(4) Shunt-Fed towers performing as vertical antennas, and
(5) The output of a transceiver of class B linear amplifier when an unfavorable VSWR condition exists.

Use BALUN transformers for matching:
(1) Half-waves dipoles and inverted V's
(2) Quad antennas
(3) Folded dipoles
(4) Rhombic and V antennas
(5) Yagi beams

*All designs, when used according to instructions, are **GUARANTEED** to give outstanding performances. **Comparisons with other matching transformers are invited.***

POWER RATING: at least 2KW continuous from 1MHz to 40 MHz.

W2FMI HIGH POWER UNUNS	IMPEDANCE MATCH	COMPLETE UNIT PRICE
2.25:1HU50	50:22.22-OHMS	$45.00
2:1-HU50	50:25-OHMS	$45.00
2:1-HDU50	50:22.22-OHMS 50:25-OHMS	$50.00
2.25:1-HU112.5	112.5:50-OHMS	$45.00
2:1-HU100	100:50-OHMS	$45.00
2:1-HDU100	112.5:50-OHMS 100:50-OHMS	$50.00
1.78:1-HU50	50:28-OHMS	$45.00
1.5:1-HU50	50:32-OHMS	$45.00
1.5:1-HU75	75:50-OHMS	$45.00
4:1-HRU50	50:12.5-OHMS	$50.00
4:1-HCU50	50:12.5-OHMS	$50.00
9:1-HRU50	50:5.56-OHMS	$50.00
9:1-HUH50	50:5.56-OHMS	$45.00
1.78:1-HDU50	50:28-OHMS 50:12.5-OHMS	$50.00
1.56:1-HDU50	50:32-OHMS 50:18-OHMS	$50.00
HMMU50(5 diff. ratios)	MULTIMATCH UNUN	$80.00
1.78:1-HMMU50 (8 different ratios)	MULTIMATCH UNUN	$90.00

Unconditional money back guarantee for 1 year on completed unit.

KIT PRICE FROM $28.00! CALL TODAY!

W2FMI HIGH POWER BALUNS	IMPEDANCE MATCH	COMPLETE UNIT PRICE
1:1-HBL50	50:50-OHMS	$55.00
4:1-HBM200	200:50-OHMS	$55.00
6:1-HB300	300:50-OHMS	$120.00
9:1-HB450	450:50-OHMS	$150.00
2.25:1-HB112.5	112.5:50-OHMS	$120.00
4:1-HB50	50:12.5-OHMS	$55.00

NOTE: OTHER BALUN & UNUN TRANSFORMERS AVAILABLE. PLEASE CALL OR WRITE FOR ADDITIONAL DETAIL.

BOOKS: 1) "Transmission Line Transformers Design Handbooks", by Jerry Sevick, W2FMI, *Amidon Associates, Inc., 1991. $8.00 ea.*
2) "Transmission Line Transformers", by Jerry Sevick, W2FMI, APRL, 1990. $20.00 ea.

ALSO AVAILABLE:

Iron Powder and Ferrite Products
Millions of Parts in Stock for Immediate Delivery. Low Cost Experimental Kits.
Call for our FREE tech. flyer.
Toroidal Cores • Shielding Beads • Shielded Coil Forms • Ferrite Rods • Pot Cores • Baluns • Etc.

AMIDON Associates, INC.
VISA MasterCard
Fast reliable service since 1963
2216 East Gladwick Street, Dominguez Hills, CA 90220
TEL: (310) 763-5770 • FAX: (310) 763-2250

COLLINS

Manual Sale: Brand New, Fresh and Crisp!! **KWM-2 & 2A – $29 • 51S-1 – $35 • 30S-1 – $29 • 32S-3 – $24 • 30L-1 – $24 • 75S-3/A – $29**

Plastic Trim Rings: Large fit all S-Line and KWM-2. Small fit 516F-2, B4, B5, etc. $29.95

Bristol Wrench Set: Complete set of 9 Bristol Spline wrenches for Collins. $29.95

TR Relay for KWM-2/A, 32S- & 30L-1: Authentic relay for Collins Equipment $49ea.

Panel Meters: New Meters for most all Collins equipment. $85ea.

Paint: (12 oz. spray) Primer–Zinc Chromate, Collins Trim Ring #126 Gray, Cabinet #180, Front Panel #250, St. James Gray #270, KWM-380 Cabinet Earth Brown. (1/2 pt. can) KWM-380 Front Panel or Cabinet. $12ea. or 6/$60

Power Cords: 51S-1–$21.95; 75S–$15; 516F-2 power–$9.95; 516F-2 interconnect– $36.95

Crystals, operating frequencies: HC-6/U holders. $8each

Crystals, BFO, Calibrator: 456.350, 453.650 & 455.8 KHz– $35each 100 KHz– $42each

KWM-2A Plug-in Relays: 970-2439-010 4PDT (X96) or 970-2439-020 6PDT (X97) $52

KWM-2A Plug-in Relay Mod Kit: Converts open frame to plug-in relays. Incl. instructions, relays & misc. $124

KWM-380–HF-380 Conversion Kit includes A3 Filter, 060 ROM, and HF-380 Emblem. $525

380 Reinforced Speaker Grill –$45; **Mic Gain Pot** 376-0276-030 –$22; **MM-280** Mobile Mike –$45; **AC-3802** Speech Processor –$350; **140 Hz** CW Filter –$195; **360 Hz** CW Filter or **1.7 KHz** RTTY/SSB/Data Filter –$109; **6 KHz** AM Filter –$79; **Power Transformer** –$45; **Front Panel Lense** –$65.

Collins equipment on hand 32S-1, 32S-3, 75S-1, 75S-2, 75S-3, 75S-3A, 75S-3B, 32V-2 (make 1 out of 2..... $950 takes both), 312B-4, KWM-2, CC-3 Suitcases(access.) Please Call!

"EIMAC" 8877 – 3CX1500A7

Last chance to stock up at up to 50% savings. New (original boxed, guaranteed!) Gain and linearity curves included with each tube. Limited quantities available. First come first served. Shipping: Add $7/ tube in US. DX please call for proforma.

Individually: $495 each (2-6) $450 (7-24) $425
Matched Pairs $1099 per pair

SGC

SG-2000	HF Transceiver, 1.8-30 Mhz, 150 watts –	$1599
SG-2000	Extra Control Head (use up to 8 per installation) –	$ 695
SG-230	Smartuner Antenna Coupler –	$ 469
SG-303	Marine/Mobile Antenna (best one for SG-230) –	$ 339
QMS	Quick Mount System (SG-230, SG-303 & QMS) –	$1199

ANNIVERSARY **FLYER 6A**

FREE! Just off the Press.... Our newest publication: Anniversary Flyer 6A. Amplifier parts, Ball Drives, Capacitors (Vacuum, Oil, Electrolytic), Relays (Vacuum, Power), SGC, NYE, DIAMOND, AEA, COLLINS PARTS, Fans, Blowers, Fingerstock, Hardline Connectors, Test Equipment, Meters, Microwave GOODIES! Send a postcard w/ mailing info to new address below or $1 for 1st class delivery.

DOORKNOB CAPACITORS

HT59	500pF	15kv	23amps	$99
HT57	25pF	15kv	13amps	$33
HT57	40pF	15kv	13amps	$29
HT57	50pF	15kv	14amps	$33
HT57	100pF	15kv	14amps	$33
HT57	200pF	15kv	15amps	$30
HT57	500pF	15kv	7amps	$30
HT57	1000pF	15kv	5.1amps	$30
HT57	1500pF	15kv	5.3amps	$33

HT58	10pF	5kv	$12	HT58	120pF	5kv	$13
HT58	25pF	7.5kv	$12	HT58	140pF	5kv	$13
HT58	30pF	5kv	$13	HT58	200pF	5kv	$12
HT58	50pF	5kv	$12	HT58	300pF	5kv	$13
HT58	66pF	5kv	$13	HT58	400pF	5kv	$13
HT58	80pF	5kv	$13	HT58	500pF	5kv	$12
HT58	100pF	5kv	$12	HT58	1000pF	5kv	$12

MINIATURE DOORKNOBS WITH WIRE LEADS

HT55	NPO	1pF	5kv	$11	HT55	NPO	6pF	5kv	$11
HT55	NPO	2pF	5kv	$11	HT55	NPO	10pF	5kv	$12
HT55	NPO	5pF	5kv	$11	HT53	N750	40pF	5kv	$11

DIAMOND ANTENNAS– Good prices too!

RCA APTs A few left in stock. Don't pass them up! Available with new ($225) or used monitor ($145)!!

DRAKE R-8 Receiver Introductory price: **$959!!** Delivered in US

MICROWAVE COMPONENTS

Flexible Waveguide 8.2-12.4GHz; 11-1/2" long; silver inside, resilient rubber outside, 1-5/8" square flange $75 ea

Mini-Circuits MIXER – TFM-2-408-1 – DC-1000Mhz $8.95 3/$24

INTERFERENCE REDUCTION FERRITE Split Beads

Beads are split in halves. Clamps around wire/ cable and chokes off unwanted interference from almost any radio transmitter.

Fits up to 1/4" cable, no cage $3.45/set • 5 sets /$16
Fits up to 3/8" cable, with cage $4.95/set • 5 sets /$23
Fits up to 1/2" cable, no cage $4.35/set • 5 sets /$20

ICs — INTEGRATED CIRCUITS

STOCK REDUCTION SALE; CLEANING HOUSE!

Send $4* for *IC* BIG LIST

(*Refunded with minimum purchase)

CIGAR – PLUG ADAPTERS

• HEAVY DUTY (UL)
• 3AG type FUSE(incl.)
• molded 18ga pigtail cord

$1.95 each
6/$10
25/$38

In-line FUSE HOLDERS
• Purple Pigtails
• Includes .5a fuse
50¢ 10/$4
50/$15

••••••• NEW ADDRESS •••••••
1502 Jones St. • Omaha, NE 68102
402-346-4750 • fax: 402-346-2939

Anniversary Flyer 6A included with your order. Please add adequate shipping. In U.S.–48 figure 30¢ per lb. to 70 lbs. (1st – 3lbs add $4 min). Others please call, fax or write for exact shipping total. We accept Visa, MC, Amexco, checks, Cash On Delivery (UPS only, add $4) or wire transfer.

Surplus Sales of Nebraska

ADVERTISER'S INDEX

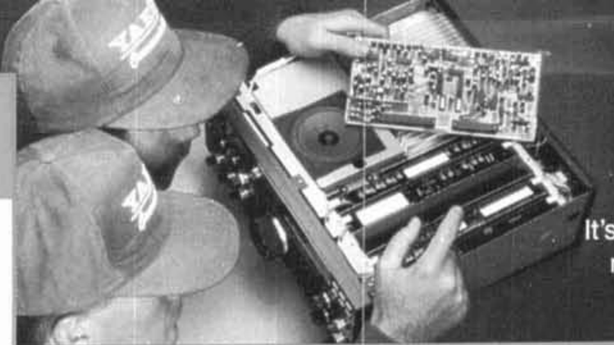

"Yaesu did it again!'

"This is the only
HF rig with a dual digital SCAF.
It's incredible on a crowded band. Look inside,
motherboard and plug-in board design.
Un-be-liev-able!"

FT-990
All-Mode
HF Transceiver

- **Frequency Coverage:** 100 kHz – 30 MHz RX (160-10 m TX)
- Built-in Dual Digital Switched Capacitance Filters
- Built-in High Speed Antenna Tuner w/39 Memories
- RF FSP (RF Frequency-Shifted Speech Processor)
- Dual VFOs with Direct Digital Synthesis (DDS)
- 90 Memories which store Frequency Mode and Bandwidth
- Full and Semi Break-in CW Operation
- Band Stacking VFO System
- Multi-mode Selection on Packet/RTTY; Easy interface to TNCs
- Adjustable RF Power
- Variable Threshold Noise Blanker
- Optional Digital Voice Recorder (DVS-2)
- Front Panel RX Antenna Selection
- **Accessories:**

FT-990DC	Available without power supply
XF-10.9M	2nd IF SSB Narrow 2.0 kHz Filter
XF-445K	2nd IF CW Narrow 250 Hz Filter
TCXO-2	High Stability TCXO
SP-6	External Desk-top Speaker
MD-1C8	Desk Microphone
DVS-2	Digital Voice Recorder Unit
YH-77ST	Lightweight Headphones
LL-5	Phone Patch Unit for SP-6 Speaker

The innovative technology of the FT-990 is inside, not outside. Like the exclusive dual digital SCAF (Switched Capacitance Audio Filter). And for long term reliability, the motherboard/plug-in module construction eliminates inter-board wiring. The FT-990 also has the same undisputed receiver performance of the FT-1000 as well as other features such as a high-speed, built-in antenna tuner with automatic storage. And, multiple DDS (Direct Digital Synthesis) for quick lock-up time and low level noise. What's more, for maximum efficiency, the FT-990 is a self-contained base station with its space-saving, built-in AC power supply.

Outside, the very functional HF front panel is simple and uncluttered with a large amber display. Easy to use, easy to see. Pure and simple QSO enjoyment – with muscle when you need it! Yaesu makes "high-tech" effortless. Now it works for you, not against you. Have your dealer show you the FT-990 today and see what we mean.

FT-990DC now available. **NEW**

YAESU

Performance without compromise.℠

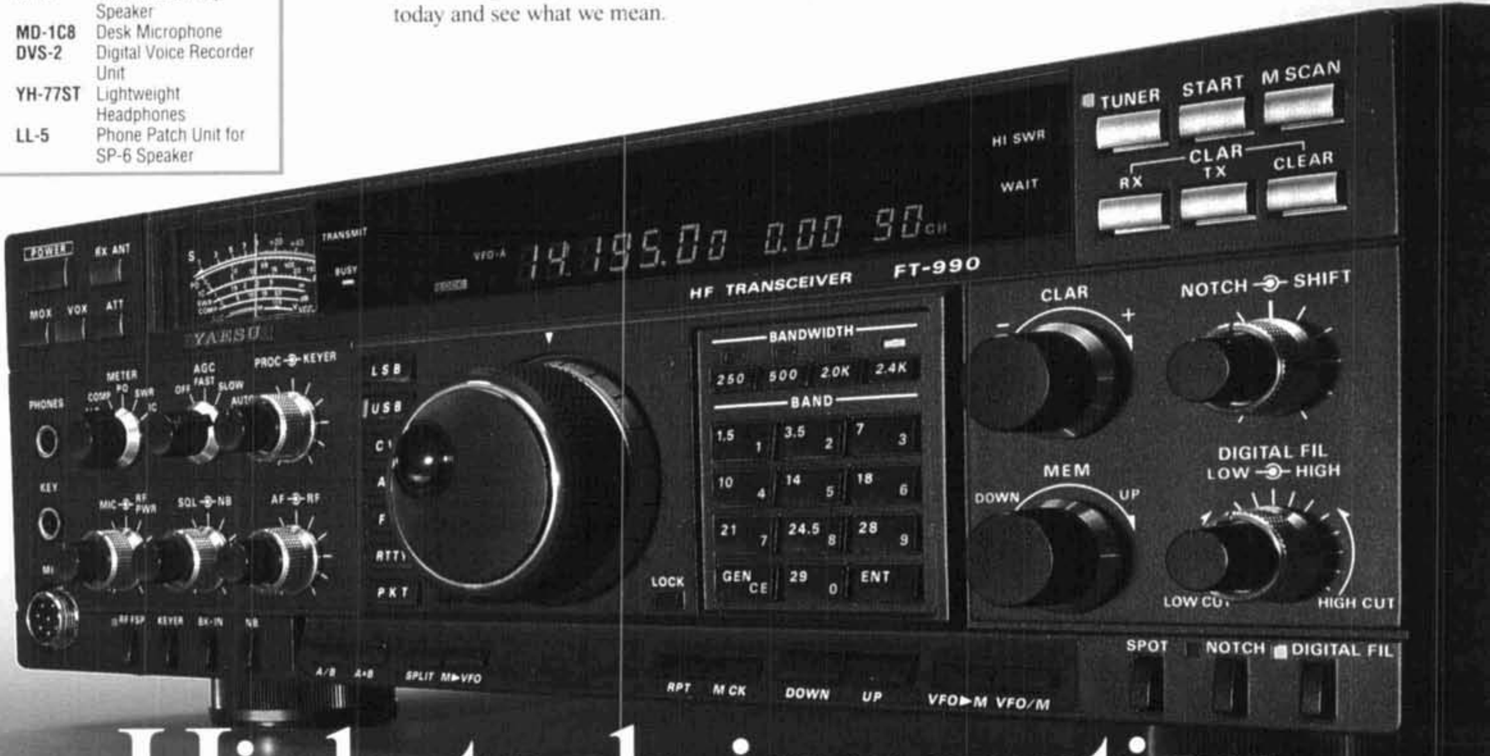

High-tech innovation isn't miniature knobs, switches, and tiny labels.